

**An investigation of the neurochemical
mechanisms underlying the contrasting
effects of *d*-amphetamine in two subregions
of the rat anterior cingulate cortex**

Elizabeth S. Ash

A thesis presented to the University of London for the degree of Doctor of

Philosophy

2007

Department of Pharmacology

University College London

Gower Street

London WC1E 6BT



UMI Number: U591363

All rights reserved

INFORMATION TO ALL USERS

The quality of this reproduction is dependent upon the quality of the copy submitted.

In the unlikely event that the author did not send a complete manuscript and there are missing pages, these will be noted. Also, if material had to be removed, a note will indicate the deletion.



UMI U591363

Published by ProQuest LLC 2013. Copyright in the Dissertation held by the Author.
Microform Edition © ProQuest LLC.

All rights reserved. This work is protected against
unauthorized copying under Title 17, United States Code.



ProQuest LLC
789 East Eisenhower Parkway
P.O. Box 1346
Ann Arbor, MI 48106-1346

Abstract

d-Amphetamine inhibits neuronal uptake, and causes impulse-independent release of monoamines. There are several reports that *d*-amphetamine increases glutamate efflux in the rat cerebral cortex, but this has not been investigated systematically. It is unclear whether this is direct or secondary to its effects on dopamine transmission. These experiments aimed to compare regulation of extracellular glutamate in two adjacent subregions of the rat anterior cingulate cortex using *in vivo* microdialysis: the rostral anterior cingulate cortex (rACC) and caudal anterior cingulate cortex (cACC), which are innervated by dopaminergic projections from different brainstem nuclei.

The first finding was that the glutamate response to *d*-amphetamine depended on subregion and route of administration. Glutamate in the cACC but not the rACC was increased by systemic *d*-amphetamine. Conversely, glutamate in the rACC but not the cACC was increased by local *d*-amphetamine. Local infusion of dopamine in the rACC mimicked the effect of *d*-amphetamine, suggesting the glutamate response is mediated by dopamine. This was confirmed by experiments where the glutamate response to local *d*-amphetamine in the rACC was blocked by the D₁-like receptor antagonist SCH23390 but not the D₂-like receptor antagonist haloperidol.

Local infusion of dihydrokainate (DHK), which inhibits the glial GLT-1 glutamate transporter, did not affect spontaneous efflux of glutamate in either subregion. However, DHK increased glutamate efflux during local infusion of *d*-amphetamine in the cACC, indicating that GLT-1 normally contributes to clearance of glutamate released by *d*-amphetamine. In contrast, infusion of DHK reduced glutamate efflux in the rACC of rats given systemic *d*-amphetamine, suggesting that

impairment of GLT-1 function leads to reduced glutamate release (possibly through activation of inhibitory autoreceptors).

Such striking neurochemical asymmetries enable spatial focussing of the response to *d*-amphetamine in the ACC and could contribute to demarcation of the role of each of its subregions in regulation of mood and behaviour.

Acknowledgments

I would like to thank my supervisor Dr. Clare Stanford for all her invaluable help and guidance throughout the course of my Ph.D, especially during the difficult stages of the experimentation and writing.

I would also like to thank Dr. David Heal for his interest in my work and the funding he provided throughout my studies. I also gratefully acknowledge the Medical Research Council for their funding of this project.

Thanks to all the members of the lab: John Stewart, Inga Herpfer, Amy Fisher and Carrie Yan for their friendship, support and encouragement and for guiding me through the experimental techniques.

Thanks also to the members of the Pharmacology Department, especially Roger Allman for his help with ordering and his good friendship throughout my Ph.D. Also thanks to Nick Hayes for his friendship and conversation, Mike Bovingdon for all his technical help and Bob Muid for IT-related help.

I would also like to thank the staff at the biological services unit for all their help.

Finally a huge thanks to all my family and friends for all their support and good times and for believing in me.

Contents

Title	1
Abstract	2
Acknowledgements	4
Contents	5
List of Figures	13
List of Tables	17
List of abbreviations	20
List of prefixes	21

Chapter 1: General introduction	21
1.1 THE PREFRONTAL CORTEX	22
1.1.1 <i>Anatomical delineation of the prefrontal cortex</i>	23
1.1.2 <i>The medial prefrontal cortex</i>	24
1.1.3 <i>The anterior cingulate cortex – structure and function</i>	24
1.2 GLUTAMATE IN THE ANTERIOR CINGULATE CORTEX	28
1.2.1 <i>Regulation of extracellular glutamate by glial cells</i>	29
1.3 MICRODIALYSIS OF GLUTAMATE	31
1.3.1 <i>Microdialysis of glutamate – what does it signify?</i>	32
1.3.2 <i>Microdialysis studies in the prefrontal cortex</i>	38
1.4 DOPAMINE AFFERENTS TO THE MEDIAL PREFRONTAL CORTEX	41
1.4.1 <i>Neuroanatomy of dopamine – pathways in the rat brain</i>	41
1.4.2 <i>Dopaminergic innervation of the prefrontal cortex</i>	43
1.5 GLUTAMATE-DOPAMINE INTERACTIONS	46

1.6 DOPAMINE-GLUTAMATE INTERACTIONS	50
1.6.1 <i>Modulation of prefrontocortical glutamate by the dopamine system – electrophysiological studies</i>	50
1.6.2 <i>Modulation of prefrontocortical glutamate by the dopamine system – microdialysis studies</i>	51
1.7 THE PHARMACOLOGY OF d-AMPHETAMINE	52
1.7.1 <i>Sites of action of d-amphetamine – experimental evidence</i>	53
1.7.2 <i>Mechanisms of action of d-amphetamine – experimental evidence</i>	56
1.8 THE PHARMACOLOGY OF DIHYDROKAINATE	60
1.9 OBJECTIVES	60
Chapter 2: Methods	62
2.1 IN VIVO NEUROCHEMICAL MONITORING TECHNIQUES	62
2.1.1 <i>The push-pull cannula</i>	62
2.1.2 <i>In vivo microdialysis</i>	63
2.1.3 <i>In vivo voltammetry</i>	64
2.1.4 <i>In vivo brain imaging</i>	64
2.1.5 <i>Composition of the perfusate</i>	65
2.1.6 <i>Neurotransmitter ‘efflux’</i>	66
2.2 THE MICRODIALYSIS PROBE	66
2.2.1 <i>Probe construction</i>	66
2.2.2 <i>Measurement of probe recovery</i>	67
2.3 MICRODIALYSIS PROCEDURES	71
2.3.1 <i>Surgical procedure</i>	71
2.3.2 <i>Collection of dialysates</i>	73
2.3.3 <i>Verification of probe placement</i>	73
2.3.4 <i>Measurement of dialysate glutamate content</i>	74

2.4 HIGH PERFORMANCE LIQUID CHROMATOGRAPHY (HPLC)	74
2.4.1 <i>Detection of glutamate</i>	74
2.4.2 <i>Theory of HPLC</i>	76
2.4.3 <i>Isocratic vs. gradient elution</i>	76
2.4.4 <i>Main components of the HPLC system</i>	79
2.4.5 <i>Choice of the mobile phase</i>	79
2.4.6 <i>Composition of the mobile phase</i>	83
2.4.7 <i>Electrochemical detection</i>	83
2.4.8 <i>Choice of the potential of oxidation</i>	84
2.4.9 <i>Calibration of the separation/detection system</i>	85
2.5 DOPAMINE HPLC	88
2.5.1 <i>Composition of the mobile phase</i>	88
2.5.2 <i>Components of the assay system</i>	88
2.5.3 <i>Calibration of the separation/detection system</i>	89
2.6 DRUG ADMINISTRATION	90
2.7 STATISTICAL ANALYSIS	91
Chapter 3: <i>d</i>-Amphetamine has contrasting effects in two subregions of the rat anterior cingulate cortex	93
3.1 INTRODUCTION	93
3.2 AIMS	96
3.3 METHODS	97
3.3.1 <i>In vivo microdialysis</i>	97
3.3.2 <i>Statistical analysis</i>	98
3.4 RESULTS	101

3.4.1 Basal glutamate efflux	101
3.4.2 Effects of local infusion (via retrodialysis) of increasing concentrations of d-amphetamine on glutamate efflux	101
3.4.3 Effects of systemic injection of d-amphetamine on glutamate efflux	105
3.5 DISCUSSION	108
3.5.1 Possible sources of glutamate (where increased efflux is observed)	109
3.5.2 Possible explanations for regional differences in the response to d-amphetamine	112
3.5.4 Summary of key findings	113
Chapter 4: Contrasting effects of d-amphetamine on dopamine efflux and dopamine on glutamate efflux in two subregions of the anterior cingulate cortex	114
4.1 INTRODUCTION	114
4.2 AIMS	115
4.3 METHODS	116
4.3.1 Experiment 1 – effects of local infusion of d-amphetamine on dopamine efflux in the cACC and rACC	116
4.3.2 Experiment 2 – effects of systemic injection of d-amphetamine on dopamine efflux in the cACC and rACC	116
4.3.3 Experiment 3 – effects of local infusion of increasing concentrations of dopamine on glutamate efflux in the cACC and rACC	117
4.3.4 Statistical analysis	117
4.4 RESULTS	120
4.4.1 Experiment 1 – effects of local infusion of d-amphetamine on dopamine efflux in the cACC and rACC	120
4.4.2 Experiment 2 – effects of systemic injection of d-amphetamine on dopamine efflux in the cACC and rACC	123

4.4.2.1 The rostral anterior cingulate cortex	123
4.4.2.2 The caudal anterior cingulate cortex	126
4.4.3 <i>Experiment 3 – effects of local infusion of dopamine on glutamate efflux in the cACC and rACC</i>	129
4.5 DISCUSSION	132
4.5.1 <i>Effects of d-amphetamine on dopamine efflux</i>	137
4.5.2 <i>Effects of local infusion of dopamine on glutamate efflux</i>	138
4.5.3 <i>Summary of key findings</i>	138
CHAPTER 5: The effect of pre-treatment with dopaminergic antagonists on the glutamate response to local infusion of d-amphetamine in the rostral anterior cingulate cortex	139
5.1 INTRODUCTION	139
5.2 AIM	142
5.3 METHODS	143
5.3.1 <i>Experiment 1 – Effects of pre-treatment with the D₂-like receptor antagonist haloperidol on the glutamate response to local infusion of d-amphetamine in the rostral anterior cingulate cortex</i>	143
5.3.2 <i>Experiment 2 – Effects of pre-treatment with the D₁-like receptor antagonist SCH23390 on the glutamate response to local infusion of d-amphetamine in the rostral anterior cingulate cortex</i>	144
5.3.3 <i>Statistical analysis</i>	144
5.4 RESULTS	147
5.4.1 <i>Effects of pre-treatment with the D₂-like receptor antagonist haloperidol on the glutamate response to local infusion of d-amphetamine in the rostral anterior cingulate cortex</i>	147

5.4.2 Effects of pre-treatment with the D₁-like receptor antagonist SCH23390 on the glutamate response to local infusion of d-amphetamine in the rostral anterior cingulate cortex	155
5.5 DISCUSSION	163
5.5.1 Effects of haloperidol and SCH23390 on spontaneous glutamate efflux in the rACC	163
5.5.2 Effects of haloperidol on the glutamate response to d-amphetamine	164
5.5.3 Effects of SCH23390 on the glutamate response to d-amphetamine	165
5.5.4 Summary of key findings	168
CHAPTER 6: Effect of pre-treatment with the GLT-1 inhibitor dihydrokainate on the glutamate response to systemic administration of d-amphetamine in the rostral and caudal anterior cingulate cortices	169
6.1 INTRODUCTION	169
6.2 AIM	172
6.3 METHODS	173
6.3.1 In vivo microdialysis	173
6.3.2 Statistical analysis	175
6.4 RESULTS	176
6.4.1 Caudal anterior cingulate cortex	176
6.4.2 Rostral anterior cingulate cortex	181
6.5 DISCUSSION	185
6.5.1 The effect of inhibition of GLT-1 on spontaneous glutamate efflux	185
6.5.1.1 The caudal anterior cingulate cortex	185
6.5.1.2 The rostral anterior cingulate cortex	185
6.5.2 The effect of inhibition of GLT-1 on d-amphetamine-evoked glutamate Efflux	186

6.5.2.1 The caudal anterior cingulate cortex	186
6.5.2.2 The rostral anterior cingulate cortex	191
6.5.3 Mechanism of decreased glutamate efflux	192
6.5.3.1 Decreased extracellular glutamate – a possible hypothesis	192
6.5.4 Summary of key findings	194

Chapter 7: Effect of pre-treatment with the GLT-1 inhibitor dihydrokainate on the glutamate response to local infusion of *d*-amphetamine in the caudal and rostral anterior cingulate cortices

7.1 INTRODUCTION	195
7.2 AIM	196
7.3 METHODS	197
7.3.1 <i>In vivo</i> microdialysis	197
7.3.2 <i>Statistical analysis</i>	199
7.4 RESULTS	200
7.4.1 <i>Caudal anterior cingulate cortex</i>	200
7.4.2 <i>Rostral anterior cingulate cortex</i>	205
7.5 DISCUSSION	209
7.5.1 <i>Caudal anterior cingulate cortex</i>	209
7.5.2 <i>Rostral anterior cingulate cortex</i>	211
7.5.3 <i>Summary of key findings</i>	213

Chapter 8: General discussion

8.1 SUMMARY OF RESULTS	214
8.2 IMPLICATIONS OF THESE RESULTS	218
References	222

List of Figures

Chapter 1: General introduction

- Figure 1.1** *Anatomical delineation of the prefrontal cortex* 24
- Figure 1.2** *Midsagittal view of the rat cingulate cortex* 25
- Figure 1.3** *Scheme depicting the position of the microdialysis probe in relation to the glutamatergic synapse* 40
- Figure 1.4** *Schematic diagram summarising the influence of glutamatergic neurotransmission on dopamine efflux in the rat prefrontal cortex* 49
- Figure 1.5** *The chemical structure of d-amphetamine* 52

Chapter 2: Methods

- Figure 2.1** *Schematic diagram showing the steps involved in constructing the microdialysis probes* 66a
- Figure 2.2** *Probe recovery as a function of flow rate* 70
- Figure 2.3** *Scheme depicting the reaction between glutamate and o-phthalaldehyde (OPA)* 78
- Figure 2.4** *Mean detector response as a function of mobile phase pH* 81
- Figure 2.5** *Examples of typical chromatograms obtained during experiments* 81a
- Figure 2.6** *Voltammogram showing the detector response to a 10 pmol/50 μ L glutamate standard as a function of the electrode potential*
85
- Figure 2.7** *Calibration curve for the detection of glutamate in a sample* 87
- Figure 2.8** *Calibration curve for the detection of dopamine in a sample* 90

Chapter 3: d-Amphetamine has contrasting effects in two subregions of the rat anterior cingulate cortex

- Figure 3.1** *Location of the two microdialysis probes in the anterior cingulate cortex in my microdialysis studies* 95
- Figure 3.2** *Time bins for statistical analysis of changes in extracellular glutamate after systemic (i.p.) injection of d-amphetamine*
99

Figure 3.3 *Time bins for statistical analysis of changes in extracellular glutamate after local infusion of d-amphetamine*

100

Figure 3.4 *The effects of local infusion (via retrodialysis) of increasing concentrations of d-amphetamine on glutamate ('GLU') efflux in the cACC or rACC of freely-moving rats*

103

Figure 3.5 *The effects of intraperitoneal (3 mg/kg) administration of d-amphetamine on glutamate ('GLU') efflux in the cACC or rACC of freely-moving rats*

106

Chapter 4: Contrasting effects of d-amphetamine on dopamine efflux and dopamine on glutamate efflux in two subregions of the anterior cingulate cortex

Figure 4.1 *Time bins for statistical analysis of changes in extracellular dopamine after local infusion of d-amphetamine*

118

Figure 4.2 *Time bins for statistical analysis of changes in extracellular dopamine after systemic (i.p.) injection of d-amphetamine*

118

Figure 4.3 *Time bins for statistical analysis of changes in extracellular glutamate after local infusion of dopamine solution*

119

Figure 4.4 *Effects of local infusion (via retrodialysis) of increasing concentrations of d-amphetamine on dopamine ('DA') efflux in cACC and rACC of freely-moving rats*

121

Figure 4.5 *Effects of intraperitoneal (3 mg/kg) administration of d-amphetamine or saline (1 ml/kg) on dopamine ('DA') efflux in the rACC of freely-moving rats*

124

Figure 4.6 *Effects of intraperitoneal administration of d-amphetamine (3 mg/kg) or saline (1 ml/kg) on dopamine ('DA') efflux in the cACC of freely-moving rats*

127

Figure 4.7 *Effects of local infusion of increasing concentrations of dopamine (via retrodialysis) on glutamate ('GLU') efflux in the cACC and rACC of freely-moving rats*

130

CHAPTER 5: The effect of pre-treatment with dopaminergic antagonists on the glutamate response to local infusion of d-amphetamine in the rostral anterior cingulate cortex

Figure 5.1 *Time bins for statistical analysis of changes in extracellular glutamate after local infusion of d-amphetamine*
145

Figure 5.2 *Effects of cumulative infusion of d-amphetamine on glutamate ('GLU') efflux in the rACC of freely-moving rats*
149

Figure 5.3 *Effects of haloperidol (0.1 mg/kg i.p.) injection on glutamate ('GLU') efflux in the rACC of freely-moving rats*
150

Figure 5.4 *Effects of cumulative infusion of d-amphetamine on glutamate ('GLU') efflux in the rACC of freely-moving rats*
152

Figure 5.5 *Effects of haloperidol (1 mg/kg i.p.) injection on glutamate ('GLU') efflux in the rACC of freely-moving rats*
153

Figure 5.6 *Effects of cumulative infusion of d-amphetamine on glutamate ('GLU') efflux in the rACC of freely-moving rats*
157

Figure 5.7 *Effects of SCH23390 (0.1 mg/kg i.p.) injection on glutamate ('GLU') efflux in the rACC of freely-moving rats*
158

Figure 5.8 *Effects of cumulative infusion of d-amphetamine on glutamate ('GLU') efflux in the rACC of freely-moving rats*
160

Figure 5.9 *Effects of SCH23390 (1 mg/kg i.p.) injection on glutamate ('GLU') efflux in the rACC of freely-moving rats*
161

CHAPTER 6: Effect of pre-treatment with the GLT-1 inhibitor dihydrokainate on the glutamate response to systemic administration of d-amphetamine in the rostral and caudal anterior cingulate cortices

Figure 6.1 *Timeline for experiments performed in Chapter 6*
174

Figure 6.2 *Time bins for statistical analysis of changes in extracellular glutamate after local infusion of DHK/Ringer's solution and systemic injection of d-amphetamine/saline*
175

Figure 6.3 *Effects of intraperitoneal administration of saline (1 ml/kg) on glutamate efflux in the cACC of freely-moving rats*
178

Figure 6.4 *Effects of intraperitoneal administration of d-amphetamine on glutamate efflux in the cACC of freely-moving rats* **180**

Figure 6.5 *Effects of intraperitoneal administration of saline on glutamate efflux in the rACC of freely-moving rats*
182

Figure 6.6 *Effects of intraperitoneal administration of d-amphetamine on glutamate efflux in the rACC of freely-moving rats* **183**

Figure 6.7 **190**

Figure 6.8 *Proposed scheme by which local infusion of DHK and systemic injection of d-amphetamine could cause a gradual, sustained decrease in glutamate efflux in the rACC*
193

Chapter 7: Effect of pre-treatment with the GLT-1 inhibitor dihydrokainate on the glutamate response to local infusion of d-amphetamine in the caudal and rostral anterior cingulate cortices

Figure 7.1 *Timeline for DHK experiment* **199**

Figure 7.2 *Time bins for statistical analysis of changes in extracellular glutamate after local infusion of DHK/Ringer's solution and local infusion of d-amphetamine*
199

Figure 7.3 *Effects of infusion of dihydrokainate (DHK) on glutamate ('GLU') efflux in the cACC and rACC of freely-moving rats* **201**

Figure 7.4 *Effects of cumulative infusion of d-amphetamine (d-AMP) on glutamate ('GLU') efflux in the cACC and rACC of freely-moving rats* **203**

Figure 7.5 *Effects of cumulative infusion of d-amphetamine ('d-AMP') on glutamate ('GLU') efflux in the caudal anterior cingulate cortex ('cACC') of freely-moving rats* **206**

Figure 7.6 *Effects of cumulative infusion of d-amphetamine ('d-AMP') on glutamate ('GLU') efflux in the rostral anterior cingulate cortex ('rACC') of freely-moving rats* **207**

Chapter 8: General discussion

Figure 8.1 *Summary diagrams showing the effects of different drug treatments on dopamine and glutamate efflux in the rat rostral and caudal anterior cingulate cortices* **221**

List of Tables

Chapter 1: General introduction

Table 1.1 *Summary of coordinates from microdialysis studies investigating glutamate efflux in the 'medial prefrontal cortex'* 39

Table 1.2 *Dopamine pathways in the rat brain* 41

Table 1.3 *In vitro K_i for the inhibition of monoamine uptake by d-amphetamine* 53

Table 1.4 *Effect of d-amphetamine on [3H]-NA, [3H]-5-HT, and [3H]-DA release from rat brain slices in vitro. Data show % release at different concentrations of d-amphetamine* 53

Chapter 2: Methods

Table 2.1 *Characteristics of chromatograms at different mobile phase pH* 82

Chapter 3: d-Amphetamine has contrasting effects in two subregions of the rat anterior cingulate cortex

Table 3.1 *Treatment groups for d-amphetamine administration* 98

Table 3.2 *Statistics generated from split-plot ANOVA summarising the effect of local infusion of d-amphetamine ('d-AMP') on glutamate efflux, in the cACC and the rACC* 104

Table 3.3 *Statistics generated from split-plot ANOVA summarising the effects of administration of d-amphetamine ('d-AMP') 3 mg/kg i.p. on glutamate efflux in the cACC and rACC* 107

Chapter 4: Contrasting effects of d-amphetamine on dopamine efflux and dopamine on glutamate efflux in two subregions of the anterior cingulate cortex

Table 4.1 *Statistics generated from split-plot ANOVA summarising the effects of local infusion of d-amphetamine on dopamine efflux in the cACC and rACC* 120

Table 4.2 *Statistics generated from split-plot ANOVA summarising the effects of administration of d-amphetamine ('d-AMP': 3 mg/kg) and saline (1 ml/kg) on dopamine efflux in the rACC*

125

Table 4.3 *Statistics generated from split-plot ANOVA summarising the effects of administration of d-amphetamine ('d-AMP': 3 mg/kg) or saline (1 ml/kg) on*

dopamine efflux in the cACC
128

Table 4.4 *Statistics generated from split-plot ANOVA summarising the effects of local infusion of dopamine solution in the cACC and the rACC* **131**

Table 4.5 *Summary of microdialysis studies investigating the effect of systemic d-amphetamine on dopamine efflux in the prefrontal cortex* **133**

Table 4.6 *The results of previous microdialysis studies investigating the effects of local infusion of d-amphetamine on dopamine efflux in the prefrontal cortex*
134

CHAPTER 5: The effect of pre-treatment with dopaminergic antagonists on the glutamate response to local infusion of d-amphetamine in the rostral anterior cingulate cortex

Table 5.1 *Treatment groups for haloperidol/saline administration. Rats were randomly assigned to one of three treatment groups for each experiment*
145

Table 5.2 *Treatment groups for SCH23390/saline administration. Rats were randomly assigned to one of three treatment groups for each experiment*
146

Table 5.3 *Statistics generated from split-plot ANOVA summarizing the effects of administration of d-amphetamine ('d-AMP') on glutamate efflux in the rACC* **151**

Table 5.4 *Statistics generated from split-plot ANOVA summarizing the effects of administration of haloperidol (0.1 mg/kg i.p.) on glutamate efflux in the rACC* **151**

Table 5.5 *Statistics generated from split-plot ANOVA summarizing the effects of administration of d-amphetamine ('d-AMP') on glutamate efflux in the rACC* **154**

Table 5.6 *Statistics generated from split-plot ANOVA summarizing the effects of administration of haloperidol (1 mg/kg i.p.) on glutamate efflux in the rACC* **154**

Table 5.7 *Statistics generated from split-plot ANOVA summarizing the effects of local infusion of d-amphetamine ('d-AMP': 10-100 μ M) on glutamate efflux in the rACC after pre-treatment with saline or SCH23390 (0.1 mg/kg i.p.)*
159

Table 5.8 *Statistics generated from split-plot ANOVA summarizing the effects of administration of SCH23390 (0.1 mg/kg i.p.) on glutamate efflux in the rACC* **159**

Table 5.9 *Statistics generated from split-plot ANOVA summarizing the effects of local infusion of d-amphetamine ('d-AMP': 10-100 μ M) on glutamate efflux in the rACC after pre-treatment with saline or SCH23390 (1 mg/kg i.p.)* **162**

Table 5.10 *Statistics generated from split-plot ANOVA summarizing the effects of administration of SCH23390 (1 mg/kg i.p.) on glutamate efflux in the rACC* **162**

CHAPTER 6: Effect of pre-treatment with the GLT-1 inhibitor dihydrokainate on the glutamate response to systemic administration of *d*-amphetamine in the rostral and caudal anterior cingulate cortices

Table 6.1 *Drug treatment groups* **174**

Table 6.2 *Statistics generated from split-plot ANOVA summarizing the effects of administration of saline on glutamate efflux in the cACC* **179**

Table 6.3 *Statistics generated from split-plot ANOVA summarizing the effects of administration of *d*-AMP on glutamate efflux in the cACC* **179**

Table 6.4 *Statistics generated from split-plot ANOVA summarizing the effects of systemic administration of saline on glutamate efflux in the rACC*
184

Table 6.5 *Statistics generated from split-plot ANOVA summarizing the effects of systemic administration of *d*-amphetamine on glutamate efflux in the rACC*
184

Chapter 7: Effect of pre-treatment with the GLT-1 inhibitor dihydrokainate on the glutamate response to local infusion of *d*-amphetamine in the caudal and rostral anterior cingulate cortices

Table 7.1 *Drug treatment groups* **198**

Table 7.2 *Statistics generated from split-plot ANOVA summarizing the effects of local infusion of DHK (1mM) on glutamate efflux in the cACC and rACC* **202**

Table 7.3 *Statistics generated from split-plot ANOVA summarizing the effects of local infusion of *d*-amphetamine on glutamate efflux in the cACC and rACC* **204**

Table 7.4 *Statistics generated from split-plot ANOVA summarising the effects of local infusion of *d*-amphetamine + DHK (1 mM) on glutamate efflux in the cACC and rACC* **208**

Abbreviations

AC adenylate cyclase

ACC anterior cingulate cortex

ACh acetylcholine

AMPA α -amino-3-hydroxy-5-methylisoxazole-4-propionic acid

ANOVA analysis of variance

ATP adenosine triphosphate

[³H] tritium

cAMP cyclic adenosine monophosphate

CCK cholecystokinin

CNS central nervous system

DA dopamine

DAT dopamine transporter

DNA deoxyribonucleic acid

DOPAC 3,4-dihydroxyphenylacetic acid

EAA excitatory amino acid

ECD electrochemical detection

F-CPA formalin-induced conditioned place avoidance

GABA gamma amino butyric acid

g gram

G_i inhibitory G-protein

GLU glutamate

h hour

HPLC high performance liquid chromatography

HVA homovanillic acid

i.p. intraperitoneal

K_i inhibition constant

L litre

m metre

M molar

mAChR muscarinic acetylcholine receptor

mGluR metabotropic glutamate receptor

min minute

mol moles
mRNA messenger ribonucleic acid
N sample size
NA noradrenaline
NET norepinephrine transporter
NMDA N-methyl-D-aspartate
PFC prefrontal cortex
ROS reactive oxygen species
SERT serotonin transporter
TTX tetrodotoxin
V volt
VMAT vesicular monoamine transporter
VTA ventral tegmental area

Prefixes

m milli ($\times 10^{-3}$)
 μ micro ($\times 10^{-6}$)
n nano ($\times 10^{-9}$)
p pico ($\times 10^{-12}$)
f femto ($\times 10^{-15}$)

Chapter 1

1.0/ General Introduction

Administration of the psychostimulant drug *d*-amphetamine is associated with increased motor arousal, psychosis and analgesia. Its influences on mood and behaviour are thought to be due to its effects on catecholamine transmission in the brain, especially the prefrontal cortex. In agreement with this, abnormal dopaminergic neurotransmission in the prefrontal cortex is associated with pathological brain states such as schizophrenia and depression.

Extensive evidence also points to disrupted glutamatergic neurotransmission in the prefrontal cortex as a potentially important factor in psychiatric disorders (e.g. Moghaddam, 2002). However, hardly any studies have investigated whether, or how, *d*-amphetamine modifies glutamate transmission in the prefrontal cortex.

d-Amphetamine has been a focus of research for many years by this laboratory and its effects on monoamines have been widely studied. As will be discussed in detail in later sections, a few published studies found that *d*-amphetamine increased glutamate in the prefrontal cortex, while other laboratories reported no effect at all. The inconsistencies of these reports could be due to the study of different subregions of the prefrontal cortex, broadly referred to as the 'prefrontal cortex'. The anterior cingulate cortex (ACC) is a subdivision of the prefrontal cortex. The dorso-ventral aspect of this subregion has been extensively studied. However, no systematic study of the rostro-caudal plane has been so far carried out, despite clear demarcation of function between the rostral and caudal ACC. Here, I investigated the effects of *d*-amphetamine on glutamate in more detail by comparing regulation of glutamatergic

neurotransmission in two subregions of the rat anterior cingulate cortex – the rostral anterior cingulate cortex (rACC) and caudal anterior cingulate cortex (cACC). Since the source and density of dopaminergic terminals varies in different regions of the ACC, this could have a profound influence on the effects of *d*-amphetamine on glutamatergic transmission. I therefore characterised the role of dopamine in regulation of glutamatergic transmission in these two subregions.

The majority of published studies of glutamate are concerned with changes in fast synaptic transmission (in the order of milliseconds). However, the changes in glutamatergic transmission associated with pathological brain states are long-lasting, and so prolonged, stable changes in glutamate are of interest also. It is now acknowledged that little, if any, extracellular glutamate is derived from neuronal release. In fact, *d*-amphetamine causes impulse-independent release of monoamines via retrotransport on neuronal transporters, which resemble glial glutamate transporters (EAAT1/GLT-1). A final objective of this study was to test whether the glutamate response to *d*-amphetamine in the rACC and cACC is modified by functional blockade of GLT-1.

1.1/ THE PREFRONTAL CORTEX

The prefrontal cortex (Figure 1.1) is involved in a range of behavioural control processes but is particularly implicated in working memory processes. Working memory is defined as the ability to retain and manipulate mnemonic information to guide ongoing behaviour (Baddeley, 1986). Two key aspects of working memory have been characterised. One important component is the short-term storage of trial-unique information, whereby information about specific stimuli is retained briefly in a

short-term memory buffer and discarded when the appropriate response has been executed. Another element of working memory involves 'executive functions', which include supervisory processes for the temporal organisation of behaviour and the use of short-term memory to plan a sequence of forthcoming responses.

1.1.1/ Anatomical delineation of the prefrontal cortex

The prefrontal cortex was originally defined as the region of the cortex with strong reciprocal connections with the mediodorsal nucleus (MD) of the thalamus (Kolb, 1984). However, in all species studied, the frontal cortical areas that receive mediodorsal inputs receive, in addition, fibres from other specific thalamic nuclei, in particular from the anterior parts of the ventral complex of the thalamus (Conde *et al.*, 1990; Musil and Olson, 1988). This anatomical feature alone cannot provide unequivocal criteria to distinguish the prefrontal cortex from the more posterior parts of the frontal lobe. Another anatomical characteristic suggested to be unique to the prefrontal cortex is the input of dopaminergic fibres from the ventral mesencephalon. However, this dopaminergic innervation does not appear to be restricted to the prefrontal cortex (Klitenick *et al.*, 1992).

The prefrontal cortex comprises several cytoarchitectonic subdivisions. The first is the medial frontal division, which can be subdivided into a dorsal region that includes precentral (PrC) and anterior cingulate (ACC) cortices and a ventral component that includes the prelimbic (PrL, also known as Cg3), infralimbic (IL) and medial orbital (MO) cortices. The second is a lateral region that includes the dorsal and ventral agranular insular (AID, AIV) and lateral orbital (LO) cortices. Finally,

there exists a ventral region, which encompasses the ventral orbital (VO) and ventral lateral orbital (VLO) cortices (Paxinos and Watson, 2005).

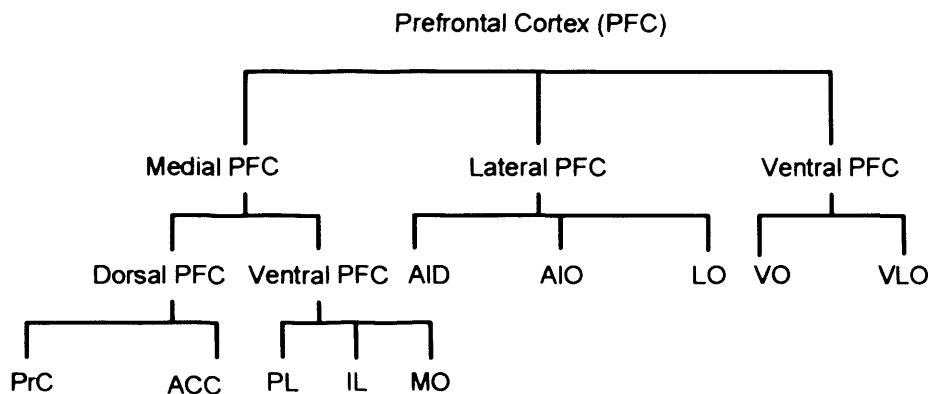


Figure 1.1 *Anatomical delineation of the prefrontal cortex.* Abbreviations AID: dorsal agranular insular cortex; AIV: ventral agranular insular cortex; LO: lateral orbital cortex; VO: ventral orbital cortex; VLO: ventral lateral orbital cortex; PrC: precentral cortex; ACC: anterior cingulate cortex; PL; prelimbic cortex; IL: infralimbic cortex; MO: medial orbital cortex.

1.1.2/ *The medial prefrontal cortex*

The medial prefrontal cortex is a component of the motive circuit involved in reward-orienting behaviours, such as those associated with drug addiction. It can be further characterised as five subdivisions: the infralimbic, prelimbic (area Cg3 of the anterior cingulate cortex), dorsal and ventral anterior cingulate (areas Cg1 and Cg2 of the anterior cingulate cortex), medial precentral and medial orbital cortices (Paxinos and Watson, 2005, see Figure 1.1).

1.1.3/ *The anterior cingulate cortex – structure and function*

In 2005, Jones *et al.* determined the topographical and laminar characteristics of intrinsic cingulate connections in the rat (see Figure 1.2). They found that the

cingulate cortices can be subdivided into at least 13 regions on the basis of the combination of cytoarchitectonic characteristics and the pattern of the intrinsic connections.

Figure 1.2 *Midsaggital view of the rat cingulate cortex.* Abbreviations ACd: dorsal anterior cingulate cortex; ACv: ventral anterior cingulate cortex; PL: Prelimbic cortex; IL: infralimbic cortex; RSd: dorsal retrosplenial cortex; RSv(a and b): ventral retrosplenial cortex (adapted from Jones *et al.*, 2005).

Furthermore, imaging studies of the human brain suggest that the anterior cingulate cortex can be divided into three functional zones (Yücel *et al.*, 2003) –

- (1) A rostral affective/visceral region (aff-ACC), located inferior and anterior to the genu of the corpus callosum. This has extensive reciprocal connections with the orbitofrontal cortex and the amygdala. This region is responsible for the regulation of autonomic and endocrine functions and is also involved in higher-order functions, such as conditioned emotional learning, assessment of motivational content and assigning emotional valence to internal and external stimuli.
- (2) A dorsal cognitive division (cog-ACC) lying superior to the callosum. This has extensive reciprocal connections with other frontal and temporal areas, especially the dorsolateral prefrontal cortex (equivalent to the medial

prefrontal cortex of the rat) and hippocampus. This region is involved with response selection and cognitively-demanding information processing.

- (3) A caudal motor region (mot-ACC) deep within the cingulate sulcus. This has extensive connections with the primary/supplementary motor and parietal regions and plays a role in premotor/skeletomotor function.

These observations in humans have been replicated in animal studies. In 2001, Johansen *et al.* examined the effects of excitotoxin-induced lesions of the ACC on the expression of both formalin-induced nociceptive behaviours and formalin-induced conditioned place avoidance. Lesions were induced in either the rostral or caudal region of the ACC (rACC or cACC, respectively). The rACC preferentially receives nociceptive input, while the cACC receives comparatively little (Berendse and Groenewegen, 1991). Lesions of neither the rACC nor the cACC affected the acute nociceptive response to formalin injection. When hind-paw injection of formalin was paired with a particular compartment in the place-conditioning apparatus, rats with sham lesions of the ACC spent less time in this compartment on the post-conditioning test day as compared with the pre-conditioning test day i.e. formalin-induced conditioned place avoidance (F-CPA) was produced. F-CPA was reduced by lesions of the rACC, but not the cACC, suggesting that the rACC encodes, at least in part, the affective component of pain in rats. The more caudal regions of the ACC are involved in motor planning as a secondary response to nociceptor stimulation (Vogt *et al.*, 1996).

These observations were confirmed in a subsequent study, where the effects of excitotoxic lesions of the rostral anterior cingulate cortex (rACC) or caudal anterior cingulate cortex (cACC) in rats on the expression of formalin-induced conditioned

place avoidance were examined (Johansen *et al.*, 2004). Destruction of neurones originating from the rACC (but not the cACC) reduced formalin-conditioned place avoidance (F-CPA) without reducing acute pain-related behaviours. Lesions of the rACC decrease the aversive aspect of the response to a nociceptive-activating stimulus, therefore decreasing the animals' motivation to avoid the compartment in which the stimulation was produced.

Recently, another study has investigated the involvement of the rACC in the consolidation of inhibitory avoidance memory (Malin *et al.*, 2007). Animals were tested for active avoidance of a test environment in which they had previously experienced an unescapable footshock. Bilateral infusion of the mAChR agonist oxotremorine into the rACC post-training enhanced inhibitory avoidance retention, but not when administered into the immediately adjacent cACC. This study therefore suggested that the anterior cingulate cortex is involved in memory consolidation for inhibitory avoidance training, and that this involvement is restricted to the rACC.

Microdialysis studies in the rat also point at a role for the rACC in nociceptive processing. In one such study, the carrageenan model of inflammatory pain in rats was used to study the effect of pain on the release of cholecystokinin-like immunoreactivity (CCK-LI) in the rACC. In animals with carrageenan-induced monoarthritis, both basal and potassium induced release of CCK-LI were significantly increased compared to controls (Erel *et al.*, 2004). This result was confirmed by a later study (Heilborn *et al.*, 2007).

All these studies consistently point to a clear demarcation of function of the rostral and caudal anterior cingulate cortices. To date, no authors have tried to elucidate the neurochemical processes underlying such differences, despite these

being of key importance when examining the role of the anterior cingulate cortex in mood and behaviour.

1.2/ GLUTAMATE IN THE ANTERIOR CINGULATE CORTEX

Glutamate is the main excitatory neurotransmitter in the brain, giving rise to excitatory postsynaptic potentials when it interacts with its receptors. This is in contrast to compounds such as the monoamines (dopamine and noradrenaline), which have a modulatory effect through their action on G-protein-coupled receptors, and do not cause inhibitory or excitatory postsynaptic potentials (Fillenz, 2005). Glutamate produces its effects in the brain through actions at both ionotropic and metabotropic receptors.

The ionotropic receptors include the N-methyl-D-aspartate (NMDA), α -amino-3-hydroxy-5-methylisoxazole-4-propionic acid (AMPA) and kainate receptors (Bigge, 1999). The ionotropic glutamate receptors are ligand-gated ion channels with a pentameric structure. NMDA receptors are assembled from 2 types of subunit, NR1 and NR2, which can exist in different isoforms and splice variants, giving rise to many receptor isoforms in the brain. The AMPA and kainate receptors are formed from GluR₁₋₇ and KA_{1,2} subunits, respectively, which are distinct from NMDA receptor subunits, despite being closely related.

The metabotropic glutamate receptors are classified into three groups (for review see Pin and Duvoisin, 1995). Group I metabotropic receptors (including mGluR1 and mGluR5) are coupled to activation of phospholipase C, which hydrolyses phosphoinositide phospholipids in the cell plasma membrane. These receptors can either be excitatory, increasing conductance and causing more glutamate

to be released from the presynaptic cell, or inhibitory. Groups II (mGluR2 and mGluR3) and III (mGluRs 4, 6, 7, and 8) prevent the formation of cyclic adenosine monophosphate (cAMP) by activating the G-protein G_i , which inhibits adenylate cyclase (AC). Receptors in groups II and III reduce the activity of synaptic potentials, both inhibitory and excitatory, in the cortex (Chu and Hablitz, 2000). The metabotropic glutamate receptors are monomeric G protein-coupled receptors, linked to second messengers.

1.2.1 / Regulation of extracellular glutamate by glial cells

Glial cells are non-neuronal cells that provide support and nutrition, maintain homeostasis, form myelin, and participate in signal transmission within the central nervous system (for review, see Haydon, 2001). Astrocytes are the most abundant glial cells within the brain and have an important role in regulating the external environment of the brain. For example, they participate in the removal of excess ions, such as potassium and recycle neurotransmitters during synaptic transmission (Volterra and Steinhauser, 2004).

One well-characterised function of astrocytes is the uptake of glutamate released into the extracellular space during synaptic transmission, thus terminating its action and preventing the process of excitotoxicity. Over-activation of NMDA receptors by excess exogenous glutamate leads to an increased influx of Na^+ and Ca^{2+} ions into neurones (for review see Choi, 1992). Accumulation of intracellular Ca^{2+} ions leads to activation of numerous enzymes, such as phospholipase C, leading to degradation of the cellular membrane and release of endonucleases, which break down DNA. The generation of reactive oxygen species (ROS), in combination with

free radicals leads to lipid peroxidation, cellular lysis and eventual demise of the cell. ROS inhibit the activity of glutamate transporters, therefore leading to increased extracellular levels of glutamate, increased stimulation of NMDA receptors and further production of ROS. This feed-forward cycle accelerates cell death.

Since synapses do not possess the means for enzymatically degrading glutamate, glutamate transporters are crucial for the termination of glutamatergic neurotransmission and prevention of excitotoxicity (Sonnewald *et al.*, 2002). A family of high-affinity glutamate transporters responsible for the clearance of glutamate from the synaptic cleft has evolved. These transporters are expressed by many cell types in the central nervous system, including astrocytes, neurons, oligodendrocytes, microglia and endothelia (Anderson and Swanson, 1999). Both Na⁺-dependent and -independent glutamate uptake systems exist, but Na⁺-independent transport accounts for only a small proportion of the total glutamate uptake (Anderson and Swanson, 2000). At least five Na⁺-dependent glutamate transporters have been cloned using different approaches (Kanai and Hediger, 2003). The standard nomenclature for these is EAATs 1-5, but many authors also use other names. EAAT1 is also known as GLAST, while EAAT2 is commonly called GLT-1 (see Alexander *et al.*, 2007 for review of nomenclature). EAAT1 (GLAST) and EAAT2 (GLT-1) are localized to astrocytes, with GLAST being predominantly a cerebellar transporter (Storck *et al.*, 1992) and GLT-1 localised to the cortex (Pines *et al.*, 1992). EAAT3 is localized to neurons throughout the CNS (Berger and Hediger, 1998, Kanai *et al.*, 1995a, Kanai *et al.*, 1995b, Rothstein *et al.*, 1994), whereas EAAT4 is largely restricted to cerebellar Purkinje cells (Nagao *et al.*, 1997). EAAT5 has been localized exclusively to the retina (Arriza *et al.*, 1997). The transport of glutamate is driven by the electrochemical gradient of Na⁺ with a stoichiometry of

three Na⁺ ions cotransported with one glutamate. There is also cotransport of a proton or the counter-transport of a hydroxyl ion (or HCO₃⁻). The existence of glutamate-activated Cl⁻ flux distinct from excitatory amino acid (EAA) transport has been proposed to counteract Na⁺-induced cellular depolarization that would otherwise decrease EAA transport.

Rothstein *et al.*, (1996) used chronic antisense oligonucleotide treatment to knock down the genes for the astrocytic glutamate transporters GLAST and GLT-1. Inactivation of the astrocytic glutamate transporters increased extracellular glutamate in the striatum, and was associated with neurodegeneration characteristic of excitotoxicity and progressive paralysis, demonstrating the importance of astrocytic glutamate transporters in controlling extracellular glutamate. Tanaka *et al.*, (1997) generated a GLT-1 knockout mouse, which shows spontaneous epileptic activity and increased susceptibility to cortical injury. Glutamate uptake in cortical crude synaptosomes of mutant mice was decreased to 5.8 % of that in synaptosomes from wild-type mice (Tanaka *et al.*, 1997). This suggests that, of the glutamate transporters, GLT-1 accounts for greater than 90 % of glutamate transport activity in the forebrain, highlighting the key role for this transporter in the regulation of extracellular glutamate.

1.3/ MICRODIALYSIS OF GLUTAMATE

In 1910, Legendre and Pieron observed that a sleep factor could be collected from the cerebral ventricles and this led to a whole host of studies devoted to the analysis of neurotransmitters released from the brain during a physiological event. Microdialysis is one such method used for monitoring the extracellular concentration

of neurotransmitter in the brain. A concentric probe, originally modelled on a capillary, is implanted into a selected brain area. The microdialysis probe consists of a semipermeable membrane surrounding two fine cannulae, through which fluid flows into and out of the portion containing the semipermeable membrane. Compounds in the extracellular space reach the perfusion fluid by diffusion (see: Chapter 2 for more details). The most widely studied classes of factors are the monoamines and their metabolites (e.g. Géranton *et al.*, 2003, Wortley *et al.*, 1999). The monoamines are released into the extracellular space and their actions are diffuse and prolonged. Their presence in the extracellular space makes them easily accessible to measurement by microdialysis. They are sensitive to Na⁺- and Ca²⁺-channel blockers, confirming that they are released from nerve terminals and represent overflow from the synaptic cleft (Westerink, 1995). The microdialysis technique has also been successfully applied to study glutamate in the brain extracellular fluid (e.g. see an early study by Benveniste *et al.*, 1984). However, care must be taken when interpreting changes in extracellular glutamate as measured by microdialysis (see next section).

1.3.1/ *Microdialysis of glutamate – what does it signify?*

The source of both drug-evoked and basal glutamate efflux, as measured by microdialysis, has long been a matter of contention. Unlike neuromodulators, such as dopamine, glutamate is released into the extracellular space by a variety of sources. In 2000, Zilberter used dual-cell recordings to measure the activity of neurones in layers 2 and 3 of the rat neocortex. They found that glutamate was released from pyramidal cell dendrites into the extracellular space. Other neuronal sources of glutamate include the terminals of cortico-cortical pyramidal cells, thalamocortical neurones and contralateral (corticofugal) projections. Glutamate is also released into

the extracellular space by non-neuronal sources, namely glial cells. This can either be via Ca^{2+} -independent release, through the cystine-glutamate antiporter, present in the glial cell membrane (Baker *et al.*, 2002) or via Ca^{2+} -dependent release (Montana *et al.*, 2006).

Microdialysis is frequently used to study changes in glutamate concentration in the extracellular space during pharmacological or behavioural activation. These fluctuations in glutamate concentration are often assumed to represent the synaptic release of glutamate, but the presence of glutamate in high concentrations doesn't necessarily mean that it has been released from nerve terminals (Herrera-Marschitz *et al.*, 1996, Timmerman and Westerink, 1997). This contrasts with neurotransmitters such as dopamine and noradrenaline (Del Arco *et al.*, 2003). Monoamines can be distinguished from the 'classical' neurotransmitters (glutamate and GABA), since they do not give rise to excitatory and inhibitory postsynaptic potentials. Rather, they act on G-protein-coupled receptors, which activate enzymes that give rise to second messengers. The actions of monoamines are diffuse and prolonged as they are released into the extracellular compartment, making them accessible to measurement by microdialysis. The extracellular levels of monoamines such as dopamine and noradrenaline, as measured by microdialysis, are reduced by the addition of drugs such as TTX and Ca^{2+} channel blockers, confirming that they are of neuronal origin (Westerink, 1995). Glutamate is present as a metabolic intermediate as well as being found in neurones and glial cells and greater than 60 % of extracellular glutamate found in the brain has a nontransmitter origin (Fonnum, 1984). The significance of changes in dialysate concentrations of glutamate is still controversial.

To investigate neuronal vs. non-neuronal sources of basal dialysate glutamate, two criteria can be applied – involvement of nerve impulses and Ca^{2+} -dependence (del

Arco *et al.*, 2003, Timmerman and Westerink, 1997). In one such study, several criteria were applied to ascertain the neuronal origin of glutamate and other neurotransmitters quantified by microdialysis (Herrera-Marschitz *et al.*, 1996). These were sensitivity to

- K⁺-depolarisation
- Na⁺-channel blockade
- Removal of extracellular Ca²⁺
- Depletion of synaptic vesicles by local administration of the selective neurotoxin α -latrotoxin.

Dopamine fulfilled all these criteria. However, glutamate levels in the brain regions of interest (neostriatum, substantia nigra, frontoparietal cortex) were not greatly affected by K⁺-depolarisation, and were paradoxically increased by TTX infusion and removal of Ca²⁺ from the infusion medium, arguing against a neuronal origin for basal extracellular glutamate. These data correlate well with neuroanatomical evidence showing that the neuronal compartment of dopamine (open synapse), but not glutamate (closed synapse), is linked to the extracellular space (Zoli and Agnati, 1996). Dopamine is released far from postsynaptic sites and there is a low density of dopamine transporters located close to the synaptic cleft so synaptic dopamine diffuses through the extracellular space to be sampled by the microdialysis probe. However, a significant diffusion of glutamate from the synaptic cleft to the extracellular space is unlikely due to the high density of astrocytic glutamate transporters around the synapse (Del Arco *et al.*, 2003). Therefore, a neuronal origin for basal extracellular glutamate cannot be assumed.

Baker *et al.*, (2002) investigated the origin and function of *in vivo* non-synaptic glutamate in the striatum in more detail. The cystine-glutamate antiporter is a membrane-bound Na⁺-independent anionic amino acid transporter, which exchanges extracellular cystine for intracellular glutamate (Danbolt, 2001). The transporter is ubiquitously distributed on cells throughout the body, although, in the brain, it may be preferentially located on glia (Pow, 2001). Blockade of glutamate release from the cystine-glutamate antiporter (using homocysteic acid (0-50 μM)) produced a decrease (60 %) in extrasynaptic glutamate levels in the striatum, whereas blockade of voltage-dependent Na⁺ and Ca²⁺ channels produced relatively minimal changes. These data indicate that the primary source of *in vivo* non-synaptic glutamate in the striatum arises from non-vesicular glutamate release by the cystine-glutamate antiporter. The activity of the cystine-glutamate antiporter is negatively regulated by group II metabotropic glutamate receptors (mGluR2/3) via a cAMP-dependent protein kinase mechanism.

In contrast to subcortical structures (Baker *et al.*, 2002, 2003), basal glutamate levels in the prefrontal cortex are not affected by blockade of the cystine-glutamate antiporter (Melendez *et al.*, 2005). However, Melendez *et al.* (2005) demonstrated that inhibition of the cystine-glutamate antiporter by (S)-4-carboxyphenylglycine (CPG) completely reversed the increase in glutamate efflux elicited by the Na⁺-dependent EAAT1-3 blocker DL-threo-β-benzyloxyaspartate (TBOA). This suggests that normally, Na⁺-dependent transporters clear glutamate released by the cystine-glutamate antiporter. When EAATs 1-3 are blocked, glutamate released from the antiporter is immediately apparent, suggesting that it does indeed contribute to basal extracellular glutamate levels. The coordinates for prefrontal cortex used by

Melendez *et al.* correspond closely to the coordinates used for the rostral part of the anterior cingulate cortex in my study (AP +2.7 ML +1.1 DV -2.0).

The origin of changes in glutamate efflux in response to physiological or pharmacological stimuli has also been a matter of contention. When an action potential reaches an excitatory synapse, glutamate is released with a latency of microseconds, reaches a high concentration in the synaptic cleft and gives rise to a synaptic potential with a duration of three milliseconds. The action of glutamate is terminated by a very efficient uptake mechanism (Kanai and Hediger, 2003, Chapter 1, section 1.2). The slow time course of stimulated glutamate release and its TTX insensitivity argue against a neuronal origin, suggesting that dialysate glutamate is not a measure of neuronal release.

A few previous microdialysis studies show increased extracellular glutamate concentrations produced by specific drugs, which can be prevented by TTX and are dependent on Ca^{2+} in the perfusion medium, although basal concentrations are not. In one such study, intracerebral microdialysis was used to study the effects of systemic cocaine (7.5 – 30 mg/kg) on glutamate efflux in the nucleus accumbens (Smith *et al.*, 1995). The highest dose of cocaine tested produced a 4-fold increase in dialysate glutamate levels, which was attenuated by local infusion of Ca^{2+} -free buffer and TTX. These findings have been interpreted as reflecting the neuronal release of glutamate. Glutamate could be diffusing from the synaptic cleft to be sampled by the microdialysis probe ('spill-over'; Del Arco *et al.*, 2003).

Astrocytes are able to release glutamate into the extracellular space (Carmignoto, 2000). Furthermore, neuronal exocytotic glutamate release may induce an astrocytic glutamate release into the extracellular space, which is therefore TTX-

and Ca^{2+} -sensitive. The release of glutamate from astrocytes is preceded by an increase of intracellular Ca^{2+} that can be propagated through the astrocyte network via gap junctions, making up calcium waves (Carmignoto, 2000), suggesting that glutamate is released by astrocytes far away from the initial stimulation point. This amplifies the astrocytic release of glutamate, and more glutamate accumulates in the extracellular compartment. The role of astrocytes in increased extracellular glutamate has been suggested by previous microdialysis studies. For example, Miele *et al* in 1996, found an increase in glutamate efflux during induced grooming (initiated by dropping water from a pipette onto the rat's nose). This increase was unaffected by local infusion of TTX. The authors speculated about the involvement of astrocytes in the changes in extracellular glutamate.

Recently, communication modes other than synaptic transmission have been proposed to exist in the central nervous system, suggesting that the classical view of communication processes should be enlarged. The terms 'wiring transmission' and 'volume transmission' were suggested as the primary conceptual categories of a systematisation of intercellular communication in the CNS (Zoli and Agnati, 1996). Wiring transmission is the intercellular communication characterised by a single 'transmission channel' made by cellular (neuronal or glial) structures and with a region of discontinuity not larger than a synaptic cleft. Conversely, volume transmission is the intercellular communication characterised by diffusion of chemical signals in a 3-dimensional fashion in the extracellular fluid (Zoli and Agnati, 1996).

Del Arco *et al* (2003) have suggested that the glutamate monitored in microdialysis studies could be acting as volume transmission signals. Glutamate diffuses from its release site to modulate the activity of neuronal-glial assemblies

surrounding the microdialysis probe (see: Figure 1.3). Glutamate in the region of the probe could preferentially activate extrasynaptic receptors to play a role in neurotransmission. There is evidence for the existence of extrasynaptic glutamate receptors (Sattler *et al.*, 2000). These receptors are localized on their own glutamate synapses (autoreceptors), on astrocytes (Gracy and Pickel, 1996) and other neurotransmitter system/ terminals such as GABAergic interneurons (heteroreceptors; Semyanov and Kullman, 2000). Much evidence has accumulated supporting the modulation of neurotransmission by extracellular glutamate through extrasynaptic receptors. In one such study, the uptake of glutamate in the striatum and nucleus accumbens was blocked by infusion of L-trans-pyrroloidine-3,4-dicarboxylic acid (PDC: a selective blocker of high-affinity glutamate uptake) through a microdialysis probe (Segovia *et al.*, 1997, 1999). Perfusion of PDC increased extracellular dopamine and these increases were correlated with an increase of extracellular glutamate. Furthermore, the increased dopamine efflux was blocked by specific ionotropic glutamatergic antagonists. No synaptic contacts exist between glutamatergic and dopaminergic terminals in these areas (Sesack and Pickel, 1992). The stimulating effects of extracellular glutamate on dopamine could be mediated through extrasynaptic receptors located on dopaminergic terminals.

1.3.2/ Microdialysis studies in the prefrontal cortex

A few microdialysis studies have demonstrated increased glutamate in different subregions of the rat medial prefrontal cortex after both local and systemic administration of *d*-amphetamine (Del Arco *et al.*, 1998, Reid *et al.*, 1997). However, *d*-amphetamine is also reported to have no effect on extracellular glutamate in the medial prefrontal cortex in other studies (Shoblock *et al.*, 2003). These inconsistencies

could be due to the use of different coordinates for subregions broadly referred to as the 'prefrontal cortex'. The rat medial prefrontal cortex extends over quite a large area of the brain and is comprised of many distinct subregions (see section 1.1). Table 1.1 summarises the wide variety of coordinates used by previous authors when referring to the medial prefrontal cortex. It is clear from this table that studies investigating the medial prefrontal cortex more systemically need to be undertaken.

Table 1.1 *Summary of microdialysis studies investigating glutamate efflux in the rat 'medial prefrontal cortex'*

Reference	Coordinates for mPFC
Reid <i>et al.</i> , 1997	AP +2.5 ML +0.6 DV-4.6
Del Arco <i>et al.</i> , 1998	AP+3.6 ML±0.9 DV-0.5
Abekawa <i>et al.</i> , 2000	AP+2.7 ML±1.4 DV-6.5
Shoblock <i>et al.</i> , 2003	AP+3.2 ML+0.1 DV-6.1
Harte and O'Connor, 2004	AP+2.7 ML+0.8 DV-1.8

Figure 1.3 *Scheme depicting the position of the microdialysis probe in relation to the glutamatergic synapse.*

Changes of extracellular glutamate are thought to be an index of the role these neurotransmitters play as volume transmission signals in the brain. Synaptic glutamate acts on extrasynaptic glutamatergic receptors located on neurones and astrocytes (•). The increase of Ca^{2+} in astrocytes causes them to release glutamate. Other neurotransmitters such as DA, NA and ACh could activate non-glutamatergic receptors (•) located on astrocytes and induce the release of glutamate. Glutamate then diffuses through the extracellular space to reach the microdialysis probe. This extracellular glutamate also modulates the activity of glial-neurone assemblies surrounding the microdialysis probe (adapted from Del Arco *et al.*, 2003).

1.4/ DOPAMINE AFFERENTS TO THE MEDIAL PREFRONTAL CORTEX

1.4.1/ *Neuroanatomy of dopamine – pathways in the rat brain*

These have been mapped using the formaldehyde (Falck *et al.*, 1962) and glyoxylic acid (Lindvall and Bjorklund, 1974) fluorescence techniques. Table 1.2 illustrates the four main dopamine pathways in the rat brain – the nigrostriatal pathway, the mesocortical pathway, the mesolimbic pathway and the tuberoinfundibular pathway.

Table 1.2 *Dopamine pathways in the rat brain*

	Cells of origin	Projections
(1) Nigrostriatal pathway	Substantia nigra	Dorsal striatum
(2) Mesocortical pathway	Ventral tegmental area	Cortex (frontal lobes)
(3) Mesolimbic pathway	Ventral tegmental area	Ventral striatum (Nucleus Accumbens)
(4) Tuberoinfundibular pathway	Mediobasal hypothalamus	Infundibular region

The system of interest to this thesis is the mesocortical dopamine pathway, projecting from the ventral tegmental area to the cortex (including the medial prefrontal cortex).

This pathway is essential for the normal cognitive function of the dorsolateral

prefrontal cortex and is thought to be involved in motivation and the emotional response.

Dopamine exerts its effects in the brain by acting through two families of receptors. These include the D₁-like (including the D₁- and D₅- receptors) and D₂-like (including the D₂-, D₃- and D₄- receptors). All are metabotropic receptors, coupled to the stimulation (D₁-like family) and inhibition (D₂-like family) of adenylyl cyclase activity. In addition, activation of D₂-like receptors opens K⁺-channels and blocks voltage-sensitive Ca²⁺-channels. Receptor binding studies have confirmed the presence of both D₁- and D₂-like receptors in the medial prefrontal cortex of the rat (Vincent *et al.*, 1993). D₁-like receptors are thought to be located preferentially on nonpyramidal neurons (i.e. interneurons) while D₂-like receptors are localized on both pyramidal and nonpyramidal neurons.

Studies in the primate prefrontal cortex have revealed that the D₁-like receptors are far more abundant in this brain region than D₂-like receptors (approximately 20-fold) (Lidow *et al.*, 1991). The distal dendrites and spines of pyramidal cells are most prominently labeled by antisera against the D₁-like receptor (Smiley *et al.*, 1994). The D₁-like receptor is also present postsynaptically to GABAergic interneurons, particularly those neurons providing the strongest inhibitory input to the perisomatic region of cortical pyramidal cells (Muly *et al.*, 1998). Specific antibodies have been produced against individual D₁-like receptors, allowing their distribution and subcellular localization in the primate prefrontal cortex to be mapped. Ultrastructural studies have revealed that D₁-like immunoreactivity is prevalent in dendritic spines (Bergson *et al.*, 1995) while the D₅ receptor is localized on the dendritic shafts of pyramidal neurons (Bergson *et al.*, 1995).

The distribution of D₂-like receptors has also been extensively mapped in the primate prefrontal cortex. D₂-like receptors have been localized to both pre- and post-synaptic structures (Negyessy and Goldman-Rakic, 2005). Postsynaptic D₂-like receptors were detected in the spines of glutamatergic pyramidal neurons as well as GABAergic interneurons of the prefrontal cortex. The study also revealed the localization of D₂-like receptors in axon terminals, consistent with the autoreceptor function of D₂-like receptors in the prefrontal cortex. These studies indicate species differences in the distribution of dopamine receptors between rats and primates.

Both D₁- and D₂-like receptors have also been localized to glial cells at least in the basal ganglia. The expression of dopamine receptors was examined *in vitro* using cultured astrocytes from the rat basal ganglia (Miyazaki *et al.*, 2004). Dopamine receptors belonging to both families were found in the astrocyte membrane (including D₁-, D₃-, D₄- and D₅-receptors) and a D₄-mediated signal transduction in response to dopamine was demonstrated.

1.4.2/ Dopaminergic innervation of the prefrontal cortex

Three different projections systems to the prefrontal cortex can be distinguished: the anteromedial, suprarhinal and supragenual systems (Van Eden *et al.*, 1987). The terminals of the anteromedial and suprarhinal systems predominantly distribute in the basal layers of the medial and orbital prefrontal cortex, respectively, and originate in the ventral tegmental area (A10). The supragenual system gives rise to a terminal plexus in the superficial layers of the supragenual part of the prefrontal cortex and originates in the substantia nigra (A9). Dopamine fibres are present in the

frontal cortex extending from the rostral pole to the retrosplenial cortex, the most caudal limit of the anterior cingulate cortex.

(1) *The anteromedial system* – The fibres of the anteromedial system are contained within the prefrontal subareas: in the medial prefrontal, anterior cingulate and prelimbic areas. The density of the dopaminergic innervation of the pregenual prefrontal cortex is much higher in the basal cortical layers (V and VI) compared to the more superficial layers (I, II and III). In addition to the laminar differences in dopamine fibre distribution, there are also regional differences, correlating well with the cytoarchitectonic subareas in this part of the cortex. The highest density of dopamine fibres is found within Cg3 (prelimbic area) of the prefrontal cortex. In comparison with this, the dorsal part of the anterior cingulate cortex contains far fewer fibres in the superficial layers I and II, while the densities in layers V and VI are comparable to that of Cg3 (Lindvall *et al.*, 1978).

(2) *The supragenual dopamine system* – This fine, superficial dopamine system is observed in the entire supragenual cingulate cortex, starting at a level immediately rostral to the genu of the corpus callosum and ending at a level within the transitional area between the anterior cingulate and retrosplenial cortices. The highest fibre density is observed in layer III of the ventral anterior cingulate area. The fibres of this system gradually become less dense in the dorsal direction to the border of the medial precentral area (Lindvall *et al.*, 1978).

(3) *The suprarhinal dopamine system* – The fibres of this system have a similar distribution to that of the anteromedial system, being rather homogeneously

distributed over the cortical layers. However, a higher density is observed in the more basal cortical layers (Lindvall *et al.*, 1978).

In general, the prelimbic and dorsal agranular insular areas contain the highest densities of dopamine fibres. Compared to the distribution of dopamine fibres in these two areas, the density of dopamine fibres in the pregenual part of the anterior cingulate and ventral agranular insular areas is less, especially in the more superficial layers. Febvret *et al.* (1991) used single- or double-immunocytochemical methods to provide further evidence that distinct subsets of dopaminergic neurones project to the rat cerebral cortex. They distinguished three classes of afferents with a distinct regional and laminar distribution. The first one was characterised by a dense meshwork of fine dotted neurotensin (NT)-positive varicosities, occupying restricted areas of the limbic system, namely the granular retrosplenial and the deep entorhinal cortices and subicular complex. Secondly, the mixed NT/DA projections identified in the prefrontal cortex extended rostrocaudally in layer VI of the whole cerebral cortex and formed cluster-like groupings in layers II-III of the medial and lateral entorhinal cortex. Thirdly, the dopamine projections to the superficial layers of the anterior cingulate, motor, retrosplenial and visual cortices were not colocalised with NT.

The mixed NT/dopaminergic fibres distribute to the deeper cortical layers V and VI and exhibit a striking rostrocaudal gradient of decreasing density from the prefrontal cortex to the visual cortex. The dopamine projections to the superficial layers of the anterior cingulate reach their cortical targets only after birth, during the first and second postnatal weeks. They distribute to the superficial cortical layers I-III and are mainly concentrated in the anterior cingulate cortex but innervate also sparsely the premotor, retrosplenial and visual cortices. The two groups of fibres have

a distinct morphology, different types of collateralisation and a different mediolateral origin in the ventral mesencephalon: ventral tegemental area (group A10) for the former, medial substantia nigra (A9) for the latter.

1.5/ GLUTAMATE-DOPAMINE INTERACTIONS

It has been well established that glutamate release in the prefrontal cortex affects the release of other neurotransmitters in this brain region, for example GABA and dopamine. Del Arco *et al.*, in 1999, used microdialysis to investigate the interactions between glutamate, GABA and dopamine in the rat prefrontal cortex. They found that intracortical infusions of the glutamate reuptake inhibitor L-trans-pyrrolidine-2,4-dicarboxylic acid (PDC: 0.5 – 32 mM) increased extracellular glutamate in the mPFC dose-dependently. This increase in glutamate was correlated with an increase in extracellular GABA and also a decrease in the extracellular concentrations of the dopamine metabolites DOPAC and HVA. The increase in extracellular GABA was blocked by co-infusion of the AMPA receptor antagonist 6,7-dinitroquinoxaline-2,3-dione (DNQX: 0.5 mM), but not the NMDA receptor antagonist 3-[(R)-2-carboxypiperazin-4-yl]-propyl-1-phosphonic acid (CPP: 1 mM), while the decrease in dopamine metabolites was blocked by the NMDA receptor antagonist only. Direct connections exist between glutamate terminals and GABAergic interneurons in the prefrontal cortex. The increase in GABA efflux produced by increased endogenous glutamate could be attributed to the effect of glutamate in these interneurons. GABA could also participate in the effects of endogenous glutamate on dopaminergic neurotransmission (i.e. the decrease in dopamine metabolites seen in this study).

Takahata and Moghaddam, in 1998, determined whether tonic activation of glutamate receptors contributes to basal dopamine release in the rat prefrontal cortex. To investigate whether tonic activation of glutamate receptors contributes to basal dopamine release, they looked at the effects of local administration of both NMDA (AP-5: 500 μ M) and AMPA (LY293558: 100 μ M) receptor antagonists on dopamine efflux. In awake rats, blockade of cortical AMPA receptors profoundly reduced dopamine efflux in the prefrontal cortex, suggesting that dopamine outflow in this area is under tonic excitatory control of AMPA receptors. Dopamine and excitatory terminals are in close apposition in the prefrontal cortex, suggesting possible presynaptic interactions between AMPA receptors and dopaminergic neurones. Blockade of cortical NMDA receptors increased dopamine efflux, suggesting that dopamine transmission is under tonic inhibitory control by NMDA receptors in this brain region. This could be an indirect effect. NMDA receptors are present on cortical GABAergic interneurons, which inhibit dopamine release (Santiago *et al.*, 1993). Antagonists of both NMDA (AP-5: 500 μ M) and AMPA (LY293558: 100 μ M) receptors, when applied into the ventral tegmental area (VTA), decreased dopamine efflux in the prefrontal cortex (Takahata and Moghaddam, 1998). This suggests an enhancement of dopaminergic neurotransmission in the prefrontal cortex by glutamate at the level of the cell bodies (see: Figure 1.4). Handling-induced increases in dopamine in the PFC were not altered by intracortical infusion of AP-5, but were blocked by LY293558, suggesting that glutamatergic transmission also regulates stimulus-induced increase of dopamine release in the PFC.

Feenstra *et al.*, in 1995, investigated the effect of local infusion of the glutamate agonist, NMDA, in the prefrontal cortex of freely-moving rats on the extracellular concentration of dopamine. Local application of NMDA (1mM)

increased dopamine to 170-1500 %. However, application of a lower concentration of NMDA (0.1 mM) decreased extracellular dopamine to 61 %. These effects were blocked by co-infusion of the competitive NMDA receptor antagonist AP-5. This demonstrates a dual action of glutamate on dopamine release, depending on the concentration of glutamatergic agonist applied. Dopamine terminals on neurones in the prefrontal cortex are often in close apposition to excitatory afferents and increased activation of these glutamatergic projections results in increased dopamine release. With respect to the inhibitory action of glutamate on dopamine efflux in the prefrontal cortex, the authors suggested a circuit involving the ventral striatum, which receives direct projections from the prefrontal cortex, and the ventral tegmental area (VTA), the location of dopaminergic neurones projecting to the prefrontal cortex. The VTA receives both direct and indirect projections from the prefrontal cortex. Thierry *et al.* in 1979, showed that stimulation of the prefrontal cortex may produce an inhibition of activity in the majority of those VTA neurones that project to the prefrontal cortex. Glutamatergic control of dopamine transmission is not restricted to the prefrontal cortex. For example, infusions of NMDA into the raphé nucleus decreased dopamine efflux, and this effect was reversed by the NMDA antagonist AP-5 (100 μ M: Smith and Whitton, 2001).

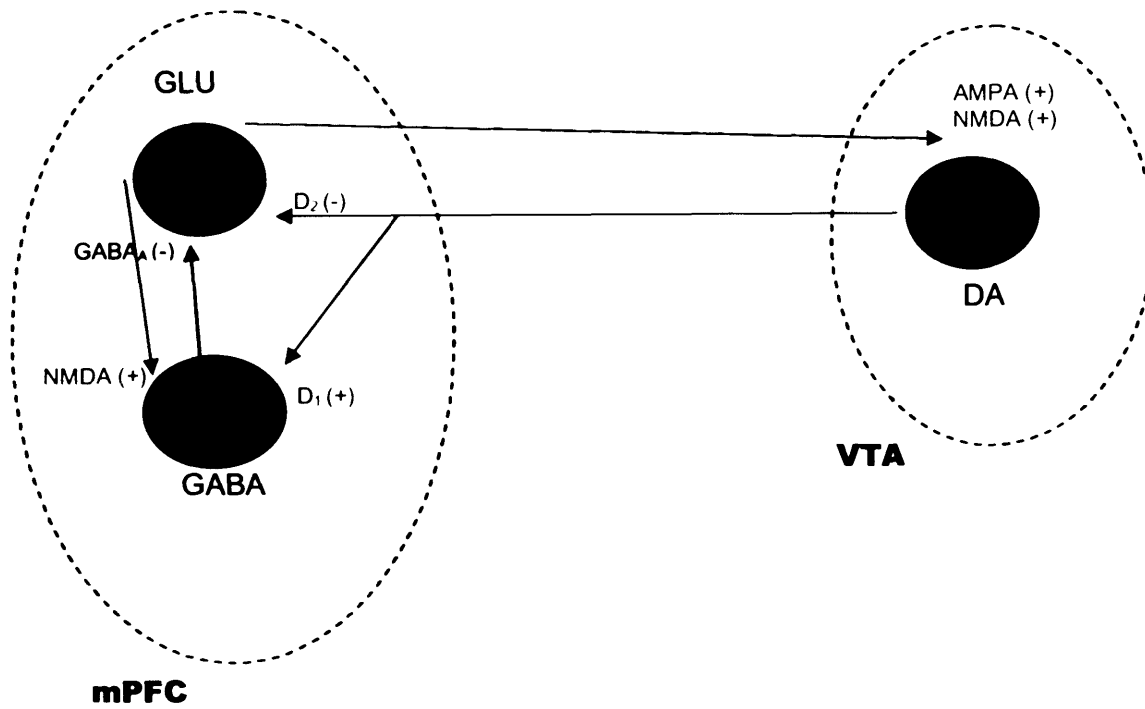


Figure 1.4 Schematic diagram summarising the interactions of dopamine, glutamate and GABA in the rat medial prefrontal cortex (mPFC) and ventral tegmental area (VTA).

1.6/ DOPAMINE-GLUTAMATE INTERACTIONS

It is clear that glutamate has a significant role in the influence of dopaminergic transmission during microdialysis studies, but fewer studies have addressed the reciprocal situation i.e. the control of glutamatergic neurotransmission by the dopamine system. Anatomical studies have consistently demonstrated the existence of a dopaminergic projection from the ventral tegmental area of the midbrain to the prefrontal cortex in rats (Lindvall and Bjorklund, 1978), comprising a portion of the mesocortical dopamine system. These dopaminergic neurones synapse on two cell types within the prefrontal cortex – pyramidal glutamatergic neurones and nonpyramidal GABAergic interneurones.

1.6.1 Modulation of prefrontocortical glutamate by the dopamine system – electrophysiological studies

Electrophysiological studies have revealed a complex action of D₁-like and D₂-like receptors in the control of cortical pyramidal neuronal activity. Activation of D₂-like receptors inhibits cortical pyramidal cells, while activation of D₁-like receptors excites cortical pyramidal neurons. In one such study, the effects of dopamine (0.1 – 30 μ M), on the passive and active membrane properties of layer V pyramidal cells from the rat prefrontal cortex was studied (Gulledge and Jaffe, 1998). Application of dopamine produced a reversible decrease in the number of action potentials evoked by a given current step. Pharmacological analysis using D₁-like and D₂-like receptor ligands suggested that decreases in the excitability of the pyramidal

cells was mediated by D₂-like receptor activation, while D₁-like receptors had no effect.

1.6.2/ Modulation of prefrontocortical glutamate by the dopamine system – microdialysis studies

To date, only a few microdialysis studies have been performed investigating the modulation of glutamatergic neurotransmission by dopamine in the prefrontal cortex. One study used dual-probe microdialysis to look at the effect of selective dopamine receptor ligands applied in the medial prefrontal cortex of rats on local and ventral tegmental area glutamate and GABA efflux (Harte and O'Connor, 2004). Intracortical infusion by reverse dialysis with the D₁-like receptor agonist SKF38393 (10 – 100 µM) decreased local extracellular glutamate and increased local extracellular GABA but had no effect on either transmitter in the ventral tegmental area. The decrease in local prefrontal glutamate efflux was reversed by co-infusion of the GABA_A antagonist bicuculline (0.1 µM), suggesting that it occurs indirectly via activation of GABAergic interneurons. Intracortical infusion with the selective D₂-like receptor agonist pergolide was associated with a decrease in local and VTA [GLU] and reversed in the presence of intracortical raclopride (10 µM). These results suggest that activation of D₁-like receptors decreases local prefrontal cortex glutamate efflux via a feed-forward activation of local GABAergic interneurons. Activation of D₂-like receptors in the medial prefrontal cortex directly decreases local glutamate efflux and inhibits the excitatory glutamatergic drive on the ventral tegmental area.

Another study investigated the effect of local infusion of the D₁-like receptor agonist SKF38393 (2 – 200 µM) on glutamate and GABA efflux in the rat prefrontal

cortex (Abekawa *et al.*, 2000). They found a dose-related decrease in local concentrations of both glutamate and GABA, which was prevented by co-infusion of the selective D₁-like receptor antagonist SCH23390 (40 μ M). These microdialysis studies suggest an inhibitory action of D₁-like and D₂-like receptors on spontaneous glutamate efflux in the prefrontal cortex.

1.7/ THE PHARMACOLOGY OF *d*-AMPHETAMINE

The main effects of *d*-amphetamine in the CNS are inhibition of reuptake (Table 1.3) of monoamines and promotion of their release out of the cell (Table 1.4). Although both actions are possible, they could happen under different conditions. However, it is difficult to distinguish between these two actions with *in vivo* experiments. The chemical structure of *d*-amphetamine is illustrated in Figure 1.5.

Figure 1.5 *The chemical structure of d-amphetamine (adapted from Sulzer et al., 2005).*

Table 1.3 *In vitro* K_i (nM) for the inhibition of monoamine uptake by *d*-amphetamine

NA		5-HT		DA		
45 (1)	39 (2)	1441 (1)	3830 (2)	132 (1)	34 (2)	78 (3)

K_i : inhibition constant (nM); (1) data from Heal *et al.*, (1998); results obtained from fronto-cortical preparations for noradrenaline and 5-HT, and from striatum preparations for dopamine; (2) data from Rothman *et al.*, (2002); results obtained from whole brain minus caudate and cerebellum for noradrenaline and dopamine, and from preparation of caudate for dopamine; (3) data from Rowley *et al.*, (2000); results obtained from nucleus accumbens preparations.

Table 1.4 *Effect of d-amphetamine on [3H]-NA, [3H]-5-HT, and [3H]-DA release from rat brain slices in vitro. Data show % release at different concentrations of d-amphetamine*

100 nM <i>d</i> -AMP			1000 nM <i>d</i> -AMP			10000 nM <i>d</i> -AMP		
NA	5-HT	DA	NA	5-HT	DA	NA	5-HT	DA
57	NS	56	135	NS	122	162	136	138

Data obtained from Heal and Cheetham, 1997.

1.7.1/ Sites of action of *d*-amphetamine - experimental evidence

In vitro and *in vivo* studies have implicated both vesicular and plasma membrane monoamine transporters as mediating the pharmacological effects of *d*-amphetamine. Secretory vesicles in neuronal and endocrine cells are important in the storage of classical neurotransmitters. At least two key components of the storage process have been identified. The first is vacuolar ATPase, which pumps protons from the cytoplasm to the inside of secretory vesicles. The second is a transporter, which exchanges vesicular protons for cytoplasmic neurotransmitter. The vesicular

monoamine transporter (VMAT) is responsible for transport of monoamines, including dopamine, noradrenaline and serotonin. Two major isoforms arising from different genes have been characterised (endocrine VMAT1 and neuronal VMAT2: for review see Parsons, 2000). The role of synaptic vesicle pools in the action of *d*-amphetamine was long doubted, mainly due to results from reserpine experiments. Reserpine irreversibly binds to storage vesicles of neurotransmitters such as dopamine, noradrenaline, and serotonin (i.e. VMAT-2), leading to depletion of monoamine transmitters. Results of *in vivo* microdialysis work investigating the effect of reserpine on *d*-amphetamine-induced dopamine release in the striatum are mixed. Some studies found little or no effect of reserpine (e.g. Callaway *et al.*, 1990), while others reported a blockade (e.g. Sabol *et al.*, 1998) of *d*-amphetamine-induced striatal dopamine release.

Several caveats should be taken into account when using reserpine as an experimental tool to investigate the pharmacology of *d*-amphetamine. For example, reserpine lowers core body temperature (Danielson *et al.*, 1985), which could attenuate dopamine release by *d*-amphetamine and leading to false positive results. It also causes a delayed upregulation of tyrosine hydroxylase activity via enhanced transcription, and produces higher levels of cytosolic dopamine (Tissari, 1982). In most studies, reserpine was administered 24 h prior to *d*-amphetamine administration, therefore the increase in newly-synthesised dopamine available for release could counteract the decrease in dopamine available from synaptic vesicles, leading to false negative results.

Newer experimental approaches using genetic manipulations have made the use of reserpine redundant. In a study by Piffl *et al.* (1995), COS-7 cells were engineered to express the plasmalemmal dopamine transporter (DAT cells), the

vesicular monoamine transporter (VAT cells) or both (DAT/VAT cells). Applying the superfusion technique, they found that a brief exposure to *d*-amphetamine (1-100 μ M for 4 min) caused a rapid and reversible increase in dopamine release from DAT cells and DAT/VAT cells but not VAT cells. The magnitude of this release was greater in DAT/VAT cells compared to DAT cells. During a prolonged exposure to *d*-amphetamine (1 μ M for 36 min), efflux from DAT cells reached a maximum after 8 min and subsequently returned to baseline in spite of the continuing presence of *d*-amphetamine. In DAT/VAT cells, a sustained increase in dopamine release was observed. This was demonstrated by a peak-shaped curve for DAT cells and a step-shaped release in DAT/VAT cells. This experiment suggests two distinct mechanisms of *d*-amphetamine-induced dopamine release. Firstly, reversal of the transport action of plasmalemmal DAT and secondly, release of dopamine from the intracellular vesicular pool, possibly by dissipation of the transmembrane pH that drives biogenic amine uptake into synaptic vesicles or by direct interaction with the substrate site of the vesicular amine transporter. This latter effect occurs at higher concentrations of *d*-amphetamine.

Another study used the technique of fast-scan cyclic voltammetry and *in vivo* microdialysis to investigate dopamine function in genetically modified mice in which the DAT gene has been deleted (Jones *et al.*, 1998). In striatal slices from wild-type mice, application of *d*-amphetamine (10 μ M) causes a gradual increase (~30 min) in extracellular dopamine, with a concomitant disappearance of the pool of dopamine available for depolarisation-evoked release as measured by cyclic voltammetry. In slices from mice lacking the dopamine transporter (DAT^{-/-}), application of *d*-amphetamine did not change baseline dopamine overflow. However, a decrease in electrically-stimulated dopamine release commenced approximately 15 min after

d-amphetamine treatment and was eliminated after 45 min. The authors deduced that *d*-amphetamine entered dopaminergic terminals and decreased vesicular stores, but could not cause release of dopamine into the extracellular space in the absence of DAT. Similarly, microdialysis measurements of dopamine after systemic *d*-amphetamine (10 mg/kg) in freely-moving animals show no change in animals lacking the DAT, whereas a 10-fold increase is observed in wild type animals.

Application of the VMAT2 inhibitor Ro4-1284 (10 μ M) to striatal slices from wild-type mice resulted in a gradual decrease in electrically-stimulated dopamine release over approximately 30 min with no accompanying increase in baseline dopamine overflow. After Ro4-1284 caused the disappearance of electrically stimulated dopamine in a slice from a wild type mouse, 10 μ M *d*-amphetamine was applied to the slice, and baseline dopamine outflow increased rapidly. These experiments illustrate the central importance of both depletion of dopamine from secretory vesicles and reversal of DAT-mediated transport in the releasing-effects of *d*-amphetamine. The plasmalemmal DAT is required for overflow of dopamine into the extracellular space, but not for vesicular depletion of vesicular dopamine by *d*-amphetamine. When endogenous, releasable dopamine was mobilised from the vesicles into the cytoplasm, the resulting increase in the dopamine concentration gradient across the plasma membrane was not sufficient to reverse DAT to a measurable degree.

1.7.2/ Mechanisms of action of d-amphetamine – experimental evidence

As mentioned in the opening paragraph of section 1.7, the main effects of *d*-amphetamine in the CNS are thought to be inhibition of reuptake of monoamines and promotion of their release out of the cell. This section will discuss some of the

experimental evidence underlying the proposed mechanisms of action of *d*-amphetamine. *In vitro* evidence for both inhibition of reuptake and release of monoamines has been provided by studies performed in the laboratory of Rudnick. In 1995, Wall *et al.* transfected LLC-PK₁ cells with cDNAs encoding the human noradrenaline transporter (NET), the rat dopamine transporter (DAT) and the rat serotonin transporter (SERT). Using these cell lines, the specificity of each transporter towards agents that inhibit substrate influx and stimulate substrate efflux across the plasma membrane was examined. MPP (1-methyl-4-phenylpyridinium) acts as a substrate for both the NET and the DAT. To measure the inhibition of monoamine transport, [³H] MPP⁺ was used as a substrate for LLC-NET and LLC-DAT cells, while [³H] 5-HT was used with LLC-SERT cells. Infusion of *d*-amphetamine (0.01 – 100 μM) potently and concentration-dependently inhibited NET- and DAT-mediated transport, with a lesser effect on SERT-mediated transport. Infusion of 50 μM *d*-amphetamine increased efflux of [³H] MPP⁺ from LLC-DAT cells. This *d*-amphetamine-induced efflux of [³H] MPP⁺ was attenuated by the presence of the transport inhibitor mazindol (50 μM) demonstrating that the *d*-amphetamine-induced increase in efflux is mediated by the transport system. This study suggests that *d*-amphetamine acts as a substrate for plasma membrane biogenic amine transporters, and, as a substrate, competes with other substrates for influx and also stimulates efflux of internal substrates by a transporter-mediated exchange. However, using this technique, the authors could only shed light on the interaction of *d*-amphetamine with plasma membrane transporters, while the experiments outlined in section 1.7.1 have demonstrated evidence for an involvement of the vesicular monoamine transporter in the pharmacological effects of *d*-amphetamine.

Piffl *et al.* (1999) used the superfusion technique to study the effect of *d*-amphetamine on the noradrenaline transporter (NAT). The cDNA of the noradrenaline transporter was transfected into COS-7 cells (NAT-cells) or cotransfected with the cDNA of the vesicular monoamine transporter (NAT/VMAT cells). As for the dopamine transporter, *d*-amphetamine released noradrenaline by 2 distinct mechanisms: reversal of the plasma membrane transporter to release cytoplasmic noradrenaline and, at higher concentrations, release of noradrenaline from the vesicular pool. At higher concentrations of *d*-amphetamine (10 and 100 μM), there was no release of noradrenaline from cells expressing only the plasma membrane transporter. However, on switching back to a *d*-amphetamine-free buffer, a prompt increase of noradrenaline release was observed. The authors inferred that *d*-amphetamine was blocking the plasma membrane transporter at high concentrations. This did not happen in cells coexpressing both transporters, where the concentration of noradrenaline, which is confined in storage vesicles, is much greater.

In vivo techniques have also been used to discriminate between uptake inhibition and release of monoamines. A study in this laboratory used *in vivo* microdialysis to investigate mechanisms by which *d*-amphetamine releases noradrenaline in the frontal cortex and hypothalamus of freely-moving rats (Géranton *et al.*, 2003). After systemic administration (10 mg/kg) or local infusion (10 μM) of *d*-amphetamine, the increase in noradrenaline efflux in the hypothalamus was greater than that in the frontal cortex. In the frontal cortex, the noradrenaline response to 10 μM *d*-amphetamine was constrained by activation of α_2 -adrenoceptors, since administration of the α_2 -adrenoceptor antagonist atipamezole (1 mg/kg i.p.) augmented noradrenaline efflux in this brain region. This suggests that, at this concentration of *d*-amphetamine, inhibition of reuptake of noradrenaline, following its

impulse-dependent release, is evident in the frontal cortex, but the noradrenaline response in the hypothalamus derives mostly from impulse-independent release (retrotransport). Blockade of α_2 -adrenoceptors by atipamezole (1 mg/kg i.p.) did not affect the noradrenaline response to 100 μ M *d*-amphetamine in either brain region, possibly because, at this higher concentration, retrotransport of noradrenaline masks any compensatory reduction in impulse-evoked release. Therefore, it seems that in the frontal cortex, the noradrenaline response to low concentrations of *d*-amphetamine seems to be constrained through activation of α_2 -adrenoceptors that blunt impulse-evoked transmitter release. No such compensatory mechanism is observed in the hypothalamus. At higher probe concentrations of *d*-amphetamine, noradrenaline efflux in both brain regions seems to derive from its impulse-independent release.

Another study in the laboratory of Kuczenski used microdialysis to characterise the hippocampal and prefrontal cortical noradrenaline responses to systemic administration of *d*-amphetamine (0.5 – 5 mg/kg i.p.; Florin *et al.*, 1994). Noradrenaline was dose-dependently increased in each brain region to a similar extent. Pre-treatment with the α_2 -adrenoceptor agonist clonidine (50 μ g/kg i.p.) decreased the noradrenaline response to 0.5 mg/kg *d*-amphetamine by approximately 75 %, but became progressively less effective as the dose of *d*-amphetamine was increased to 1.75 and 5 mg/kg. This result suggests that *d*-amphetamine increases extracellular noradrenaline through two consequences of its interaction with the neuronal transport carrier:

- (1) reuptake blockade, which predominates at the lower doses
- (2) release, which is prevalent at higher doses

In summary, two scenarios have emerged from studies investigating the effects of more than one dose of *d*-amphetamine. Results of *in vitro* studies (Piffl *et al.*, 1999) suggested that *d*-amphetamine releases noradrenaline by retrotransport, but, with high doses (perfusion of 10 and 100 μ M) *d*-amphetamine accumulates outside the cell and blocks the transporter. Consequently, noradrenaline cannot leave the cell *via* the transporter, and there is no increase in noradrenaline efflux. In contrast, *in vivo* microdialysis studies from Florin *et al.* (1994) and Géranton *et al.*, (2003), in the frontal cortex, suggested that low doses of *d*-amphetamine increase noradrenaline efflux by reuptake inhibition, but retrotransport increases with the dose.

1.8/ THE PHARMACOLOGY OF DIHYDROKAINATE (DHK)

Dihydrokainate (DHK) is a selective, nontransportable inhibitor of the GLT-1 glutamate transporter (Arriza *et al.*, 1994; see section 1.2 for details about GLT-1). This pharmacological inactivation of GLT-1 by DHK distinguishes it from the other glutamate transporter subtypes. In 1991, Robinson *et al.* measured the transport of L-[³H]glutamate into crude synaptosomal fractions prepared from the rat forebrain. They showed that DHK inhibited transport of glutamate with an IC₅₀ of approximately 100 μ M. It has also been reported that DHK has weak agonist actions at ionotropic glutamate receptors (AMPA and NMDA) in cultured hippocampal neurones (Maki *et al.*, 1994).

1.9/ OBJECTIVES

The overall aim of the experiments performed in this thesis was to compare the regulation of glutamatergic neurotransmission in two areas of the rat anterior

cingulate cortex: the rostral anterior cingulate cortex (rACC) and caudal anterior cingulate cortex (cACC).

- To determine whether the glutamate and dopamine responses to *d*-amphetamine differ in the cACC and rACC and to distinguish local vs. polysynaptic release mechanisms (Chapters 3 and 4).
- To determine the role of dopamine in the regulation of glutamatergic transmission in the cACC and rACC (Chapters 4 and 5).
- To determine the role of the glial glutamate transporter, GLT-1, in the regulation of glutamate transmission in the cACC and rACC (Chapters 6 and 7).

Chapter 2

2.0 Methods

2.1/ *IN VIVO* NEUROCHEMICAL MONITORING TECHNIQUES

Four main techniques are used for the monitoring of neurotransmitter efflux *in vivo*. These can be classified as follows:

- Sampling techniques with *ex situ* analysis of the samples:
 1. The push-pull cannula, which can result in extensive damage of the tissue in contact with the perfusate.
 2. *In vivo* microdialysis.
- Monitoring techniques with *in situ* analysis of neurotransmitter efflux:
 1. *In vivo* voltammetry (see Stamford, 1989)
 2. *In vivo* functional brain imaging.

2.1.1/ *The push-pull cannula*

The earliest attempt to monitor chemical changes in the extracellular compartment of the brain of conscious animals was the push-pull technique developed by Gaddum (Gaddum, 1961). The push-pull cannula is composed of two concentric hollow fibres or steel cannulae, the inner for the delivery of perfusion medium, the outer for the collection of the fluid. Two pumps are required, one to push the fluid into the tissue and the other to pull the perfusate out into a collecting tube. Neurotransmitters and other substances are taken up by the flow of fluid from the cannula for subsequent analysis.

Over the years, this design has evolved, which has eliminated some of the problems encountered during perfusion of an animal. An open flow system is a requirement for this type of perfusion, so tissue damage or bacterial contamination at the site of perfusion is possible. A lesion can arise if the rate of flow in the push and pull lines are not calibrated precisely or if a particle of tissue blocks the pull tube.

2.1.2/ *In vivo* microdialysis

In 1966, Bito *et al.*, published the first results obtained with a method that would later become *in vivo* microdialysis. By placing a permeable sack, containing 6 % dextran in saline, into the brain of dogs, they managed to collect and analyse amino acids and ions. The sack was removed 10 weeks after implantation and one single sample obtained. The use of the sack enabled the integrity of brain tissue to be preserved and provided clean samples. Over the subsequent years, the method has been refined. Delgado *et al.*, (1972) introduced the dialytrode, which made continuous sampling possible. It consisted of two cannulae (one shorter than the other one) arranged side-by-side and closed at the tips by a small porous bag. The perfusion system is the same as the one used for the push-pull cannula.

Brain microdialysis consists of the continuous sampling of endogenous molecules in the brain, with minimal perturbation of the system under study. The samples are analysed *ex situ*, after collection. A concentric probe, originally modelled on a capillary is implanted into a selected brain region. The microdialysis probe consists of a semipermeable membrane surrounding two fine cannulae through which fluid flows into and out of the portion containing the semipermeable membrane. The perfusion rate varies from 0.5-3 $\mu\text{l}/\text{min}$ and collection time varies from 1-20 min. Compounds reach the perfusion fluid by diffusion and the size of the solutes

penetrating the probe is limited by the properties of the dialysis membrane. The concentration of solute in the dialysate is not the same as its extracellular concentration, but depends on probe recovery. The recovery of a probe *in vivo* is a measure of the rate at which a substance is delivered to the perfusate. This depends on perfusion barriers in the brain (the 'tortuosity' of the tissue), properties of the dialysis membrane and the rate of perfusion. The probe can also be used for the local application of drugs by 'reverse dialysis'.

2.1.3/ *In vivo* voltammetry

For *in vivo* voltammetry, a voltage is applied to an electrode immersed in a solution/tissue. The electroactive species, with a suitable oxidation potential, are oxidised and a current generated, which enables detection and quantification of the electroactive species. This technique is only suitable for the measurement of catecholamines and serotonin, as these readily diffuse from the synaptic cleft. *In vivo* voltammetry offers better spatial resolution than *in vivo* microdialysis and excellent temporal resolution. However, it is difficult to detect separately the different catecholamines and other electroactive solutes and therefore impossible to study the interactions between different neurotransmitter systems.

2.1.4/ *In vivo* brain imaging

In vivo brain imaging techniques exploit a property of molecules called nuclear magnetic resonance (NMR) to obtain information about the concentrations of these molecules over time. In this way, the rates of change of concentration of specific metabolites can be determined. All nuclei, which contain odd numbers of protons and neutrons, have an intrinsic magnetic moment and angular momentum. The most commonly measured nuclei are ^1H and ^{13}C and NMR resonant frequencies

for a particular substance are directly proportional to the strength of the applied magnetic field. NMR aligns magnetic nuclei with an applied constant magnetic field and perturbing this alignment using an alternating magnetic field, the fields being orthogonal. The resulting response to the perturbing electromagnetic field is the phenomenon that is exploited in magnetic resonance spectroscopy (MRS) and magnetic resonance imaging (MRI).

In vivo MRS of the brain was first reported in the 1970s in animal models using systems adapted from high-resolution NMR spectroscopy (Chance *et al.*, 1978). Since this paper, ¹H MRS has been used to provide valuable insights into glutamate-glutamine neurotransmission cycling, the GABA neuronal system, and the second messenger system by measuring the metabolite levels of N-acetylaspartate (NAA), glutamate, glutamine, GABA and *myo*-inositol (for review see Stanley, 2002). The main advantage of *in vivo* brain imaging is that is completely non-invasive when compared to the other neurochemical monitoring techniques described above.

2.1.5 Composition of the perfusate

In order to prevent fluid removal from the brain interstitial compartment, it is necessary to use a perfusion fluid of composition and ionic strength as close as possible to the one of the interstitial fluid (Stenken, 1999). The composition of interstitial and cerebrospinal fluid is unknown and a variety of perfusion fluids can be used for microdialysis, which differ widely in their composition and pH. The perfusion solution used in this laboratory is based on a modified Ringer's solution, with a composition close to that of plasma: (mM) NaCl 145, KCl 4, CaCl₂ 1.3 and pH 6.8. It is important to maintain the composition of the perfusion fluid as close to that

of the interstitial fluid as possible. Infusion of a perfusate with a lower Ca^{2+} concentration than that in the extracellular fluid will induce a decrease in Ca^{2+} concentration around the probe resulting in a decrease in dialysate neurotransmitter concentration (Westerink and De Vries, 1988). Infusion of a perfusate with a Ca^{2+} concentration higher than that of the interstitial fluid increases dialysate neurotransmitter concentration (Moghaddam and Bunney, 1989). Small variations in the concentrations of Mg^{2+} and K^+ in the perfusate can affect basal dialysate dopamine in the striatum (Osborne, 1991).

2.1.6/ Neurotransmitter 'efflux'

There exist in brain tissue three fluid compartments: the intracellular fluid, the extracellular fluid and the vascular fluid. When neurotransmitters are released, they diffuse into the extracellular fluid. At the same time, these neurotransmitters are cleared from the extracellular fluid by reuptake and enzymatic degradation. Therefore, dialysis is sampling the net result of these processes. It is not measuring release, but rather the concentration of substances that pass into the extracellular fluid, which is determined by the balance of release and reuptake/degradation. The term 'efflux' is used to describe the amount of neurotransmitter reaching the probe.

2.2/ THE MICRODIALYSIS PROBE

2.2.1/ Probe construction

Figure 2.1 illustrates the construction of a typical microdialysis probe used in this laboratory.

Microdialysis Probe Construction

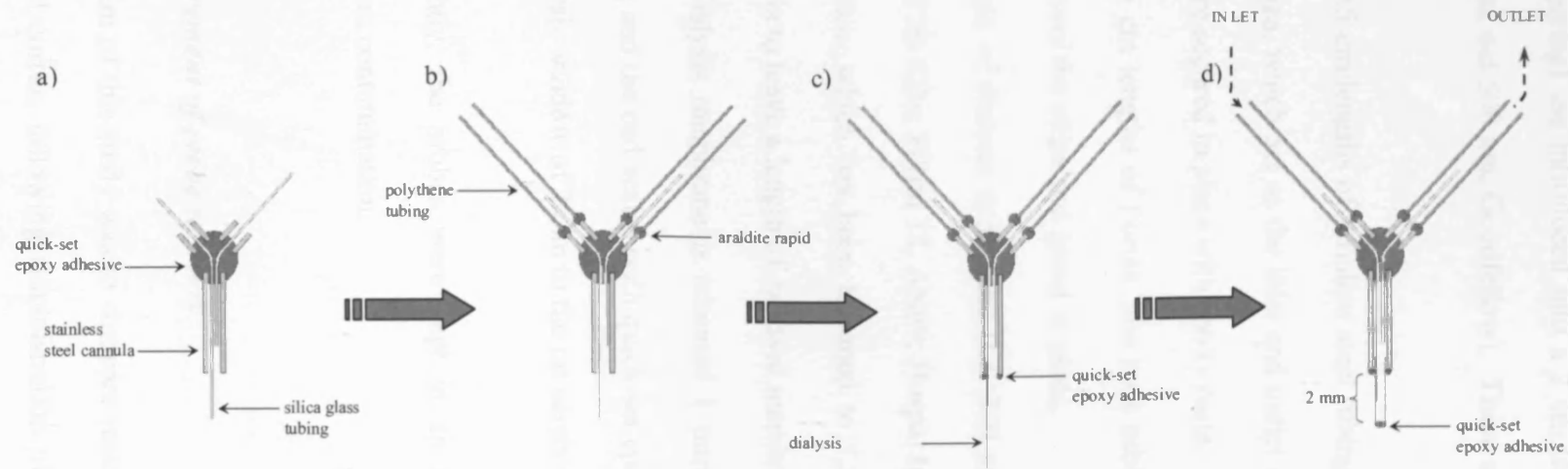


Figure 2.1. Schematic diagram showing the steps involved in constructing the microdialysis probes:
a) the stainless steel cannulae and silica glass tubing are secured using quick-set epoxy adhesive
b) polythene inlet and outlet tubing is attached to the 'arms' of the probe using araldite rapid
c) dialysis tubing is slid over the silica glass tubing (trimmed to 1.5 mm) and sealed with the stainless steel cannula using quick-set epoxy adhesive
d) the dialysis tubing is trimmed 1 mm from the end of the silica glass tubing and the end sealed with quick-set epoxy adhesive.

- Two 4cm lengths of silica tubing (i.d. 75 μm , o.d. 150 μm , Scientific Glass Engineering) are introduced into a 2 cm length of stainless steel tubing (i.d. 380 μm , o.d 500 μm , Goodfellow). These are glued in place with epoxy resin (RS).
- Two 0.5 cm lengths of stainless steel tubing are placed over the fixed ends of the silica, which act as the inlet and outlet channels. The lengths of stainless steel are secured in place with epoxy resin.
- Two 5 cm lengths of Portex fine bore tubing (i.d. 280 μm o.d. 610 μm) are fitted over the silica and glued in place.
- A length of dialysis membrane (i.d. 240 μm , o.d. 300 μm ; molecular weight cut-off 20 KDa; Filtral 12, AN69; Hospal Industries) is placed over the end of the silica, which has been trimmed to 1.5 mm, and glued inside the steel cannula to leave a length of exposed membrane.
- The dialysis membrane is trimmed 1 mm from the end of the silica glass tubing and the end sealed with quick-set epoxy adhesive (RS). This presented a dialysis window of 2 mm to the rat cerebral cortex.

Subsequently, the probes were kept in an air-tight container to protect the membrane from contamination.

2.2.2/ Measurement of probe recovery

The aim of this study was to compare relative changes in glutamate efflux in the rat frontal cortex, following administration of various CNS agents. Moreover, previous work in this laboratory has shown that probe recovery is reasonably constant

between probes and over the range of solute concentrations so that results are comparable across experiments. Therefore, measurements were not corrected for probe recovery. However, as glutamate has not been previously measured in this laboratory, it was necessary to determine probe recovery for a range of probe infusion rates. In the past, it was thought that the main factor limiting diffusion, during the draining of solutes from the brain, was the membrane. However, it is now known that the *in vivo* recovery of a solute strongly depends on the properties of the surrounding tissue. Evidence that the main factor limiting diffusion is not the membrane has been provided by Hsiao *et al.* (1990). They compared the recoveries for acid metabolites, *in vitro* and *in vivo*, in the striatum, of three membranes mounted on probes of concentric design: cuprophane, polycarbonate ether, and polyacrylonitrile membrane. They found major differences between the *in vitro* extraction fractions of the three types of probes, but no differences between the *in vivo* values. This supported the view that, *in vitro*, the membrane is the major limit to diffusion whereas, *in vivo*, the limiting factor is the diffusion in the tissue itself.

The water recovery method has been traditionally used to measure the extraction fraction of solutes *in vitro* (Zetterstrom *et al.*, 1982). This involves measuring the recovery of a probe by inserting it into an aqueous solution containing a known concentration of the solute of interest, and perfusing the probe with a solution free of this solute. The *in vitro* recovery is the ratio between the concentration in the outflow and the concentration in the solution. To determine the probe perfusion rate which gave the optimum recovery of glutamate, the probes were immersed in a solution of 2×10^{-7} M glutamate and continuously perfused with Ringer's solution devoid of glutamate. After the beginning of probe perfusion, successive 20 min samples were obtained for each probe. The effect of different flow

rates on relative recoveries was determined at flow rates of 1, 2, 3, 4 and 5 $\mu\text{l}/\text{min}$. Samples of the solution surrounding the probes were taken at intervals throughout the day to correct recoveries for any degradation of glutamate.

It was found that a flow rate of 1 $\mu\text{l}/\text{min}$ gave the maximum recovery and this value decreased when the flow rate was increased to 2 $\mu\text{l}/\text{min}$ and remained fairly constant across the higher flow rates (Figure 2.2). Diffusion of solutes in the brain tissue is a greater limiting factor than diffusion through the membrane. Therefore, *in vitro* recovery cannot be considered to be a true reflection of *in vivo* recovery. However, applying this method allowed determination of the optimal value for perfusion flow rate. From the results obtained in this study, I decided to use a flow rate of 2 $\mu\text{L}/\text{min}$. This provided a good *in vitro* recovery of glutamate and the volume of sample obtained was large enough for injection into the HPLC system. Other factors that can be determined from the water recovery method include membrane area and the composition of the perfusion fluid that yields optimal recovery.

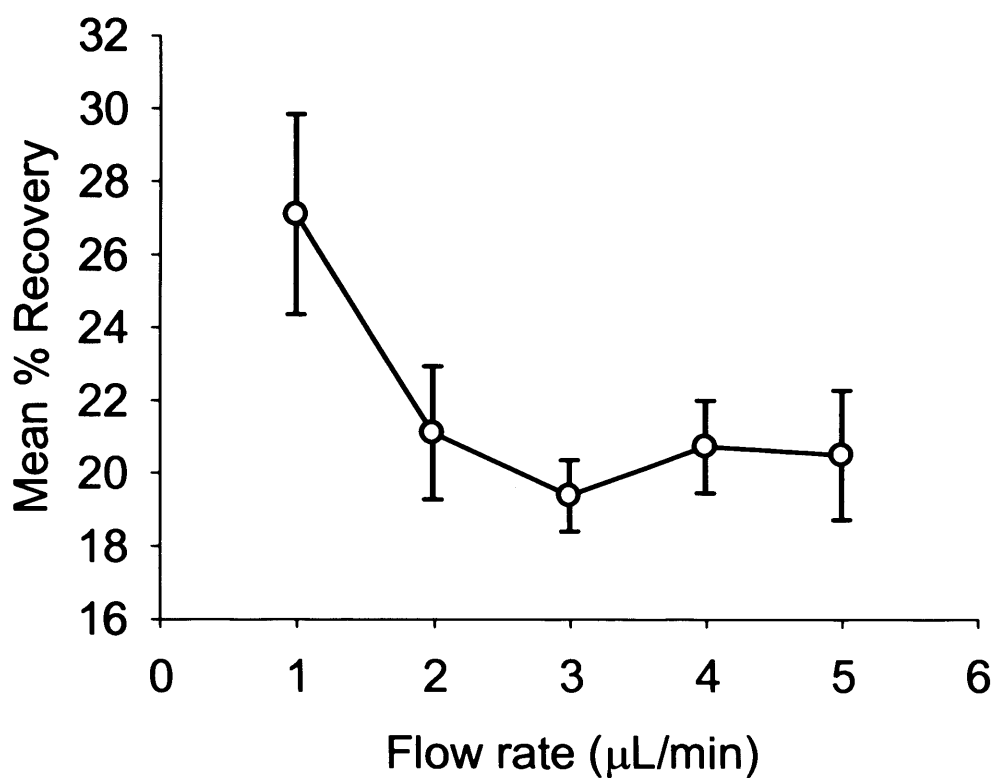


Figure 2.2 Probe recovery as a function of flow rate

Microdialysis probes were immersed in a solution of glutamate of 2×10^{-7} M (which gives a concentration of 50 pmol/50 μL glutamate on the HPLC column). N=12-16.

Since *in vitro* calibration has little application in microdialysis *in vivo*, other *in vivo* methods can also be employed to calibrate the probe. The reverse dialysis method is commonly used to estimate the recovery of exogenous compounds. The probe is inserted in a drug-free environment and perfused with different concentrations of the test drug. By plotting mass transport (i.e. the difference between C_{in} , the perfusate, and C_{out} , collected in the dialysate) versus C_{in} , a straight line can be obtained by linear regression. Its slope is the recovery of the probe. The no net flux method is popular for calibrating probe recovery for endogenous substances (Lonroth *et al.*, 1987). It consists of perfusing the probe with solutions of different concentrations of the substance of interest, greater and less than the expected one. By plotting mass transport versus C_{in} , a line is obtained by linear regression. Its slope is the extraction fraction and its intercept with the X-axis is the No Net Flux point. This point is an estimate of the concentration of unbound solute surrounding the membrane.

2.3/ MICRODIALYSIS PROCEDURES

2.3.1/ Surgical procedure

All procedures complied with the UK Scientific Procedures (Animals) Act 1986. Male outbred Sprague-Dawley rats (250 – 300 g) were obtained from the colony at University College London. They were housed in groups of 4 at 21 °C and 55 % humidity with a light-dark cycle of 12 h (lights on at 8.00 am). Animals had free access to food and water at all times.

Anaesthesia of rats was induced by inhalation of 5 % halothane in combination with 95% O₂/5% CO₂ delivered through an induction chamber at 2 l/min.

Following loss of the righting reflex, rats were transferred to a stereotaxic frame (David Kopf, model 900) and the anaesthetic delivered *via* a face mask (2-2.5 % halothane in 95 % O₂/5% CO₂ at 1 l/min). The head was set in the flat-skull position (incisor bar set at 3.3 mm below the interaural line) using blunted, non-rupture ear bars. Core body temperature was maintained at 37 °C using a homeothermic heating pad and rectal probe (Harvard Instruments).

A small incision was made in the skin and the skull surface exposed to reveal Bregma. A small hole was made through the skull using a trepanning drill burr where the probes were to be inserted: mm caudal anterior cingulate cortex (cACC): AP +1.0 ML ±0.6, rostral anterior cingulate cortex (rACC): AP +2.5 ML ±0.6 according to the atlas of Paxinos and Watson (2005). A screw was inserted into the skull in order to anchor the dental cement that would secure the probes after insertion.

The dura was carefully broken using a needle and a probe primed with Ringer's solution slowly lowered vertically to its final position: mm cACC: DV -3.6, rACC: DV -4.6, according to the atlas of Paxinos and Watson (2005). The probe was secured to the skull surface using acrylic dental cement. When the cement had dried, the inlet and outlet tubing of the probe were sealed with bone wax to prevent blockage prior to the beginning of the experiment. The rats were allowed to recover from the anaesthesia in an incubation chamber (about 30 to 45 min according to the surgery). They were then transferred into individual plastic cages overnight.

2.3.2/ Collection of dialysates.

On the day after probe implantation, rats were kept individually in their home cages and moved to the experimental laboratory. The probe inlet and outlet were connected *via* a length of Portex tubing (i.d. 580 μm o.d. 960 μm) to a gas-tight syringe (Terrumo) containing Ringer's solution, fitted to an infusion pump. The probes were perfused with Ringer's solution at a rate of 2 $\mu\text{l}/\text{min}$ for the duration of the experiment. The inlet and outlet tubing were guided through a liquid swivel, held in a clamp, over the top of the cage, allowing the rat to move freely around the cage. Dialysis samples (40 μl) were collected every 20 min and derivatised with 20 μl of complete *o*-phthaldehyde reagent (Sigma, UK) before injection into the HPLC system. Once three successive samples had established a stable base-line, a test drug was administered.

2.3.3/ Verification of probe placement

At the end of the experiments, animals were deeply anaesthetised with halothane and sacrificed by cervical dislocation. The brains were removed and fixed in formalin solution overnight. The next day, probe placements were verified by cutting the brains and observing the probe tracts, which were clearly visible under a light microscope. The probe tracts were compared by eye with the atlas of Paxinos and Watson to confirm whether or not they were in the right place. Animals implanted with probes, which were obviously out of range of the desired coordinates, were excluded from the final analysis. Several animals were excluded as the probes were found to be located too lateral to the midline (see: Chapter 6 for more details).

2.3.4/ Measurement of dialysate glutamate content

Dialysate samples are applied to a chromatography column that separates the various compounds according to their size, charge and lipophilicity. They are assayed electrochemically at a downstream electrode, where the sequentially eluted compounds are oxidised and give rise to a series of currents (see section 2.4).

2.4/ HIGH PERFORMANCE LIQUID CHROMATOGRAPHY (HPLC)

2.4.1/ Detection of glutamate

Since the identification of a number of amino acids as neurotransmitters, their measurement in brain tissue and fluids is of increasing importance. Traditional approaches to amino acid analysis have included ion-exchange procedures using sulphonated cation exchange resins, post-column reaction with ninhydrin and detection with spectrophotometry (Moore and Stein, 1951) or colorimetry (Spackman *et al*, 1958). However, post-column derivitisation schemes are not suitable for the detection of amino acids in brain samples as the sensitivity is too low and unable to detect micromolar concentrations. In the past 10 years, pre-separation derivitisation methods have dominated the field of amino acid analysis. Separation of derivatised amino acids is accomplished by high-performance liquid chromatography (HPLC), or more increasingly, capillary electrophoresis (CE). HPLC can be coupled to different modes of detection depending on the analytes to be measured and the sensitivity required e.g. UV absorbance, fluorescence, mass spectrometry and electrochemistry.

Traditionally, HPLC has been coupled with fluorescence detection. Simple aliphatic amines such as glutamate lack a chromophore and cannot be readily analysed by HPLC using fluorescence detection. This problem can be overcome by derivatisation to introduce a chromophore or fluorophore. Several derivatisation methods exist for the conversion of amines, such as glutamate, to detectable forms. Derivatisation schemes include those based on ninhydrin, *o*-phthaldehyde, fluorescamine, dansyl chloride, and dabsyl chloride. Fluorescence methods using *o*-phthaldehyde (OPA) as a derivatising reagent have become popular, although they face certain limitations, such as insensitivity of the assay and the instability of the fluorescent derivatives of the reaction: 1-(alkylthio)-2-alkylisoindoles (see figure 2.3, Rowley *et al.*, 1995). Attempts have been made to increase the stability of the derivatives by reacting them with either tert-butylthiol and also 2- or 3-mercaptopropionic acid. The 1-(alkylthio)-2-alkylisoindoles can also undergo anodic oxidation at moderate potential, permitting the use of electrochemistry for their determination. The electrochemical properties of the derivative are thought to be far less susceptible than fluorescence to changes in the derivative's structure (Joseph and Davies, 1983). A popular alternative to the use of HPLC-ECD method for amino acid analysis is the use of OPA derivatisation in conjunction with capillary electrophoresis (CE) and laser-induced fluorescence (LIF) detection. These systems provide extremely high sensitivity and excellent temporal resolution when coupled to microdialysis due to the low volume of sample required for analysis (Dawson *et al.*, 1995, Silva *et al.*, 2000).

2.4.2/ Theory of HPLC

For the analysis of glutamate content in brain dialysates, HPLC coupled with ECD was used. This highly sensitive assay is used to separate the components of the dialysate prior to their measurement with electrochemical detection. Separation is achieved by exploiting differences in the relative affinities of the constituent compounds to a solid, non-polar phase (the 'stationary phase') and a polar, liquid phase (the 'mobile phase'). In this 'reversed phase' chromatography, the stationary phase is a hydrocarbon-bonded surface, usually octadecyl silyl (ODS) bonded to silica. The particulate phase is densely packed within a length of stainless steel housing (the 'column'). The mobile phase is a pH buffered water/methanol mixture. Samples are introduced into the flow of mobile phase and passed through the stationary phase at a constant flow rate. The most polar components of the sample will elute first, having lowest affinity for the non-polar stationary phase. By adjusting the pH of the buffer, the polarity of compounds within the sample can be adjusted, therefore determining their retention to the stationary phase. Individual components are identified by their 'retention time' i.e. the time taken to pass through the column and onto the electrochemical cell.

2.4.3/ Isocratic vs. gradient elution

Elution of solutes of interest can be achieved using either gradient or isocratic elution. The main purpose of gradient elution is to move strongly retained components of the mixture more quickly, but having the least well retained component well resolved. The least concentration of the organic solvent in the eluent

allows the least retained components to be separated. Strongly retained components will sit on the adsorbent surface on the top of the column, or will move very slowly. As the amount of the organic solvent (e.g. acetonitrile) is increased then strongly retained components start to move faster. When the solvent composition remains constant throughout the analysis, the elution is called isocratic. Gradient elution is necessary when the resolution of a number of amino acids in one sample is desired. This is because with isocratic elution, most of the amino acids elute quickly and are not resolved.

For the purpose of these studies, isocratic elution was employed, since there was only one solute of interest (glutamate). Isocratic elution removes the need for an intervening re-equilibration step, as found in gradient systems. Glutamate was derivatised with complete *o*-phthaldehyde (OPA; Sigma) reagent before injection onto an octadecylsilan (ODS) column. This stationary phase consists of silica derivatised with octadecyl groups. Rather than making up the OPA reagent from scratch every day, which is a lengthy and time-consuming procedure, 'complete' reagent purchased from Sigma UK was used. This requires no further preparation for use. Pilot experiments demonstrated that the amount of electroactive derivative increased with reaction time, and a peak was reached at 7-10 min. After 15 min of reaction time, the amount of electroactive derivative decreased and a smaller peak was obtained on the chromatogram. For my microdialysis experiments, I found that a reaction time of 8 min produced the optimum amount of derivative on the column, while fitting in with the run-time of the chromatograms and the sampling time of the experiments. The reaction time was kept consistently at 8 min for each sample to prevent any variation in the concentration of electroactive derivative from day to day.

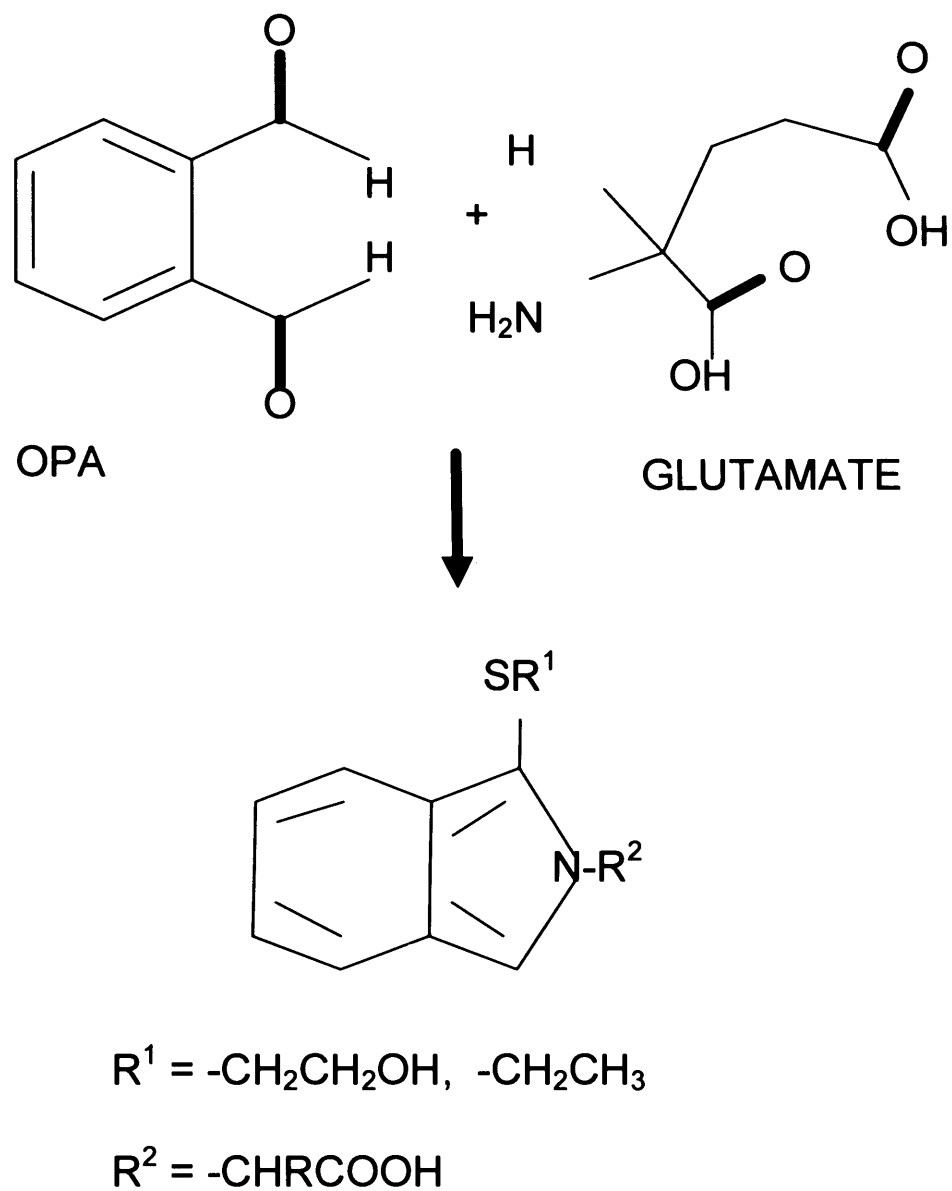


Figure 2.3 Scheme depicting the reaction between glutamate and *o*-phthalaldehyde (OPA).

The structure of the (1-(alkylthio)-2-alkylisoindole is also shown.

2.4.4/ Main components of the HPLC/ECD system

- LKB 2150 isocratic HPLC pump (delivering the mobile phase at a rate of 1 mL/min)
- Rheodyne injection valve (50 μ L sampling loop)
- Electrochemical detector (ESA Coulochem 2.1)
- Microdialysis cell (ESA 5014A)
- Guard cell (ESA 5021)
- Pulse Damper
- SupercosilTMLC-18 15cm x 4.6mm, 5 μ m reverse-phase column

2.4.5/ Choice of the mobile phase

The retention time of solutes depends on the composition of the mobile phase: for example, the nature and concentration of the organic modifier, the pH, and also the end-capping of the column. Therefore, the correct conditions need to be chosen so that all the solutes are separated from one another and from the solvent front. The original mobile phase used in these studies was based on a modified version of the buffer used by Rowley *et al* in 1995. To assess the concentration of glutamate in a sample, a range of conditions in which the pH of the buffer was changed, were tested in order to determine the optimal conditions to detect glutamate. The results shown in Figure 2.4 were obtained by testing different pHs of the mobile phase within the range 6.36 to 7.33. For a given concentration of glutamate injected onto the column, the mean detector response varied with the pH of the mobile phase. As the pH of the mobile phase increased, the mean detector response increased for a given concentration of glutamate. This would suggest that the highest pH tested would be optimal for the measurement of glutamate in samples. However, other features of the

chromatograms obtained at this high pH meant that it was unsuitable for use in experiments (see table 2.1). For example, as the pH of the mobile phase was increased, the size of the solvent front also increased and sometimes it was hard to resolve the glutamate peak from the solvent front. Also, interfering reagent peaks were observed at a higher pH. As the pH of the mobile phase was decreased, the peak height of the chromatogram for glutamate decreased until, at a pH below 6.4, a response was no longer obtained. A late-eluting and saturating peak was consistently seen and, as the pH was lowered, the elution time of this peak increased dramatically. This caused it to interfere considerably with subsequent chromatograms. Therefore, a pH of 7.2 was regarded as optimal for the detection of glutamate. This gave desirable resolution of the analyte peak from the solvent front and a good detector response. Figure 2.5 (a) shows a typical chromatogram derived from injection of a glutamate standard solution containing 50 pMol/50 μ L into the HPLC system. The peak corresponding to glutamate is indicated by the arrow. Figure 2.5 (b) shows a typical chromatogram obtained after injection of brain dialysate sample into the HPLC system. The glutamate peak is large and easily discernable from the solvent front. The contaminating peaks are thought to be due to the presence of the reagent in the system.

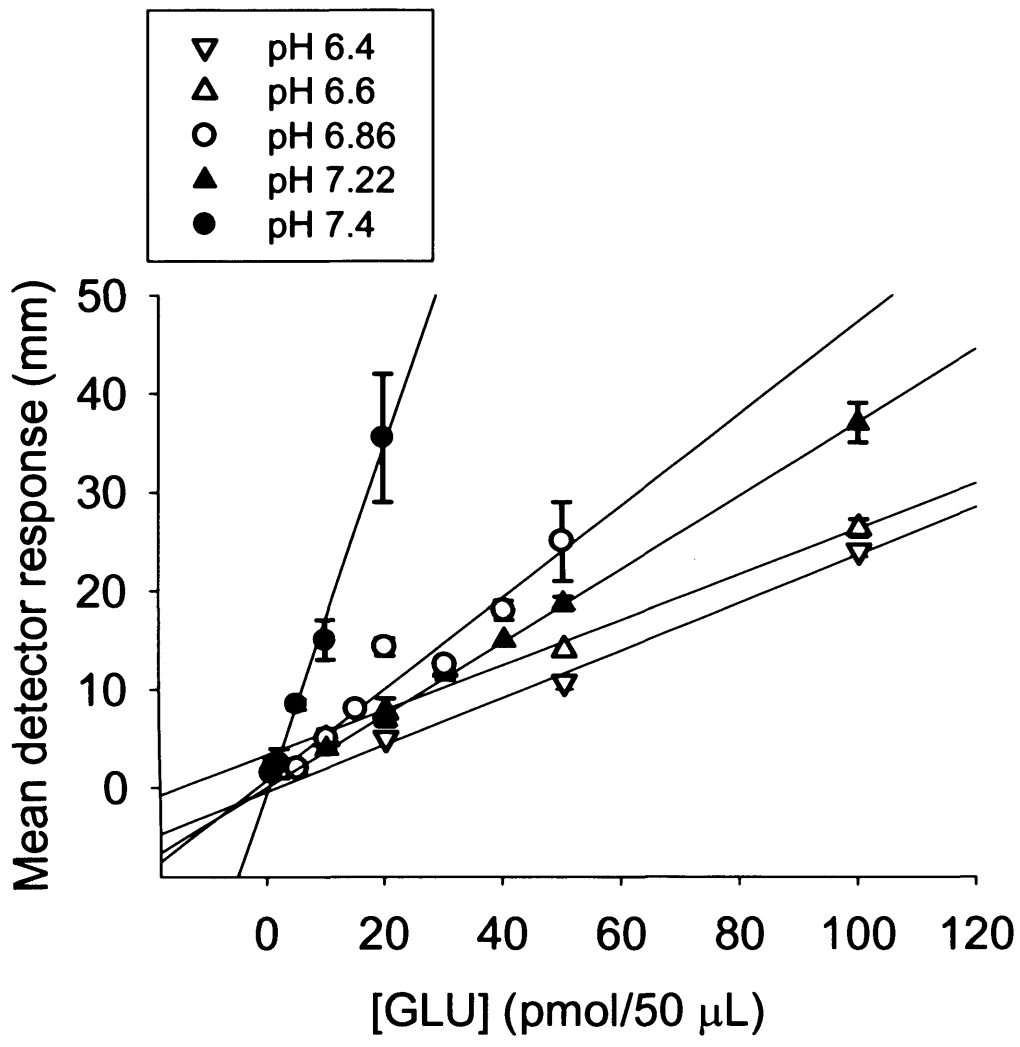


Figure 2.4 Mean detector response as a function of mobile phase pH.

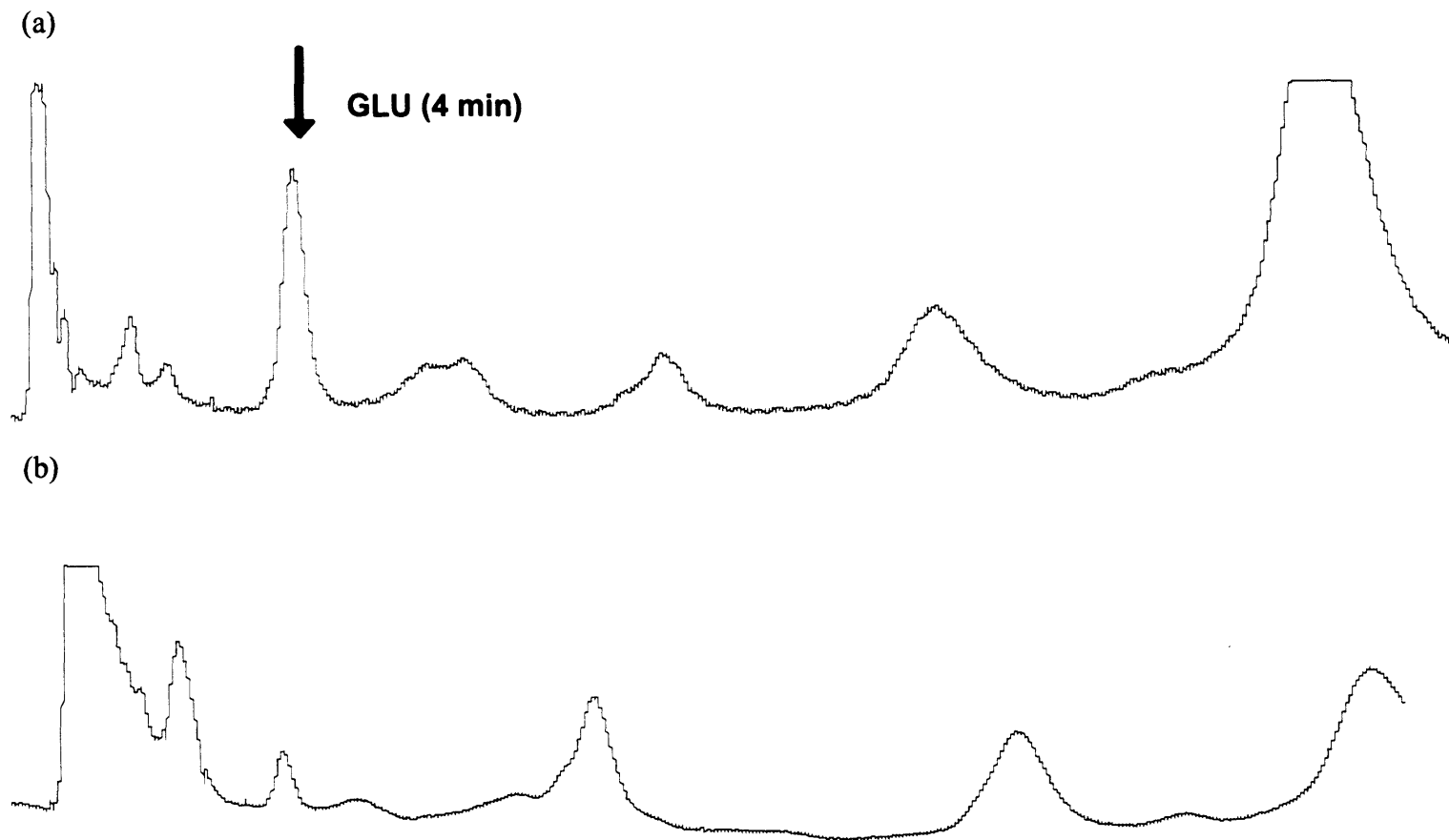


Figure 2.5 – examples of typical chromatograms obtained during experiments

- a) A typical chromatogram obtained on injection of a glutamate standard solution containing 50 pmol/50 μ l glutamate.
- b) A typical chromatogram obtained on injection of a brain sample from the same experimental day

Table 2.1 Characteristics of chromatograms at different mobile phase pH

pH of mobile phase	Retention time of glutamate peak	Comments
7.33	5 min 45 s	Large solvent front, sometimes glutamate cannot be resolved. Very large peak at 4-5 min, sometimes interferes with glutamate peak. Large late-eluting peak.
7.22	5 min 55 s	Solvent front smaller, doesn't interfere with glutamate peak. Other peaks seen at 4 min 30s and 7 min, but do not interfere with solvent front. Large late-eluting peak.
6.86	6 min 05 s	Small solvent front (only lasts 2 min 30s). Other peaks seen at 4 min 30 s and 5 min 30 s, which could interfere with glutamate peak. Large late-eluting peak.
6.6	7 min 20 s	Very small solvent front. Other peaks at 4 min (very narrow). Large late-eluting peak.
6.4	7 min 30 s	Very small solvent front. Other peaks at 4 min and 4 min 30 s. Large peak at 7 min, which sometimes interferes with glutamate peak. Late-eluting peak interferes with subsequent chromatograms.
5.75	No discernible glutamate peak	Late-eluting peaks interfere with subsequent chromatograms.

2.4.6/Composition of the mobile phase:

- 0.1 mM phosphate buffer
 1. 64 mM Na₂HPO₄ (99 %, Fischer)
 2. 16 mM NaH₂PO₄ (99 %, Fischer)
- 50 mg/L EDTA (99.5 %, AnalaR)
- 25 % methanol (99.8 %, Prolabo)
- Adjust to pH 6.5 – 7.0 with phosphoric acid

The mobile phase was filtered through 0.45 μM Millipore filters and degassed to prevent bubbles forming in the system.

2.4.7/ Electrochemical detection (ECD)

Once the solutes have crossed the column, they are detected by an electrochemical cell. The cell consists of two glassy carbon electrodes in series. A negative potential is applied to the first one to condition the mobile phase containing the solutes. A positive potential is applied to the second cell where the reaction of detection takes place (an oxidation). The transfer of electrons at the electrode during the oxidation gives rise to a current measured by the detector and expressed as a peak on a chromatogram by the chart recorder. The current obtained is proportional to the difference between the rate of oxidation and reduction reactions at the electrode.

2.4.8/ Choice of the potential of oxidation

According to work done previously, the conditioning electrode (E1) located in the electrochemical cell was set at -280mV. To determine the optimal potential for the second electrode (E2), a current/potential calibration curve for GLU was constructed. A constant amount of GLU (10 pmol/50 μ L) was injected into the system and the detector response recorded to E2 over the range 200 to 700mV whilst E1 was kept constant at -280mV. By changing the potential of the second electrode (E2), the rate of oxidation of solutes is altered, and therefore the current flowing across the electrode changes, giving rise to different size peaks on the chromatograms.

The voltammogram obtained (Figure 2.6) by oxidation of GLU was stable from 700mV down to about 400mV. At 400mV, the height of the peak on the chromatogram began to decrease severely in a linear relationship with the potential E2, until no response was detected when E2 fell below 250mV. Despite larger peaks being obtained at larger potentials, a value of 350mV was chosen for E2, since too many interfering peaks were seen at potentials above this, possibly caused by oxidation of the mobile phase.

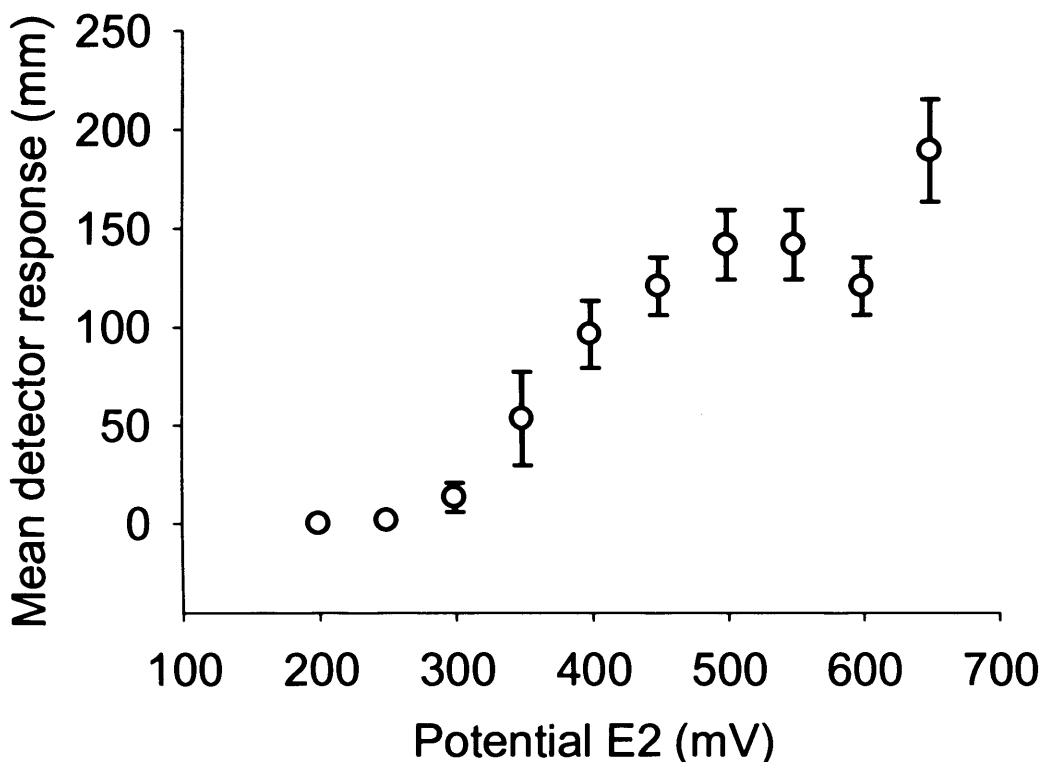


Figure 2.6 Voltammogram showing the detector response to a 10 pmol/50 μ L glutamate standard as a function of the electrode potential. N=3.

2.4.9/ Calibration of the separation/detection system

Before application of the HPLC-ECD technique to measure glutamate in microdialysis samples, regular calibration of the system in a wide range of concentrations of glutamate was necessary, as well as determination of the detection limit of the assay. Solutions containing a range of concentrations of glutamate (0.5 to 30 pmol/50 μ l) were injected into the system, under the conditions already described.

A typical calibration curve obtained is presented in figure 2.7. The relationship between the height of the peak and the concentration of glutamate was linear. The detection limit for glutamate using this assay was 0.5 pmol/50 μ l. At this

concentration, the signal was more than twice as high as the basal noise. A calibration of the HPLC-ECD system was required every day prior to the microdialysis experiment. It was done within a range of glutamate concentrations close to those expected to be measured during the experiment (5 – 50 pmol/50 μ L).

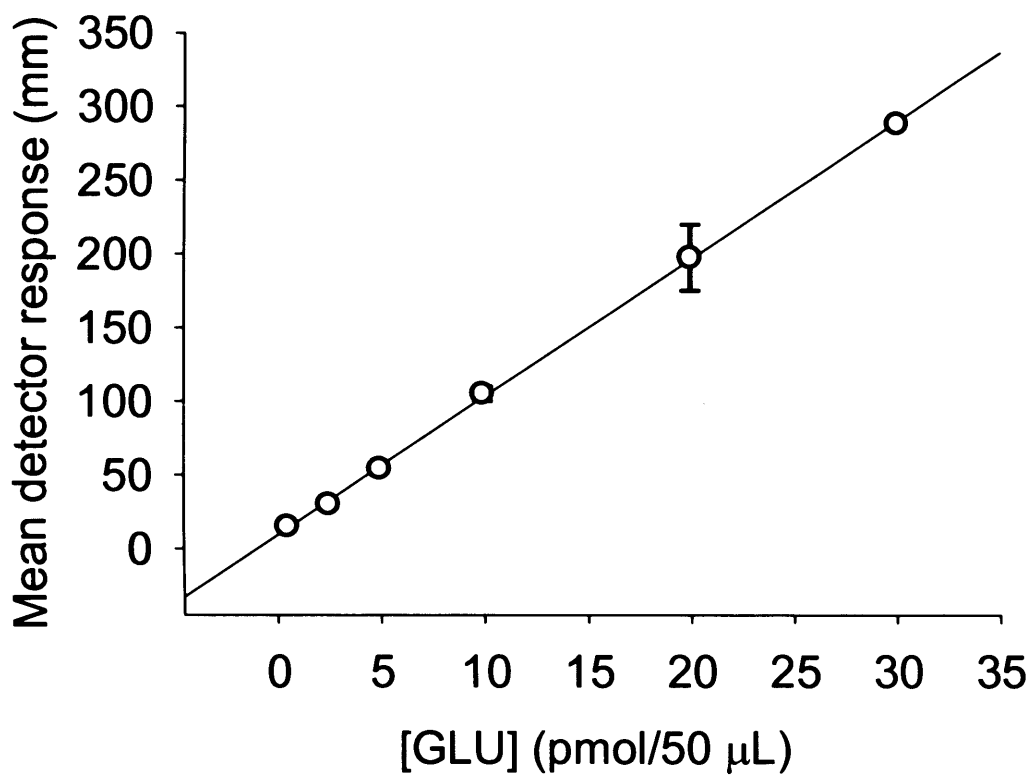


Figure 2.7 Calibration curve for the detection of glutamate in a sample.

The height of the peak representing the oxidation of the *o*-phthaldialdehyde derivative was plotted against the concentration of glutamate in the sample. N=3.

2.5/ DOPAMINE HPLC

Monoamines such as dopamine are readily oxidised without the need for a derivatisation step. Therefore, samples can be injected straight onto the column. After passing through the column, the mobile phase undergoes oxidation at the electrochemical cell. A positive potential is applied to the working electrode of the cell in contact with the mobile phase. The release of electrons creates a current, which is amplified and detected. The amount of current produced is directly proportional to the number of molecules of DA present in the sample, in accordance with Faraday's Law.

2.5.1/ *Composition of the mobile phase*

- NaH₂PO₄ 83 mM (99 %, Fischer)
- OSA 0.23 mM (98 %, Sigma)
- EDTA 0.84 mM (99.5 % AnalaR)
- Methanol 17 % (99.8 %, Prolabo)
- Adjust to pH 4.0 with orthophosphoric acid

2.5.2/ *Components of the assay system –*

The HPLC-ECD system consisted of:

- Shimadzu LC 6A isocratic dual piston pump ESA 582, delivering the mobile phase at 1.15 ml/min
- Pulse dampener (ESA)
- 50 µl stainless steel injection loop (Anachem) attached to a Rheodyne 7125 injection port

- Aquapore guard column (7 μ M particle size, 30 x 4.6 mm, Brownlee, Perkin, Elmer)
- Column (Hypersil ODS; 5 μ M; 250 x 4.6 mm; Thermo Hypersil Ltd., UK), maintained at 26 °C by a column heater (Jones Chromatography, model 7955)
- An analytical cell: ESA 5014 electrochemical cell, with 2 electrodes in series; a conditioning electrode set at -280 mV and a measuring electrode set at +180 mV
- An ESA model 5100A coulometric detector
- A Spectraphysics Chromjet integrator

2.5.3/ Calibration of the separation/detection system

As with the assay for measuring glutamate, regular calibration of the system in a range of concentrations of dopamine was necessary. Solutions of dopamine of concentrations 25 – 100 fmol/50 μ l sample were injected into the system, under the conditions already described.

A typical calibration curve is presented in figure 2.8. The relationship between the height of the peak and the concentration of dopamine in the sample was linear. A calibration of the HPLC-ECD system was required every day prior to the microdialysis experiment. It was done within a range of dopamine concentrations close to those expected to be measured during the experiment.

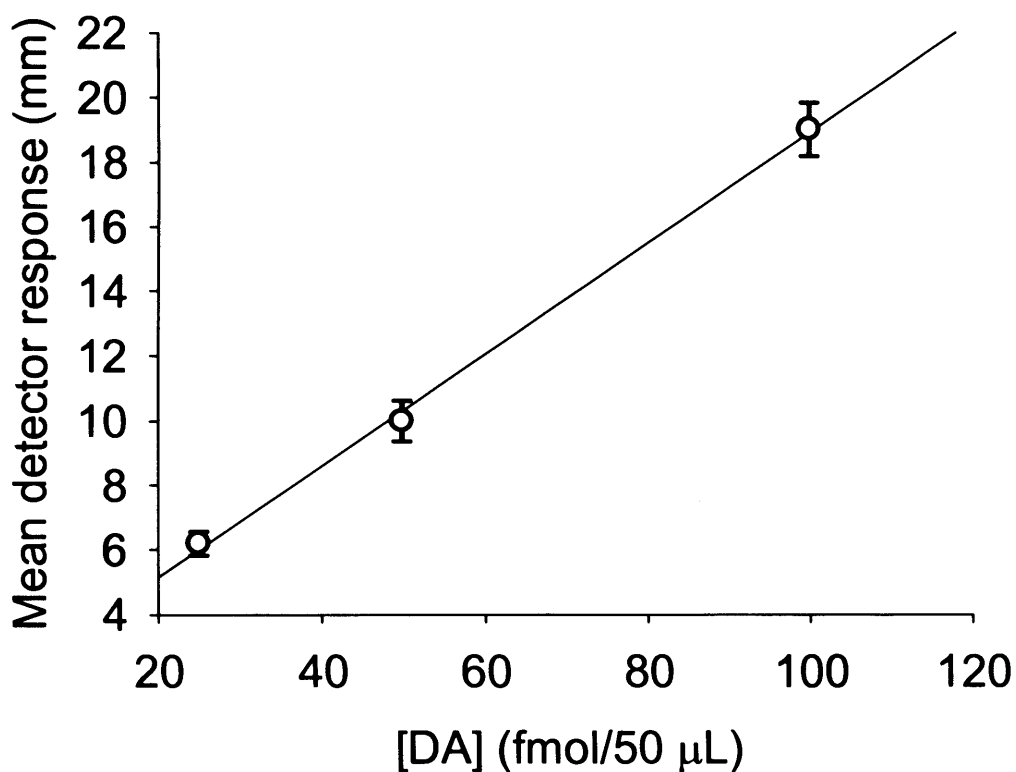


Figure 2.8 Calibration curve for the detection of dopamine in a sample.

The height of the peak representing the oxidation of dopamine was plotted versus the concentration of dopamine in the sample. N=5.

2.6/ DRUG ADMINISTRATION

In this study, 4 different drugs were used:

- *d*-amphetamine sulphate (Sigma, UK)
- haloperidol, 4-[4-(*p*-Chlorophenyl)-4-hydroxy-piperidino]-4'-fluorobutyrophenone (Sigma, UK)
- SCH23390 (Schering, UK)
- dihydrokainate (Tocris, UK)

When given by injection (i.p.), test drugs were dissolved in 0.9 % saline and administered in a volume of 1 ml/kg. When infused locally into the terminal field, *via* the dialysis probe, test drugs were diluted in the perfusate.

Perfusate: Modified Ringers solution:

- NaCl 145 mM
- KCl 4 mM
- CaCl₂ 1.3 mM

2.7/ STATISTICAL ANALYSIS

Statistical analysis of the net change in glutamate efflux was carried out routinely. This was calculated by subtraction of the mean efflux in the 3 consecutive basal samples, collected immediately before drug administration, from all subsequent samples. When comparing drug-induced changes and basals, statistical analysis of the raw data was carried out. The significance of any differences in glutamate efflux was assessed using analysis of variance (ANOVA) with repeated measures on SPSS. 'Time' was considered as a 'within subjects' factor and when comparing the effect of drug treatments on a given brain area, 'drug treatment' was considered as a 'between subjects' factor.

When comparing the effect of a given treatment in the caudal anterior cingulate cortex and rostral anterior cingulate cortex, 'brain area' was considered as a second 'within subjects' factor. When necessary, the Greenhouse-Geisser ' ϵ ' correction was applied to compensate for any violation of sphericity of the variance-covariance matrix.

When drug-induced glutamate efflux was compared with basal levels, the analysis was carried out on bins of three consecutive samples (see results Chapters for specific details of analysis) so as to balance the number of samples in the ANOVA matrix. In all cases, the criterion for significance was set at $P \leq 0.05$.

Chapter 3

3.0/ *d*-Amphetamine has contrasting effects in two subregions of the rat anterior cingulate cortex

3.1/ INTRODUCTION

In vivo microdialysis studies have shown that *d*-amphetamine increases the extracellular concentration of monoamine neurotransmitters in the brain by inhibition of reuptake and retrotransport (see: Chapter 1). Increased extracellular concentrations of monoamines, particularly dopamine, are thought to be responsible for the behavioural effects of *d*-amphetamine, with nigrostriatal and mesolimbic areas considered particularly important (Fuchs *et al.*, 2005; Louis and Clarke, 1998). In an early paper, Kuczenski and Segal (1990) investigated the effects of systemic *d*-amphetamine (0.5-5.0 mg/kg i.p.) on dopamine release in the striatum. They found a rapid, dose-dependent increase in extracellular dopamine. There was also a relationship between *d*-amphetamine-induced increases in behavioural perseveration and the magnitude of the dopamine response.

The effect of *d*-amphetamine on dopamine efflux in different subregions of the rat prefrontal cortex has been systematically studied using microdialysis (Mazei *et al.*, 2002). Dopamine release in response to local infusion of *d*-amphetamine (100 μ M) was found to depend on brain region, with a greater dopamine efflux observed in the prelimbic (Cg3) compared to the anterior cingulate cortex (Cg1 and Cg2; Mazei *et al.*, 2002). The dopamine response to *d*-amphetamine correlated with the dopaminergic

innervation of the prefrontal cortex (a greater density of dopaminergic terminals is found in the deeper layers (i.e. Cg3) when compared to the more superficial layers (i.e. Cg1 and Cg2)). The two subregions also receive dopaminergic inputs from different brain stem nuclei (Lindvall, 1978; Chapter 1). So far, one study has shown an increase in glutamate efflux in the rostral anterior cingulate cortex in response to systemic administration of *d*-amphetamine (2 mg/kg i.p.; Reid *et al.*, 1997). However, no studies to date have compared the effects of *d*-amphetamine on glutamate efflux in subregions of the prefrontal cortex. Given that the source and density of dopaminergic innervation varies in different regions of the prefrontal cortex, any modulation of glutamatergic neurotransmission by dopamine is likely to vary also. If there are subregional differences, this could help explain the various effects of *d*-amphetamine on mood and behaviour.

The rostral anterior cingulate cortex (coordinates: AP +2.5 ML \pm 0.6 DV -4.6) was chosen for these studies as systemic *d*-amphetamine has already been shown to increase glutamate efflux in this subregion (Reid *et al.*, 1997). The neighbouring caudal anterior cingulate cortex (coordinates: AP +1.0 ML \pm 0.6 DV -3.6) was also studied. Figure 3.1 shows the positions of the two microdialysis probes used for these studies. As discussed in Chapter 1, these two subregions have very different functions and I was interested in exploring any variations in neurochemistry, which may underlie these.

Figure 3.1 *Location of the two microdialysis probes in the anterior cingulate cortex in my microdialysis studies. Abbreviations: ACd, dorsal anterior cingulate cortex; ACv, ventral anterior cingulate cortex; PL, prelimbic cortex; IL, infralimbic cortex; RSd, retrosplenial cortex (adapted from Jones et al., 2005).*

Two routes of administration were used in these studies – local infusion and systemic (intraperitoneal) injection. This allowed a comparison of whether glutamate efflux is regulated locally or by afferent inputs. Local infusion delivers the drug directly into the brain area of interest, enabling investigation of drug effects in the terminal fields. After systemic injection, the drug has the potential to affect targets all over the body. The doses of *d*-amphetamine were based on previous studies in this and other laboratories. For local infusion, doses of 1-100 μ M were used, which consistently increase noradrenaline efflux in the frontal cortex of freely-moving rats (Géranton *et al.*, 2003, Wortley *et al.*, 1999). For systemic administration, a dose of 3 mg/kg i.p. was chosen. This dose was found to increase noradrenaline efflux in the frontal cortex of halothane-anaesthetised rats (Wortley *et al.*, 1999) and was within the range of the dose of 2 mg/kg i.p. used in a previous study found to increase glutamate efflux in the rACC (Reid *et al.*, 1997).

3.2/ AIMS

- *To compare whether extracellular glutamate ('efflux') in two adjacent areas of the rat cerebral cortex differs in response to d-amphetamine – the rostral anterior cingulate cortex and the caudal anterior cingulate cortex.*
- *To determine the extent to which the effects of d-amphetamine depend on route of administration.*

3.3/ METHODS

3.3.1/ *In vivo* microdialysis

Experiments were performed on freely-moving rats (250-300g on day of surgery).

Rats were implanted with microdialysis probes in either the cACC or rACC on the day before experimenting. *d*-Amphetamine was dissolved in 0.9 % saline to make a 3 mg/ml solution. This was administered in a volume of 1 ml/kg (i.e. 3 mg/kg). For local infusion, *d*-amphetamine was dissolved in Ringer's to make 1, 10 and 100 μ M solutions. Rats were randomly assigned to one of four treatment groups (see: Table 3.1 for treatment groups). Once stable basal glutamate efflux was established, *d*-amphetamine was administered systemically either, by i.p. injection, or locally infused *via* the dialysis probe by changing the perfusion solution for Ringer's containing the drug. The last three basal samples were designated T₋₄₀-T₀, with infusion or systemic injection of *d*-amphetamine starting immediately after T₀. Microdialysis sampling continued for a further 5 h. The two lowest concentrations of *d*-amphetamine were infused for 80 min each and the highest concentration infused for 160 min. At the end of each experiment animals were deeply anaesthetised using halothane and killed by cervical dislocation. Brains were removed and stored overnight in formalin solution. The next day, probe placement was verified under a light microscope. The concentration of glutamate in brain dialysates is expressed as pmol/20min without correction for recovery. In addition to analysing the raw data, net changes were calculated by subtracting the mean of the last 3 basal samples from all samples in the time course. The calculation of net changes in glutamate efflux

allowed any differences between two groups to be shown clearly, if there were slight variations in basal glutamate efflux between the two groups i.e. the data were normalised. The calculation of net efflux also has less propensity to distort the data, when compared to percentage change.

Table 3.1 *Treatment groups for d-amphetamine administration.* Rats were randomly assigned to one of four treatment groups.

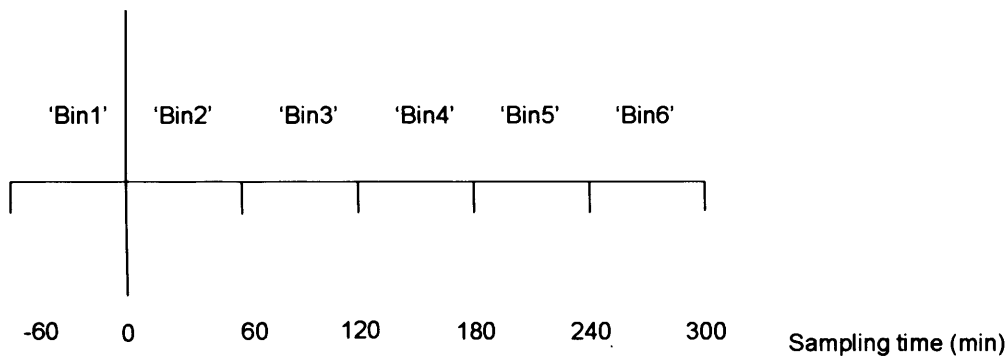
GROUP	BRAIN REGION		ROUTE OF ADMINISTRATION	
	cACC	rACC	Local infusion	Sytemic
1 (N = 10)	X		X	
2 (N = 10)		X	X	
3 (N = 11)	X			X
4 (N = 10)		X		X

3.3.2/ *Statistical analysis*

All data were analysed for significance using two-way ANOVA with repeated measures. For each experiment, ‘time’ was a ‘within subjects’ factor and ‘route of drug administration’ and ‘brain region’ (i.e. local infusion vs. systemic administration and rACC vs.cACC) were ‘between subjects’ factors.

For systemic administration, data were divided into six 'bins' with three consecutive samples per bin. Therefore, each bin represents 1 h of sampling after injection of *d*-amphetamine (Figure 3.2). 'Bin' was second 'within subjects' factor.

Figure 3.2 Time bins for statistical analysis of changes in extracellular glutamate after systemic (*i.p.*) injection of *d*-amphetamine.



For local infusion, data were divided into four 'bins' with four consecutive samples per bin (each bin therefore corresponded to infusion of one concentration of *d*-amphetamine; Figure 3.3). 'Bin 1' represents basal efflux (i.e. $T_{40}-T_0$). For bins representing glutamate efflux during drug infusion, the last three samples during each concentration of drug were used. Therefore, bin 2 = 1 μM ($T_{40}-T_{80}$), bin 3 = 10 μM ($T_{120}-T_{160}$), bin 4 = 100 μM ($T_{200}-T_{240}$) and bin 5 = 100 μM ($T_{280}-T_{320}$). 'Bin' was a second 'within subjects' factor. The Greenhouse-Geisser ' ϵ ' correction was performed where Mauchley's test of sphericity was significant.

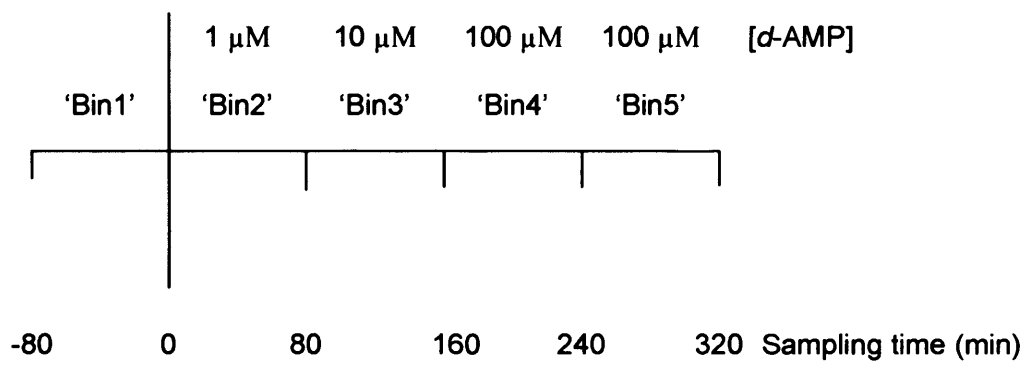


Figure 3.3 Time bins for statistical analysis of changes in extracellular glutamate after local infusion of *d*-amphetamine.

3.4/ RESULTS

3.4.1/ *Basal glutamate efflux*

Mean basal glutamate efflux in the rACC (across both treatment groups) was 12.7 ± 1.4 pmol/20min and in the cACC was 10.2 ± 1.1 pmol/20min. For clarity, the effects of local infusion and systemic administration of *d*-amphetamine will be discussed separately, despite rats being randomised to the 4 treatment groups.

3.4.2/ *Effects of local infusion (via retrodialysis) of increasing concentrations of d-amphetamine on glutamate efflux.*

There was no difference in basal glutamate efflux in the cACC and the rACC of animals destined for local infusion of *d*-amphetamine (i.e. between groups 1 and 2). Basal glutamate efflux obtained from the pooled data was 14.7 ± 1.3 pmol/20min for the rACC and 12.1 ± 1.5 pmol/20min for the cACC.

After infusion of $100 \mu\text{M}$ *d*-amphetamine, 3-way ANOVA revealed a significant BIN*SUBREGION interaction – $F(1,18)=4.600$ $P<0.05$. At this concentration, there was also a main effect of BIN – $F(1,18)=4.274$ $P<0.05$, and SUBREGION – $F(1,18)=4.577$ $P<0.05$.

Local infusion of *d*-amphetamine increased glutamate efflux in the rACC. This increase attained statistical significance after infusion of $1 \mu\text{M}$ *d*-amphetamine and was dose-related (see: Table 3.2 for statistical analysis). A maximum net increase of 14 ± 9 pmol/20 min was reached after infusion of the highest concentration of

d-amphetamine (100 μ M). However, the glutamate response to each concentration of *d*-amphetamine was phasic in nature, and declined in amplitude during subsequent sampling. Infusion of a higher concentration of *d*-amphetamine caused a resurgence of the glutamate response, which peaked after two samples and declined rapidly thereafter (Figure 3.4).

In the cACC, there was no increase in glutamate efflux after infusion of any concentration of *d*-amphetamine (Figure 3.4 and see: Table 3.2 for statistical analysis).

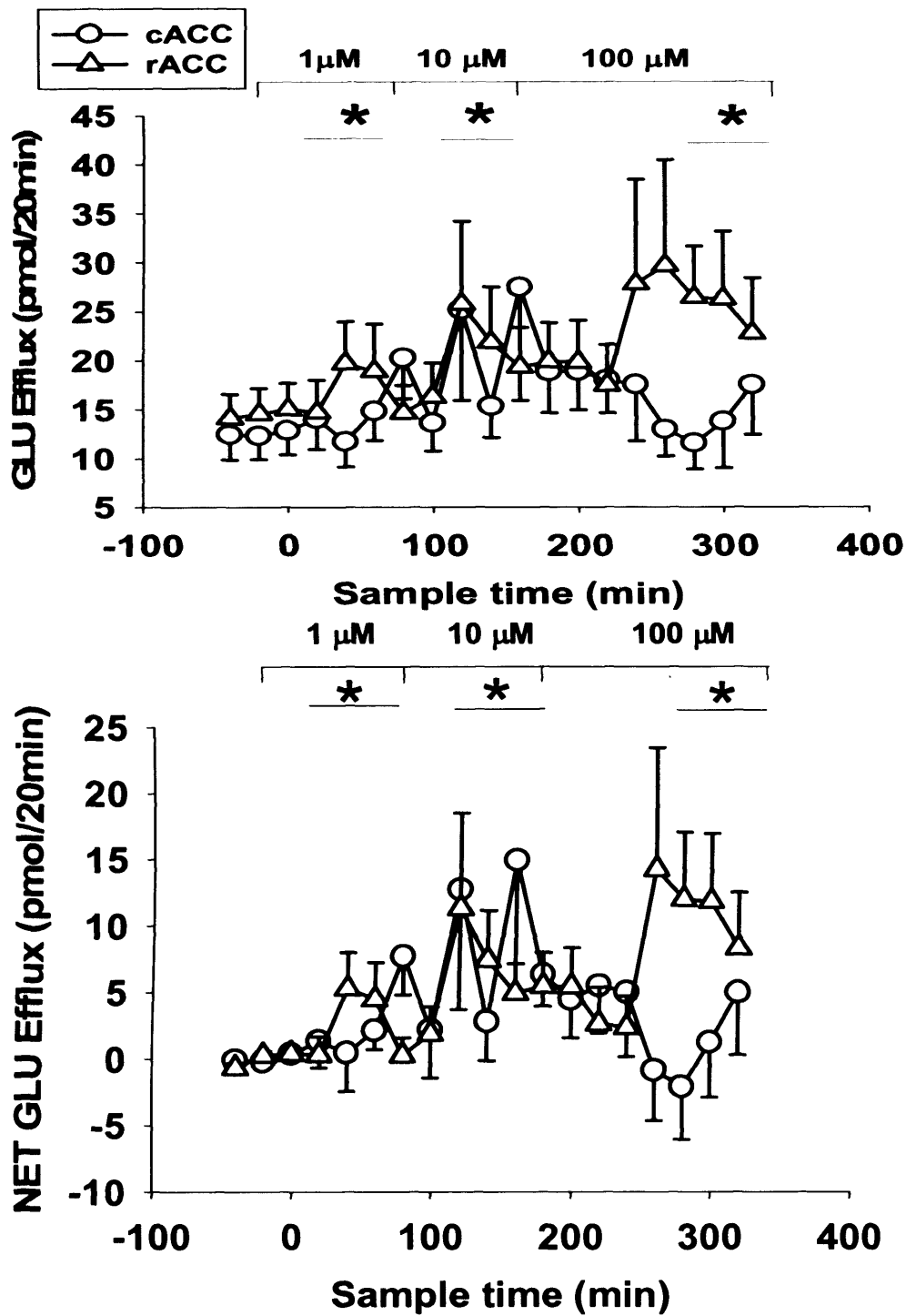


Figure 3.4 The effects of local infusion (via retrodialysis) of increasing concentrations of *d*-amphetamine on glutamate ('GLU') efflux in the cACC or rACC of freely-moving rats. The top graph shows raw data and the bottom graph net data set. * $P < 0.05$.

d-Amphetamine infusion was initiated at T_0 , as indicated by the line. GLU efflux is expressed as pmol/20min. Points show mean \pm s.e. mean GLU efflux in the cACC (open circles) and the rACC (open triangles). $N=10$ in each group.

Table 3.2 Statistics generated from split-plot ANOVA summarising the effect of local infusion of *d*-amphetamine (*'d-AMP'*) on glutamate efflux, in the *cACC* and the *rACC*. Glutamate efflux after each treatment was compared, over 4-sample increments, with efflux in the cluster of basal samples. Significant differences are shown in **bold**.

Treatment	<i>d</i> -AMP (local infusion)	
	<i>rACC</i>	<i>cACC</i>
[<i>d</i> -AMP] (μM)		
1 μM	F(1,9)=4.857 $P<0.05$	F(1,7)=0.209 $P<0.7$
10 μM	F(1,9)=5.155 $P<0.05$	F(1,8)=1.165 $P<0.3$
100 μM	F(1,8)=3.783 $P<0.1$	F(1,9)=3.188 $P<0.1$
100 μM	F(1,9)=5.770 $P<0.04$	F(1,9)=0.006 $P<0.9$

3.4.3/ Effects of systemic injection of d-amphetamine on glutamate efflux.

There was no difference in basal efflux between the cACC and the rACC of animals destined for intraperitoneal injection of *d*-amphetamine (i.e. between groups 3 and 4). Basal glutamate efflux obtained from the pooled data was 9.1 ± 0.9 pmol/20min for the cACC and 10.4 ± 1.0 pmol/20min for the rACC. To minimise suffering and reduce the number of animals used, saline controls were not included in all my experiments. Also, I was only interested in comparing subregional differences in the response to *d*-amphetamine, rather than comparing drug and saline effects. It would have been advantageous to include saline controls during these experiments to determine if the *d*-amphetamine effect was real. In the cACC injection of saline did not affect glutamate efflux at any time (see: Chapter 6, Figure 6.3). In the rACC, injection of saline increased glutamate efflux during the first 2 h of sampling. However, this quickly returned to basal levels for the remainder of the sampling time (see: Chapter 6, Figure 6.5).

Intraperitoneal injection of 3 mg/kg *d*-amphetamine caused a gradual increase in glutamate efflux in the anterior cingulate cortex with a maximum net increase (at T₈₀), of 11.1 ± 7 pmol/20min (Figure 3.5). Efflux remained greater than basal for the remainder of the sampling time (see: Table 3.3 for statistical analysis). In contrast, there was no increase in glutamate efflux in the rACC at any time (see: Table 3.3 for statistical analysis). Despite the lack of any effect on glutamate efflux in the rACC, it is notable that there were frequent fluctuations in extracellular glutamate (Figure 3.5).

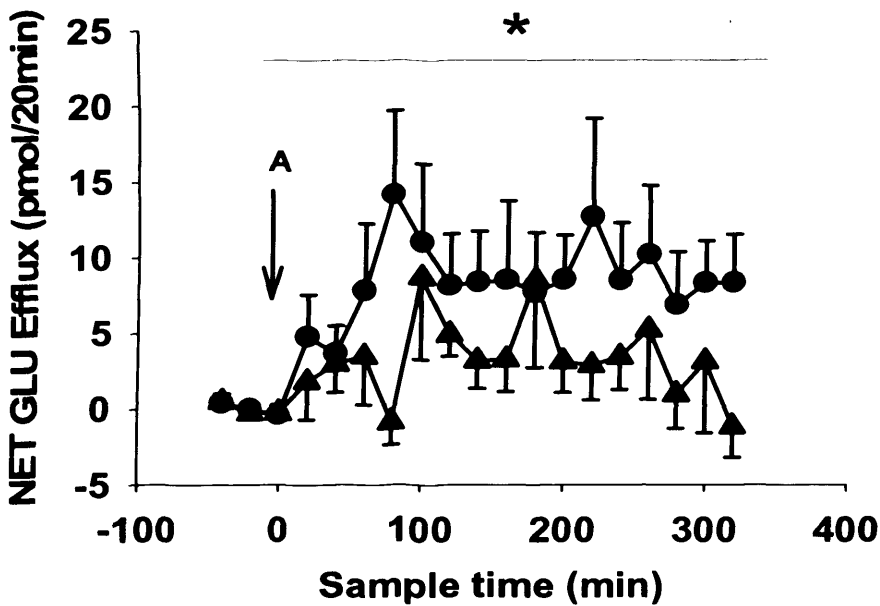
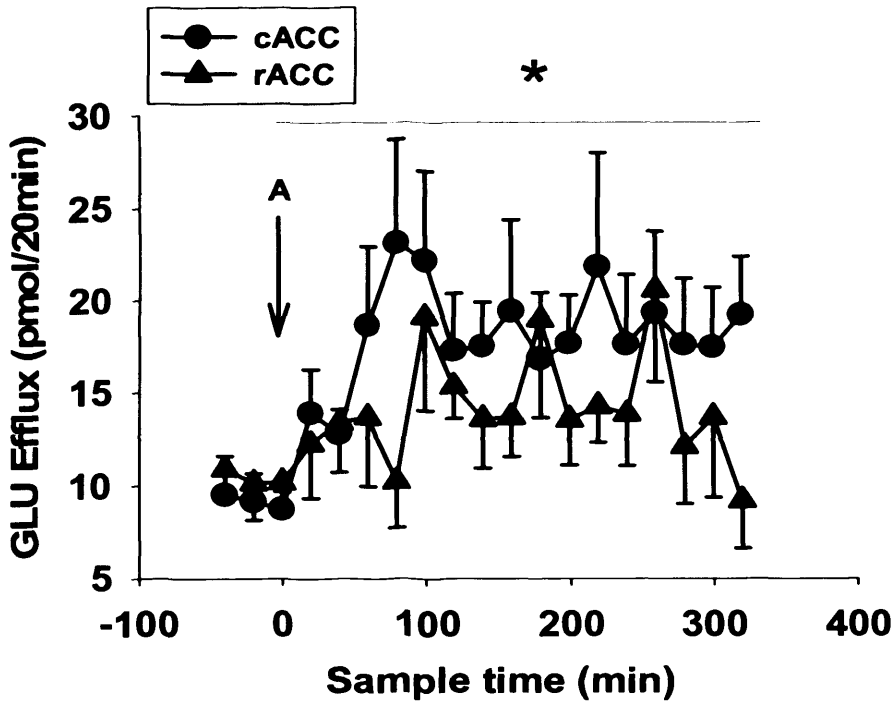


Figure 3.5 The effects of intraperitoneal (3 mg/kg) administration of *d*-amphetamine on glutamate ('GLU') efflux in the cACC or rACC of freely-moving rats. The top graph shows raw data and the bottom graph net data set. * $P < 0.05$.

d-Amphetamine was administered at T0, as indicated by the arrow. GLU efflux is expressed as pmol/20min. Points show mean \pm s.e. mean GLU efflux in the cACC and the rACC. N=10/11 in each group.

Table 3.3 Statistics generated from split-plot ANOVA summarising the effects of administration of *d*-amphetamine ('*d*-AMP') 3 mg/kg *i.p.* on glutamate efflux in the *cACC* and *rACC* (main effect of 'BIN'). Glutamate efflux after each treatment was compared, over 1-h increments, with efflux in the cluster of basal samples. Significant differences are in **bold**.

Treatment	<i>d</i> -AMP 3 mg/kg N=10/11	
	<i>rACC</i>	<i>cACC</i>
Time		
T ₂₀ -T ₆₀	F(1,7)=0.759 <i>P</i> <0.4	F(1,9)=8.591 <i>P</i><0.02
T ₈₀ -T ₁₂₀	F(1,9)=2.298 <i>P</i> <0.2	F(1,8)=8.398 <i>P</i><0.02
T ₁₄₀ -T ₁₈₀	F(1,9)=3.908 <i>P</i> <0.08	F(1,10)=6.273 <i>P</i><0.03
T ₂₀₀ -T ₂₄₀	F(1,9)=2.804 <i>P</i> <0.1	F(1,20)=5.896 <i>P</i><0.04
T ₂₆₀ -T ₃₀₀	F(1,9)=1.160 <i>P</i> <0.3	F(1,20)=8.392 <i>P</i><0.02

3.5/ DISCUSSION

One previous study has reported increases in glutamate efflux in the cingulate region of the rat prefrontal cortex after systemic injection or local infusion of *d*-amphetamine (Reid *et al.*, 1997). So far, none has investigated the effect of *d*-amphetamine on glutamate efflux in the cACC. Here, single-probe microdialysis was used to compare the effects of *d*-amphetamine in the rACC and cACC, providing a qualitative and quantitative comparison of the glutamate response to systemic and local *d*-amphetamine in different areas of the rat cortex. The results of this study reveal marked regional differences in the glutamate response to *d*-amphetamine.

The first finding was that local infusion of *d*-amphetamine increased glutamate efflux in the rACC, but there was no response in the cACC. The second finding was that systemic *d*-amphetamine increased glutamate efflux in the cACC, but there was no response in the rACC. The effects of systemic *d*-amphetamine were investigated at a dose within the range of that reported to increase glutamate efflux in the cerebral cortex of awake rats (2 mg/kg i.p.; Reid *et al.*, 1997). This result is not in agreement with the one previous study looking at the effect of systemic *d*-amphetamine on glutamate efflux in the rACC (Reid *et al.* 1997). However, this is the first time that such a variation in the glutamate response to *d*-amphetamine in these two adjacent subregions of the rat frontal cortex has been reported. The reasons for these reciprocal differences are as yet unclear but will be investigated in experiments in the following chapters.

3.5.1/ Possible sources of glutamate (where increased efflux is observed)

Glutamatergic pyramidal neurones are abundant in the frontal cortex, constituting approximately 80 % of the cell types in this brain region. There is also a dense glutamatergic projection to this region from the mediodorsal nucleus (MD) of the thalamus (Groenewegen *et al.*, 1997). Glutamate is a fast excitatory neurotransmitter within the brain and is released from neurones with a latency of microseconds, reaches a high concentration within the synaptic cleft and gives rise to synaptic potentials with millisecond durations (Fillenz, 2005). The action of glutamate is terminated by the highly efficient uptake system surrounding the synapse, which means there is little overflow of glutamate from the synapse into the extracellular space (Kanai and Hediger, 2003).

A neuronal origin for the increased extracellular glutamate in the rACC, after local infusion of *d*-amphetamine, and the cACC, after systemic administration of *d*-amphetamine, cannot be ruled out. This could either be a direct effect of *d*-amphetamine on neuronal glutamate transporters (causing impulse-independent release)/vesicular glutamate transporters (causing impulse-dependent release) or an indirect effect.

The indirect effect of *d*-amphetamine could be mediated by monoamine neurotransmitters (see: Chapter 1 for pharmacology of *d*-amphetamine). The effect of monoamine neurotransmitters on glutamatergic neurotransmission has been widely studied (see: Chapter 1). For example, hallucinogenic drugs, such as lysergic acid diethylamide (LSD) increase glutamate efflux in the medial prefrontal cortex through the activation of postsynaptic 5-HT_{2A} receptors on the terminals of glutamatergic pyramidal cells (Muschamp *et al.*, 2004). *d*-Amphetamine acts on the serotonin

transporter to increase release of 5-HT in the brain. An involvement of dopamine in *d*-amphetamine-induced release of glutamate is also a possibility. The role of dopamine in the rACC is complex and electrophysiological studies have demonstrated both inhibitory and excitatory effects of dopamine on glutamatergic pyramidal cell excitability (Gonzalez-Islas and Hablitz, 2003, Gullledge and Jaffe, 1998, see: Chapter 1). Such studies show that the action of monoamine transmitters at their receptors can indirectly evoke increases in glutamatergic transmission.

Glial cells have been suggested as an alternative source of glutamate in the subcortical areas, such as the striatum (Baker *et al.*, 2002) and a number of mechanisms for release, leading to increased extracellular glutamate, have been identified:

1. Reversal of uptake by glutamate transporters (Szatkowski *et al.*, 1990)
2. Ca^{2+} -dependent exocytosis (Parpura *et al.*, 1994)
3. Anion channel opening induced by cell swelling (Kimelberg *et al.*, 1990)
4. Glutamate exchange via the cystine-glutamate antiporter (Warr *et al.*, 1999)
5. Diffusional release through ionotropic purinergic receptors (Duan *et al.*, 2003)
6. Functional 'hemichannels' or unpaired connexons on the cell surface (Ye *et al.*, 2003)

In subsequent experiments, I shall focus on the first two theories. Glutamate is released through the high-affinity Na^+ -dependent transporter, GLT-1, located in the astrocyte membrane, leading to increased extracellular concentrations. However, there is no alteration in the expression of the glutamate transporter subtypes GLT-1 and EAAC1 (quantified by Western blotting) in the rat prefrontal cortex after either

acute or chronic exposure to *d*-amphetamine (Sidiropoulou *et al.*, 2001). There is no evidence in the literature that *d*-amphetamine binds directly to this transporter, although blockade of GLT-1 does lead to increased extracellular glutamate in the rat striatum (Fallgren and Paulsen, 1996). It is possible that *d*-amphetamine influences this transporter indirectly to increase release of glutamate.

Expression of a number of neurotransmitter receptors in the membrane of astrocytes renders them sensitive to changes in the extracellular concentrations of these neurotransmitters. There is evidence of glutamatergic, GABAergic, adrenergic, purinergic, serotonergic, muscarinic and peptidergic receptors on astrocytes *in situ* and *in vivo* (for review, see Porter and McCarthy, 1997). Stimulation of group I metabotropic glutamate receptors (mGluRs) can trigger an increase in intracellular Ca^{2+} , which has complex temporal and spatial patterns (Cai *et al.*, 2000). Astrocytes are connected by gap junctions, channels allowing the passage of ions between coupled cells, providing a pathway for direct, intercellular communication. These gap junctions allow the propagation of Ca^{2+} waves, which lead to release of glutamate from the astrocytes. Such Ca^{2+} -mediated release of glutamate has been demonstrated *in vitro* with cultured cortical astrocytes (Parpura *et al.*, 1994) and has many features common to vesicular exocytosis in nerve terminals. In fact astrocytes express the many of the proteins required for vesicular release of neurotransmitter (Wilhelm *et al.*, 2004). The function of this astrocytic-derived glutamate is not yet clear. However, it may be involved in the spatial coordination and synchronisation of neuronal activity and synaptic networks (Fellin *et al.*, 2004).

3.5.2/ Possible explanations for regional differences in the response to *d*-amphetamine

Since local infusion of *d*-amphetamine had no effect, actions upstream of the cACC must explain the increased glutamate efflux seen in this subregion. The differences in the two subregions suggest that the rACC and cACC may receive inputs from different subcortical nuclei, with different excitatory and inhibitory influences. The noradrenergic innervation (derived from the locus coeruleus) of the rat cerebral cortex is known to be homogeneous to all cortical subregions (Lindvall *et al.*, 1978, Audet *et al.*, 1988). Therefore, regional variation in noradrenergic innervation is unlikely to explain the differential glutamate response to *d*-amphetamine. The different subregions of the prefrontal cortex receive dopaminergic innervation from different parts of the A10 cell group (Lindvall *et al.*, 1978). This regional variation in dopamine innervation is a strong candidate for investigation when attempting to explain the differences in the glutamate response to *d*-amphetamine. Differences in the serotonergic innervation of the cerebral cortex have also been demonstrated with the highest densities observed in the Cg3, when compared to Cg2 (Audet *et al.*, 1989). However, as discussed in Chapter 1, *d*-amphetamine has a much lower affinity for SERT compared to NET and DAT (see Tables 1.3 and 1.4).

Histochemical studies have demonstrated the presence of inhibitory heteroreceptors in glutamatergic nerve terminals. These include the D₂-like receptor and the 5-HT_{1A} receptor (Vincent *et al.*, 1993, Kia *et al.*, 1996): stimulation of these receptors decreases terminal release of glutamate into the rACC, as measured by microdialysis. These receptors are also present on the cell bodies of pyramidal cells, where they decrease the firing rate of glutamatergic neurones (Arandeda and Andrade,

1991, Gullledge and Jaffe, 1998). Where no increase in cortical glutamate efflux is seen after administration of *d*-amphetamine, this could be explained by activation of monoamine heteroreceptors by the increase in extracellular glutamate.

A final possibility is that there may be a more efficient transport system for clearance of glutamate in the cACC compared to the rACC. Indeed, regional differences in the glutamate response to local infusion of glutamate transport inhibitor have been demonstrated (Semba and Wakuta, 1998). Differential distributions of glutamate transporters in the two subregions could explain any differences in the glutamate response to *d*-amphetamine. Any or all of these possibilities may explain the regional difference in the glutamate response to *d*-amphetamine.

3.5.3/ Summary of key findings

- Systemic administration of *d*-amphetamine increases glutamate efflux in the caudal anterior cingulate cortex, but not the rostral anterior cingulate cortex.
- Local infusion of *d*-amphetamine increases glutamate efflux in the rostral anterior cingulate cortex, but not the caudal anterior cingulate cortex

Chapter 4

4.0 Contrasting effects of *d*-amphetamine on dopamine efflux and dopamine on glutamate efflux in two subregions of the anterior cingulate cortex

4.1/ INTRODUCTION

In the previous experiments, the glutamate response to *d*-amphetamine depended on both route of administration and subregion. Systemic administration of *d*-amphetamine increased glutamate efflux in the cACC, but not the rACC, while local infusion of *d*-amphetamine increased glutamate efflux in the rACC, but not the cACC (see: Chapter 3). Here, I explored in more detail the mechanisms underlying the glutamate response in the anterior cingulate cortex. One of the main pharmacological effects of *d*-amphetamine is to increase impulse-independent release of dopamine in various brain regions by reversal of the dopamine reuptake transporter (DAT). Therefore, any effects of *d*-amphetamine on the glutamatergic system could be secondary to an increase in dopaminergic neurotransmission.

To explore this possibility, I first investigated the effect of *d*-amphetamine on dopamine efflux in the cACC and the rACC. A lack of increase of dopamine efflux by *d*-amphetamine would invalidate the hypothesis outlined above. The effects of both local infusion (10 and 100 μ M) and systemic injection (3 mg/kg i.p.) of *d*-amphetamine on dopamine efflux in the cACC and the rACC were investigated. These doses/concentrations were based on our previous experiments, which demonstrated a clear increase in glutamate efflux at these concentrations (see: Chapter 3).

Finally, we explored the effect of dopamine on glutamate efflux in the cACC and the rACC. The simplest way to achieve this is to infuse a solution of dopamine directly down the microdialysis probe into the cortex. One previous microdialysis study has investigated the effect of infusion of dopamine on noradrenaline efflux in the prefrontal cortex (Pan *et al.*, 2004). This demonstrated an increase in extracellular noradrenaline on infusion of 12, 20 and 40 nM dopamine. Similar concentrations of dopamine were chosen for this study, including solutions with two-fold higher concentrations.

4.2/ AIMS

- *To discover whether local infusion of d-amphetamine affects dopamine efflux in the cACC and/or the rACC.*
- *To discover whether systemic injection of d-amphetamine affects dopamine efflux in the cACC and/or the rACC.*
- *To discover whether local infusion of dopamine increases glutamate efflux in the cACC and/or the rACC.*

4.3/ METHODS

4.3.1/ Experiment 1 – Effects of local infusion of d-amphetamine on dopamine efflux in the cACC and rACC

Rats were implanted with microdialysis probes in both the cACC and the rACC on the day before experimenting i.e. dual-probe microdialysis was performed. For local infusion, *d*-amphetamine was dissolved in Ringer's solution to make 10 and 100 μM concentrations. Once stable basal dopamine efflux was established, 10 μM *d*-amphetamine was locally infused *via* the probe for 2 h, followed by Ringer's solution for 1 h and finally 100 μM *d*-amphetamine for 2 h.

4.3.2/ Experiment 2 – Effects of systemic injection of d-amphetamine on dopamine efflux in the cACC and rACC

Rats were implanted with microdialysis probes in both the cACC and the rACC on the day before experimenting i.e. dual-probe microdialysis was performed. This allows a direct, simultaneous comparison of the effects of *d*-amphetamine on dopamine efflux in both brain regions. For systemic injection, *d*-amphetamine was dissolved in 0.9 % saline to make a 3 mg/ml solution. This was administered in a volume of 1 ml/kg (i.e. 3 mg/kg). Once stable basal dopamine efflux was established, *d*-amphetamine was administered systemically by intraperitoneal injection. Microdialysis sampling continued for a further 5 h.

4.3.3/ Experiment 3 – Effects of local infusion of increasing concentrations of dopamine on glutamate efflux in the cACC and rACC

Rats were implanted with microdialysis probes in both the cACC and the rACC on the day before experimenting i.e. dual-probe microdialysis was employed. Dopamine was dissolved in Ringer's solution to make concentrations of 0.05, 0.5, 5 and 50 μM . These concentrations were based on a previous microdialysis study where an increase in noradrenaline efflux was seen after infusion of dopamine concentrations within this range (Pan *et al.*, 2004). Once basal glutamate efflux was established and at least three stable basal samples taken, dopamine was infused locally *via* the dialysis probe by substituting the perfusion solution for Ringer's containing dopamine. Four successive concentrations from 0.05-50 μM were infused for 80 min each.

4.3.4/ Statistical analysis

For experiment 1 (local infusion of *d*-amphetamine) both 'time' and 'brain region' were 'within subjects' factors. The data were divided into five 'bins' with three consecutive samples per bin (each bin corresponded to one hour of infusion of *d*-amphetamine or Ringer's solution; Figure 4.1) and 'bin' was a 'within subjects' factor.

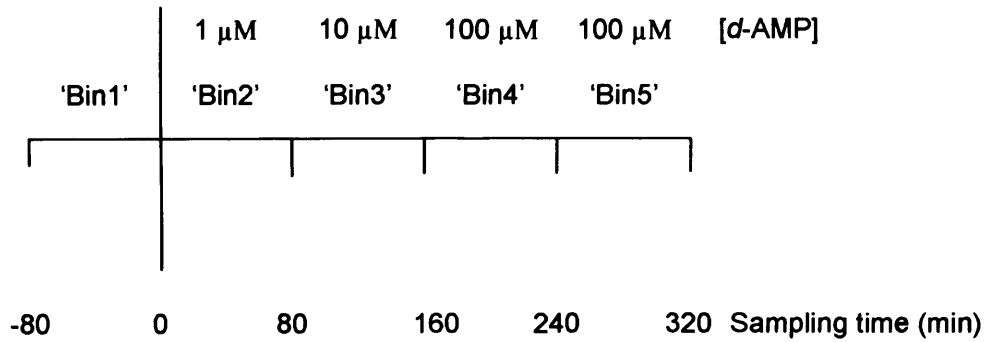


Figure 4.1 Time bins for statistical analysis of changes in extracellular dopamine after local infusion of *d*-amphetamine.

For experiment 2 (systemic *d*-amphetamine), ‘time’ was a ‘within subjects’ factor and ‘treatment’ was a ‘between subjects’ factor. The data were divided into six ‘bins’ with three consecutive samples per bin (each bin therefore corresponded to one hour of sampling after injection of *d*-amphetamine; Figure 4.2) and ‘bin’ was a ‘within subjects’ factor.



Figure 4.2 Time bins for statistical analysis of changes in extracellular dopamine after systemic (*i.p.*) injection of *d*-amphetamine.

For experiment 3 (dopamine infusion), both ‘time’ and ‘brain region’ (i.e. cACC or rACC) were ‘within subjects’ factors. The data were divided into five ‘bins’ with four consecutive samples per bin (each bin therefore corresponded to infusion of one concentration of dopamine; Figure 4.3) and ‘bin’ was a ‘within subjects’ factor. ‘Bin 1’ represents basal efflux (i.e. T_{-40} - T_0). For the purposes of the statistical analysis, the

last three samples during infusion of each concentration of dopamine were used. Therefore, 'bin 2' = $0.05\mu\text{M}$ (T_{40} - T_{80}), 'bin 3' = $0.5\mu\text{M}$ (T_{120} - T_{160}), 'bin 4' = $5\mu\text{M}$ (T_{200} - T_{240}) and 'bin 5' = $50\mu\text{M}$ (T_{280} - T_{320}).

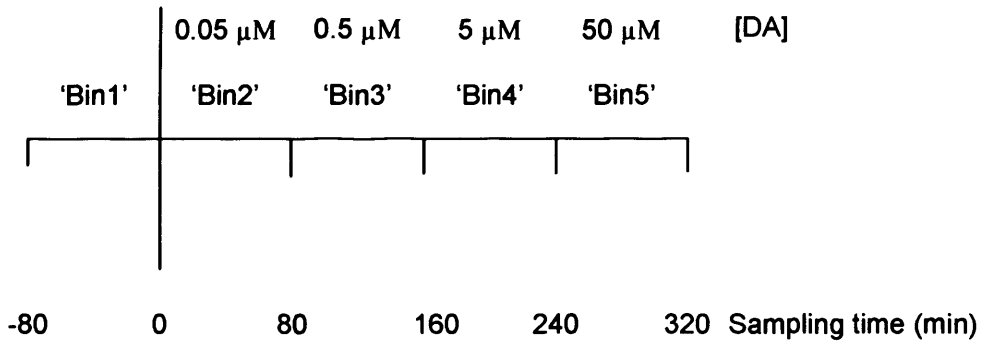


Figure 4.3 Time bins for statistical analysis of changes in extracellular glutamate after local infusion of dopamine solution.

The Greenhouse-Geisser ϵ -correction was performed where Mauchley's test of Sphericity was significant.

4.4/ RESULTS

4.4.1/ *Experiment 1 – Effects of local infusion of d-amphetamine on dopamine efflux in the cACC and rACC*

There was no difference in basal efflux of dopamine in the cACC and the rACC of animals destined for local infusion of *d*-amphetamine. Basal efflux of dopamine of the pooled data (from the group given local *d*-amphetamine only) was 13.6 ± 4.5 fmol/20min for the cACC and 15.7 ± 1.5 fmol/20min for the rACC.

Infusion of $10 \mu\text{M}$ *d*-amphetamine, via the microdialysis probe, starting at T_0 , caused an immediate increase in dopamine efflux in the rACC (see Figure 4.4). The maximum increase was reached at T_{40} (33 ± 11 fmol/20min) and this was sustained for the remainder of the infusion (2 h). Subsequent infusion of Ringer's, starting at T_{140} for 1 h, led to a progressive decrease in dopamine efflux. On infusion of $100 \mu\text{M}$ *d*-amphetamine, an immediate resurgence of the dopamine response was seen, with a maximum increase seen at T_{260} (63 ± 21 fmol/20min) i.e. the amplitude of the dopamine response was dose-related. Again, this increase in extracellular dopamine was sustained for the remainder of the *d*-amphetamine infusion (Figure 4.4 and see: Table 4.1 for statistical analysis).

No significant increase in dopamine efflux was observed in the cACC at any time (Figure 4.4 and see: Table 4.1 for statistical analysis).

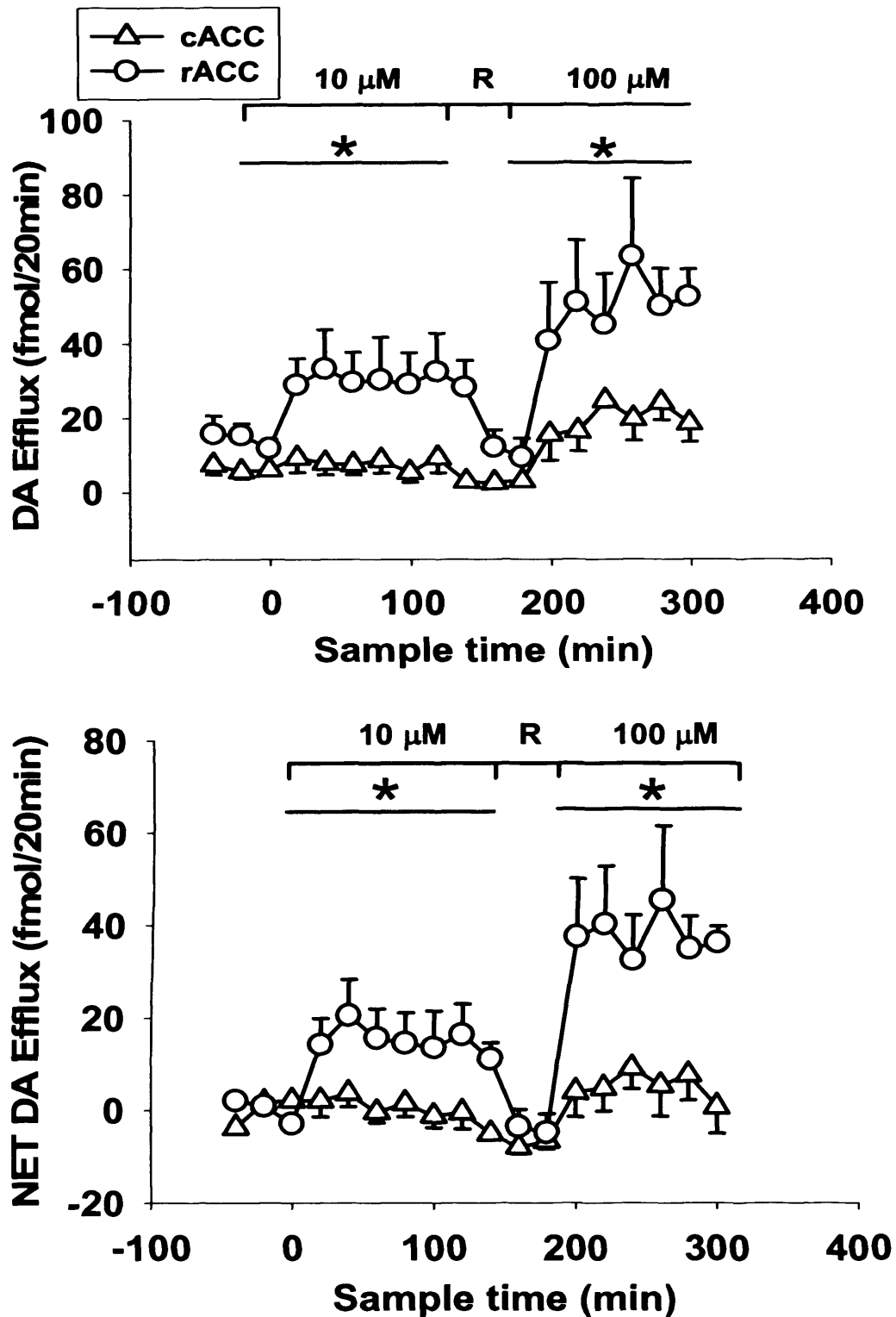


Figure 4.4 Effects of local infusion (via retrodialysis) of increasing concentrations of *d*-amphetamine on dopamine ('DA') efflux in cACC and rACC of freely-moving rats.

The top graph shows raw data and the bottom graph shows net data set. *d*-Amphetamine infusion was initiated at T_0 as indicated by the line. Points show mean \pm s.e. mean DA efflux in the cACC (open triangles) and rACC (open circles). R=Ringer's. N=7. * - $P < 0.05$.

Table 4.1 Statistics generated from split-plot ANOVA summarising the effects of local infusion of *d*-amphetamine on dopamine efflux in the cACC and rACC.

Treatment	<i>d</i> -Amphetamine (local infusion)	
	cACC	rACC
<i>[d</i> -AMP] μ M		
10 (1 st hour)	F(1,6)=0.550 <i>P</i> <0.5	F(1,6)=9.124 <i>P</i><0.02
10 (2 nd hour)	F(1,6)=0.001 <i>P</i> <0.9	F(1,6)=6.320 <i>P</i><0.05
Ringers	F(1,6)=4.094 <i>P</i> <0.1	F(1,5)=0.513 <i>P</i> <0.5
100 (1 st hour)	F(1,5)=0.663 <i>P</i> <0.5	F(1,6)=11.044 <i>P</i><0.02
100 (2 nd hour)	F(1,4)=0.076 <i>P</i> <0.8	F(1,6)=58.180 <i>P</i><0.000

Dopamine efflux after each treatment was compared, over 1-h increments with efflux in the cluster of basal samples. Significant differences are highlighted in **bold**.

Significant BIN*SUBREGION interactions were seen at both concentrations of *d*-amphetamine – T₂₀-T₆₀ F(1,6)=6.293 *P*<0.046, T₈₀-T₁₂₀ F(1,6)=5.699 *P*<0.05, T₂₆₀-T₃₀₀ F(1,4)=14.430 *P*<0.02.

4.4.2/ Experiment 2 – Effects of systemic administration of *d*-amphetamine on dopamine efflux in the cACC and the rACC

There was no difference in basal dopamine efflux in the cACC and the rACC of animals destined for intraperitoneal injection of *d*-amphetamine. Basal efflux of dopamine obtained from the pooled data (for the group given systemic *d*-amphetamine only) was 5.7 ± 0.8 fmol/20min for the cACC and 4.4 ± 0.4 fmol/20min for the rACC.

4.4.2.1/ The rostral anterior cingulate cortex

Systemic injection of saline did not alter dopamine efflux in the rACC (see Figure 4.5). Injection of *d*-amphetamine caused an immediate increase in dopamine efflux, which reached a maximum of 27 ± 8 fmol/20min at T₄₀. Efflux remained greater than that in the basal samples for the next 2 h at least (Figure 4.5 and see: Table 4.2 for statistical details). There was a significant BIN*DRUG interaction during the first and second hours after injection – T₂₀-T₆₀ F(1,7)=8.366 $P<0.02$, T₈₀-T₁₂₀ F(1,5)=7.946 $P<0.04$.

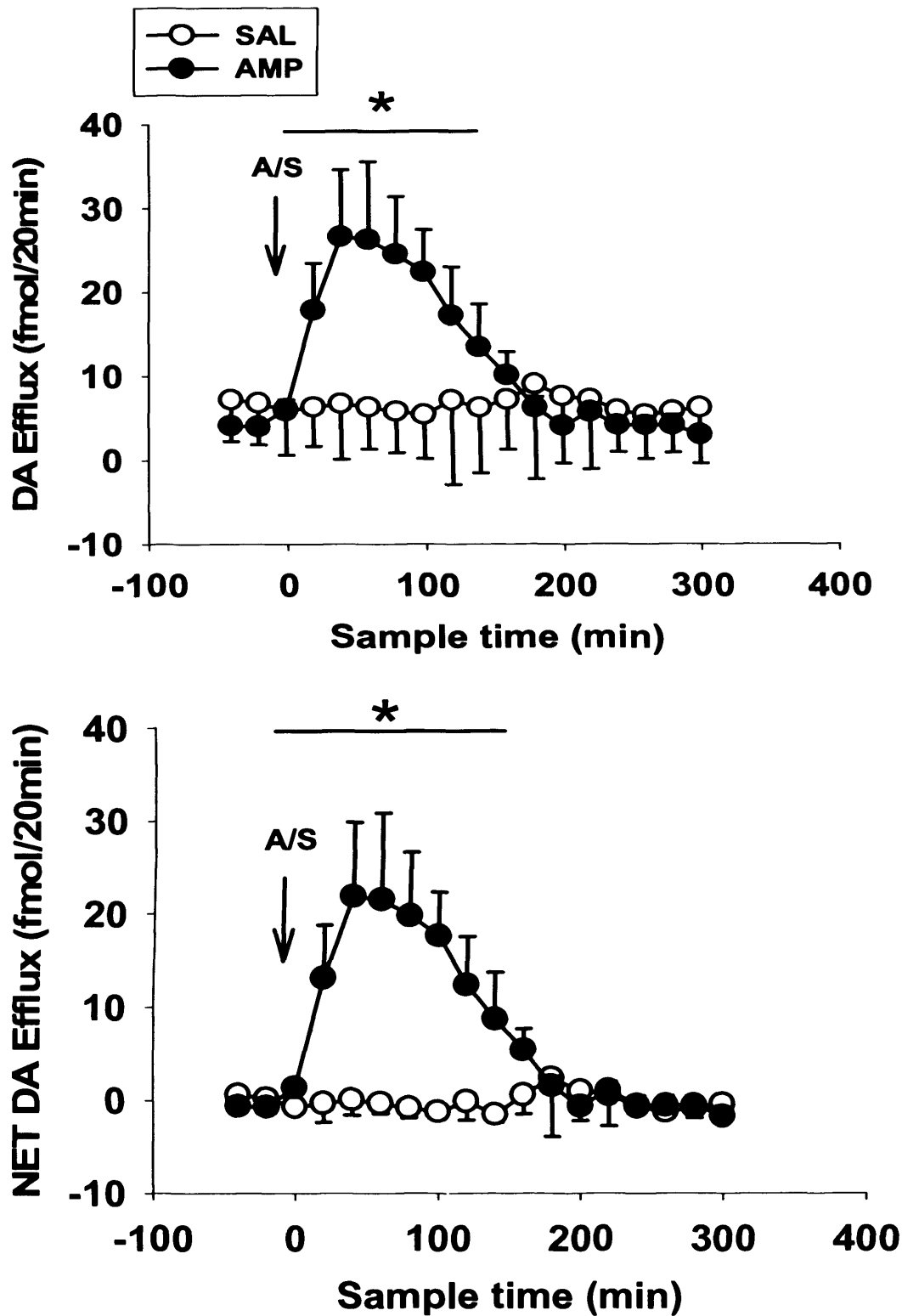


Figure 4.5 Effects of intraperitoneal (3 mg/kg) administration of *d*-amphetamine or saline (1 ml/kg) on dopamine ('DA') efflux in the rACC of freely-moving rats.

The top graph shows raw data and the bottom graph net data set. *d*-Amphetamine was administered at T₀, as indicated by the arrow. DA efflux is expressed as fmol/20min. Points show mean ± s.e. mean DA efflux in the rACC after administration of saline (closed circles) or *d*-amphetamine (open circles). N=5-6 in each group. * - P<0.05.

Table 4.2 Statistics generated from split-plot ANOVA summarising the effects of administration of *d*-amphetamine ('*d*-AMP': 3 mg/kg) and saline (1 ml/kg) on dopamine efflux in the rACC.

Brain region	Rostral anterior cingulate cortex	
	Saline	<i>d</i> -AMP
Time		
T ₂₀ -T ₆₀	F(1,3)=0.320 <i>P</i> <0.611	F(1,4)=10.352 <i>P</i><0.03
T ₈₀ -T ₁₂₀	F(1,2)=0.917 <i>P</i> <0.439	F(1,3)=9.970 <i>P</i><0.05
T ₁₄₀ -T ₁₈₀	F(1,2)=4.837 <i>P</i> <0.159	F(1,4)=4.463 <i>P</i> <0.10
T ₂₀₀ -T ₂₄₀	F(1,3)=1.508 <i>P</i> <0.307	F(1,4)=0.007 <i>P</i> <0.9
T ₂₆₀ -T ₃₀₀	F(1,3)=2.101 <i>P</i> <0.243	F(1,4)=9.966 <i>P</i><0.03

Dopamine efflux after each treatment was compared, over 1-h increments, with efflux in the cluster of basal samples. Significant differences are highlighted in **bold**.

4.4.2.2/ *The caudal anterior cingulate cortex*

Systemic injection of saline did not alter dopamine efflux in the cACC (see Figure 4.6). On injection of *d*-amphetamine there was no statistically significant increase in dopamine efflux in the cACC at any time as indicated by the statistical analysis (Figure 4.6 and see Table 4.3 for statistical details). This response is in marked contrast to the glutamate response in the cACC, which was consistently increased after injection of *d*-amphetamine (see: Chapter 3).

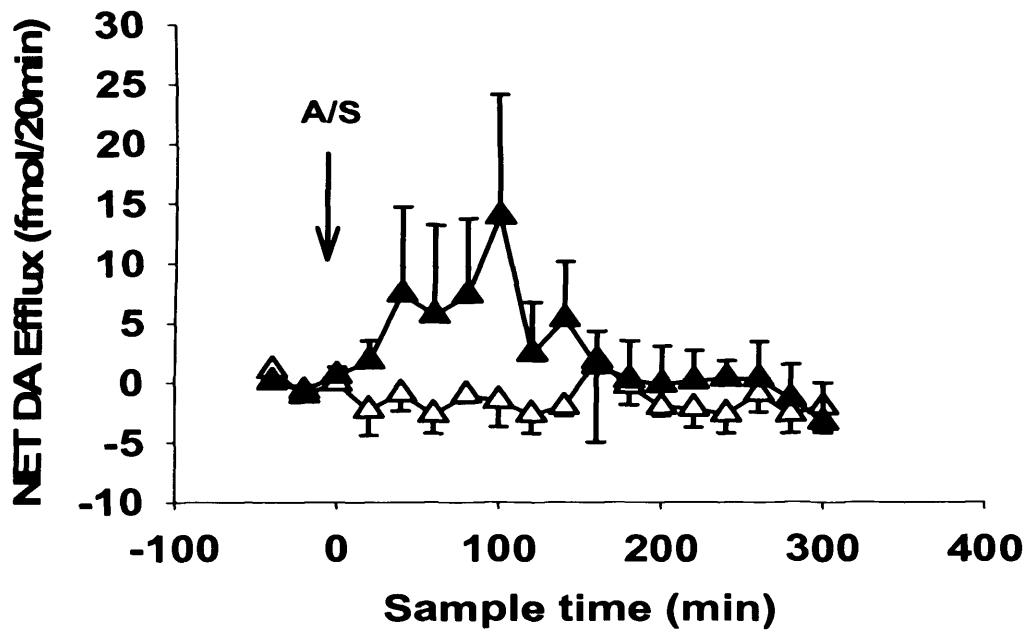
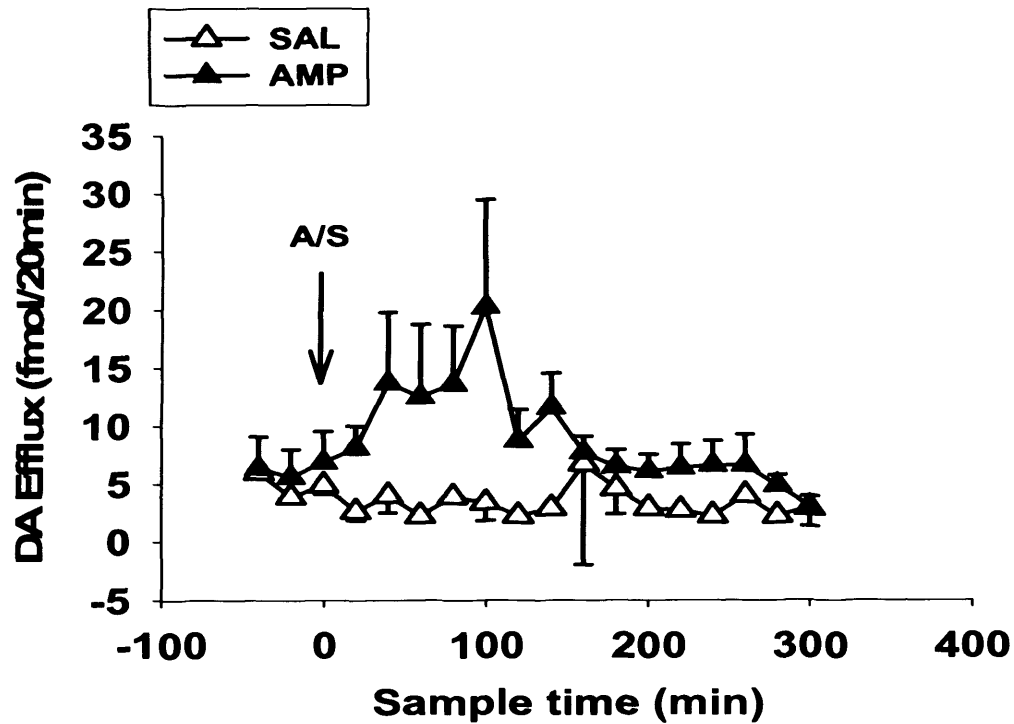


Figure 4.6 Effects of intraperitoneal administration of *d*-amphetamine (3 mg/kg) or saline (1 ml/kg) on dopamine ('DA') efflux in the cACC of freely-moving rats.

The top graph shows raw data and the bottom graph net data set. *d*-Amphetamine was administered at T_0 , as indicated by the arrow. DA efflux is expressed as fmol/20min. Points show mean \pm s.e. mean DA efflux in the cACC on administration of saline (open triangles) or *d*-amphetamine (closed triangles). N=5-6 in each group.

Table 4.3 Statistics generated from split-plot ANOVA summarising the effects of administration of *d*-amphetamine ('*d*-AMP': 3 mg/kg) or saline (1 ml/kg) on dopamine efflux in the cACC.

Brain region	Caudal anterior cingulate cortex	
	<i>d</i> -AMP	Saline
Time		
T20-T60	F(1,3)=2.913 <i>P</i> <0.2	F(1,4)=0.566 <i>P</i> <0.5
T80-T120	F(1,3)=5.271 <i>P</i> <0.1	F(1,4)=1.577 <i>P</i> <0.3
T140-T180	F(1,3)=0.006 <i>P</i> <0.9	F(1,4)=0.398 <i>P</i> <0.6
T200-T240	F(1,3)=6.022 <i>P</i> <0.1	F(1,4)=0.001 <i>P</i> <0.9
T260-T300	F(1,3)=2.199 <i>P</i> <0.2	F(1,4)=0.261 <i>P</i> <0.6

Dopamine efflux after each treatment was compared, over 1-h increments, with efflux in the cluster of basal samples.

4.4.3/ Experiment 3 – Effects of local infusion of increasing concentrations of dopamine on glutamate efflux in the cACC and the rACC

There was no difference in basal glutamate efflux in the cACC and the rACC of animals destined for local infusion of dopamine. Basal efflux of glutamate obtained from the pooled data was 10.0 ± 1.3 pmol/20min for the cACC and 10.7 ± 0.9 pmol/20min for the rACC.

A significant BIN*SUBREGION interaction was seen after infusion of $50 \mu\text{M}$ dopamine – $F_{(1,9)}=5.135$ $P<0.05$. Local infusion of dopamine solution caused an increase in glutamate efflux in the rACC, while no effect on glutamate efflux was seen in the cACC at any time (Figure 4.7 and see: Table 4.4 for statistical details).

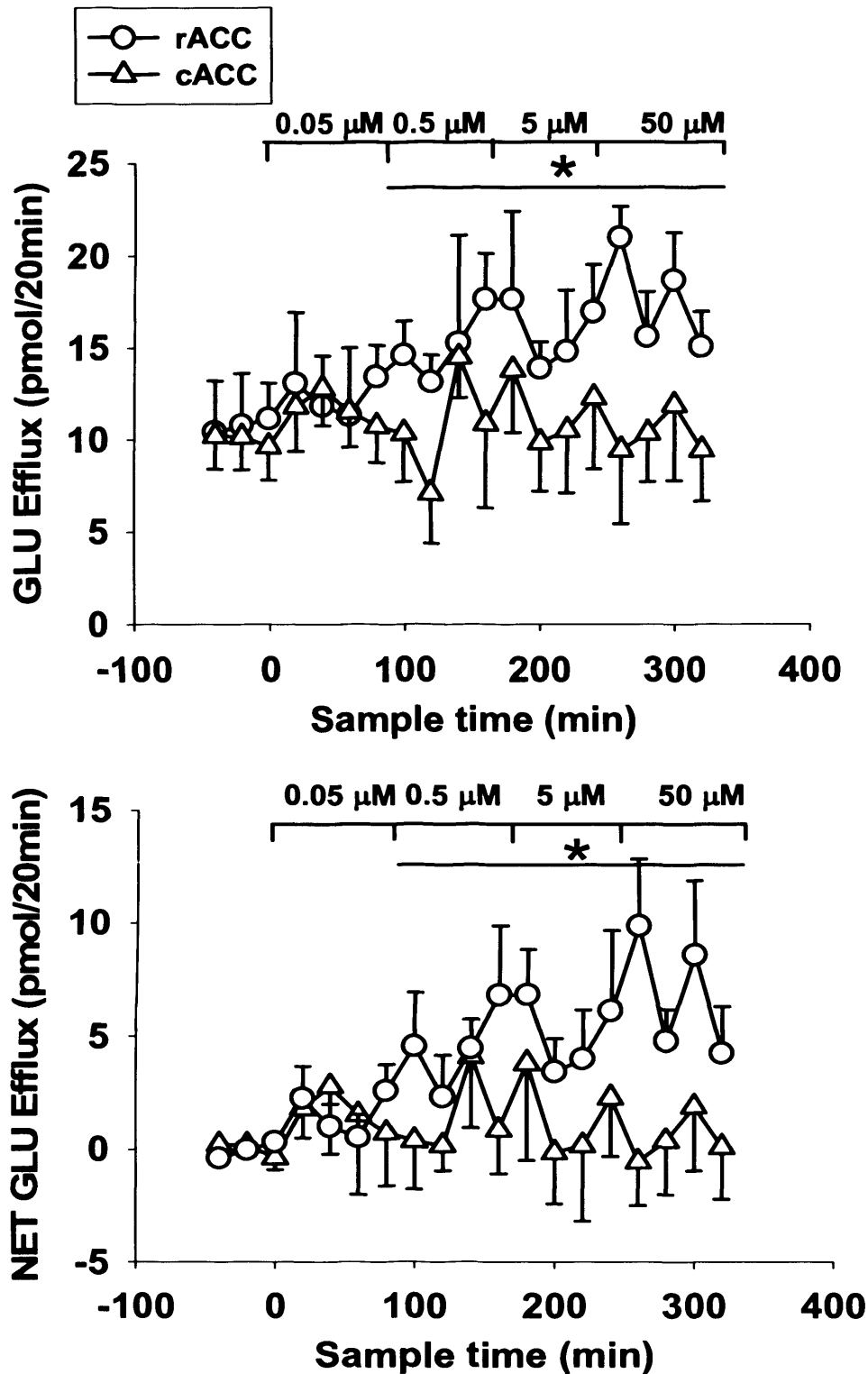


Figure 4.7 Effects of local infusion of increasing concentrations of dopamine (via retrodialysis) on glutamate ('GLU') efflux in the cACC and rACC of freely-moving rats.

Top graph shows raw data and bottom graph net data set. Dopamine infusion was initiated at T_0 as indicated by the line. GLU efflux is expressed as pmol/20min. Points show mean \pm s.e. mean GLU efflux in the cACC (open triangles) and rACC (open circles). $N=12/14$. * - $P<0.05$

Table 4.4 *Statistics generated from split-plot ANOVA summarising the effects of local infusion of dopamine solution in the cACC and the rACC.*

Treatment	Dopamine (local infusion)	
	cACC	rACC
[DA] μ M		
0.05	F(1,11)=1.193 $P<0.2$	F(1,13)=1.834 $P<0.1$
0.5	F(1,7)=0.742 $P<0.4$	F(1,12)=5.850 $P<0.03$
5	F(1,10)=0.165 $P<0.7$	F(1,12)=6.819 $P<0.02$
50	F(1,11)=0.063 $P<0.8$	F(1,11)=10.911 $P<0.001$

Glutamate efflux was compared, for each concentration of dopamine, with efflux in the cluster of basal samples. Significant differences are highlighted in **bold**.

4.5/ DISCUSSION

In my previous experiments, there was a regional difference in the glutamate response to *d*-amphetamine (see: Chapter 3). *d*-Amphetamine is translocated inside the cell *via* the plasma membrane dopamine transporter. Once inside the cell, *d*-amphetamine disrupts storage of dopamine within the vesicles, which causes leakage of dopamine into the cytoplasm (see: Chapter 1). Therefore, it was proposed that an increase in extracellular dopamine could underlie the glutamate response to *d*-amphetamine. In this chapter, the experiments explored the effects of both local infusion and systemic administration of *d*-amphetamine on dopamine efflux in the cACC and rACC. I also investigated the effects of local infusion of dopamine on glutamate efflux in both subregions.

4.5.1/ *Effects of d-amphetamine on dopamine efflux*

Systemic administration of *d*-amphetamine increased dopamine efflux in the rACC relative to saline. Systemic administration of *d*-amphetamine did not increase dopamine efflux in the cACC relative to saline. To date, no studies have looked at the effect of systemic *d*-amphetamine on dopamine efflux in this brain area and directly compared it to the rACC by using dual-probe microdialysis. Since systemic *d*-amphetamine did not affect dopamine efflux in this brain region, it can be inferred that an increase in dopamine efflux in the terminal field does not underlie the increase in extracellular glutamate in this subregion.

Table 4.5 summarises the results of previous microdialysis studies investigating dopamine efflux in various subregions of the medial prefrontal cortex after systemic

administration of *d*-amphetamine. In most subregions, an increase in dopamine efflux was seen. However, Hédou *et al.* (2001) reported a decrease in dopamine efflux on administration of 1.5 mg/kg *d*-amphetamine. This discrepancy could be caused by the use of anaesthetised animals by Hédou *et al.* rather than conscious, freely-moving rats as used in my experiments. They were also studying a different subregion of the rat prefrontal cortex.

Table 4.5 Summary of microdialysis studies investigating the effect of systemic *d*-amphetamine on dopamine efflux in the prefrontal cortex.

Reference	Dose of <i>d</i> -amphetamine	Effect on dopamine efflux	Coordinates
Hédou <i>et al.</i> , 2001	1.5 mg/kg i.p.	Decreased	<i>Dorsal mPFC</i> AP+2.7 ML+0.5 DV -4.0 <i>Ventral mPFC</i> AP+3.2 ML+0.5 DV -6.0
Berridge <i>et al.</i> , 2002	0.15 and 0.25 mg/kg s.c.	Increased (+125 % cf. basals)	AP +3.2 ML +1.0 DV -5.0
Shoblock <i>et al.</i> , 2003	2 mg/kg i.p.	Increased	AP+3.2 ML+0.1 DV -6.1

Local infusion of *d*-amphetamine dose-dependently increased dopamine efflux in the rACC. However, no change was observed in the cACC at any concentration tested. The regional dopamine response to local infusion of *d*-amphetamine mirrored that of the glutamate response in both subregions and so the increase in extracellular glutamate seen in the rACC after local infusion of *d*-amphetamine could be occurring secondary to increased dopaminergic neurotransmission. Table 4.6 summarises the

results of previous microdialysis experiments investigating dopamine efflux in various subregions of the medial prefrontal cortex after local infusion of *d*-amphetamine. In both studies, an increase in dopamine efflux was seen after *d*-amphetamine infusion.

Table 4.6 *The results of previous microdialysis studies investigating the effects of local infusion of d-amphetamine on dopamine efflux in the prefrontal cortex.*

Reference	Dose of <i>d</i> -amphetamine	Effect on dopamine efflux	Coordinates
Mazei <i>et al.</i> , 2002	10, 50, 100 μ M	Increased	<i>Cingulate</i> AP +3.2 ML +0.8 DV 0.0 to -2.5 <i>Prelimbic</i> AP +3.2 ML +0.8 DV -2.5 to -5.0
Balla <i>et al.</i> , 2001	10 μ M	Increased	AP +4.1 ML+1.0 DV-1.0

The mechanisms by which *d*-amphetamine causes increased extracellular dopamine in the rACC have been outlined in the introduction (see: Chapter 1). It is less clear why there should be no such increase in the cACC after either systemic or local administration of *d*-amphetamine. Dopamine transporters (DAT) are present in the prefrontal cortex, albeit in lower numbers than in the striatum (Sesack *et al.*, 1998). There is subregional variation in DAT density in the prefrontal cortex, with higher numbers being present in the more superficial areas, such as the anterior cingulate cortex, than the deeper layers, such as the prelimbic cortex (Sesack *et al.*, 1998). Therefore, if the main effect of *d*-amphetamine is to cause impulse-independent release of dopamine through DAT, one would expect to see increased dopamine efflux in the cACC, where the probes were located in the more superficial laminae of the cortex. The variation in the subregional response to *d*-amphetamine

seen in the present study seems to correlate more closely with their dopamine innervation densities (see later paragraphs).

In terms of dopaminergic connectivity, the prefrontal cortex receives a dense dopaminergic innervation from the ventral tegmental area (VTA or A10) of the midbrain (Lindvall *et al.*, 1978). As discussed in Chapter One, the two subregions of study receive dopaminergic afferent input from different brainstem nuclei. The dopaminergic projection to the medial prefrontal cortex and the superficial layers of the anterior cingulate cortex (i.e. the cACC) originates in the medial part of the A10 cell group, while the projection to the deeper layers of the anterior cingulate subregion (i.e. the rACC) originates in the ventrolateral part and also the mediolateral substantia nigra (A9; Emson and Koob, 1977). This could explain the differences in the dopamine response to *d*-amphetamine between the two subregions.

Mazei *et al.*, (2002) investigated the effect of local infusion of *d*-amphetamine on dopamine efflux in different subregions of the rat prefrontal cortex (the dorsally localised anterior cingulate cortex and the more ventrally localised prelimbic cortex). They found that local infusion of 100 μ M *d*-amphetamine differentially increased dopamine efflux in the two subregions of the prefrontal cortex. Thus *d*-amphetamine-induced dopamine efflux was significantly greater in the prelimbic area compared to the anterior cingulate subregion. These results correspond to the dopamine innervation density of these two subregions, with the prelimbic area demonstrating a greater dopamine innervation density than the anterior cingulate area. Studies using tritiated dopamine or proline have found that the prelimbic area has a denser dopamine innervation compared to the more dorsal anterior cingulate area (Descarries *et al.*, 1987, Javitch *et al.*, 1985). Thus the dopamine response to *d*-amphetamine in this study is correlated with dopamine innervation densities.

More recent anatomical studies have confirmed a greater density of dopaminergic innervation in the deep layers of the medial prefrontal cortex compared to the more superficial layers (Ciliax *et al.*, 1995). Therefore, in the rostral anterior cingulate cortex (as investigated during this study), the high dopamine innervation density compared to the caudal anterior cingulate cortex could contribute to the differential dopamine response to *d*-amphetamine. The presence of fewer dopaminergic terminals in the caudal anterior cingulate cortex means that there would be less dopamine available for extrusion by the transporter when compared to the rostral anterior cingulate cortex. The reason for the differential dopamine innervation densities between the two brain regions could be explained in terms of their afferent inputs. As explained earlier in the discussion, the dopaminergic projection to the deeper layers of the prefrontal cortex originates in the medial part of the A10 cell group. The projection to the more superficially-located anterior cingulate cortex originates in the ventromedial part/A9 (Lindvall *et al.*, 1978).

d-Amphetamine also acts on the noradrenaline transporter (NET) to increase release of noradrenaline (Piffl *et al.*, 1999). The NET is responsible for the clearance of the majority of the extracellular dopamine from the prefrontal cortex (Wayment *et al.*, 2001). Therefore, *d*-amphetamine could be releasing dopamine from the NET. However, unlike the dopamine innervation density, the noradrenergic innervation of different subregions of the prefrontal cortex is homogeneous and derived from the same brain region (the locus coeruleus; Lindvall *et al.*, 1978). Therefore, the differential dopamine response to *d*-amphetamine in subregions of the prefrontal cortex is unlikely to be due to any action of *d*-amphetamine on the NET.

To summarise, there were subregional differences in the dopamine response to *d*-amphetamine. Both systemic injection and retrodialysis of *d*-amphetamine

increased dopamine efflux in the rACC, but neither route had any appreciable effect in the cACC. The dopamine response to *d*-amphetamine in the rACC was similar, regardless of the route of administration. Therefore, the dopamine response to local *d*-amphetamine is not confounded by afferent inputs.

4.5.2/ Effects of local infusion of dopamine on glutamate efflux

Local infusion of dopamine dose-dependently increased glutamate efflux in the rACC, while no effect in the cACC was seen at any concentration tested. This response profile mimics the effects of local infusion of *d*-amphetamine in these subregions. Therefore, an increase in dopaminergic neurotransmission could underlie the glutamate response to local infusion of *d*-amphetamine in the rACC. These results are in contention with some previous microdialysis studies investigating the effects of dopaminergic agents on extracellular glutamate. The selective D₁-like receptor agonist SKF38393 and pergolide (which has actions on D₁, D₂ and D₃-like receptors) both decreased spontaneous glutamate efflux in the rACC of freely-moving rats (Harte and O'Connor, 2004). Electrophysiological studies have demonstrated both increased and decreased excitability of glutamatergic pyramidal cells after application of dopamine and dopamine receptor ligands (Gonzalez-Islas and Hablitz, 2003, Gullledge and Jaffe, 1998). These studies suggest a complex role of dopamine in the modulation of glutamatergic neurotransmission in the rACC.

The explanation for the differing glutamate response to local infusion of dopamine in the rACC and cACC is unclear. As mentioned in section 4.1, there is a differential dopaminergic innervation of different subregions of the prefrontal cortex. Dopamine has a greater propensity to affect glutamate efflux in the rACC when

compared to the cACC due to the greater dopaminergic innervation of the prefrontal cortex (Ciliax *et al.*, 1995). A differential distribution of dopamine receptors has also been demonstrated in the two subregions. The D₁-like receptor in the rat cortex has a relatively homogeneous pattern in most regions except the deeper laminae (V and VI), which contain more receptors than the superficial layers. D₂-like receptors are distributed in all regions of the cerebral cortex in rats and are very homogeneous in their regional distribution and laminar pattern compared to the D₁-like receptor (Richfield *et al.*, 1989). The pattern of the glutamate response to local infusion of dopamine therefore correlates with the density of D₁-like receptors in the cortex.

4.5.3/ SUMMARY OF KEY FINDINGS

- Both local infusion and systemic administration of *d*-amphetamine increased dopamine efflux in the rACC, suggesting that dopamine efflux is not constrained by afferent inputs.
- In the cACC, dopamine efflux was not affected by either local infusion or systemic administration of *d*-amphetamine, suggesting that an increase in dopamine efflux does not underlie the glutamate response to systemic *d*-amphetamine in this subregion.
- Local infusion of dopamine solution increased glutamate efflux in the rACC but not the cACC. This gives more credence to the idea that an increase in dopaminergic neurotransmission underlies the glutamate response to *d*-amphetamine.

Chapter 5

5.0/ The effect of pre-treatment with dopaminergic antagonists on the glutamate response to local infusion of *d*-amphetamine in the rostral anterior cingulate cortex

5.1/ INTRODUCTION

In Chapter 3, local infusion of *d*-amphetamine produced a dose-related increase in extracellular glutamate in the rACC, while no change in glutamate efflux was observed in the cACC. It was hypothesised that an increase in dopaminergic neurotransmission could underlie the *d*-amphetamine-induced increase in glutamate efflux in the rACC. This proposal was supported by subsequent experiments (see: Chapter 4). These experiments demonstrated that local infusion of *d*-amphetamine increased dopamine efflux in the rACC, but not the cACC. Local infusion of dopamine also increased glutamate efflux in the rACC, but not the cACC. Therefore, it is a possibility that the *d*-amphetamine-induced increase in glutamate efflux in the rACC is occurring secondary to an increase in dopaminergic neurotransmission.

The aim of these experiments was to investigate further the possibility that an increase in dopaminergic neurotransmission underlies the glutamate response to *d*-amphetamine in the rACC and to characterise the subtype(s) of dopamine receptors involved. The rACC was chosen for study as local infusion of *d*-amphetamine into this brain region gave a reliable, dose-related increase in glutamate efflux. No change in extracellular glutamate was observed in the cACC in response to *d*-amphetamine. To further investigate the possibility of a dopaminergic involvement in the glutamate

response to local infusion of *d*-amphetamine in the rACC, two dopaminergic antagonists were chosen: the D₂-like receptor antagonist haloperidol and the D₁-like receptor antagonist SCH23390. Both these drugs have been well characterised using radioligand binding. The ED₅₀ for receptor occupancy in the rat brain (striatum and cerebellum) by haloperidol is 0.2 mg/kg (Barth *et al.*, 2006). To the best of my knowledge, the ED₅₀ for SCH23390 is not readily available. Doses of haloperidol were chosen, which, according to these radioligand binding assays, should block D₂-like receptors *in vivo*: 0.1 and 1 mg/kg. The doses of SCH23390 were based on previous microdialysis studies, which show an effect on pharmacologically-evoked glutamate release in the ventral tegmental area (Wolf and Xue, 1999). To date, no study has looked at the effect of pre-treatment with dopaminergic antagonists on the glutamate response to *d*-amphetamine in the rACC. However, one previous study found that pre-treatment with SCH23390 (0.1 mg/kg i.p.) completely prevented the increased extracellular glutamate in the ventral tegmental area in response to systemic administration of *d*-amphetamine (5 mg/kg i.p., Wolf and Xue, 1999). Another study looked at glutamate efflux in the rACC in response to another psychostimulant, cocaine (Reid *et al.*, 1997). The authors found that the increased glutamate efflux in response to systemic cocaine (30 mg/kg) was completely blocked by pre-treatment with systemic SCH23390 (0.02 mg/kg i.p.), but not by haloperidol (0.2 mg/kg i.p.). Cocaine and *d*-amphetamine have some common pharmacological characteristics. They both increase extracellular dopamine levels by actions on the plasma membrane dopamine transporter (Pifl *et al.*, 1995). Therefore, the data obtained by Reid *et al.* may be comparable with the results of the experiments performed in Chapter 5.

d-Amphetamine was administered into the rACC by local infusion at doses of 10 and 100 μ M. These doses were based on the experiments performed in chapters 3

and 4, which produced a measurable increase in glutamate efflux. Local infusion delivers the drug directly into the brain area of interest. It therefore enables investigation of drug effects in the terminal fields. Limited diffusion of *d*-amphetamine from the probe has been demonstrated in microdialysis studies (Westerink and De Vries, 2001).

The dopaminergic antagonists were administered 2 h before local infusion of *d*-amphetamine. This time period was chosen to allow glutamate efflux to stabilize before *d*-amphetamine treatment. The pharmacokinetics of haloperidol have been examined in young and aged male Fischer-344 rats (Kapetanovic *et al.*, 1982). The elimination half-life of a bolus (0.5 mg/kg i.p.) dose of haloperidol in young (3-4 month) rats was found to be 2.62 h, while in aged (32-34 month) rats, it was 3.50 h. The concentration of haloperidol in the brain would have declined by nearly half when *d*-amphetamine infusion was initiated. However, in rodents, D₂-like receptor occupancy by haloperidol, in the striatum at least, is in excess of 80 % at doses of haloperidol of 0.1 mg/kg or greater (Mukherjee *et al.*, 2001). In the present experiments, both dopaminergic antagonists were administered systemically in order to be distributed throughout the body. Local infusion of *d*-amphetamine delivers the drug directly into the rACC and therefore enables investigation of drug effects in the terminal fields. These two routes of drug administration were chosen to avoid pharmacokinetic artefacts created by giving two drugs simultaneously down the probe. If a compound is locally infused into the brain, it is impossible to predict its exact concentration in the terminal fields. This situation would be complicated by the addition of two drugs to the perfusion fluid, as the concentration of each drug accessing the brain extracellular fluid could vary from experiment to experiment.

There is also the possibility of chemical interaction between the two compounds in the perfusion fluid.

5.2/ AIM

- *To determine if the glutamate response to d-amphetamine in the rACC can be prevented by pre-treatment with either the D2-like receptor antagonist haloperidol or the D1-like receptor antagonist SCH23390*

5.3/ METHODS

Experiments were performed on freely-moving rats (250-300 g on the day of surgery).

5.3.1/ Experiment 1 – Effects of pre-treatment with the D₂-like receptor antagonist haloperidol on the glutamate response to local infusion of d-amphetamine in the rostral anterior cingulate cortex

Rats were implanted with microdialysis probes in the rACC on the day before experimenting. Haloperidol was dissolved in 0.9 % saline to make a 0.1 mg/ml solution. This was administered at a volume of 1 ml/kg (i.e. 0.1 mg/kg). This dose of haloperidol was based on previous *in vivo* studies where blockade of D₂-like receptors has been reported. For local infusion, *d*-amphetamine was dissolved in Ringer's solution to make 10 and 100 μ M solutions. These doses were based on the studies carried out in chapter 3, which demonstrated measurable increases in glutamate efflux in the rACC at these concentrations. Rats were randomly assigned to one of three treatment groups (Table 5.1, Experiment 1). Once stable basal glutamate efflux was established, 0.1 mg/kg haloperidol or 1 ml/kg saline were administered by i.p. injection. The last three basal samples were designated T₋₄₀-T₀, with injection of haloperidol or saline immediately after T₀. Sampling continued for a further 2 h after haloperidol or saline injection. After the 2 h stabilisation period, *d*-amphetamine was locally infused via the probe by changing the perfusion solution for Ringer's containing *d*-amphetamine in two groups only. Two successive concentrations of *d*-amphetamine were infused for 80 min each. For the haloperidol-Ringer's groups, sampling continued for a further 280 min without the addition of *d*-amphetamine.

The concentration of glutamate in dialysates was expressed as pmol/20 min without correction for recovery.

This experiment was then repeated with a higher dose of haloperidol (1 mg/kg i.p., Table 5.1 Experiment 2).

5.3.2/ Experiment 2 – Effects of pre-treatment with the D1-like receptor antagonist SCH23390 on the glutamate response to local infusion of d-amphetamine in the rostral anterior cingulate cortex

Rats were implanted with microdialysis probes on the day before experimenting and Experiment 1 was repeated, substituting SCH23390 (0.1 and 1 mg/kg) for haloperidol (see: Table 5.2, experiments 1 and 2).

5.3.3/ Statistical analysis

All data were analysed for significance using three- and two-way analysis of variance with repeated measures. In addition to raw data, net changes were calculated by subtracting the mean of the last three basal samples from all the samples in the time course. Data for each treatment group were pooled and the mean and s.e.m. calculated.

‘Time’ was a ‘within subjects’ factor and ‘pre-treatment’ (i.e. dopamine antagonist treatment vs. saline) was a ‘between subjects’ factor. The data were divided in three ‘bins’ with four consecutive samples per bin (each bin therefore corresponded to infusion of one concentration of d-amphetamine or Ringer’s solution; Figure 5.1).

'Bin' was a 'within subjects' factor. 'Bin 1' represents basal efflux (i.e. $T_{40}-T_0$). The last three samples during infusion of each concentration of *d*-amphetamine were used for the analysis.

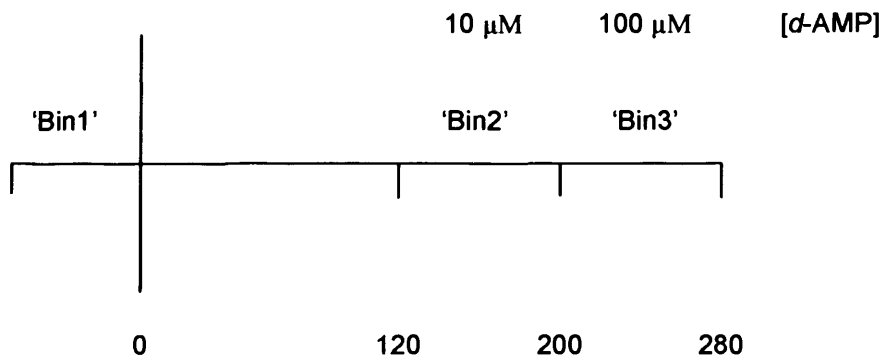


Figure 5.1 Time bins for statistical analysis of changes in extracellular glutamate after local infusion of *d*-amphetamine.

Therefore, 'bin 2'=10 μM ($T_{160}-T_{200}$) and 'bin 3'=100 μM ($T_{240}-T_{280}$). The Greenhouse-Geisser ϵ -correction was performed where Mauchley's test of Sphericity was significant.

Table 5.1 Treatment groups for haloperidol/saline administration. Rats were randomly assigned to one of three treatment groups for each experiment.

Group Number	Experiment 1	Experiment 2
1	Saline-- <i>d</i> -amphetamine	Saline-- <i>d</i> -amphetamine
2	Haloperidol (0.1)-- <i>d</i> -amphetamine	Haloperidol (1)-- <i>d</i> -amphetamine
3	Haloperidol (0.1)--Ringers	Haloperidol (1)--Ringers

Table 5.2 *Treatment groups for SCH23390/saline administration. Rats were randomly assigned to one of three treatment groups for each experiment.*

Group Number	Experiment 1	Experiment 2
1	Saline-- <i>d</i> -amphetamine	Saline-- <i>d</i> -amphetamine
2	SCH23390 (0.1)-- <i>d</i> -amphetamine	SCH23390 (1)-- <i>d</i> -amphetamine
3	SCH23390 (0.1)--Ringers	SCH23390 (1)--Ringers

5.4/ RESULTS

5.4.1/ Effects of pre-treatment with the D₂-like receptor antagonist haloperidol on the glutamate response to local infusion of d-amphetamine in the rostral anterior cingulate cortex

There was no difference in basal efflux of glutamate in the rACC of animals in the treatment groups:

Experiment 1(a)

SAL+AMP	14.27 ± 1.20 pmol/20min
HAL(0.1)+AMP	15.48 ± 1.27 pmol/20min
HAL(0.1)+RINGERS	7.64 ± 0.50 pmol/20min

Experiment 1(b)

SAL+AMP	10.59 ± 1.50 pmol/20min
HAL (1)+AMP	10.76 ± 0.93 pmol/20min
HAL(1)+RINGERS	8.5 ± 0.85 pmol/20min

Experiment 1(a)

Injection of saline did not affect glutamate efflux. Subsequent infusion of *d*-amphetamine (10 μM) caused an immediate increase in glutamate efflux to a maximum of 33.09 ± 7.80 pmol/20min, which was sustained for the remainder of the experiment. Infusion of 100 μM *d*-amphetamine did not cause any further increase in glutamate efflux (Figure 5.2 and see Table 5.3 for statistical analysis). Injection of 0.1 mg/kg haloperidol produced a transient increase in glutamate efflux in the rACC

(to 26.85 ± 6.68 pmol/20min), which quickly returned to basal levels in the subsequent sample. In the presence of 0.1 mg/kg haloperidol, *d*-amphetamine retained to ability to increase glutamate efflux at both concentrations tested. Extracellular glutamate reached a maximum value of 40.15 ± 11.21 pmol/20min on infusion of *d*-amphetamine (Figure 5.2 and see Table 5.3 for statistical analysis). Injection of haloperidol (0.1 mg/kg) alone increased glutamate efflux in the rACC at 3 and 4 h after injection (Figure 5.3 and see Table 5.4 for statistical analysis).

Experiment 1(b)

Injection of saline did not affect glutamate efflux in the rACC. Infusion of 10 μ M *d*-amphetamine caused an immediate increase in glutamate efflux to a maximum of 19.14 ± 2.41 pmol/20min, which declined rapidly in the next two samples. Subsequent infusion of 100 μ M *d*-amphetamine caused a resurgence of the glutamate response, which reached a peak of 22.64 ± 7.70 pmol/20min after one sample and then started to decline rapidly (Figure 5.4 and see Table 5.5 for statistical analysis). *d*-Amphetamine retained the ability to increase extracellular glutamate in the presence of 1 mg/kg haloperidol (Figure 5.4 and see Table 5.5 for statistical analysis). Injection of 1 mg/kg haloperidol alone did not affect glutamate efflux in the rACC at any time (Figure 5.5 and see Table 5.6 for statistical analysis).

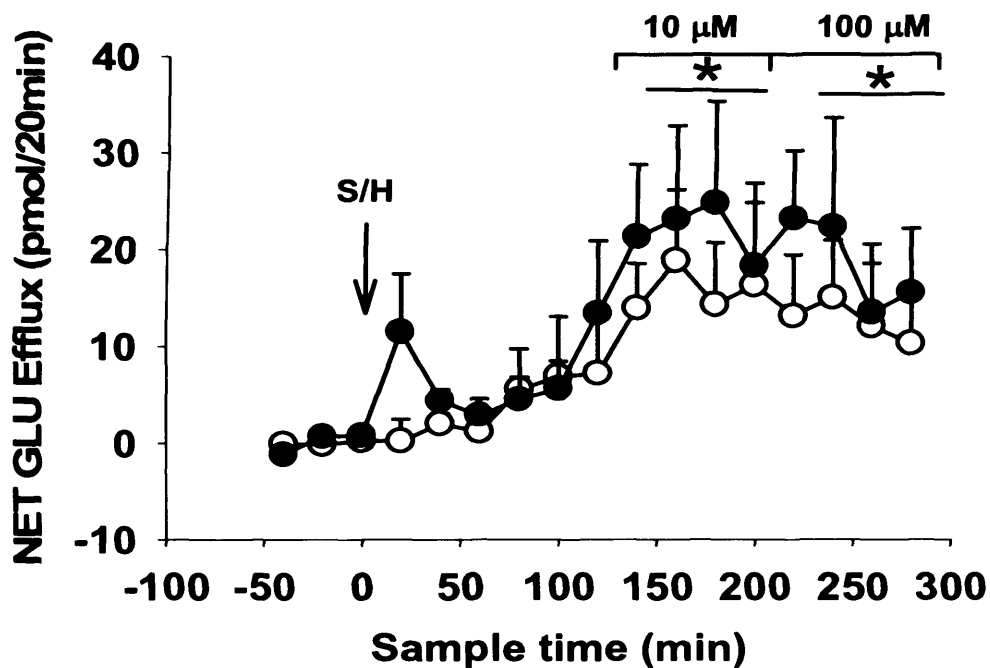
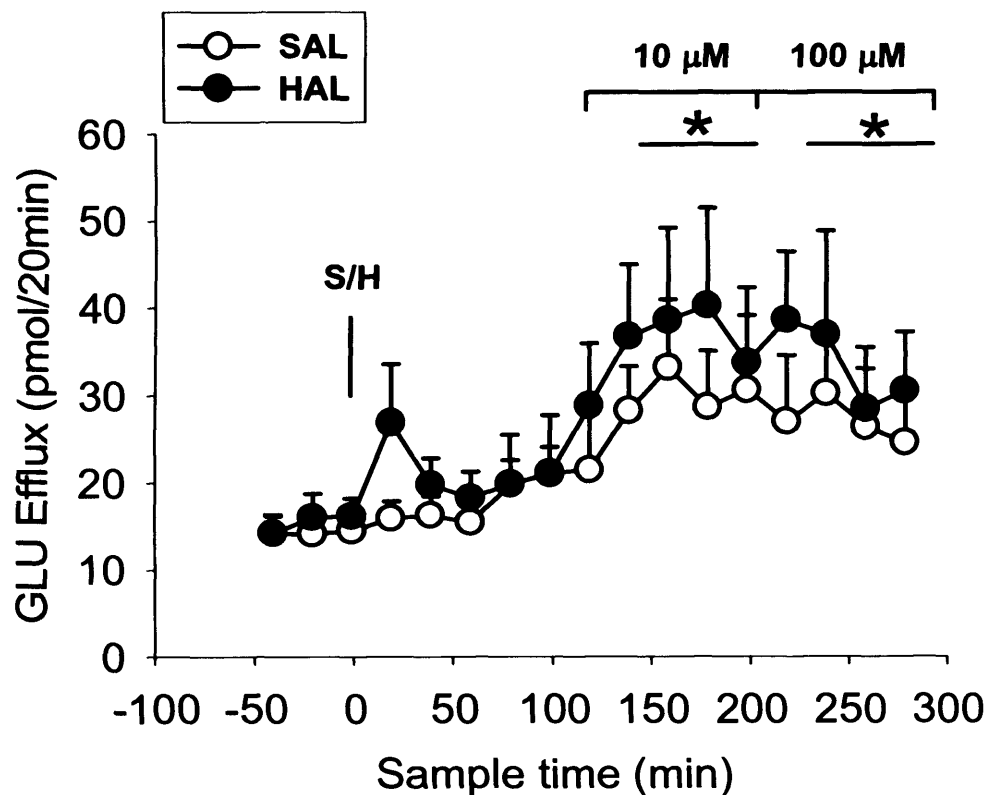


Figure 5.2 Effects of cumulative infusion of *d*-amphetamine on glutamate ('GLU') efflux in the rACC of freely-moving rats.

Haloperidol (0.1 mg/kg i.p.) or saline (1 ml/kg i.p.) were injected at T_0 as indicated by the arrow. *d*-AMP (10 μ M: 80 min, 100 μ M: 80 min) infusion was initiated at T_{120} as indicated by the line. Glutamate efflux is expressed as pmol/20min. Points show mean \pm s.e. mean GLU efflux after injection of HAL (closed circles) or saline (open circles). $N=9$. Top graph shows raw data and bottom graph net data set.

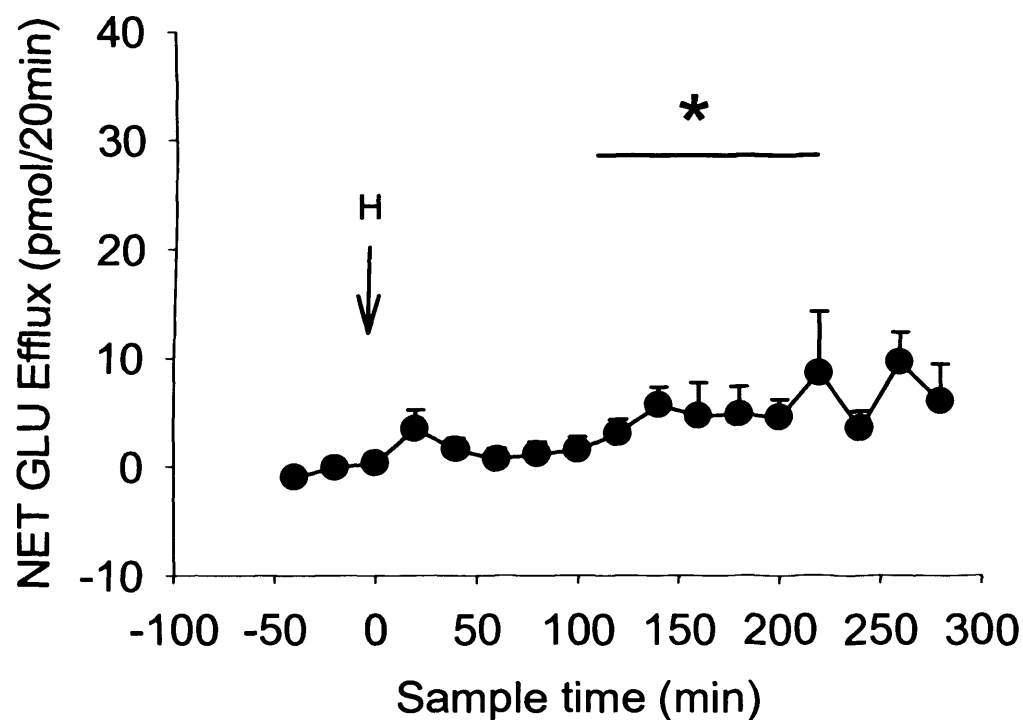
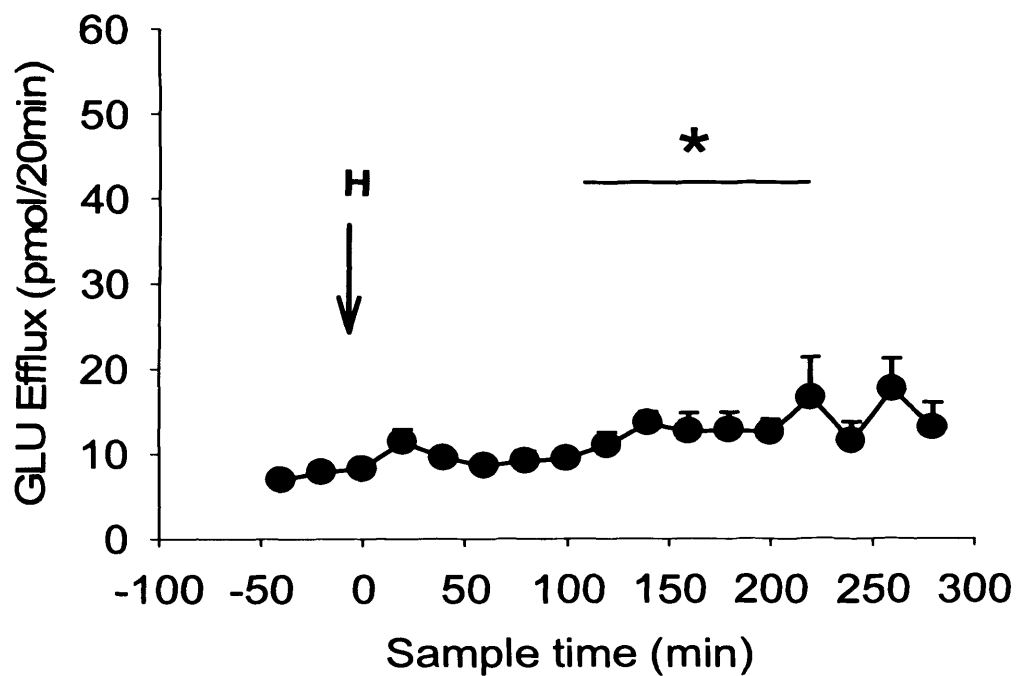


Figure 5.3 Effects of haloperidol (0.1 mg/kg i.p.) injection on glutamate ('GLU') efflux in the rACC of freely-moving rats
 Haloperidol was injected at T_0 as indicated by the arrow. Glutamate efflux is expressed as pmol/20min. Points show mean \pm s.e. mean GLU efflux. $N=7$. Top graph shows raw data and bottom graph net data set. * - $P<0.05$.

Table 5.3 Statistics generated from split-plot ANOVA summarizing the effects of administration of *d*-amphetamine (*'d-AMP'*) on glutamate efflux in the rACC. Rats were pre-treated with either saline (*'SAL'*: 1 ml/kg) or haloperidol (*'HAL'*: 0.1 mg/kg) 2 h before local infusion of *d*-amphetamine. Glutamate efflux after each treatment was compared, over 1-h increments, with efflux in the cluster of basal samples. Significant differences are shown in **bold**.

Treatment	<i>d</i> -AMP (local infusion)	
	SAL	HAL
[<i>d</i> -AMP] μ M		
10	F(1,10)=7.116 <i>P</i><0.02	F(1,9)=9.662 <i>P</i><0.01
100	F(1,8)=6.094 <i>P</i><0.04	F(1,8)=6.684 <i>P</i><0.03

Table 5.4 Statistics generated from split-plot ANOVA summarizing the effects of administration of haloperidol (0.1 mg/kg i.p.) on glutamate efflux in the rACC. Glutamate efflux was compared, over 1-h increments, with efflux in the cluster of basal samples.

Treatment	Haloperidol (0.1 mg/kg i.p.)
Time	
T ₂₀ -T ₆₀	F(1,12)=10.722 <i>P</i><0.02
T ₈₀ -T ₁₂₀	F(1,12)=0.768 <i>P</i><0.03
10 μ M	F(1,12)=6.857 <i>P</i><0.01
100 μ M	F(1,12)=6.461 <i>P</i><0.03

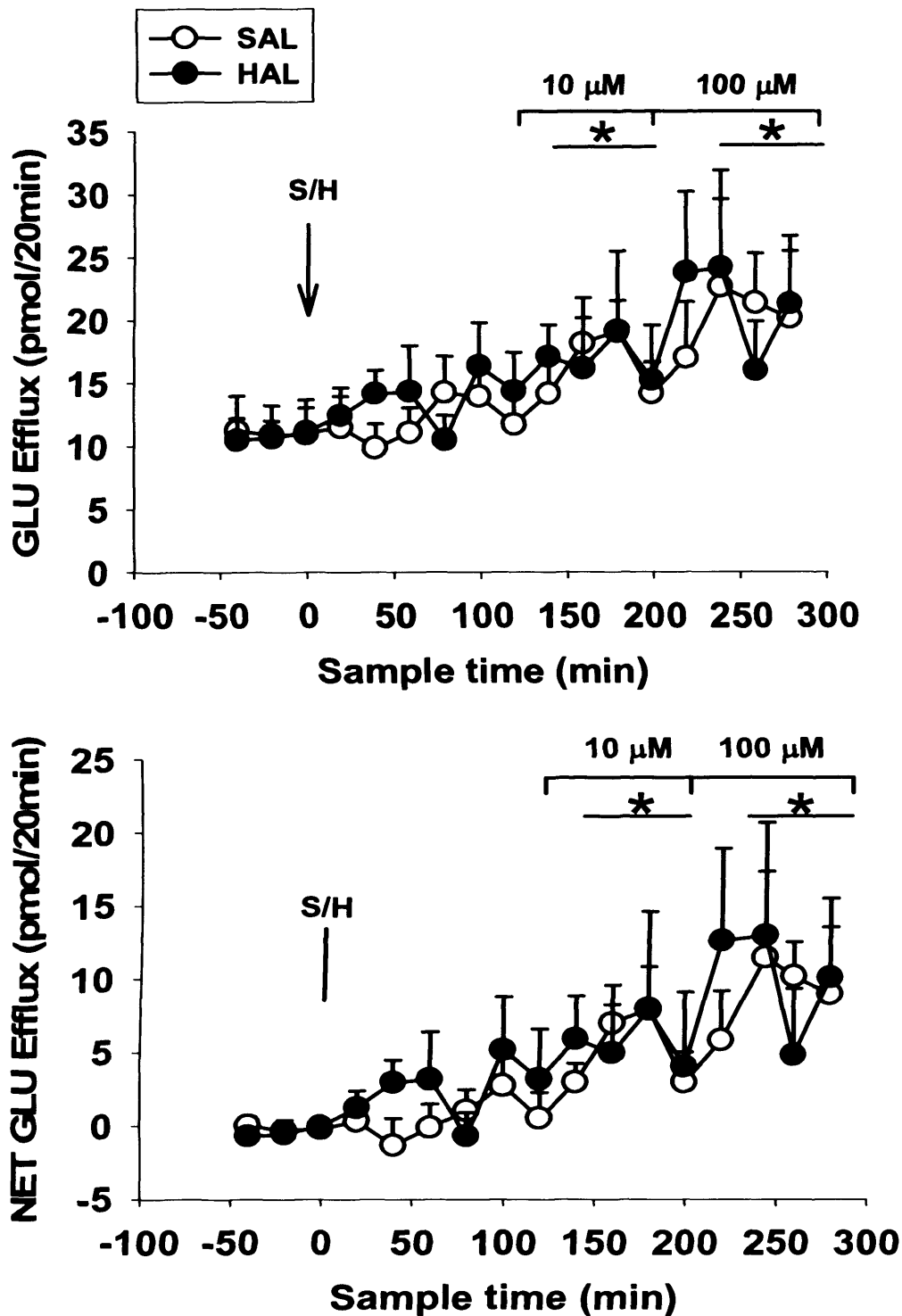


Figure 5.4 Effects of cumulative infusion of *d*-amphetamine on glutamate ('GLU') efflux in the rACC of freely-moving rats.

HAL (1 mg/kg i.p.) or saline (1 ml/kg i.p.) were injected at T_0 as indicated by the arrow. *d*-AMP (10 μ M: 80 min, 100 μ M: 80 min) infusion was initiated at T_{120} as indicated by the line. Glutamate efflux is expressed as pmol/20min. Points show mean \pm s.e. mean after injection of HAL (closed circles) or saline (open circles). $N=9$. The top graph shows raw data and the bottom graph net data set.

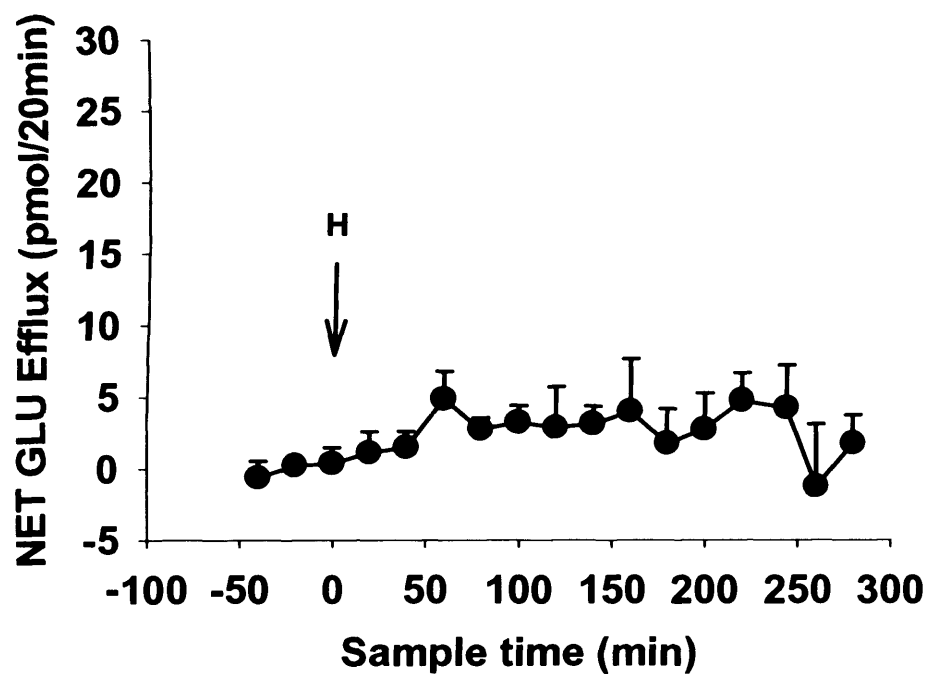
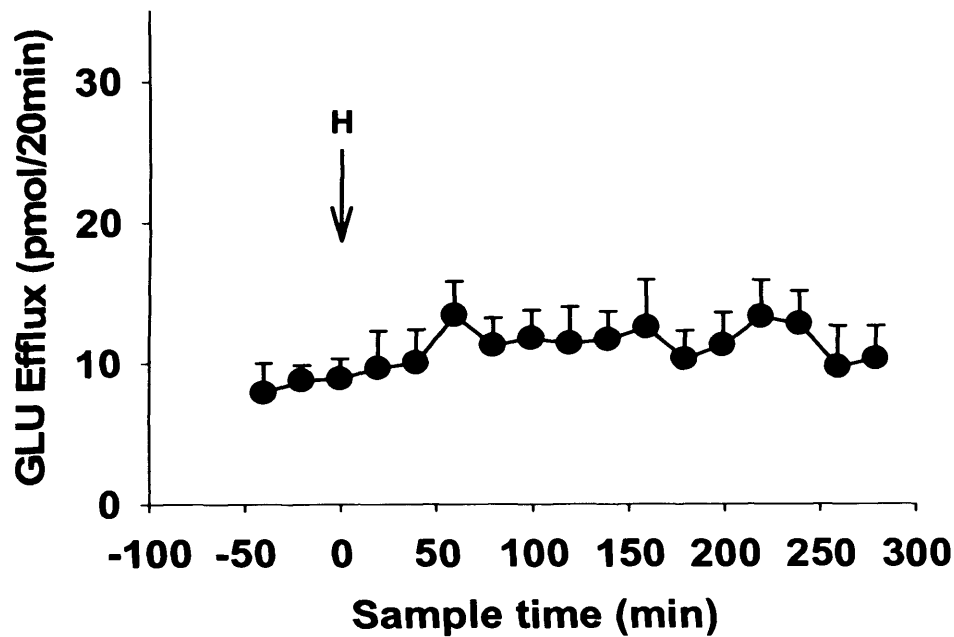


Figure 5.5 Effects of haloperidol (1 mg/kg i.p.) injection on glutamate ('GLU') efflux in the rACC of freely-moving rats.

Haloperidol was injected at T₀ as indicated by the arrow. Glutamate efflux is expressed as pmol/20min. Points show mean ± s.e. mean GLU efflux. N=4. The top graph shows raw data and the bottom graph net data set.

Table 5.5 *Statistics generated from split-plot ANOVA summarizing the effects of administration of d-amphetamine ('d-AMP') on glutamate efflux in the rACC. Rats were pre-treated with either saline (1 mg/kg) or haloperidol (1 mg/kg) 2 h before local infusion of d-amphetamine. Glutamate efflux after each treatment was compared with efflux in the basal samples. Glutamate efflux after each treatment was compared, over 1 h increments, with efflux in the cluster of basal samples. Significant differences are in bold.*

Treatment	<i>d</i> -AMP (local infusion)	
	SAL	HAL
[<i>d</i> -AMP] μ M		
10	F(1,7)=11.713 <i>P</i><0.01	F(1,6)=4.086 <i>P</i> <0.1
100	F(1,7)=6.400 <i>P</i><0.04	F(1,6)=6.272 <i>P</i><0.05

Table 5.6 *Statistics generated from split-plot ANOVA summarizing the effects of administration of haloperidol (1 mg/kg i.p.) on glutamate efflux in the rACC. Glutamate efflux was compared, over 1-h increments with that in the cluster of basal samples.*

Treatment	Haloperidol (1 mg/kg i.p.)
Time	
T ₂₀ -T ₆₀	F(1,3)=4.830 <i>P</i> <0.1
T ₈₀ -T ₁₂₀	F(1,3)=7.068 <i>P</i> <0.1
10 μ M	F(1,3)=0.996 <i>P</i> <0.4
100 μ M	F(1,2)=1.493 <i>P</i> <0.3

5.4.2/ Effects of pre-treatment with the D₁-like receptor antagonist SCH23390 on the glutamate response to local infusion of d-amphetamine in the rostral anterior cingulate cortex.

There was no difference in basal glutamate efflux in the rACC of animals destined for systemic injection of saline or SCH23390.

Experiment 2(a)

SAL+AMP	12.56 ± 1.26 pmol/20min
SCH(0.1)+AMP	7.72 ± 0.83 pmol/20min
SCH (0.1)+RINGERS	11.58 ± 1.60 pmol/20min

Experiment 2(b)

SAL+AMP	10.25 ± 0.90 pmol/20min
SCH (1)+AMP	10.90 ± 0.83 pmol/20min
SCH(1)+RINGERS	9.44 ± 0.81 pmol/20min

Experiment 2(a)

Injection of saline did not affect glutamate efflux. Infusion of 10 μ M d-amphetamine produced a delayed increase in glutamate efflux, which was sustained throughout the experiment and reached a maximum of 21.08 ± 5.16 pmol/20min. Infusion of 100 μ M d-amphetamine did not produce any further increase in glutamate efflux (Figure 5.6 and see Table 5.7 for statistical analysis). Injection of 0.1 mg/kg SCH23390 did not affect glutamate efflux. In the presence of SCH23390, d-amphetamine retained the ability to increase glutamate efflux at 100 μ M (Figure 5.6

and see Table 5.7 for statistical analysis). Injection of 0.1 mg/kg SCH23390 alone produced an immediate increase in glutamate efflux (to 18.75 ± 3.15 pmol/20min), which quickly declined to basal levels in the subsequent sample (Figure 5.7 and see Table 5.8 for statistical analysis).

Experiment 2(b)

Injection of saline did not affect glutamate efflux in the rACC. Infusion of 10 μ M *d*-amphetamine caused an immediate increase in glutamate efflux to 20.9 ± 5.83 pmol/20min, which declined rapidly in the subsequent two samples. Infusion of 100 μ M *d*-amphetamine caused a resurgence of the glutamate response, which reached a peak of 20.35 ± 5.15 pmol/20min after two samples and then declined rapidly (Figure 5.8 and see Table 5.9 for statistical analysis). Injection of 1 mg/kg SCH23390 did not affect glutamate efflux in the rACC. In the presence of SCH23390, *d*-amphetamine no longer had the ability to increase glutamate efflux at either dose tested (Figure 5.8 and see Table 5.9 for statistical analysis). Injection of 1 mg/kg SCH23390 alone did not affect glutamate efflux at any time (Figure 5.9 and see Table 5.10 for statistical analysis).

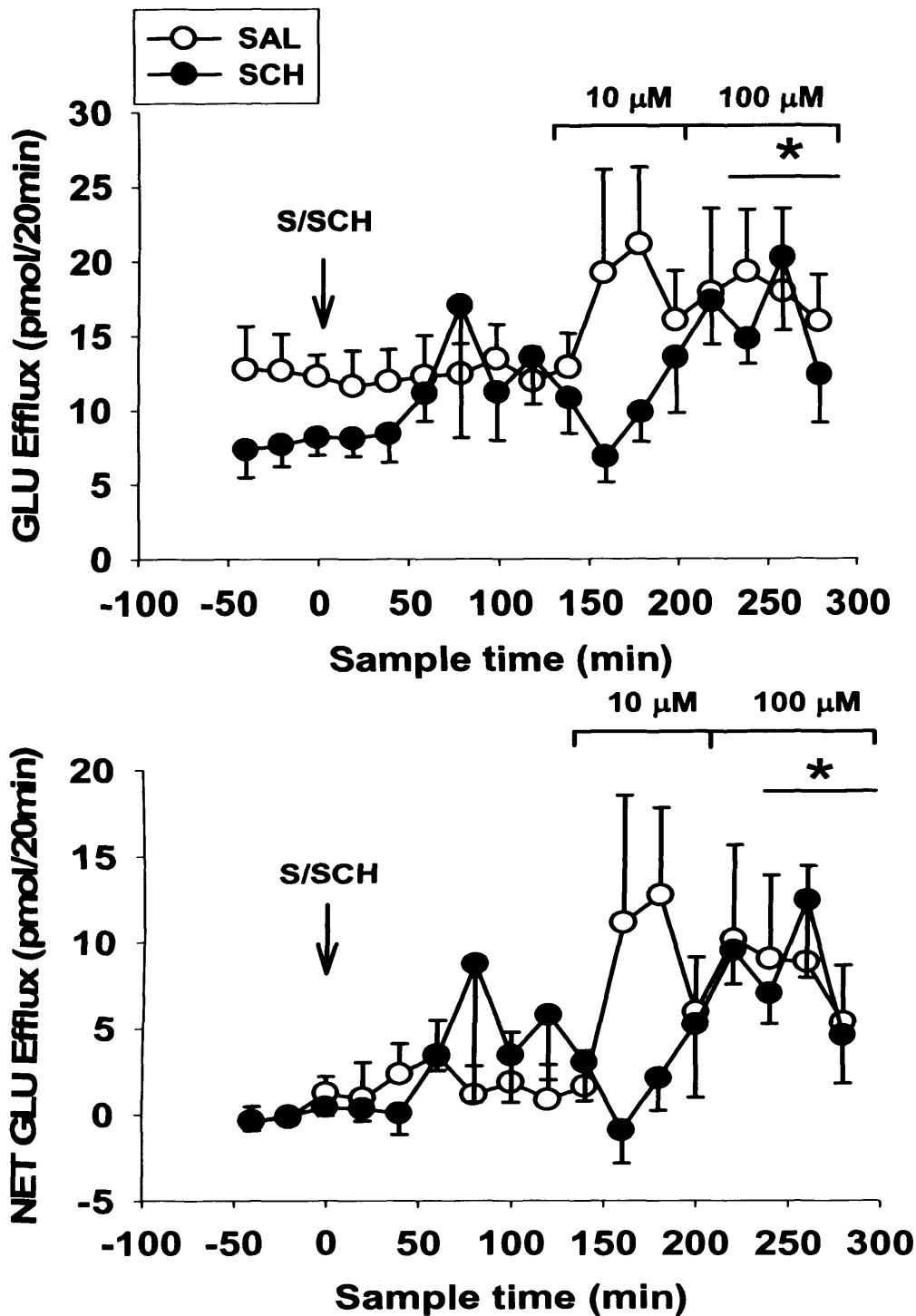


Figure 5.6 Effects of cumulative infusion of *d*-amphetamine on glutamate ('GLU') efflux in the rACC of freely-moving rats.

SCH23390 (0.1 mg/kg i.p.) or saline (1 ml/kg i.p.) were injected at T_0 as indicated by the arrow. *d*-AMP (10 μ M: 80 min, 100 μ M: 80 min) infusion was initiated at T_{120} as indicated by the line. Glutamate efflux is expressed as pmol/20min. Points show mean \pm s.e. mean GLU efflux after injection of SCH23390 (closed circles) or saline (open circles). $N=6$ in each group. The top graph shows raw data and the bottom graph net data set.

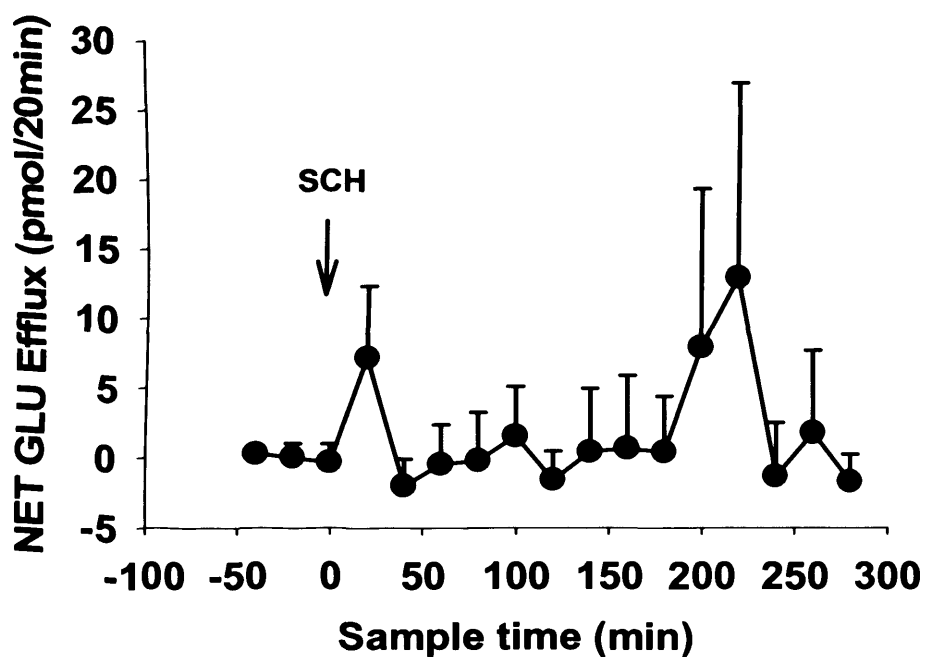
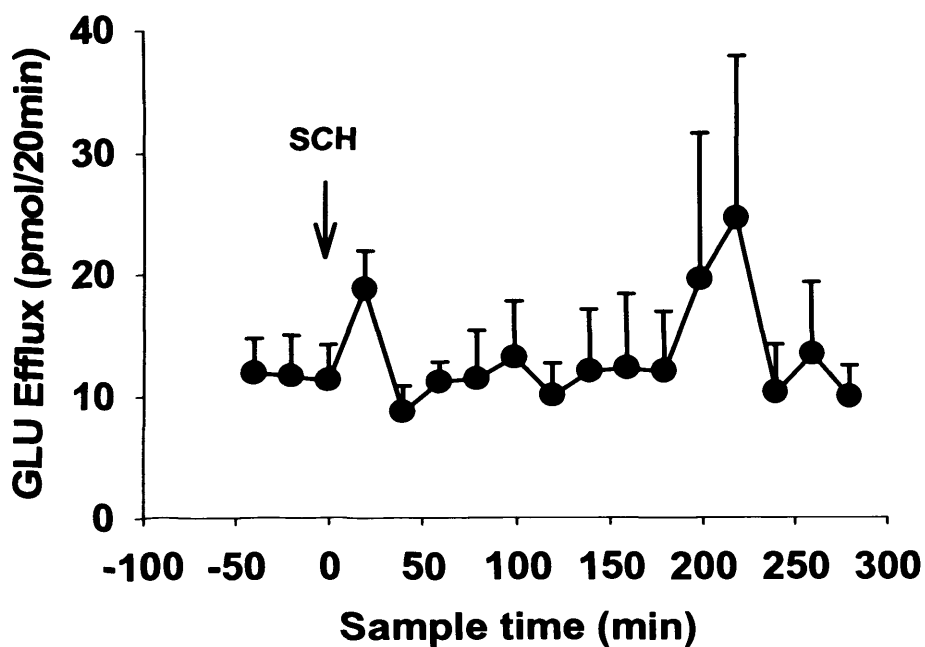


Figure 5.7 Effects of SCH23390 (0.1 mg/kg i.p.) injection on glutamate ('GLU') efflux in the rACC of freely-moving rats

SCH23390 was injected at T₀ as indicated by the arrow. Glutamate efflux is expressed as pmol/20min. Points show mean ± s.e. mean GLU efflux. N=4. The top graph shows raw data and the bottom graph net data set.

Table 5.7 Statistics generated from split-plot ANOVA summarizing the effects of local infusion of *d*-amphetamine ('*d*-AMP':10-100 μ M) on glutamate efflux in the rACC after pre-treatment with saline or SCH23390 (0.1 mg/kg i.p.).

Glutamate efflux after each treatment was compared, over 1-h increments, with efflux in the cluster of basal samples. Significant differences are shown in **bold**.

Treatment	<i>d</i> -AMP (local infusion)	
	SAL	SCH23390
[<i>d</i> -AMP] μ M		
10	F(1,4)=3.998 <i>P</i> <0.1	F(1,4)=1.062 <i>P</i> <0.4
100	F(1,4)=7.369 <i>P</i><0.05	F(1,5)=11.085 <i>P</i><0.02

Table 5.8 Statistics generated from split-plot ANOVA summarizing the effects of administration of SCH23390 (0.1 mg/kg i.p.) on glutamate efflux in the rACC. Glutamate efflux in each time bin was compared with that in the basal samples.

Treatment	SCH23390 (0.1 mg/kg i.p.)
Time	
T ₂₀ -T ₆₀	F(1,2)=0.338 <i>P</i> <0.6
T ₈₀ -T ₁₂₀	F(1,3)=0.001 <i>P</i> <0.9
10 μ M	F(1,3)=0.012 <i>P</i> <0.9
100 μ M	F(1,3)=0.382 <i>P</i> <0.6

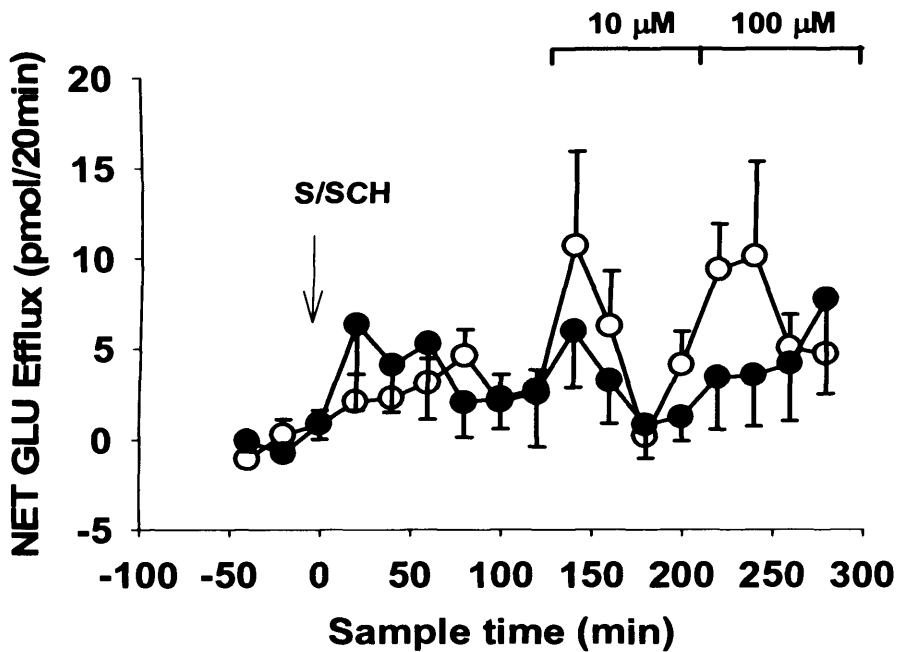
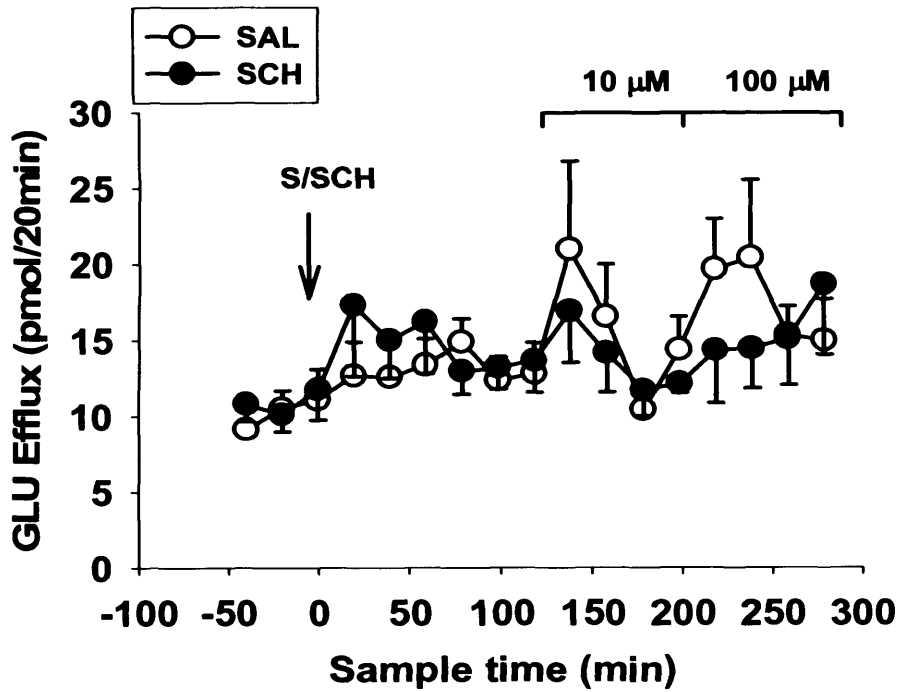


Figure 5.8 Effects of cumulative infusion of *d*-amphetamine on glutamate ('GLU') efflux in the rACC of freely-moving rats. SCH23390 (1 mg/kg i.p.) or saline (1 ml/kg i.p.) were injected at T₀ as indicated by the arrow. *d*-AMP (10 μM: 80 min, 100 μM: 80 min) infusion was initiated at T₁₂₀ as indicated by the line. Glutamate efflux is expressed as pmol/20min. Points show mean ± s.e. mean GLU efflux after SCH (closed circles) and saline (open circles) injection. N=8/11 in each group. The top graph shows raw data and the bottom graph net data set.

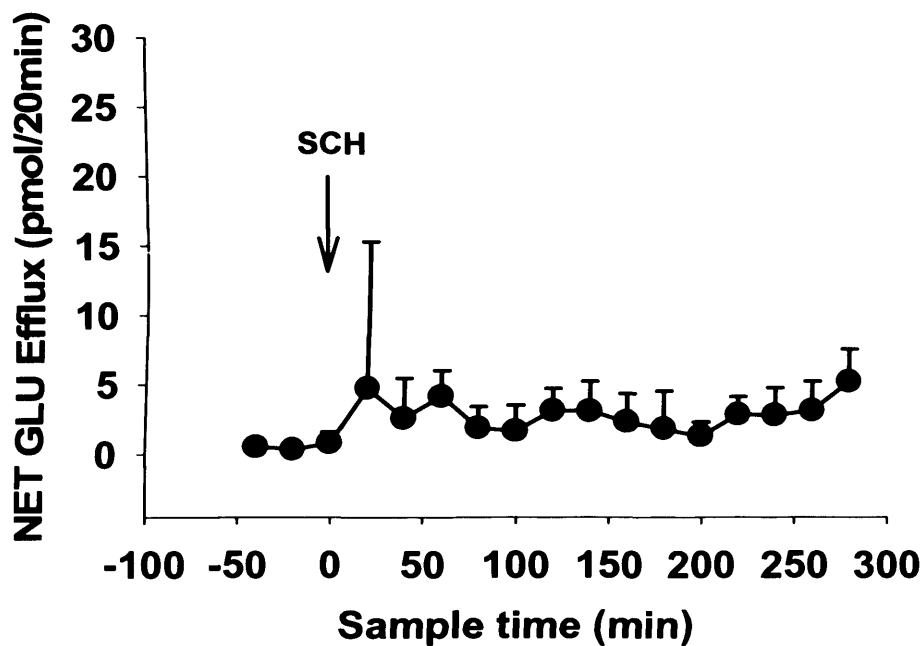
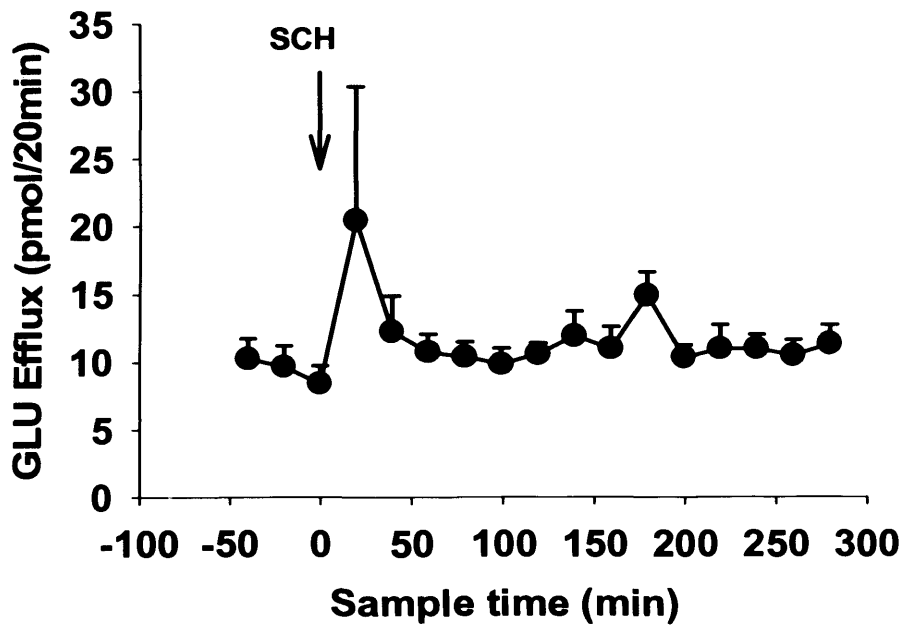


Figure 5.9 Effects of SCH23390 (1 mg/kg i.p.) injection on glutamate ('GLU') efflux in the rACC of freely-moving rats

SCH23390 (1 mg/kg i.p.) was injected at T_0 as indicated by the arrow. Glutamate efflux is expressed as pmol/20min. Points show mean \pm s.e. mean GLU efflux. $N=7$. The top graph shows raw data and the bottom graph net data set.

Table 5.9 Statistics generated from split-plot ANOVA summarizing the effects of local infusion of *d*-amphetamine (*'d*-AMP': 10-100 μ M) on glutamate efflux in the rACC after pre-treatment with saline or SCH23390 (1 mg/kg i.p.).

Glutamate efflux after each treatment was compared, over 1-h increments, with efflux in the cluster of basal samples. Significant differences are shown in **bold**.

Treatment	<i>d</i> -AMP local infusion	
	SAL	SCH23390
[<i>d</i> -AMP] μ M		
10	F(1,9)=5.796 P<0.04	F(1,7)=2.221 P<0.2
100	F(1,7)=11.437 P<0.01	F(1,7)=3.433 P<0.1

Table 5.10 Statistics generated from split-plot ANOVA summarizing the effects of administration of SCH23390 (1 mg/kg i.p.) on glutamate efflux in the rACC. Glutamate efflux in each time bin was compared with that in the basal samples.

Treatment	SCH23390 (1 mg/kg i.p.)
Time	
T ₂₀ -T ₆₀	F(1,5)=3.325 P<0.1
T ₈₀ -T ₁₂₀	F(1,4)=0.740 P<0.4
10 μ M	F(1,5)=1.553 P<0.3
100 μ M	F(1,5)=0.565 P<0.5

5.5/ DISCUSSION

In previous experiments, it was discovered that local infusion of dopamine at increasing concentrations increased glutamate efflux in the rostral anterior cingulate cortex, while no change was observed in the caudal anterior cingulate cortex at any time. Local infusion of *d*-amphetamine also increased dopamine efflux in the rACC, but not the cACC. Based on these observations, we proposed that an increase in dopamine neurotransmission could underlie the glutamate response to local infusion of *d*-amphetamine in the rACC. In this chapter, the experiments further explored the possibility that an increase in dopaminergic neurotransmission underlies the glutamate response to local infusion of *d*-amphetamine in the rACC and also attempted to elucidate the subtype of dopamine receptor responsible for the glutamate response to *d*-amphetamine.

5.5.1/ Effects of haloperidol and SCH23390 on spontaneous glutamate efflux in the rACC

Systemic administration of neither antagonist affected spontaneous glutamate efflux in the rACC, suggesting a lack of tonic control of extracellular glutamate by both D₁-like and D₂-like receptors in this brain region. This result agrees with the study by Reid *et al.*, in 1997, which investigated glutamate efflux in the same region of the ACC as me.

5.5.2/ Effects of haloperidol on the glutamate response to d-amphetamine

To determine the role of D₂-like receptors in modulating the glutamate response to local infusion of *d*-amphetamine in the rACC, the D₂-like receptor antagonist haloperidol (0.1 and 1 mg/kg i.p.) was administered 2 h before the *d*-amphetamine treatment. The plasma half-life of haloperidol in the rat is approximately 3 h (Kapetanovic *et al.*, 1982), so the concentration of haloperidol in the brain would have declined progressively during the experiment. However, haloperidol has a high affinity for the D₂-like receptor in the rat brain (K_i = 28 nM), so only low concentrations are required for optimal receptor occupancy. In these experiments, pre-treatment with systemic haloperidol did not affect the glutamate response to *d*-amphetamine. In other words, *d*-amphetamine retained the ability to increase glutamate efflux at both doses tested. This result indicates that there is no modulation of glutamate efflux by D₂-like receptors after impulse-dependent or independent release by *d*-amphetamine. However, the possibility that the concentration of haloperidol in the cortex declined too much to permit occupation of D₂-like receptors cannot be ruled out.

This is the first time that an attempt has been made to elucidate the subtype of dopamine receptor responsible for mediating the glutamate response to local infusion of *d*-amphetamine in the rACC. Several previous authors have investigated the mechanisms underlying evoked glutamate efflux in different subregions of the prefrontal cortex by other psychostimulants. For example, systemic administration of the glutamatergic antagonist phencyclidine ('PCP': 5 mg/kg i.p.) increased glutamate efflux in the prefrontal cortex (Adams and Moghaddam, 2001). This increase in glutamate efflux was not prevented by pre-treatment with haloperidol (0.1 mg/kg i.p.)

20 min before administration of PCP. Similarly, systemic administration of cocaine (15-30 mg/kg i.p.) stimulated glutamate efflux in the cingulate region of the prefrontal cortex (Reid *et al.*, 1997). This was unaffected by pre-treatment with haloperidol (0.2 mg/kg i.p.) 60 min before administration of cocaine. The pharmacology of PCP differs greatly compared to *d*-amphetamine (see: Chapter 1 for details of *d*-amphetamine pharmacology). PCP is an antagonist at NMDA receptors, while *d*-amphetamine is a releaser of dopamine. The mechanisms by which these drugs increase glutamate efflux are probably different to those recruited by *d*-amphetamine. The pharmacology of cocaine exhibits some similarity to the pharmacology of *d*-amphetamine (both influence the plasma membrane dopamine transporter to increase extracellular levels of dopamine, albeit by different mechanisms), so may be predictive of some of the actions of *d*-amphetamine on glutamatergic transmission in the rat cortex.

5.5.3/ Effects of SCH23390 on the glutamate response to d-amphetamine

To determine the role of D₁-like receptors in modulating the glutamate response to local infusion of *d*-amphetamine in the rACC, the D₁-like receptor antagonist SCH23390 (0.1 and 1 mg/kg i.p.) was administered 2 h before *d*-amphetamine treatment. In these experiments, systemic administration of SCH23390 at the lower dose (0.1 mg/kg i.p.) did not affect the glutamate response to local infusion of *d*-amphetamine. No pharmacokinetic data regarding SCH23390 are freely available. Nevertheless, the glutamate response to both doses of *d*-amphetamine was attenuated by pre-treatment with the higher dose of SCH23390 (1 mg/kg i.p.), indicating a role for D₁-like receptors in *d*-amphetamine-evoked

glutamate release. This agrees with the high density of D₁-like compared to D₂-like receptors in the prefrontal cortex, with D₁-like receptors being about 20 times more abundant than D₂-like receptors in the prefrontal cortex (Lidow *et al.*, 1991).

These data are in contradiction with a couple of previous microdialysis studies investigating the effects of D₁-like receptors on glutamatergic neurotransmission. Abekawa *et al.* (2000) measured extracellular glutamate in the rat prefrontal cortex (coordinates: AP +2.7 ML \pm 1.4 DV -6.5) using microdialysis. They found that local infusion of a selective D₁-like receptor agonist SKF38393 (2-200 μ M) dose-dependently decreased extracellular glutamate and that this effect was reversed by co-perfusion with the selective D₁-like receptor antagonist SCH23390 (40 μ M). Another study also demonstrated a dose-dependent decrease in extracellular glutamate in the prefrontal cortex (coordinates: AP +2.7 ML -0.8 DV -1.8) after local infusion of SKF38393 (10-500 μ M; Harte and O'Connor, 2004). The action of these agonists on presynaptic D₁-like receptors present on glutamatergic pyramidal neurones was proposed to underlie these decreases in extracellular glutamate. These studies were clearly performed in different regions of the rat prefrontal cortex when compared to my study and investigated the effects of dopaminergic agents on spontaneous glutamate efflux, rather than drug-evoked increases. The authors also used local infusion to deliver two drugs at once into the region of study. This could have caused pharmacokinetic artifacts leading to a false positive result, explaining the discrepancies between our data.

In light of these previous microdialysis studies, it is not clear how dopamine acting at D₁-like receptors could be increasing glutamate efflux in the rACC. A study by Reid *et al.*, in 1997, found an increase in glutamate efflux after systemic administration of cocaine (30 mg/kg i.p.). The increased glutamate efflux was

blocked by pre-treatment with SCH23390 (0.02 mg/kg i.p.) but not haloperidol (0.2 mg/kg i.p.). The authors speculated that this was mediated by D₁-like receptors present on the collaterals of prefrontal-VTA glutamatergic neurones. Clearly, further work is required to elucidate the exact mechanism underlying my result.

In vivo and *in vitro* receptor competition studies have shown that SCH23390 potently interacts with brain 5-HT₂ receptors (Bischoff *et al.*, 1986, McQuade *et al.*, 1988). This could explain the attenuation of the glutamate response to *d*-amphetamine by SCH23390. Both systemic (0.1 mg/kg i.p.) and intracortical (10 μM) administration of 5-HT_{2A/C} agonists, such as lysergic acid increase glutamate efflux in the rat prefrontal cortex (Muschamp *et al.*, 2004). This increase in glutamate efflux is blocked by pre-treatment with the selective 5-HT_{2A} antagonist M100,907 (0.05 mg/kg i.p.). These studies suggest that *d*-amphetamine-induced glutamate efflux occurring secondary to release of 5-HT cannot be ruled out.

5.5.4/ Summary of key findings

- There is no tonic control of glutamate release in the prefrontal cortex by either D₁-like or D₂-like receptors
- The increased extracellular glutamate in response to local infusion of *d*-amphetamine in the prefrontal cortex is unaffected by pre-treatment with the D₂-like receptor antagonist haloperidol
- Activation of D₁-like receptors contributes to the *d*-amphetamine-induced increase in glutamate efflux in the rACC

Chapter 6

6.0/ Effect of pre-treatment with the GLT-1 inhibitor dihydrokainate on the glutamate response to systemic administration of *d*-amphetamine in the rostral and caudal anterior cingulate cortices

6.1/ INTRODUCTION

In experiments described in Chapter 3, the glutamate response to administration of *d*-amphetamine was found to depend on both brain region and route of administration. Systemic *d*-amphetamine caused a gradual, sustained increase in glutamate efflux in the cACC, while, in the rACC, no increase in glutamate efflux was observed at any time. Conversely, local infusion of *d*-amphetamine increased glutamate efflux in the rACC but had no effect in the cACC. Subsequent experiments focused on elucidating the role of dopamine receptors in the glutamate response to local infusion of *d*-amphetamine in the rACC (see: Chapters 4 and 5). Here, I explored further the possible mechanisms underlying the increased extracellular glutamate in the cACC evoked by systemic administration of *d*-amphetamine. The rACC was also studied.

Uptake is necessary for the clearance of glutamate from the extracellular fluid, since there is no extracellular enzyme, which can metabolise it. Glutamate uptake is accomplished by means of transporter proteins, which use the electrochemical gradient of Na⁺ across the plasma membrane as a driving force for uptake. To date, five subtypes of glutamate transporters have been cloned, including both neuronal and

glial transporters: GLAST, GLT-1, EAAC-1, EAAT4 and EAAT5. GLAST and GLT-1 are predominantly localised to astrocytes, while EAAC-1, EAAT4 and EAAT5 are neuronal (for review see Danbolt, 2001). Previous studies suggest that GLT-1 accounts for the majority of glutamate uptake in the forebrain (Haugeto *et al.*, 1996; Tanaka *et al.*, 1997, Chapter 1).

Increased glutamate efflux in the ventral tegmental area, measured by *in vivo* microdialysis, stimulated by either systemic injection or local infusion of *d*-amphetamine is independent of Ca^{2+} in the perfusion medium, suggesting that it does not depend on exocytotic (impulse-dependent) release (Wolf *et al.*, 2000). Impulse-independent release of glutamate can occur *via* both neurones and glial cells. During brain ischaemia, increased extracellular Na^+ concentrations lead to reversal of glutamate transporters. It is uncertain which transporters are involved, and evidence for both glial and neuronal transporters has been derived (Seki *et al.*, 1999; Dawson *et al.*, 2000; Rossi *et al.*, 2000). Studies in the laboratory of Attwell have favoured the involvement of neuronal glutamate transport (Harmann *et al.*, 2002; Rossi *et al.*, 2000). Harmann *et al.* (2002) studied the effects of ischaemia on hippocampal slices from mice lacking the GLT-1 transporter. After a few minutes of simulated ischaemia, pyramidal cells in wild-type mice showed a large and sudden glutamate-evoked current, which declined to a less inward plateau. In GLT-1 knockout mice, the characteristics of this current were indistinguishable from those of hippocampal slices from wild-type mice, suggesting that GLT-1 does not contribute significantly to glutamate release or removal from the extracellular space during early ischaemia. Seki *et al.*, in 1999, induced forebrain ischaemia in rats by bilateral occlusion of the carotid artery for 30 min. This led to increased extracellular glutamate, as measured by microdialysis. Dihydrokainate ('DHK': 1 mM) attenuated this increased glutamate

efflux. DHK is a non-transportable inhibitor of the glial glutamate transporter, GLT-1. Infusion of the anion channel blocker 4,4'-dinitrostilben-2,2'-disulfonic acid (DNDS; 1 mM) also attenuated extracellular glutamate levels. DHK inhibited the early ischaemic response more strongly than DNDS. This suggests the existence of two Ca^{2+} -independent mechanisms of glutamate release during ischaemia – a rapid reversal of the astrocytic glutamate transporter, GLT-1, as well as a more slowly developing cell swelling-induced release of glutamate.

There is evidence for impulse-independent release of glutamate by GLT-1 in response to challenge with *d*-amphetamine. For example, glutamate efflux in the ventral tegmental area was increased by i.p. injection of *d*-amphetamine (5 mg/kg; Wolf *et al.*, 2000). This increase in glutamate efflux was abolished by pre-treatment with local dihydrokainate ('DHK'; 1 mM). In addition, blockade of GLT-1 by DHK led to increased glutamate efflux as measured by microdialysis in the striatum, suggesting that GLT-1 is responsible for clearance of extracellular glutamate in this brain region (Massieu *et al.*, 1995; Del Arco *et al.*, 1999). It is therefore conceivable that *d*-amphetamine could be acting on this transporter, either directly or indirectly, to increase glutamate efflux. Glial cells also release glutamate into the extracellular space by Ca^{2+} -dependent vesicular release (for review see Haydon, 2001) and non-vesicular release, via the cystine-glutamate antiporter present on glial cells. This non-vesicular release by the cystine-glutamate antiporter is thought to constitute a major proportion (60 %) of the basal extracellular concentration of glutamate in the striatum at least (Baker *et al.*, 2002).

The purpose of these experiments was to investigate the role of GLT-1 in the increase in glutamate efflux in the cACC induced by systemic administration of *d*-amphetamine. This was tested by examining the effect of glutamate transporter

inhibition with dihydrokainate (DHK). The effect of DHK in the rACC was also investigated to ascertain whether GLT-1 would have any influence on glutamatergic neurotransmission in this brain area. It is conceivable that the lack of effect of *d*-amphetamine on glutamate efflux in this subregion is because GLT-1 efficiently sequesters any increased extracellular glutamate. The dose of DHK (1 mM) was based on that used in a previous study in the ventral tegmental area, which demonstrated a blockade of the *d*-amphetamine-induced increase in glutamate efflux in this region (Wolf *et al.*, 2000). The dose of *d*-amphetamine (3 mg/kg i.p.) was based on our previous studies (see: Chapter 3), showing a reliable increase in glutamate efflux in the cACC.

6.2/ AIM

- *To determine and compare the effect of pre-treatment with the GLT-1 blocker dihydrokainate (DHK) on the glutamate response to systemic administration of d-amphetamine in the caudal and rostral anterior cingulate cortices.*

6.3/ METHODS

6.3.1/ *In vivo* microdialysis

Experiments were performed on freely-moving rats (250-300g on day of surgery).

Rats were implanted with a microdialysis probe in either the cACC or rACC on the day before experimenting. *d*-Amphetamine was dissolved in 0.9 % saline to a concentration of 3 mg/ml. This was administered in a volume of 1 ml/kg (i.e. 3 mg/kg). This dose of *d*-amphetamine was based on our previous experiments in which there was an increase in glutamate efflux in the cACC (see: Chapter 3). For local infusion, dihydrokainate ('DHK') was dissolved in Ringer's to make a 1 mM solution. This dose of DHK was based on a previous study, which demonstrated a blockade of *d*-amphetamine-induced glutamate efflux in the rat ventral tegmental area (Wolf *et al.*, 2000).

Once stable basal glutamate efflux was established, DHK/Ringer's was infused locally down the probe for the duration of the experiment. One hour later, the rats received an intraperitoneal injection of either saline or *d*-amphetamine and sampling continued for a further 5 h (Figure 6.1). The rats were randomly assigned to one of four treatment groups for measurement of glutamate efflux in both the cACC and rACC (Table 6.1).

Table 6.1 Drug treatment groups. Rats were randomly assigned to 1 of 4 treatment groups for either the caudal or rostral ACC.

	Local infusion		Systemic injection	
	RINGER'S	DHK	SALINE	<i>d</i> -AMP
1	X		X	
2	X			X
3		X	X	
4		X		X

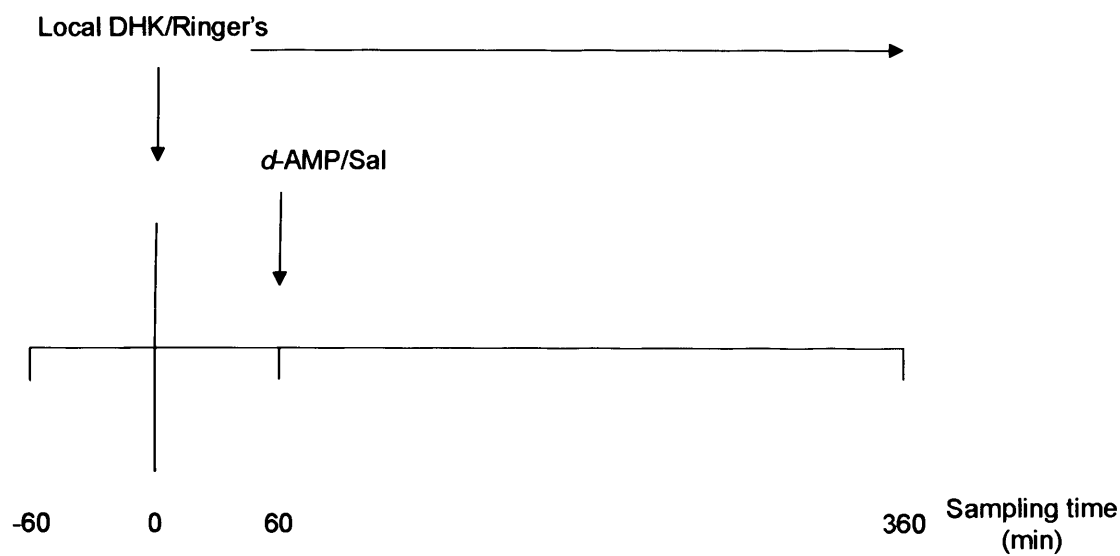


Figure 6.1 Timeline for experiments performed in Chapter 6. After 3 stable basal samples were taken, DHK/Ringer's solution was infused at time T_0 for the remainder of the experiment. At time T_{60} , 3 mg/kg *d*-amphetamine/saline was given by i.p. injection.

6.3.2/ Statistical analysis

All data were analysed for statistical significance using two-way ANOVA with repeated measures. 'Time' was a 'within subjects' factor and 'pretreatment' was a 'between subjects' factor. Data were also divided into 'bins' with three consecutive samples per bin. Therefore, each bin represents 1 h of sampling (Figure 6.2). 'Bin' was a 'within subjects' factor.

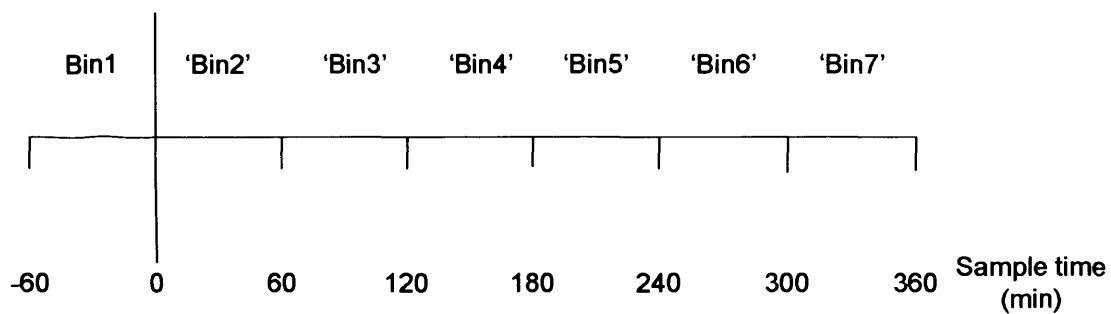


Figure 6.2 Time bins for statistical analysis of changes in extracellular glutamate after local infusion of DHK/Ringer's solution and systemic injection of d-amphetamine/saline.

6.4/ RESULTS

6.4.1/ Caudal Anterior Cingulate Cortex

There was no difference in basal glutamate efflux in the cACC in the four treatment groups:

Ringers-saline	8.3 ± 3.4 pmol/20min
DHK-saline	9.2 ± 1.5 pmol/20min
Ringers-amphetamine	5.1 ± 2.0 pmol/20min
DHK-amphetamine	9.3 ± 2.1 pmol/20min

Glutamate efflux was unaffected by infusion of Ringer's and subsequent injection of saline. There was a transient increase in glutamate efflux during the first hour of sampling after initiation of infusion of DHK, which quickly returned to basal levels for the next 3 h of sampling (Figure 6.3). Glutamate efflux rose steadily during the final 2 h, but this did not attain statistical significance (see: Table 6.2 for statistical analysis).

During infusion of Ringer's solution, systemic injection of *d*-amphetamine caused a large, transient increase in glutamate efflux (+ 500 % *cf.* basal). After the transient increase, glutamate efflux decreased (+ 200 % *cf.* basal) and remained at this level for the remainder of the experiment (Figure 6.4 and see: Table 6.3 for statistical analysis). The transient increase in glutamate efflux induced by systemic injection of *d*-amphetamine was unaffected by local infusion of DHK. There was only a

negligible effect of DHK on the sustained increase in glutamate efflux 2 h after injection of *d*-amphetamine ($T_{120-T_{220}} \text{ DRUG*BIN } F_{1,26} = 4.480 \text{ } P < 0.04$). Subsequently, glutamate efflux increased during the final 2 h of sampling until it reached the same level as in the Ringer's-*d*-AMP group (Figure 6.4 and see: Table 6.3 for statistical analysis).

In the Ringer's-saline group, four of the rats had to be excluded due to incorrect probe placement.

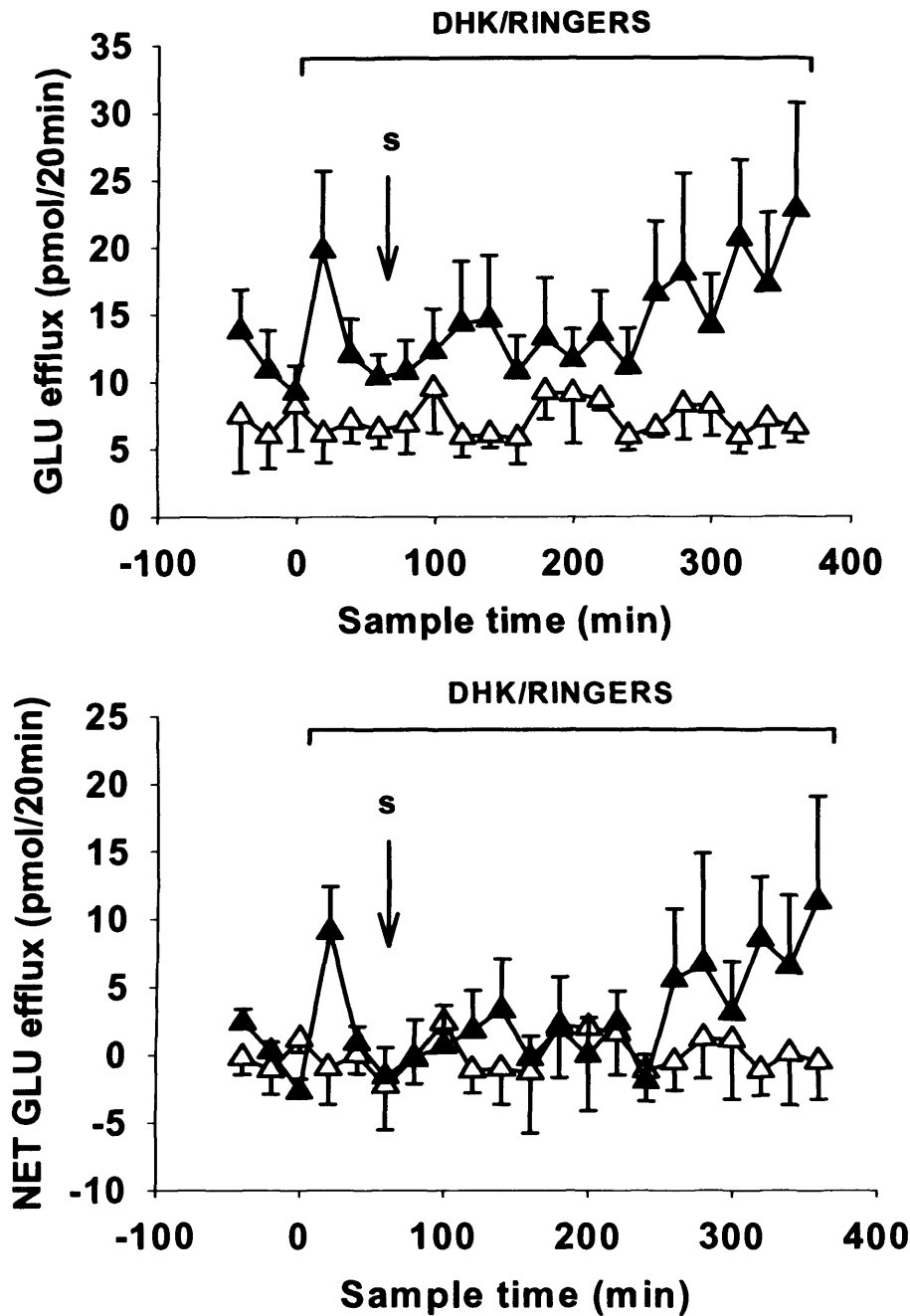


Figure 6.3 Effects of intraperitoneal administration of saline on glutamate efflux in the cACC of freely-moving rats.

Infusion of DHK (1 mM) or Ringer's solution was initiated at T_0 and maintained for the entire experiment, as indicated by the line. Saline was administered at T_{60} as indicated by the arrow. Glutamate efflux is expressed as pmol/20min. Points show mean \pm s.e. mean GLU efflux after infusion of DHK (closed triangles) or Ringer's solution (open triangles). The top graph shows raw data and bottom graph net data set. Ringer's group: N=4, DHK group: N=10.

Table 6.2 Statistics generated from split-plot ANOVA summarizing the effects of administration of saline on glutamate efflux in the cACC. Rats were pre-treated with either DHK (1 mM) or Ringer's solution 1 h before systemic injection of saline. Glutamate efflux in each time bin was compared with efflux in the basal samples. Significant differences are highlighted in **bold**.

Treatment	Saline (1 ml/kg)	
	Ringer's	DHK
Time (min)		
T ₂₀ -T ₆₀	F(1,2)=0.711 <i>P</i> <0.5	F(1,8)=16.372 <i>P</i> <0.004
T ₈₀ -T ₁₂₀	F(1,2)=0.002 <i>P</i> <0.9	F(1,9)=0.160 <i>P</i> <0.7
T ₁₄₀ -T ₁₈₀	F(1,2)=0.016 <i>P</i> <0.9	F(1,9)=0.369 <i>P</i> <0.6
T ₂₀₀ -T ₂₄₀	F(1,2)=0.011 <i>P</i> <0.9	F(1,9)=0.010 <i>P</i> <0.9
T ₂₈₀ -T ₃₀₀	F(1,2)=0.010 <i>P</i> <0.9	F(1,8)=0.541 <i>P</i> <0.5
T ₃₂₀ -T ₃₆₀	F(1,2)=0.093 <i>P</i> <0.8	F(1,8)=2.643 <i>P</i> <0.1

Table 6.3 Statistics generated from split-plot ANOVA summarizing the effects of administration of *d*-AMP on glutamate efflux in the cACC. Rats were pre-treated with either DHK (1 mM) or Ringer's solution 1 h before systemic injection of *d*-AMP. Glutamate efflux in each time bin was compared with efflux in the basal samples. Significant differences are highlighted in **bold**.

Treatment	<i>d</i> -AMP (3 mg/kg)	
	Ringer's	DHK (1 mM)
Time (min)		
T ₂₀ -T ₆₀	F(1,6)=0.069 <i>P</i> <0.8	F(1,7)=5.732 <i>P</i><0.05
T ₈₀ -T ₁₂₀	F(1,6)=6.725 <i>P</i><0.04	F(1,6)=6.029 <i>P</i><0.05
T ₁₄₀ -T ₁₈₀	F(1,6)=8.949 <i>P</i><0.05	F(1,6)=0.144 <i>P</i> <0.7
T ₂₀₀ -T ₂₄₀	F(1,6)=0.299 <i>P</i> <0.6	F(1,7)=0.148 <i>P</i> <0.7
T ₂₆₀ -T ₃₀₀	F(1,6)=1.391 <i>P</i> <0.3	F(1,5)=6.924 <i>P</i> <0.5
T ₃₂₀ -T ₃₆₀	F(1,6)=1.288 <i>P</i> <0.3	F(1,7)=2.058 <i>P</i> <0.2

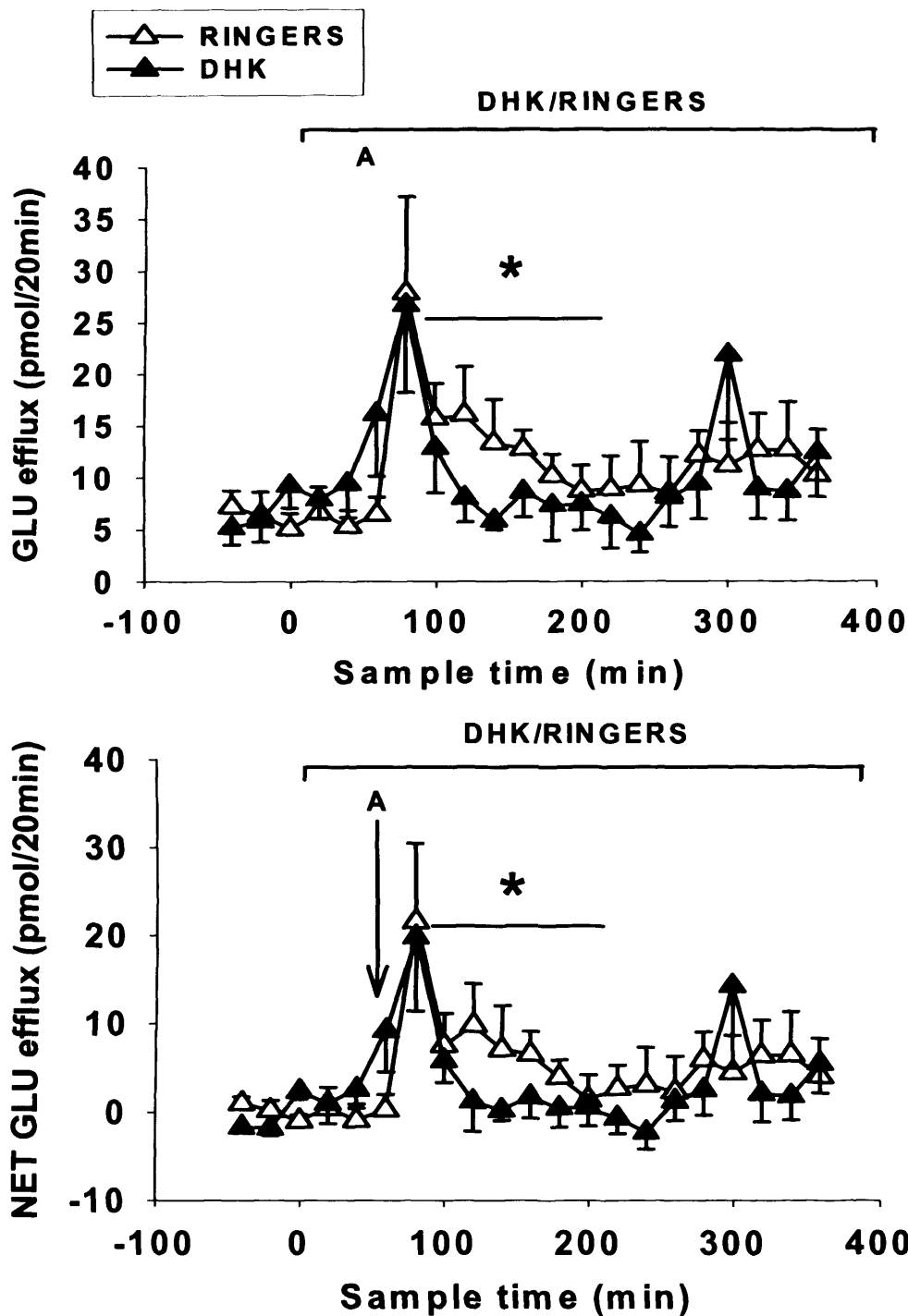


Figure 6.4 Effects of intraperitoneal administration of *d*-amphetamine on glutamate efflux in the cACC of freely-moving rats.

Infusion of DHK (1 mM) or Ringer's solution was initiated at T_0 and maintained for the entire experiment as indicated by the line. *d*-Amphetamine (3 mg/kg i.p.) was administered at T_{60} as indicated by the arrow. Glutamate efflux is expressed as pmol/20min. Points show mean \pm s.e. mean GLU efflux after infusion of DHK (closed triangles) or Ringer's (open triangles). The top graph shows raw data and bottom graph net data set. $N=8$ for both groups. * - $P<0.05$.

6.4.2/ Rostral Anterior Cingulate Cortex

There was no difference in basal glutamate efflux in the rACC in the four treatment groups:

Ringers-saline	8 ± 1.5 pmol/20min
DHK-saline	9.7 ± 3.0 pmol/20min
Ringers-amphetamine	12.6 ± 2.3 pmol/20min
DHK-amphetamine	10.9 ± 1.9 pmol/20min

Glutamate efflux was increased by systemic injection of saline during the first 2 h post-injection (Figure 6.5 and see: Table 6.4 for statistical analysis). Infusion of DHK and subsequent injection of saline did not affect glutamate efflux at any time (Figure 6.5 and see: Table 6.4 for statistical analysis) i.e. DHK blocked the glutamate response to systemic saline.

During infusion of Ringer's solution, systemic injection of *d*-amphetamine caused a small, transient increase in glutamate efflux (+ 50 % *cf.* basal). After the transient increase, glutamate efflux returned to basal levels and remained stable for the remainder of the experiment (Figure 6.6 and see: Table 6.5 for statistical analysis). The transient increase in glutamate efflux induced by systemic *d*-amphetamine was significantly attenuated by local infusion of DHK (T_{80} - T_{120} DRUG: $F_{1,17} = 5.105$ $P < 0.04$). Subsequently, a progressive decrease in glutamate efflux was observed (- 50 % *cf.* basal; Figure 6.6).

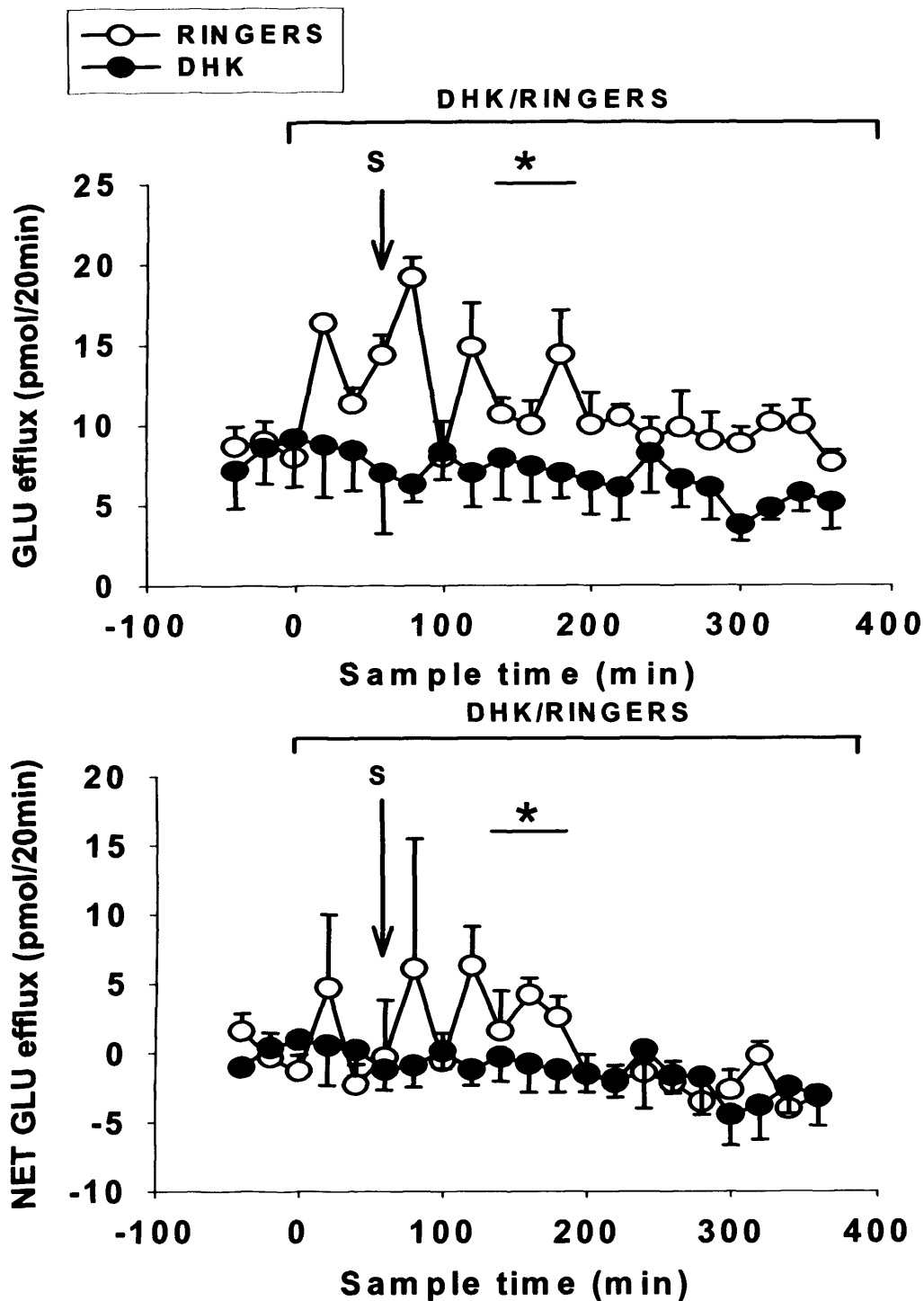


Figure 6.5 Effects of intraperitoneal administration of saline on glutamate efflux in the rACC of freely-moving rats.

Infusion of DHK (1 mM) or Ringer's solution was initiated at T_0 and maintained for the entire experiment as indicated by the line. Saline (1 ml/kg i.p.) was administered at T_{60} as indicated by the arrow. Glutamate efflux is expressed as pmol/20min. Points show mean \pm s.e. mean GLU efflux after administration of DHK (closed circles) or Ringer's (open circles). The top graph shows raw data and bottom graph shows net data set. $N=4/6$

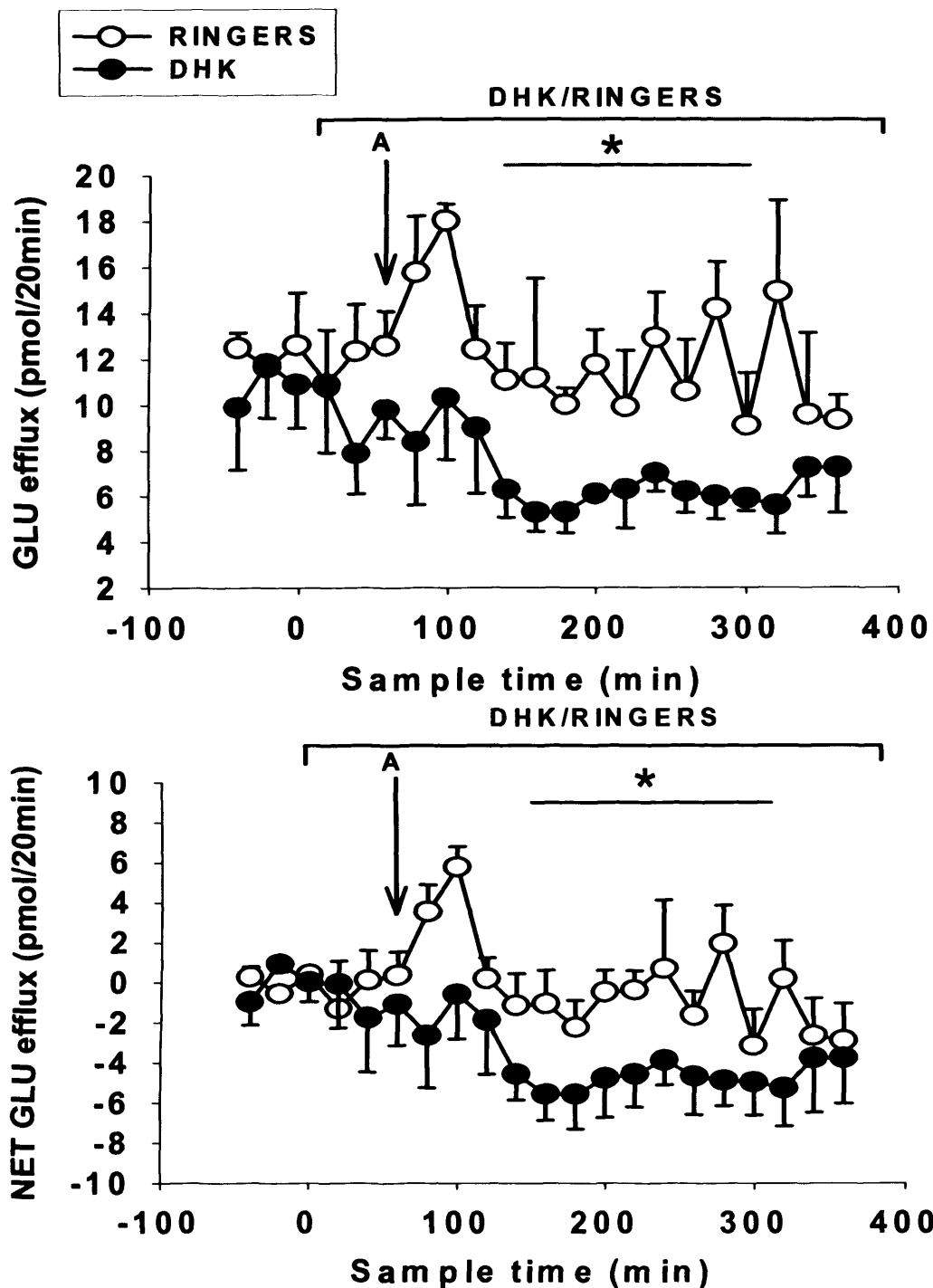


Figure 6.6 Effects of intraperitoneal administration of *d*-amphetamine on glutamate efflux in the rACC of freely-moving rats.

Infusion of DHK (1 mM) or Ringer's solution was initiated at T_0 and maintained for the entire experiment as indicated by the line. *d*-Amphetamine (3 mg/kg i.p.) was administered at T_{60} as indicated by the arrow. Glutamate efflux is expressed as pmol/20min. Points show mean \pm s.e. mean GLU efflux after infusion of DHK (closed circles) or Ringer's (open circles). Top graph shows raw data and bottom graph net data set. $N=5/6$. * $P<0.05$

Table 6.4 Statistics generated from split-plot ANOVA summarizing the effects of systemic administration of saline on glutamate efflux in the rACC. Rats were pre-treated with either DHK (1 mM) or Ringer's solution 1 h before systemic injection of saline. Glutamate efflux in each time bin was compared with efflux in the basal samples. Significant differences are shown in **bold**.

Treatment	Saline (1 ml/kg)	
	Ringer's	DHK (1 mM)
Time (min)		
T ₂₀ -T ₆₀	F(1,3)=0.017 <i>P</i> <0.9	F(1,5)=0.035 <i>P</i> <0.9
T ₈₀ -T ₁₂₀	F(1,2)=8.286 <i>P</i> <0.1	F(1,4)=0.704 <i>P</i> <0.4
T ₁₄₀ -T ₁₈₀	F(1,3)=12.912 <i>P</i><0.04	F(1,5)=0.417 <i>P</i> <0.5
T ₂₀₀ -T ₂₄₀	F(1,3)=0.291 <i>P</i> <0.6	F(1,4)=0.656 <i>P</i> <0.5
T ₂₆₀ -T ₃₀₀	F(1,3)=0.611 <i>P</i> <0.5	F(1,3)=1.835 <i>P</i> <0.3
T ₃₂₀ -T ₃₆₀	F(1,3)=0.595 <i>P</i> <0.5	F(1,4)=3.866 <i>P</i> <0.1

Table 6.5 Statistics generated from split-plot ANOVA summarizing the effects of systemic administration of *d*-amphetamine on glutamate efflux in the rACC. Rats were pre-treated with either DHK (1 mM) or Ringer's solution 1 h before systemic injection of *d*-amphetamine. Glutamate efflux in each time bin was compared with efflux in the basal samples. Significant differences are highlighted in **bold**.

Treatment	<i>d</i> -AMP (3 mg/kg)	
	Ringer's	DHK (1 mM)
Time (min)		
T ₂₀ -T ₆₀	F(1,5)=0.905 <i>P</i> <0.4	F(1,3)=0.179 <i>P</i> <0.7
T ₈₀ -T ₁₂₀	F(1,5)=1.508 <i>P</i> <0.3	F(1,2)=1.459 <i>P</i> <0.4
T ₁₄₀ -T ₁₈₀	F(1,5)=0.531 <i>P</i> <0.5	F(1,3)=12.484 <i>P</i><0.04
T ₂₀₀ -T ₂₄₀	F(1,4)=0.392 <i>P</i> <0.6	F(1,3)=10.736 <i>P</i><0.05
T ₂₆₀ -T ₃₀₀	F(1,5)=0.528 <i>P</i> <0.5	F(1,3)=9.459 <i>P</i><0.05
T ₃₂₀ -T ₃₆₀	F(1,5)=1.033 <i>P</i> <0.4	F(1,2)=1.542 <i>P</i> <0.3

6.5/ DISCUSSION

6.5.1/ *The effect of inhibition of GLT-1 on spontaneous glutamate efflux*

6.5.1.1/ The caudal anterior cingulate cortex

A marked increase in extracellular glutamate efflux was observed in the cACC during the first hour of DHK infusion in the DHK-SALINE group. This quickly returned to basal levels for the next 3 h of sampling. One previous microdialysis study infused increasing concentrations of the glutamate uptake inhibitor *L-trans*-pyrrolidine-2,4-dicarboxylic acid (PDC; 0.1-10 mM) and found a dose-dependent increase in extracellular glutamate in the frontal cortex (but not the anterior cingulate cortex; Semba and Wakuta, 1998). My result is inconsistent with previous data, in that the increased glutamate efflux was not sustained throughout infusion of DHK. In the present experiments, glutamate efflux only increased during the first hour of infusion, but then returned to basal levels even after continued infusion of DHK. In the study by Semba and Wakuta, the increase in glutamate efflux was maintained throughout DHK infusion.

6.5.1.2/ The rostral anterior cingulate cortex

In the rACC, no increase in glutamate efflux in response to DHK was observed at any time. Previous microdialysis studies have infused DHK in the striatum, and demonstrated a clear, dose-related increase in glutamate efflux (Del Arco *et al.*, 1999). Any change in glutamate efflux could have been masked by reuptake of glutamate by other transporters surrounding the synapse, for example, the neuronal

transporter EAAC1 (Kanai and Hediger, 2003). Alternatively, any glutamate released by the transporter could be acting on presynaptic metabotropic glutamate receptors to decrease neuronal release and thus normalising the levels of synaptic glutamate. The group II family of metabotropic glutamate receptors are highly enriched in the prefrontal cortex (Ohishi *et al.*, 1993). At an ultrastructural level, mGluR2 has been localised to presynaptic structures at the periphery of the synaptic area (Petralia *et al.*, 1996), which fits with the modulation of glutamatergic transmission in the prefrontal cortex. The highly selective mGluR2 agonist LY354740 (10 mg/kg) administered 20 min before PCP, completely abolished the increased glutamate efflux in the prefrontal cortex normally seen after systemic administration of PCP (5 mg/kg i.p., Moghaddam and Adams, 1998).

6.5.2/ The effect of inhibition of GLT-1 on d-amphetamine-induced glutamate efflux

6.5.2.1/ The Caudal Anterior Cingulate Cortex

In the cACC, injection of *d*-amphetamine led to a large, transient increase in glutamate efflux (+ 500 % *cf.* basal), which was quickly dissipated to a plateau (+ 200 % *cf.* basal). Due to the delayed nature of the increase in VTA glutamate efflux induced by systemic *d*-amphetamine, it is thought to involve inhibition or reversal of glutamate transporters, rather than Ca²⁺-dependent release associated with neurotransmission (Wolf *et al.*, 2000). These authors discovered that blockade of the glial glutamate transporter GLT-1 by dihydrokainate prevented the increase in glutamate efflux induced by systemic *d*-amphetamine. I was interested in finding out

if blockade of GLT-1 had the same effect on the increase in extracellular glutamate in the cACC. To do this, dihydrokainate ('DHK'), a nontransportable inhibitor of the GLT-1 subtype of glutamate transporter, was used. Pre-treatment with DHK by local infusion did not prevent the transient increase in glutamate efflux within the cACC, suggesting that this does not depend on the glial glutamate transporter GLT-1. As systemic *d*-amphetamine did not affect dopamine efflux in the cACC (see: Chapter 4), it can be inferred that the increased glutamate efflux is unlikely to occur secondary to an increase in dopaminergic neurotransmission.

The more sustained response to *d*-amphetamine was attenuated by DHK 2-4 h after injection of *d*-amphetamine, suggesting that GLT-1 has some effect on glutamate release governed by afferent inputs to this area. Reversal of the glutamate transporter by *d*-amphetamine and extrusion of glutamate into the extracellular space could play a minor role, although more experiments would be needed to corroborate this finding. Previous microdialysis studies have suggested that reversal of GLT-1 and efflux of glutamate is responsible for the increase in glutamate efflux seen after systemic *d*-amphetamine. Intraperitoneal *d*-amphetamine (5 mg/kg) led to a delayed increase in glutamate efflux in the ventral tegmental area (VTA). This was completely inhibited by pre-treatment with the non-competitive glial glutamate transporter inhibitor dihydrokainate, infused 60 min before systemic administration of *d*-amphetamine ('DHK' 1mM; Wolf *et al.*, 2000). Another study found increased striatal glutamate in response to local infusion of *d*-amphetamine (54 mM). This was attenuated by co-perfusion with blockers of GLT-1, DHK (8 mM) and L-trans-pyrrolidine-2,4-dicarboxylic acid ('PDC' 4mM; Del Arco *et al.*, 1999).

These authors suggested that oxidative stress and generation of free radicals by *d*-amphetamine treatment was mediating reversal of GLT-1. Indeed, there have been

several reports in the literature suggesting that both acute and chronic administration of *d*-amphetamine leads to oxidative stress and production of free radicals. For example, infusion of *d*-amphetamine (10 μ M) directly into the striatum caused an increased formation of hydroxyl radicals (Wan *et al.*, 2000, see also Huang *et al.*, 1997). These effects of *d*-amphetamine suggest a mechanism of action similar to that induced by ischaemia/hypoxia. During ischaemia, the activity of the Na⁺/K⁺-ATPase is markedly suppressed and the ionic gradient of Na⁺ is reduced, resulting in reversed operation of astrocytic and neuronal glutamate transporters (for review see Camacho and Massieu, 2006). Therefore, glutamate and Na⁺ are transported to the extracellular space (Szatkowski *et al.*, 1990). The ischaemia-induced rise in extracellular glutamate caused by reversed uptake occurs mainly via GLT-1. This has been demonstrated using microdialysis in the hippocampal CA1 region of mice lacking GLT-1 (Mitani and Tanaka, 2003). During a 5 min ischaemic period, the increase in glutamate levels seen in GLT-1 mutant mice was greater than that observed in wild type mice. This result indicates that GLT-1 takes up extracellular glutamate to protect neurones against delayed neuronal death. However, during a 20 min ischaemic period, the increase in extracellular glutamate measured by microdialysis was higher in wild type mice compared to GLT-1 mutant mice during the last 12.5 min of ischaemia. Neurotoxicity was also observed in this group. This indicates release of glutamate, triggering acute neuronal death in the later stages of an ischaemic episode. These observations lead to the conclusion that during the first minutes of ischaemia, when energy levels are not exhausted, glutamate transporters operate normally eliminating released glutamate. However, when energy metabolism is severely altered, glutamate transporters operate in the reverse direction extruding glutamate to the extracellular space and contributing to cell death.

Further evidence for a hypoxic effect of *d*-amphetamine comes from a microdialysis study performed in the striatum (Del Arco *et al.*, 1999). Intracerebral infusions of *d*-amphetamine (5-20 $\mu\text{g}/\mu\text{l}$) caused a decrease of extracellular Na^+ and an increase of extracellular lactate. Co-infusion of the α -adrenoceptor antagonist phenoxybenzamine (PBZ: 1mM) with 20 $\mu\text{g}/\mu\text{l}$ *d*-amphetamine significantly attenuated the increase in glutamate efflux produced by *d*-amphetamine, suggesting that the decrease in oxygen availability was caused by constriction of blood vessels. As a consequence of the decrease in oxygen concentration in the cell, cellular ATP synthesis is reduced. This impairs the function of the ATPase pumps responsible for pumping Na^+ out of the cell. Thus, intracellular $[\text{Na}^+]$ increases and facilitates reversal of the Na^+ -dependent neurotransmitter transporters (see: Figure 6.7).

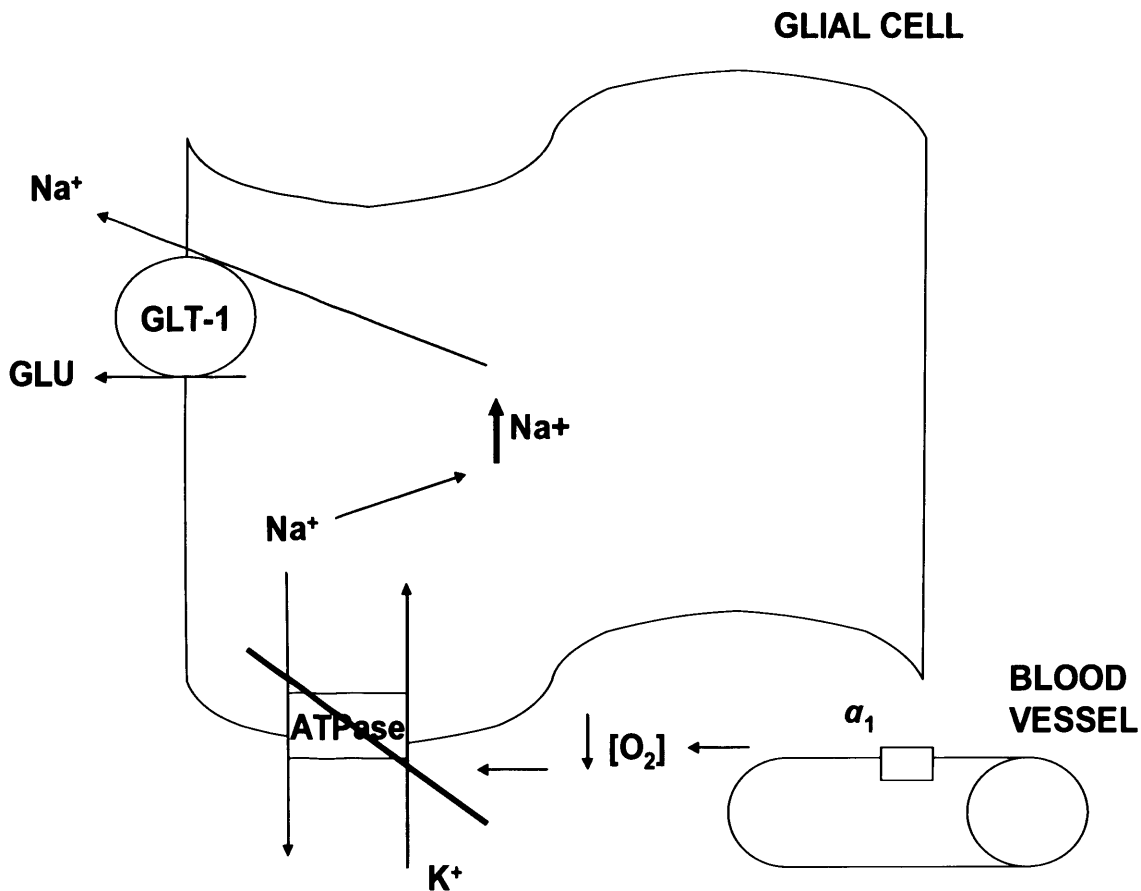


Figure 6.7 Schematic diagram showing the suggested mechanisms through which *d*-amphetamine may act to increase the extracellular concentrations of neurotransmitters

- *d*-Amphetamine acts through α₁-adrenoceptors of the brain blood vessels to produce a vasoconstriction
- This results in a decrease in oxygen availability for the cell
- As a consequence of the decrease in oxygen availability, function of the glial Na⁺K⁺-ATPase is reduced
- This leads to an increase in intracellular Na⁺, facilitating reversal of the Na⁺-dependent glial transporter, GLUT-1 and extrusion of glutamate into the extracellular space

Since the increased glutamate efflux induced by systemic *d*-amphetamine in the cACC was only attenuated after 2-4 h by pre-treatment with DHK, it follows that the some of the glutamate released by *d*-amphetamine is derived from another source. Other possible sources of glutamate release have been discussed in previous chapters, and include Ca²⁺-dependent exocytotic release by both neurons and astrocytes, or glutamate release through other subtypes of glutamate transporter.

6.5.2.2/ The Rostral Anterior Cingulate Cortex

In the rACC, systemic administration of *d*-amphetamine led to a small, transient increase in glutamate efflux (+ 50 % *cf.* basal), which quickly returned to basal levels after 40 min. Again, I examined the role of glial glutamate transporters in *d*-amphetamine-induced glutamate efflux. The small, transient glutamate response to *d*-amphetamine was significantly attenuated by pre-treatment with DHK and could rest on retrotransport at the glial glutamate transporter. However, after this, there was a gradual, sustained and marked decrease in glutamate efflux in the DHK-AMP group (-50 % *cf.* basal) compared to the RINGERS-AMP group. To the best of my knowledge, this is the first time that such a decrease in glutamate efflux in the rat cortex in response to *d*-amphetamine has been reported. Disturbances of glutamatergic neurotransmission have been implicated in the pathophysiology of schizophrenia (Tsai *et al.*, 1995), with decreased glutamatergic neurotransmission observed during psychosis. This correlates well with my result.

6.5.3/ Mechanism of decreased glutamate efflux

6.5.3.1/ Decreased extracellular glutamate – a possible hypothesis

I propose that glutamate released into the synapse by the action of *d*-amphetamine is taken up by the activity of high-affinity glutamate transporters present in both neurones and glia surrounding the synaptic cleft (e.g. the glial glutamate transporter GLT-1 or the neuronal glutamate transporter EAAC1) (Kanai and Hediger, 2003). The glial glutamate transporter GLT-1 is responsible for the vast majority of glutamate transport activity in the rat forebrain (>90 %; Tanaka *et al.*, 1997). Under normal conditions, any increase in glutamate efflux evoked by systemic injection of *d*-amphetamine is cleared by GLT-1, so no overall change in extracellular glutamate sampled by the probe is seen. When local GLT-1 is blocked by infusion of DHK, the concentration of glutamate within the synaptic cleft is transiently increased. This released glutamate acts on inhibitory autoreceptors, such as mGluR2 to inhibit its own release, and, thus, the concentration of extracellular glutamate sampled by the probe decreases (see Figure 6.8).

Candidates for this autoreceptor inhibition include the mGluR5 receptors, which are thought to act presynaptically in the prefrontal cortex (Fazal *et al.*, 2003). Microdialysis studies have also shown that selective group II mGluR agonists block ketamine-stimulated glutamate release in the rat prefrontal cortex (Lorrain *et al.*, 2003), as well as decreasing basal glutamate efflux in the rat nucleus accumbens (Xi *et al.*, 2003). However, Melendez *et al.* (2005) reported no effect on basal extracellular glutamate levels in the rat medial prefrontal cortex by either group I- or group II-selective ligands. These results suggest that GLT-1 normally masks glutamate release governed by afferent inputs to the rACC.

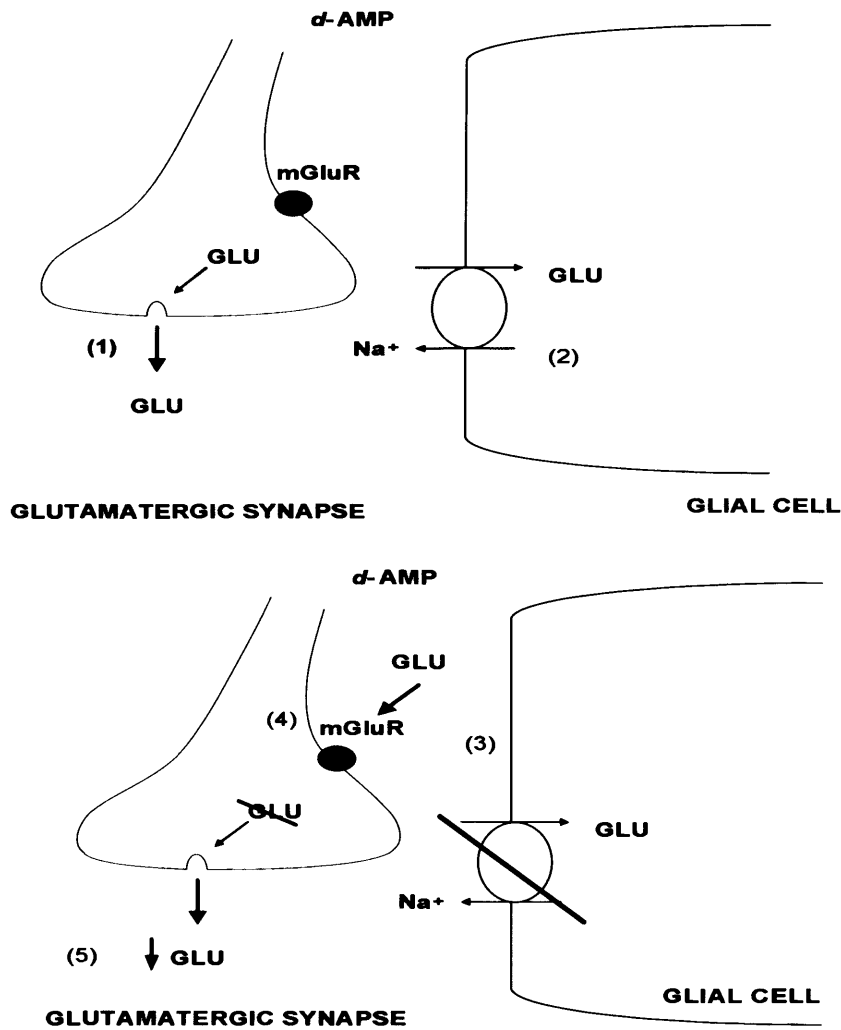


Figure 6.8 Proposed scheme by which local infusion of DHK and systemic injection of *d*-amphetamine could cause a gradual, sustained decrease in glutamate efflux in the rACC.

1. Systemic administration of *d*-amphetamine leads to increased glutamate efflux in the rACC
2. Under normal circumstances, this increased extracellular glutamate is rapidly taken up by the glial glutamate transporter, GLT-1, thus masking increased extracellular glutamate
3. Blockade of GLT-1 and subsequent injection of *d*-amphetamine leads to a transient increase in extracellular glutamate
4. This increased glutamate acts on inhibitory mGluRs present on the terminals of glutamatergic pyramidal neurones to decrease release of glutamate
5. Consequently, a decrease in extracellular glutamate is seen

6.5.4/ SUMMARY OF KEY FINDINGS

- In the cACC, GLT-1 has some contribution to release of glutamate governed by afferent influences, but another mechanism accounts for a large proportion of glutamate released
- In contrast, in the rACC, GLT-1 limits the concentration of extracellular glutamate seen after systemic administration of *d*-amphetamine
- Spontaneous efflux of glutamate in either subregion was not affected by DHK, suggesting that GLT-1 is not essential for clearance of extracellular glutamate in the rat anterior cingulate cortex

Chapter 7

7.0/ Effect of pre-treatment with the GLT-1 inhibitor dihydrokainate on the glutamate response to local infusion of *d*-amphetamine in the caudal and rostral anterior cingulate cortices.

7.1/ INTRODUCTION

In my previous studies, systemic *d*-amphetamine caused a sustained increase in glutamate efflux in the cACC (see: Chapter 3). This was unaffected by pre-treatment with the glial glutamate transporter inhibitor dihydrokainate directly into the cACC (see: Chapter 6). In the rACC, only a transient increase in glutamate efflux was observed after systemic administration of *d*-amphetamine, after which glutamate levels quickly returned to basal concentrations. This transient increase in glutamate efflux did not attain criteria for statistical significance. Pre-treatment with DHK caused sustained decrease (below baseline) in glutamate efflux in the DHK-AMP group (see: Chapter 6).

In the cACC, inhibition of GLT-1 had little impact on the increase in extracellular glutamate produced by systemic *d*-amphetamine. In the rACC, the small, transient response to systemic administration of *d*-amphetamine could rest on efflux at the transporter, but the mechanism underlying the subsequent, sustained decrease in glutamate efflux will require further studies to elucidate. It is possible that extracellular glutamate, which would normally undergo clearance by GLT-1, activates glutamatergic autoreceptors, which inhibit its release. Again, an asymmetry in the regulation of glutamatergic neurotransmission between the cACC and rACC is evident from these experiments. The glutamate response to systemic *d*-amphetamine

in the rACC is constrained by uptake of glutamate at GLT-1, while GLT-1 plays no role in the glutamate response in the cACC.

The purpose of the experiments performed in this Chapter was to further characterise the mechanisms underlying the increase in glutamate efflux in the cACC and rACC induced by local infusion of *d*-amphetamine. The effect of pre-treatment with the glial glutamate transporter inhibitor dihydrokainate on the glutamate response to local infusion of *d*-amphetamine was determined in each subregion. The concentration of DHK (1 mM) was based on our previous studies, which demonstrated a constraint of the glutamate response to systemic *d*-amphetamine in the rACC by GLT-1 (see: Chapter 6, Wolf *et al.*, 2000). The concentrations of *d*-amphetamine (10 and 100 μ M) were based on my previous studies, which demonstrated a reliable increase in glutamate efflux in the rACC (see: Chapters 3 and 5).

7.2/ AIM

- *To compare the effects of pre-treatment with the GLT-1 blocker dihydrokainate on the glutamate response to local infusion of d-amphetamine in the caudal and rostral anterior cingulate cortices.*

7.3/ METHODS

7.3.1/ *In vivo* microdialysis

Experiments were performed on freely-moving rats (250-300 g on day of surgery).

Rats were implanted with microdialysis probes under halothane anaesthesia in both the cACC and the rACC (i.e. dual-probe) the day before experimenting. For local infusion, dihydrokainate was dissolved in Ringer's to make a 1 mM solution and *d*-amphetamine was dissolved in Ringer's to make 10 and 100 μ M solutions. These doses of *d*-amphetamine were based on previous experiments carried out in the laboratory, which demonstrated a clear increase in glutamate efflux (see: Chapter 3). The dose of DHK was based on a previous study, which demonstrated a blockade of *d*-amphetamine-induced glutamate efflux in the rat ventral tegmental area (Wolf *et al.*, 2000).

Rats implanted with dual-probes were assigned to one of three treatment groups. There were six treatment groups in total and rats were randomised between these treatment groups (see: Table 7.1 for details of treatment groups).

Table 7.1 Drug treatment groups. Rats were randomly assigned to 1 of 6 treatment groups.

	Pre-treatment		Treatment	
	DHK	Ringer's	DHK	<i>d</i> -amphetamine
1- cACC	X		X	
2- cACC		X		X
3- cACC	X			X
4- rACC	X		X	
5- rACC		X		X
6- rACC	X			X

Once stable basal glutamate efflux was established, DHK/Ringer's was infused locally down both probes for the duration of the experiment. One hour later, the perfusion fluid was changed for Ringer's/DHK solution containing 10 μ M *d*-amphetamine and samples collected for another 2 h. After 2 h, the perfusion fluid was changed for Ringer's/DHK solution containing 100 μ M *d*-amphetamine and sampling continued for a further 2 h (Figure 7.1).

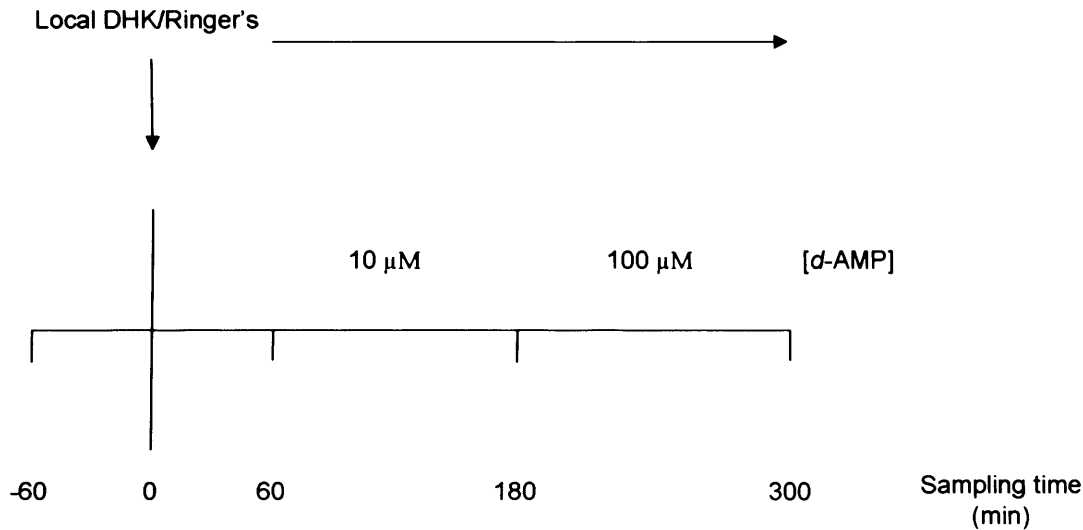


Figure 7.1 *Timeline for DHK experiment.* After 3 stable basal samples were taken, DHK/Ringer's solution was infused at Time T_0 for the remainder of the experiment. At Time T_{60} , 10 μM *d*-amphetamine was locally infused. At Time T_{180} , 100 μM *d*-amphetamine was locally infused.

7.3.2/ Statistical analysis

All data were analysed for statistical significance using two-way ANOVA with repeated measures. 'Time' and 'brain region' were both 'within subjects' factors. 'Pretreatment' was a 'between subjects' factor. Data were also divided into 'bins' with three consecutive samples per bin. Therefore, each bin represents 1 h of sampling (Figure 7.2). 'Bin' was a 'within subjects' factor.

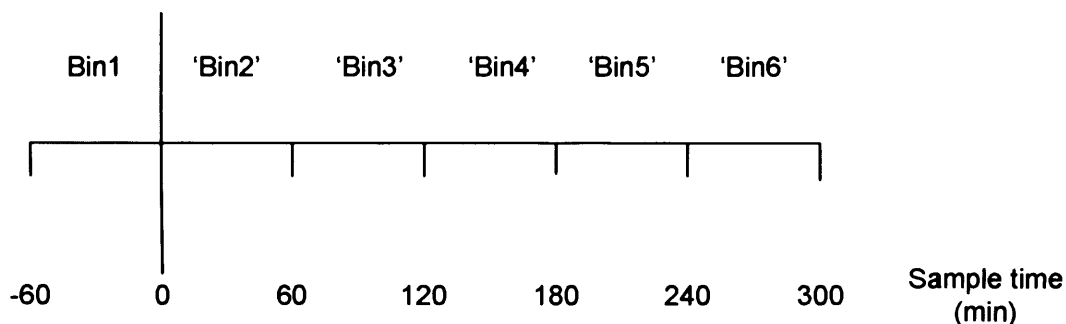


Figure 7.2 *Time bins for statistical analysis of changes in extracellular glutamate after local infusion of DHK/Ringer's solution and local infusion of d-amphetamine.*

7.4/ RESULTS

7.4.1/ Caudal anterior cingulate cortex

There was no difference in basal glutamate efflux in the cACC in the three treatment groups:

DHK-DHK	10.6 ± 1.5 pmol/20min
RINGERS-AMP	14.7 ± 2.7 pmol/20min
DHK-AMP	13.9 ± 6.1 pmol/20min

Local infusion of DHK (1 mM) did not significantly increase glutamate efflux at any time (Figure 7.2 and see Table 7.2 for statistical analysis). Local infusion of increasing concentrations of *d*-amphetamine did not significantly increase glutamate efflux at any time (Figure 7.3 and see Table 7.3 for statistical analysis). Co-infusion of DHK and *d*-amphetamine, led to a significant increase in glutamate efflux during the first hour of infusion of the lowest concentration (10 μM), when compared to glutamate efflux after infusion of *d*-amphetamine alone: PRETREATMENT*BIN F(1,18)=6.574 P<0.02 (Figure 7.4). After 1 h, glutamate efflux returned to basal levels for the remainder of the experiment (Figure 7.4) i.e. DHK enhanced the glutamate response to the lowest concentration of *d*-amphetamine (10 μM) during the first hour of infusion (see Table 7.4 for statistical analysis).

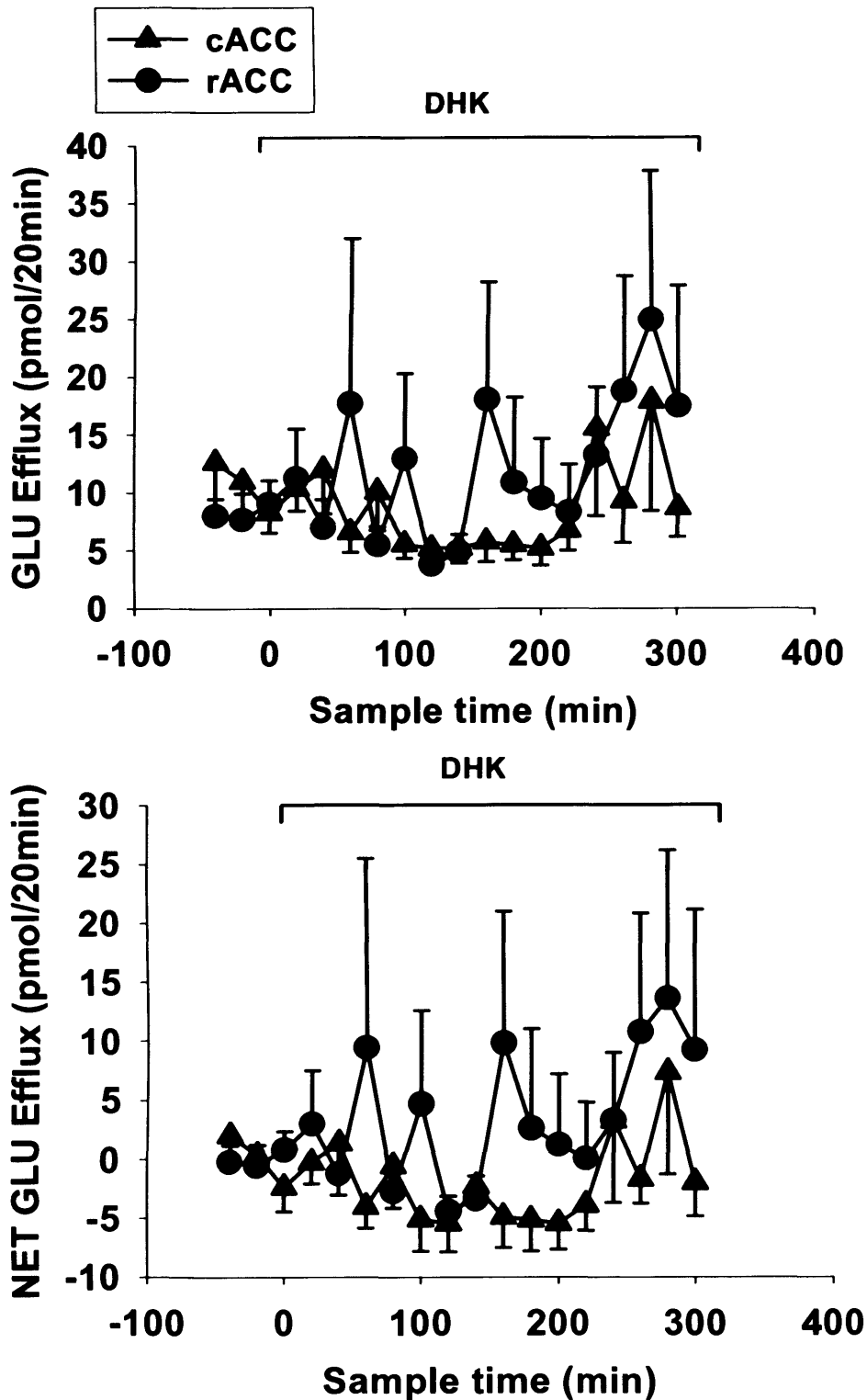


Figure 7.3 Effects of infusion of dihydrokainate (DHK) on glutamate ('GLU') efflux in the cACC and rACC of freely-moving rats
 Infusion of DHK (1 mM) was initiated at T₀. GLU efflux is expressed as pmol/20 min. Points show mean ± s.e.mean GLU efflux in the cACC (closed triangles) and rACC (closed circles). N=7/8. The top graph shows raw data and the bottom graph net data set.

Table 7.2 Statistics generated from split-plot ANOVA summarizing the effects of local infusion of DHK (1mM) on glutamate efflux in the cACC and rACC. Glutamate efflux in each time bin was compared with efflux in the basal samples. Significant differences are highlighted in **bold**.

Treatment	DHK (1 mM)	
	cACC	rACC
Time (min)		
T ₂₀ -T ₆₀	F _(1,18) =0.177 <i>P</i> <0.6	F _(1,14) =0.694 <i>P</i> <0.4
T ₈₀ -T ₁₂₀	F _(1,18) =2.139 <i>P</i> <0.1	F _(1,14) =0.124 <i>P</i> <0.7
T ₁₄₀ -T ₁₈₀	F_(1,17)=7.339 <i>P</i><0.02	F _(1,14) =0.369 <i>P</i> <0.6
T ₂₀₀ -T ₂₄₀	F _(1,17) =0.494 <i>P</i> <0.4	F _(1,14) =0.097 <i>P</i> <0.8
T ₂₆₀ -T ₃₀₀	F _(1,16) =0.253 <i>P</i> <0.6	F _(1,13) =1.629 <i>P</i> <0.2

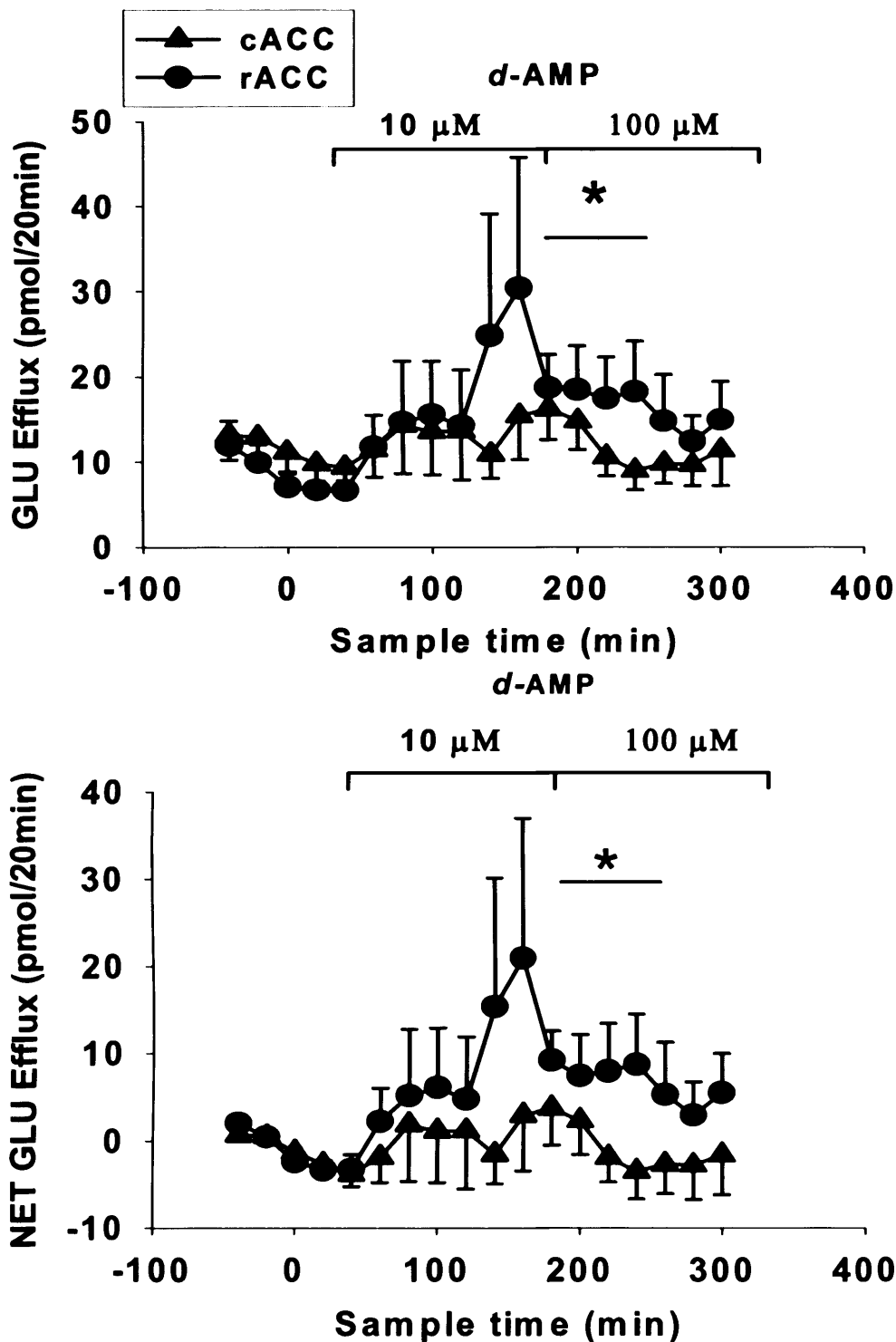


Figure 7.4 Effects of cumulative infusion of d-amphetamine (d-AMP) on glutamate ('GLU') efflux in the cACC and rACC of freely-moving rats

Infusion of Ringer's was maintained until T₄₀. Infusion of d-AMP (10 μM: 120 min, 100 μM: 120 min) was initiated at T₆₀ as indicated by the line. GLU efflux is expressed as pmol/20min. Points show mean ± s.e.mean GLU efflux in the cACC (closed triangles) and rACC (closed circles). N=8/10. The top graph shows raw data and the bottom graph net data set.

Table 7.3 *Statistics generated from split-plot ANOVA summarizing the effects of local infusion of d-amphetamine on glutamate efflux in the cACC and rACC. Glutamate efflux in each time bin was compared with efflux in the basal samples. Significant differences are highlighted in bold.*

Treatment	<i>d</i> -AMP	
	cACC	rACC
[<i>d</i> -AMP] (μ M)		
10 (1 h)	$F_{(1,24)}=0.050$ $P<0.8$	$F_{(1,21)}=0.526$ $P<0.4$
10 (2 h)	$F_{(1,24)}=0.126$ $P<0.7$	$F_{(1,21)}=1.875$ $P<0.2$
100 (1 h)	$F_{(1,24)}=0.094$ $P<0.8$	$F_{(1,20)}=4.356$ $P<0.05$
100 (2 h)	$F_{(1,23)}=1.647$ $P<0.2$	$F_{(1,21)}=1.398$ $P<0.3$

7.4.2/ Rostral Anterior Cingulate Cortex

There was no difference in basal glutamate efflux in the prefrontal cortex in the three treatment groups:

DHK-DHK	7.2 ± 0.9 pmol/20min
RINGERS-AMP	8.9 ± 1.9 pmol/20min
DHK-AMP	11.0 ± 7.3 pmol/20min

Local infusion of DHK (1 mM) did not increase glutamate efflux at any time (Figure 7.2 and see Table 7.2 for statistical analysis). A dose-related increase in glutamate efflux was observed after local infusion of *d*-amphetamine (Figure 7.3 and see Table 7.3 for statistical analysis). This increase attained statistical significance at the highest dose tested (100 μM) when compared to glutamate efflux in the anterior cingulate cortex: REGION T₂₀₀-T₃₀₀ F_(1,14)=4.495 P<0.05. A maximum net increase of 20.9 ± 16.0 pmol/20min was observed after infusion of 100 μM *d*-amphetamine. The *d*-amphetamine-induced glutamate efflux was phasic in nature, and declined in amplitude during subsequent samples. Pre-treatment with 1 mM DHK did not affect the glutamate response to *d*-amphetamine (no significant effect of 'pretreatment' was seen; Figure 7.5). *d*-Amphetamine retained the ability to increase glutamate efflux even in the presence of 1 mM DHK (Figure 7.5 and see Table 7.4 for statistical analysis). Frequent fluctuations in glutamate efflux were seen in this treatment group, with efflux increasing for a couple of samples before returning to basal levels again.

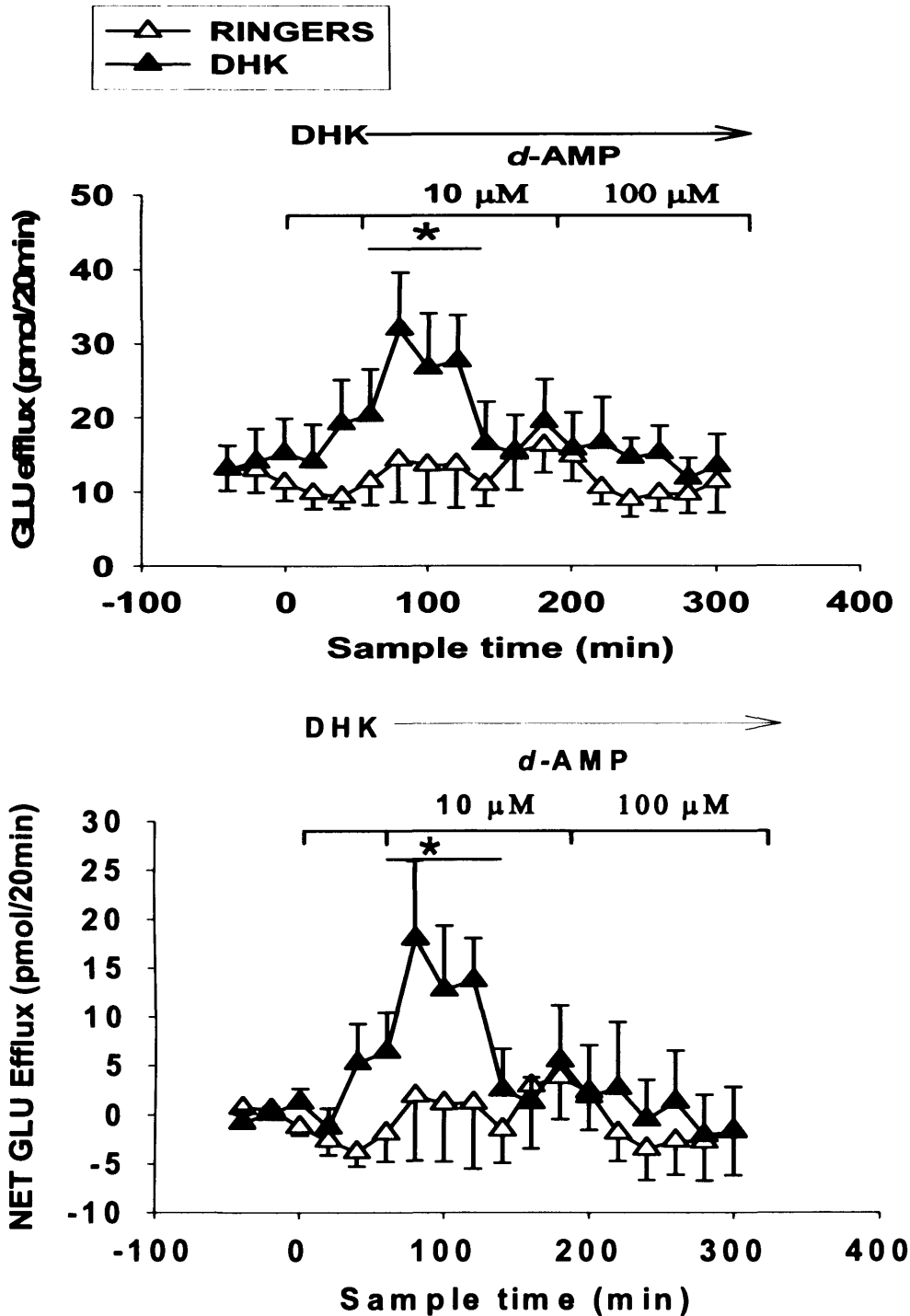


Figure 7.5 Effects of cumulative infusion of *d*-amphetamine (*d*-AMP) on glutamate (*GLU*) efflux in the caudal anterior cingulate cortex (*cACC*) of freely-moving rats. Infusion of DHK (1 mM) or Ringer's solution was initiated at T_0 and maintained throughout as indicated by the line. Infusion of *d*-AMP (10 μ M: 120 min, 100 μ M: 120 min) was initiated at T_{60} as indicated by the line. *GLU* efflux is expressed as pmol/20min. Points show mean \pm s.e. mean *GLU* efflux after infusion of DHK (closed triangles) or Ringer's (open triangles). $N=8/11$. The top graph shows raw data and the bottom graph net data set.

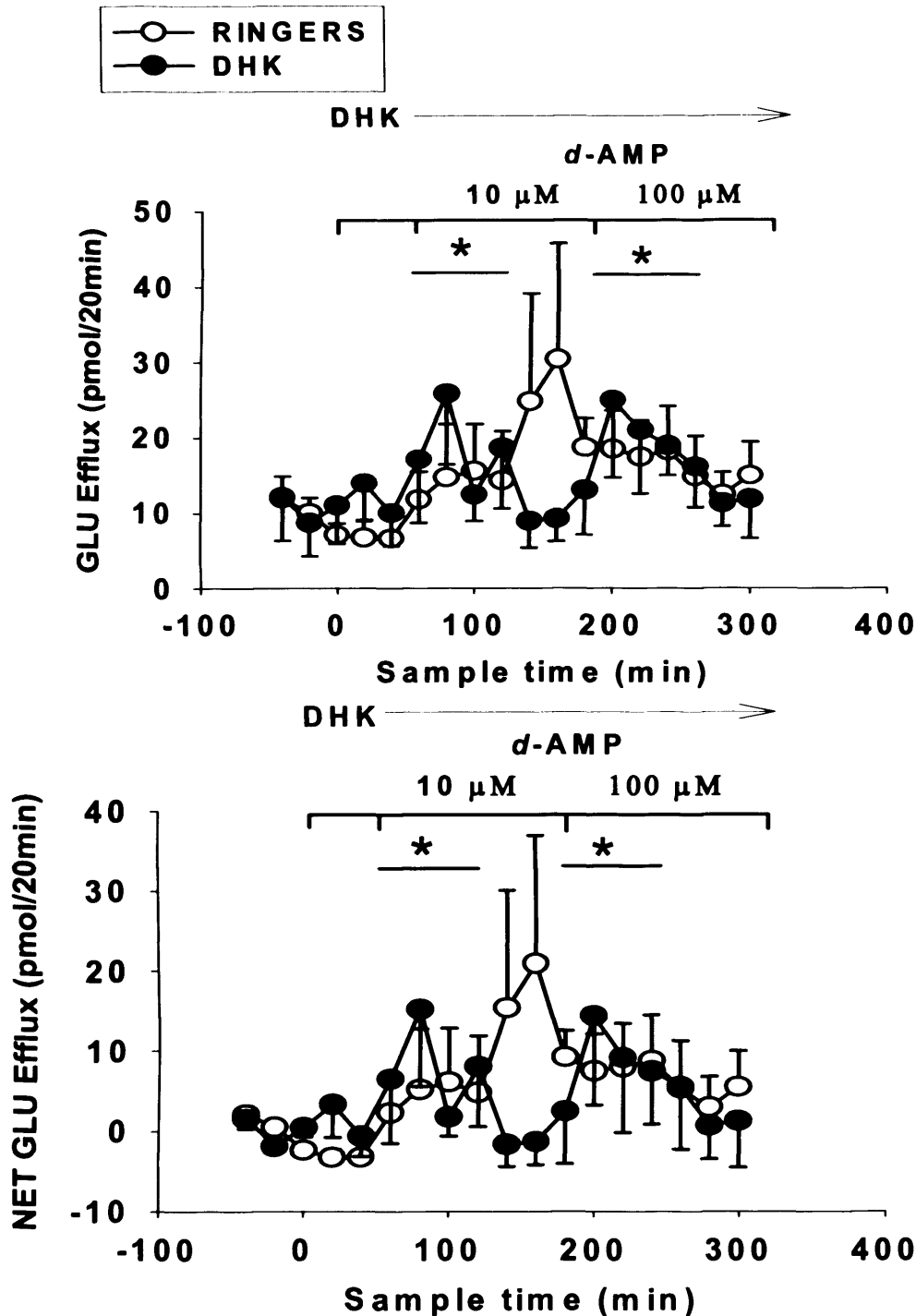


Figure 7.6 Effects of cumulative infusion of d-amphetamine ('d-AMP') on glutamate ('GLU') efflux in the rostral anterior cingulate cortex ('rACC') of freely-moving rats. Infusion of DHK (1 mM) or Ringer's solution was initiated at T₀ and maintained throughout as indicated by the arrow. Infusion of d-AMP (10 μM: 120 min, 100 μM: 120 min) was initiated at T₆₀ as indicated by the line. GLU efflux is expressed as pmol/20min. Points show mean ± s.e. mean GLU efflux after infusion of DHK (closed circles) or Ringer's (open circles). N=9/12. The top graph shows raw data and the bottom graph net data set.

Table 7.4 Statistics generated from split-plot ANOVA summarising the effects of local infusion of *d*-amphetamine + DHK (1 mM) on glutamate efflux in the cACC and rACC. Glutamate efflux in each time bin was compared with efflux in the cluster of basal samples. Significant differences are highlighted in **bold**.

Treatment	<i>d</i> -AMP + DHK (1 mM)	
	cACC	rACC
[<i>d</i> -AMP] (μM)		
10 (1 h)	F_(1,18)=8.666 P<0.01	F_(1,14)=8.291 P<0.01
10 (2 h)	F _(1,18) =0.126 P<0.7	F _(1,14) =1.352 P<0.3
100 (1 h)	F _(1,17) =0.083 P<0.8	F_(1,14)=9.135 P<0.01
100 (2 h)	F _(1,18) =0.054 P<0.8	F _(1,14) =3.024 P<0.1

7.5/ DISCUSSION

7.5.1/ *Caudal Anterior Cingulate Cortex*

Consistent with my previous studies, neither local infusion of DHK nor *d*-amphetamine affected glutamate efflux in the cACC (see: Chapter 3 and Chapter 6).

An increase in glutamate efflux was seen during the first hour of co-infusion of both DHK and the lower concentration of *d*-amphetamine (10 μ M). This quickly returned to basal levels and remained at this concentration for the remainder of the experiment, despite infusion of a higher concentration (100 μ M) of *d*-amphetamine. When *d*-amphetamine is infused locally in the cACC, any increase in glutamate efflux could be masked by uptake at the glial glutamate transporter, GLT-1. This transporter is responsible for greater than 90 % of glutamate transport activity in the rat forebrain (Tanaka *et al.*, 1997). However, when uptake at this transporter is blocked by the addition of DHK to the perfusion medium, the *d*-amphetamine-induced glutamate efflux is immediately evident. After the initial increase in glutamate efflux, the extracellular concentration quickly returned to basal levels and remained at this concentration for the remainder of the experiment.

The mechanism by which the glutamate response to local infusion of the higher concentration of *d*-amphetamine is switched off in the cACC is unclear. It is possible that the response is being switched off by glutamate hetero/autoreceptors in the terminal fields by the increased extracellular glutamate. Candidates for this include mGlu5, which are thought to act presynaptically in the prefrontal cortex (Fazal *et al.*, 2003). Members of the group II family of mGluRs are enriched in the prefrontal

cortex (Ohishi *et al.*, 1993) and have an inhibitory effect on PCP-evoked glutamate release (Moghaddam and Adams, 1998).

Actions of *d*-amphetamine mediated by other neurotransmitters (e.g. noradrenaline and serotonin) were also possible. Local infusion with the NMDA antagonist 3-[(R)-2-carboxypiperazin-4yl]-propyl-1-phosphoric acid (CPP; 100 μ M) increased extracellular glutamate in the rat prefrontal cortex (Calcagno *et al.*, 2006). Intracortical perfusion with the 5-HT_{1A} agonist 8-OH-DPAT (3 μ M) completely prevented the rise in extracellular glutamate. This effect was reversed by co-perfusion with the 5-HT_{1A} antagonist WAY-100635 (100 μ M). Any increase in extracellular glutamate induced by *d*-amphetamine in the anterior cingulate cortex could be inhibited by an action of 5-HT on inhibitory 5-HT_{1A} receptors. 5-HT_{1A} receptors are enriched in the prefrontal cortex and particularly on glutamatergic pyramidal neurons (Amargos-Bosch *et al.*, 2004, Santana *et al.*, 2004). To date, no microdialysis studies have been performed investigating the effects of noradrenergic agents on drug-evoked increases in extracellular glutamate.

Alternatively, the supplies of neuronal glutamate to be released into the extracellular space and sampled by the microdialysis probe could be exhausted by the continued infusion of *d*-amphetamine. Neurones are not capable of synthesizing glutamate since they lack pyruvate carboxylase, which is the main anaplerotic enzyme in the brain (Shank *et al.*, 1985). They rely on the astrocytic supply of TCA cycle intermediates, as every drain of neuronal amino acids would otherwise lead to a shortage of neurotransmitter precursors. Astrocytes also take up neuronal glutamate, which will lead to a further depletion of transmitters in neurons. Pyruvate carboxylase in astrocytes converts pyruvate to oxaloacetate, resulting in the formation of α -ketoglutarate. From α -ketoglutarate, glutamate can be formed and converted to

glutamine, which is transferred to neurons and emerges as glutamate (Kvamme *et al.*, 2000). This is the so-called 'glutamate-glutamine' cycle. Once the supply of neuronal glutamate has been exhausted by the addition of *d*-amphetamine to the infusion medium, it may take some time for it to be replenished. Continued infusion of *d*-amphetamine would exacerbate the situation, meaning that there would never be sufficient neuronal concentrations of glutamate to be released into the extracellular space.

In addition to competitive inhibition of GLT-1, DHK also acts as a weak agonist of ionotropic glutamate receptors (see: Chapter 1, section 1.8). Infusion of the glutamate agonists NMDA and kainate increases glutamate efflux in the striatum of rats (Hashimoto *et al.*, 2000). Assuming that these results can be generalised to the entire rat brain, this property of DHK could explain the potentiation of the glutamate response to the lower concentration of *d*-amphetamine. However, as infusion of DHK alone did not increase glutamate efflux in the cACC, this is unlikely.

7.5.2/ Rostral Anterior Cingulate Cortex

Consistent with our previous studies, local infusion of DHK did not affect extracellular glutamate concentrations in this brain region. A concentration-dependent increase in glutamate efflux was observed on local infusion of *d*-amphetamine, which attained statistical significance after infusion of the highest concentration (100 μ M). Again, the increased glutamate efflux observed in the rACC was phasic in nature, with the increased extracellular glutamate rapidly returning to basal levels in the subsequent samples. This phasic glutamate efflux has been a constant feature of these studies (see: Chapter 3, Figure 3.3). Pre-treatment with

DHK did not affect the glutamate response to *d*-amphetamine in the rACC. Therefore, the *d*-amphetamine-induced increase in extracellular glutamate does not rest on efflux at the glial glutamate transporter and it is not essential for clearance.

There are theoretical problems associated with the simultaneous infusion of two drugs down the microdialysis probe. During local infusion, the extracellular concentration of the drug will not be the same as the concentration dissolved in the Ringer's and it is hard to predict how much of the drug will remain in the infusion fluid. Dissolving two different drugs in Ringer's will complicate this situation further and could lead to variable concentrations of drug in the extracellular fluid from animal to animal. The compounds could also interact chemically within the Ringer's solution, therefore further influencing their pharmacokinetics.

7.5.3/ SUMMARY OF KEY FINDINGS

- In the caudal anterior cingulate cortex, the glutamate response to the lower concentration (10 μ M) of *d*-amphetamine but not the higher concentration was enhanced by pre-treatment with DHK
- In the rostral anterior cingulate cortex, pre-treatment with DHK did not prevent the glutamate response to local infusion of *d*-amphetamine
- Local infusion of DHK did not affect spontaneous glutamate efflux in either subregion at any time, suggesting that GLT-1 is not essential for regulation of extracellular glutamate under baseline conditions

Chapter 8

8.0/ General Discussion

8.1/ SUMMARY OF RESULTS

The rat anterior cingulate cortex shows functional specialisation. The aim of these experiments was to look for possible neurochemical coding of this by comparing regulation of glutamatergic neurotransmission in two adjacent subregions of the rat anterior cingulate cortex – the caudal anterior cingulate cortex (cACC: AP +1.0 ML +0.6 DV -3.6) and the rostral anterior cingulate cortex (rACC: AP +2.5 ML +0.6 DV -4.6). The rACC is responsible for mediating the affective response to a noxious stimulus, while the cACC contributes to the motor response to the unconditioned stimulus, only. Both single and dual-probe microdialysis studies were performed in freely-moving rats to investigate the effects of *d*-amphetamine on both dopamine and glutamate efflux in the two subregions.

Systemic administration of *d*-amphetamine increased glutamate efflux in the cingulate region of the prefrontal cortex (corresponding to the rACC in my studies; Reid *et al.*, 1997). *d*-Amphetamine has also been shown to differentially affect dopamine efflux in different subregions of the rat medial prefrontal cortex (which receive inputs from different brainstem areas: Mazei *et al.*, 2002). It follows that the effect of *d*-amphetamine on glutamate efflux could also differ in different subregions of the anterior cingulate cortex. So far, this has not been investigated systematically.

The experiments performed in Chapter 3 indicated that the glutamate response to *d*-amphetamine in the anterior cingulate cortex depends on both subregion and route of administration. Local infusion of *d*-amphetamine (1-100 μ M; *via*

'retrodialysis') dose-dependently increased glutamate efflux in the rACC but not the cACC. Systemic administration of *d*-amphetamine (3 mg/kg i.p.) increased glutamate efflux in the cACC but not the rACC. This suggests that in the rACC, actions of *d*-amphetamine in the terminal fields are increasing glutamate efflux, while the glutamate response to systemic *d*-amphetamine is constrained by afferent influences. In the cACC, the reverse situation is occurring, with the effects of *d*-amphetamine depending on actions upstream of this subregion.

The next experiments attempted to elucidate some of the mechanisms responsible for the glutamate response to local infusion of *d*-amphetamine in the rACC. The rACC receives a dense dopaminergic projection from the ventral tegmental area of the midbrain, which could influence glutamatergic transmission. Firstly, it was important to determine the effect of *d*-amphetamine on dopamine efflux in the two subregions (Chapter 4). Both local infusion (10-100 μ M; *via* retrodialysis) and systemic administration (3 mg/kg i.p.) of *d*-amphetamine increased dopamine efflux in the rACC. Therefore, the dopamine response in the rACC is not modulated by afferent inputs.

In contrast, there was no dopamine response in the cACC either after local infusion or systemic administration of *d*-amphetamine. These data fit well with the dopaminergic innervation of the rat prefrontal cortex, which is highest in the deeper layers (V-VI) of the prelimbic cortex (corresponding to area Cg3 of the rACC) and lowest in the superficial layers of the dorsal anterior cingulate area. They also suggest that an increase in dopaminergic neurotransmission could underlie the increased glutamate transmission in the rACC in response to local infusion of *d*-amphetamine. In contrast, the increased extracellular glutamate in the cACC in response to systemic injection of *d*-amphetamine cannot be related to an increase in dopamine efflux. To

confirm these results, a dose-dependent increase in glutamate efflux in the rACC, but not the cACC, in response to local infusion of dopamine solution was seen. These data all point to an involvement of increased extracellular dopamine in the glutamate response to local *d*-amphetamine in the rACC only.

To characterise further the mechanisms underlying the increased rACC glutamate in response to local infusion of *d*-amphetamine, rats were pre-treated with one of two dopaminergic antagonists 2 h before local infusion of *d*-amphetamine (10-100 μ M; *via* retrodialysis: Chapter 5). Pre-treatment with either dose of the D₂-like receptor antagonist haloperidol (0.1 and 1 mg/kg *i.p.*), did not affect the glutamate response to local *d*-amphetamine in the rACC, suggesting that any increase in glutamate efflux is not secondary to an action of dopamine on D₂-like receptors. Similarly, pre-treatment with the D₁-like receptor SCH23390 at the lower dose (0.1 mg/kg *i.p.*) did not affect the glutamate response to local infusion of *d*-amphetamine. However, the *d*-amphetamine-induced increase in extracellular glutamate was blunted by the higher dose of SCH23390 (1 mg/kg *i.p.*, see Figure 8.1 (a)). This suggests that an action of dopamine on D₁-like receptors contributes to the glutamate response to local infusion *d*-amphetamine in the rACC. This result is in agreement with anatomical studies investigating the distribution of D₁-like receptors in the prefrontal cortex. D₁-like receptors are more prominent in the deeper layers (V-VI) of the cortex, with a more homogeneous distribution in the superficial layers. D₁-like receptors also greatly outnumber D₂-like receptors in this brain region.

It is conceivable that, where no increase in glutamate efflux was seen after administration of *d*-amphetamine, this was due to uptake of glutamate by highly efficient glutamate transporters surrounding the glutamatergic synapse. The glial glutamate transporter GLT-1, present on glial cells, is the most abundant glutamate

transporter in the rat forebrain. The experiments performed in Chapter 6 sought to investigate the role of this transporter in the glutamate response to systemic *d*-amphetamine in both the rACC and cACC. The sustained increase in glutamate efflux was partly attenuated by DHK, 2-4 h after treatment with *d*-amphetamine. This suggests that DHK has some effect on the glutamate response to *d*-amphetamine, and a small proportion could rest on reversal of GLT-1 and subsequent release of glutamate. However, it seems that a large proportion of glutamate is released by another mechanism.

In the rACC, systemic injection of *d*-amphetamine caused a small, transient increase in glutamate efflux (nonsignificant), which quickly returned to basal levels in the next sample. Pretreatment with DHK caused a progressive, sustained decrease in glutamate efflux below baseline compared to the animals, which had received *d*-amphetamine injection alone. The glutamate response to systemic *d*-amphetamine in the rACC therefore depends on GLT-1. This reduction could arise from inhibition of glutamate uptake by GLT-1 and subsequent activation of terminal autoreceptors by the increased extracellular glutamate, which inhibit its release. Local infusion of DHK alone did not affect spontaneous glutamate efflux in either the cACC or rACC, suggesting that uptake of glutamate by GLT-1 is not essential for clearance of glutamate in either subregion.

Finally, in Chapter 7, I determined the effect of inhibition of glial glutamate transport on the glutamate response to local infusion of *d*-amphetamine in the rACC and cACC. In the cACC, as before, neither local infusion of *d*-amphetamine nor DHK affected glutamate efflux. However, DHK augmented the response to the lower concentration (10 μ M) of *d*-amphetamine for the first hour of infusion. In the rACC, as before, local infusion of DHK did not affect glutamate efflux and local infusion of

d-amphetamine increased extracellular glutamate. DHK did not affect the glutamate response to local infusion of *d*-amphetamine in this brain region and so the increased extracellular glutamate does not depend on GLT-1. These experiments suggest that, in the cACC, the glutamate response to local *d*-amphetamine is masked by uptake of glutamate by GLT-1, while GLT-1 does not influence the glutamate response in the rACC (see Figure 8.1 (b)).

8.2/ IMPLICATIONS OF THESE RESULTS

This is the first time that a systematic investigation of the regulation of glutamatergic neurotransmission along the rostro-caudal axis of the anterior cingulate cortex has been performed. It is clear from these studies that different mechanisms are responsible for governing glutamatergic transmission in the rostral and caudal anterior cingulate cortices. The striking asymmetry in the regulation of glutamate efflux between the cACC and rACC is the most notable feature of these experiments. To summarise, systemic *d*-amphetamine increased glutamate efflux in the cACC, but not the rACC. Conversely, local infusion of *d*-amphetamine increased glutamate efflux in the rACC but not the cACC. As regards the glial glutamate transporter, GLT-1, this plays an important role in the constraint of the glutamate response to *d*-amphetamine in both subregions. However, in the rACC, GLT-1 is responsible for limiting the concentration of extracellular glutamate arising governed by afferents to the rACC, i.e. only seen following systemic administration of *d*-amphetamine, whereas, in the cACC, GLT-1 limits any increase in glutamate efflux arising from local actions of *d*-amphetamine. GLT-1 has no effects on the local actions of *d*-

amphetamine in the rACC and only a limited action on the effects of *d*-amphetamine governed by afferent influences to the cACC.

Despite being contiguous, the cACC and rACC are functionally heterogeneous. Lesion and behavioural studies have implicated a role for the rACC in the affective component of pain (Lei *et al.*, 2004), while the cACC is thought to be responsible for motor planning as a secondary response to nociceptor stimulation. The reciprocal responses to *d*-amphetamine suggest that different mechanisms are responsible for the control of glutamatergic transmission in the two brain regions. These regional differences in the regulation of glutamatergic transmission discovered in the present experiments could help to explain their differential function.

Previous studies have indicated a role for glutamate in the regulation of dopamine neurotransmission in rat cortical areas (Feensta *et al.*, 1995; Smith and Whitton, 2001). My studies have shown that the reverse situation is also relevant. Only a few laboratories have used microdialysis to study the influence of dopamine on glutamatergic transmission in the rat cerebral cortex, despite the fact that dopamine is a neuromodulator in an ideal position to regulate glutamatergic neurotransmission. Dopamine-glutamate interactions are clearly very important for the pathogenesis of diseases such as schizophrenia and major depressive disorder. Elucidating the precise nature of these interactions will undoubtedly aid in further understanding the mechanisms of these neurological disorders and finding more effective treatment.

To my knowledge, this is the first time that a decrease in extracellular glutamate in a subregion of the prefrontal cortex in response to *d*-amphetamine has been demonstrated. It has been well documented that chronic use of *d*-amphetamine by human subjects leads to psychotic symptoms characteristic of schizophrenia. Clinical studies have suggested that decreased glutamate transmission in the

prefrontal cortex (including the anterior cingulate cortex) is a cardinal feature of chronic schizophrenia in man (Ohrmann, 2005). Numerous animal models of psychosis exist and many of these involve decreased glutamate transmission (Zuo *et al.*, 2006). My experiments, in which decreased glutamate efflux was observed after a single dose of *d*-amphetamine, suggest that impairment of GLT-1 function could contribute to *d*-amphetamine psychosis or schizophrenia.

This model also fits in well with the proposed role for glial cells in the pathogenesis of schizophrenia. The importance of glial-neuronal interactions for glutamate metabolism has been highlighted, and, in particular, the 'glutamate-glutamine' cycle, by which glutamate released by neurones is taken up by astrocytes. Once inside the astrocyte, glutamate enters the TCA cycle and is converted to glutamine, which can be transferred to neurones and hydrolysed to glutamate by phosphate-activated glutaminase. Disruption of glial-neuronal interactions is thought to be a key feature of schizophrenia (Kondziella *et al.*, 2006). In the anterior cingulate cortex of schizophrenics, an estimated glial cell loss of 15-20 % can be found in layers V and VI. This glial cell loss is reflected in the hypometabolism of the prefrontal cortex of schizophrenics and agrees with the initial glutamatergic excitotoxicity and subsequent NMDA receptor hypofunction characteristic of this disorder (Kondziella *et al.*, 2007). My experiments could be effectively modelling the glial cell loss, leading to eventual glutamatergic hypofunction, which is a cardinal feature of schizophrenia.

In conclusion, these studies revealed notable asymmetry in the neurochemical regulation of dopaminergic and glutamatergic transmission in the rACC and cACC, which could explain the differential functions of these subregions.

Figure 8 (a)

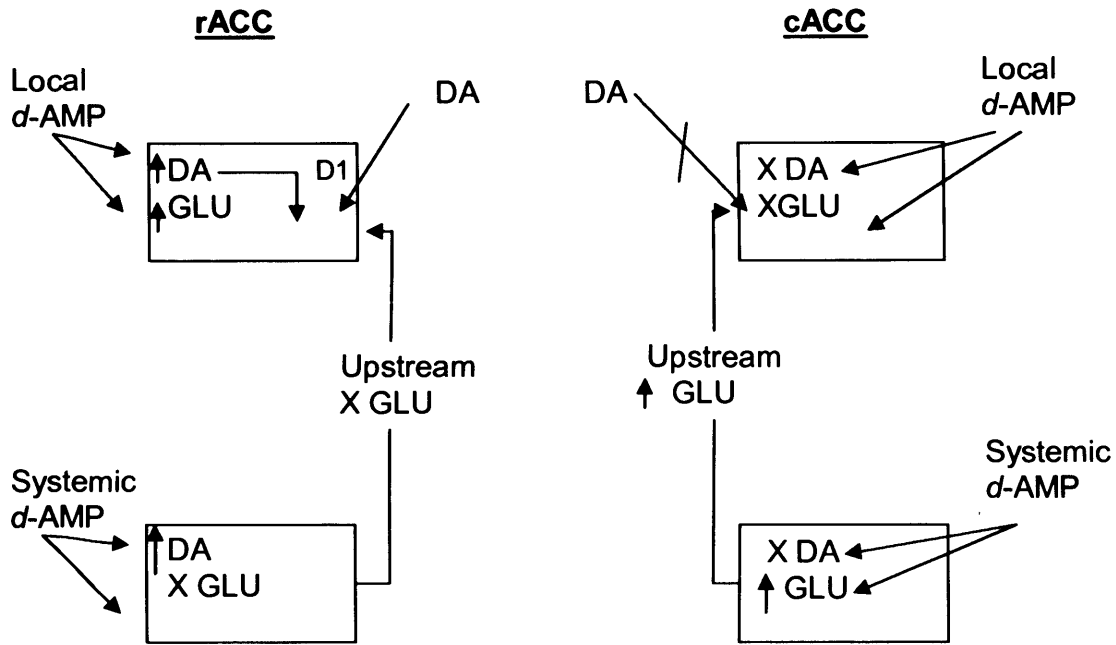


Figure 8 (b)

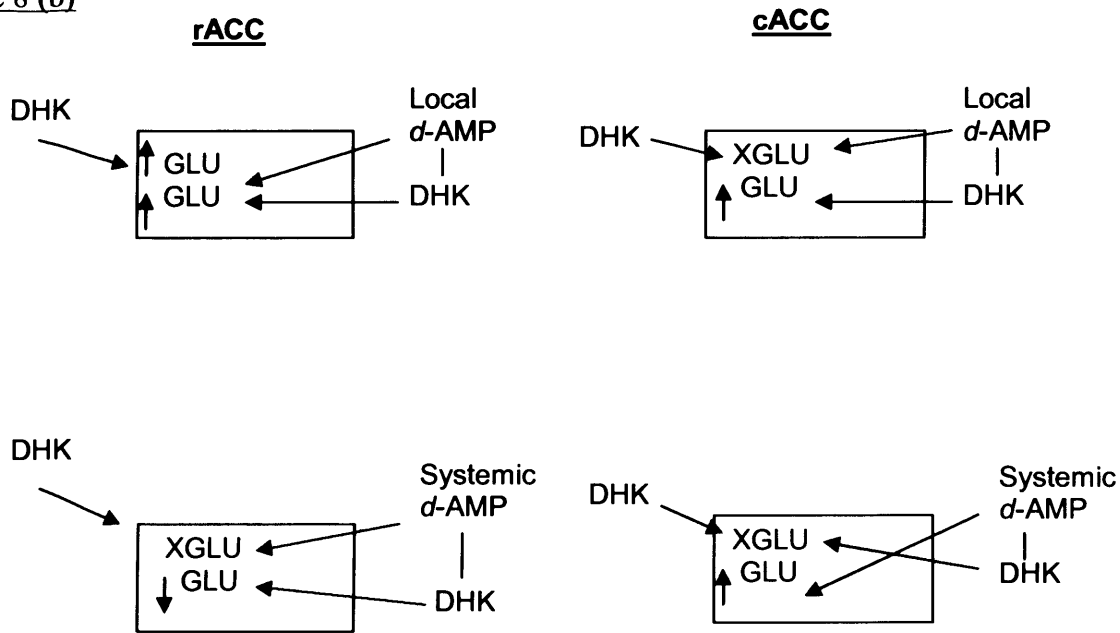


Figure 8.1 Summary diagrams showing the effects of different drug treatments on dopamine and glutamate efflux in the rat rostral and caudal anterior cingulate cortices

- (a) Effects of local and systemic *d*-AMP on glutamate efflux and modulation by dopaminergic neurotransmission.
- (b) Effects of local and systemic *d*-AMP on glutamate efflux and modulation by glial glutamate transport.

References

Abekawa T., Ohmori T., Ito K. and Koyama T. (2000). D₁ dopamine receptor activation reduces extracellular glutamate and GABA concentrations in the medial prefrontal cortex. *Brain Res.* **867**:250-254.

Adams B.W. and Moghaddam B. (2001). Effect of clozapine, haloperidol, or M100907 on phencyclidine-activated glutamate efflux in the prefrontal cortex. *Biol. Psychiatry* **50**:750-757.

Alexander S.P.H., Mathie A. and Peters J.A. (2007). Cell surface transmitter transporters. *Br. J. Pharmacol.* **250**:S137-138.

Anderson C.M. and Swanson R.A. (2000). Astrocyte glutamate transport: review of properties, regulation, and physiological functions. *Glia* **32**:1-14.

Araneda R. and Andrade R. (1991). 5-Hydroxytryptamine₂ and 5-hydroxytryptamine_{1A} receptors mediate opposing responses on membrane excitability in rat association cortex. *Neuroscience* **40**:399-412.

Armagos-Bosch M., Bortolozzi A., Puig M.V., Serrats J., Adell A., Celada P., Toth M., Mengod G. and Artigas F. (2004). Co-expression and *in vivo* interaction of serotonin_{1A} and serotonin_{2A} receptors in pyramidal neurons of prefrontal cortex. *Cereb. Cortex* **14**:281-99.

Arriza J.L., Fairman W.A., Waddiche J.L., Murdoch G.H., Kavanaugh M.P. and Amara S.G. (1994). Functional comparisons of three glutamate transporter subtypes cloned from human motor cortex. *J. Neurosci.* **14**:5559-69.

Audet M.A., Doucet G., Oleskevich S. and Descarries L. (1988). Quantified regional and laminar distribution of the noradrenergic innervation in the anterior half of the adult rat cerebral cortex. *J. Comp. Neurol.* **274**:307-18.

Audet M.A., Descarries L. and Doucet G. (1989). Quantified regional and laminar distribution of the serotonin innervation in the anterior half of the adult rat cerebral cortex. *J. Chem. Neuroanat.* **2**:29-44.

Baddeley A. (1986). Working memory. Oxford University Press.

Baker D.A., Xi Z.X., Shen H., Swanson C.J. and Kalivas P.W. (2002). The origin and neuronal function of *in vivo* nonsynaptic glutamate. *J. Neurosci.* **22**:9134-9141.

Balla A., Hashim A., Burch S., Javitt S.C., Lajtha A. and Sershen H. (2001). Phencyclidine-induced dysregulation of dopamine response to amphetamine in prefrontal cortex and striatum. *Neurochem. Res.* **26**:1001-6.

Barth V.N., Chernet E., Martin L.J., Need A.B., Rash K.S., Morin M. and Phebus L.A. (2006). Comparison of rat dopamine D₂ receptor occupancy for a series of antipsychotic drugs measured using radiolabeled or nonlabeled raclopride tracer. *Life Sci.* **78**:3007-12.

Beneyto M., Kristiansen L.V., Oni-Orisan A., McCullumsmith R.E. and Meador-Woodruff J.H. (2007). Abnormal glutamate receptor expression in the medial temporal lobe in schizophrenia and mood disorders. *Neuropsychopharmacology (Epub ahead of printing)*:1-15.

Benveniste H., Drejer J., Schousboe A. and Diemer N.H. (1984). Elevation of the extracellular concentrations of glutamate and aspartate in rat hippocampus during transient cerebral ischaemia monitored by intracerebral microdialysis. *J. Neurochem.* **43**:1369-74.

Berendse H.W. and Groenewegen H.J. (1991). Restricted cortical termination fields of the midline and intralaminar thalamic nuclei in the rat. *Neurosci.* **42**:73-102.

Berger U.V. and Hediger M.A. (1998). Comparative analysis of glutamate transporter expression in rat brain using differential double in situ hybridization. *Anat. Embryol. (Berl)* **198**:13-30.

Bergson C., Mrzljak L., Smiley T.F., Pappy M., Levenson R. and Goldman-Ralkic P.S. (1995). Regional, cellular and subcellular variations in the distribution of D₁ and D₅ dopamine receptors in primate brain. *J. Neurosci.* **15**:7821-36.

Berridge C.W. and Stalnaker T.A. (2002). Relationship between low-dose amphetamine-induced arousal and extracellular norepinephrine and dopamine levels within prefrontal cortex. *Synapse* **46**:140-9.

Bigge C.F. (1999). Ionotropic glutamate receptors. *Curr. Opin. Chem. Biol.* **3**:441-7

Bischoff S., Heinrich M., Sonntag J.M. and Krauss J. (1986). The D₁ dopamine receptor antagonist SCH23390 also interacts potently with brain serotonin (5-HT₂) receptors. *Eur. J. Pharmacol.* **129**:367-70.

Bito L., Davson H., Levin E., Murray M. and Snider M. (1966). The concentrations of free amino acids and other electrolytes in cerebrospinal fluid, *in vivo* dialysate of brain, and blood plasma of the dog. *J. Neurochem.* **13**:1057-67.

Cai Z., Schools G.P. and Kimelberg H.K. (2000). Metabotropic glutamate receptors in acutely isolated hippocampal astrocytes: developmental changes of mGluR₅ mRNA and functional expression. *Glia* **29**:70-80.

Calcagno E., Carli M. and Invernizzi R.W. (2006). The 5-HT_{1A} receptor agonist 8-OH-DPAT prevents prefrontocortical glutamate and serotonin release in response to blockade of cortical NMDA receptors. *J. Neurochem.* **96**:853-60.

Callaway C.W., Kuczenski R. and Segal D.S. (1989). Reserpine enhances amphetamine stereotypies without increasing amphetamine-induced changes in striatal dialysate dopamine. *Brain Res.* **505**:83-90.

Carmignoto G. (2000). Reciprocal communication systems between astrocytes and neurons. *Prog. Neurobiol.* **62**:561-81.

Chance B., Nakase Y., Bond M., Leigh J.S. Jr. and McDonald G (1978). Detection of ³¹P nuclear magnetic resonance signals in brain by in vivo and freeze-trapped assays. *Proc. Natl. Acad. Sci. USA.* **75**:4925-9.

Choi D.W. (1992). Excitotoxic cell death. *J. Neurobiol.* **23**:1261-1276.

Chu Z. and Hablitz J.J. (2000). Quisqualate induces an inward current via mGluR activation in neocortical pyramidal neurons. *Brain Res.* **879**:88-92.

Ciliax B.J., Heilman C., Demchyshyn L.L. Pristupa Z.B., Ince E., Hersch S.M., Niznik H.B. and Levey A.I. (1995). The dopamine transporter: immunochemical characterisation and localisation in brain. *J. Neurosci.* **15**:1714-23.

Condé F., Audinat E., Maire-Lepoivre E. and Crepel F. (1990). Afferent connections of the medial frontal cortex of the rat. A study using retrograde transport of fluorescent dyes. I. Thalamic afferents. *Brain Res. Bull.* **24**:341-54.

Danbolt N.C. (2001). Glutamate uptake. *Prog. Neurobiol.* **65**:1-105.

Danielson T.J., Coutts R.T., Coutts K.A., Keashly R. and Tang A. (1985). Reserpine-induced hypothermia and its reversal by dopamine agonists. *Life Sci.* **37**:31-38.

Dawson L.A. and Routledge C. (1995). Differential effects of potassium channel blockers on extracellular concentrations of dopamine and 5-HT in the striatum of conscious rats. *Br. J. Pharmacol.* **116**: 3260-4.

Dawson L.A., Djali S., Gonzales C., Vinegra M.A. and Zaleska M.M. (2003). Characterization of transient focal ischaemia-induced increases in extracellular glutamate and aspartate in spontaneously hypertensive rats. *Brain Res. Bull.* **53**:767-76.

Delgado J.M., Defendis F.V., Roth R.H., Ryugo D.K. and Mitruka B.M. (1972). Dialytrode for long term intracerebral perfusion in awake monkeys. *Arch. Int. Pharmacodyn. Ther.* **198**:9-21.

Del Arco A., Martinez R. and Mora F. (1998). Amphetamine increases glutamate efflux in the prefrontal cortex of the awake rat: a microdialysis study. *Neurochem. Res.* **23**:1153-1158.

Del Arco A. and Mora F. (1999). Effects of endogenous glutamate on extracellular concentrations of GABA, dopamine and dopamine metabolites in the prefrontal cortex of the freely-moving rat: involvement of NMDA and AMPA/KA receptors. *Neurochem. Res.* **24** :1027-1035.

Del Arco A., Segovia G., Fuxe K. and Mora F. (2003). Changes in dialysate concentrations of glutamate and GABA in the brain: an index of volume transmission mediated actions? *J. Neurochem.* **85**:23-33.

Descarries L., Lemay B., Doucet G. and Berger B. (1987). Regional and laminar density of the dopamine innervation in the rat cerebral cortex. *Neuroscience* **21**:807-24.

Duan S., Anderson C.M., Keung E.C., Chen Y. and Swanson R.A. (2003). P₂X₇ receptor-mediated release of excitatory amino acids from astrocytes. *J. Neurosci.* **23**:1320-8.

Ellison G.D. and Eison M.S. (1983). Continuous amphetamine intoxication: an animal model of the acute psychotic episode. *Psychol. Med.* **13**:751-61.

Emson P.C. and Koob G.F. (1978). The origin and distribution of dopamine-containing afferents to the rat frontal cortex. *Brain Res.* **142**:249-67.

Erel U., Arborelius L. and Brodin E. (2004). Increased cholecystikinin release in rat anterior cingulate cortex during carrageenan-induced arthritis. *Brain Res.* **1022**:39-46.

Falck B., Hillarp N.-A., Thieme G. and Torp A. (1962). Fluorescence of catecholamines and related compounds condensed with formaldehyde. *J. Histochem. Cytochem.* **10**:348-354.

Fallgren A.B. and Paulsen R.E. (1996). A microdialysis study in rat brain of dihydrokainate, a glutamate uptake inhibitor. *Neurochem. Res.* **21**:19-25.

Fazal A., Parker F., Palmer A.M. and Croucher M.J. (2003). Characterisation of the actions of group I metabotropic glutamate receptor subtype selective ligands on excitatory amino acid release and sodium-dependent re-uptake in rat cerebrocortical minislices. *J. Neurochem.* **86**:1346-58.

Febvret A., Berger B., Gasper P. and Verney C. (1991). Further indication that distinct dopaminergic subsets project to the rat cerebral cortex: lack of colocalization with neurotensin in the superficial dopaminergic fields of the anterior cingulate, motor, retrosplinal and visual cortices. *Brain Res.* **547**:55-61.

Feenstra M.G., van der Weij W. and Botterblom M.H. (1995). Concentration-dependent dual action of locally applied N-methyl-D-aspartate on extracellular dopamine in the rat prefrontal cortex *in vivo*. *Neurosci. Lett.* **201**:175-178.

Fellin T., Pascual O., Gobbo S., Pozzan T., Haydon P.G. and Carmignoto G. (2004). Neuronal synchrony mediated by astrocytic glutamate through activation of extrasynaptic NMDA receptors. *Neuron* **43**:729-43.

Fillenz M. (2005). *In vivo* neurochemical monitoring and the study of behaviour, *Neurosci. Biobehav. Rev.* **29**:949-62.

Florin S.M., Kuzcenski R. and Segal D.S. (1994). Regional extracellular norepinephrine responses to amphetamine and cocaine and effects of clonidine pre-treatment. *Brain Res.* **654**:53-62.

Fonnum F. (1984). Glutamate: a neurotransmitter in mammalian brain. *J. Neurochem.* **42**:1-11.

Fuchs H., Nagel J. and Hauber W. (2005). Effects of physiological and pharmacological stimuli on dopamine release in the rat globus pallidus. *Neurochem. Int.* **47**: 474-81.

Gaddum J.H. (1961). Push-pull cannulae. *J. Physiol.* **155**:1P.

Gadea A. and López-Colomé A.M. (2001). Glial transporters for glutamate, glycine and GABA. 1. Glutamate transporters. *J. Neurosci. Res.* **63**:453-460.

Géranton S.M., Heal D.J. and Stanford S.C. (2003). Differences in the mechanisms that increase noradrenaline efflux after administration of *d*-amphetamine: a dual-probe microdialysis study in rat frontal cortex and hypothalamus. *Br. J. Pharmacol.* **139**:1441-1448.

Gonzalez-Islas C. and Hablitz J.J. (2003). Dopamine enhances EPSCs in layer II-III pyramidal neurones of the rat prefrontal cortex. *J. Neurosci.* **23**: 867-75.

Gracy K.N. and Pickel V.M. (1996). Ultrastructural immunocytochemical localisation of the N-methyl-D-aspartate receptor and tyrosine hydroxylase in the shell of the rat nucleus accumbens. *Brain Res.* **739**:169-81.

Groenewegen H.J., Wright C.I. and Uylings H.B.M. (1997). The anatomical relationships of the prefrontal cortex with limbic structures and the basal ganglia. *J. Psychopharmacol.* **11**: 99-106.

Gulledge A.T. and Jaffe D.B. (1998). Dopamine decreases the excitability of layer V pyramidal cells in the rat prefrontal cortex. *J. Neurosci.* **18**:9139-9151.

Hamann M., Rossi D.J., Marie H. and Attwell D. (2002). Knocking out the glial glutamate transporter GLT-1 reduces glutamate uptake but does not affect hippocampal glutamate dynamics in early simulated ischaemia. *Eur. J. Neurosci.* **15**:308-14.

Harte M. and O'Connor W.T. (2004). Evidence for a differential medial prefrontal dopamine D₁ and D₂ receptor regulation of local and ventral tegmental area glutamate and GABA release: a dual probe microdialysis study in the awake rat. *Brain Res.* **1017**:120-129.

Hashimoto A., Kanda J. and Oka T. (2000). Effects of N-methyl-D-aspartate, kainate or veratridine on extracellular concentrations of free D-serine and L-glutamate in rat striatum: an in vivo microdialysis study. *Brain Res. Bull.* **53**:347-51.

Haugeto O., Ullensvang K., Levy L.M., Chaudhry E.A., Honore T., Nielsen M., Lehre K.P. and Danbolt N.C. (1996). Brain glutamate transporter proteins form homomultimers. *J. Biol. Chem.* **271**:27715-22.

Haydon P.G. (2001) Glia: listening and talking to the synapse. *Nat. Rev. Neurosci.* **2**:185-93.

Hédou G., Homberg J., Feldon J. and Heidbreger C.A. (2001). Expression of sensitisation and dynamics of dopamine neurotransmission in different laminae of the rat medial prefrontal cortex. *Neuropharm.* **40**:366-82.

Heal D.J., Cheetham S.C., Prow M.R., Martin K.F. and Buckett W.R. (1998). A comparison of the effects of central 5-HT function of sibutramine hydrochloride and other weight-modifying agents. *Br. J. Pharmacol.* **125**:301-308.

Heal D.J. and Cheetham S.C. (1997). The pharmacology of sibutramine, the first serotonin and noradrenaline reuptake inhibitor to be developed in the treatment of obesity. *La lettre du pharmacologue* **11 (suppl.10)**:3-8.

Heilborn H., Rost B.R., Arborelius L. and Brodin E. (2007). Arthritis-induced increase in cholecystokinin release in rat anterior cingulate cortex is reversed by diclofenac. *Brain Res.* **1136**:51-8.

Herrera-Marschitz M., You Z.B., Goiny M., Meana J.J., Silveira R., Godukhin O.V., Chen Y., Espinoza S., Pettersson E., Loidl C.F., Lubec G., Andersson K., Nylander I., Terenius L. and Ungerstedt U. (1996). On the origin of extracellular glutamate levels monitored in the basal ganglia of the rat by *in vivo* microdialysis. *J. Neurochem.* **66**:1726-1735.

Hsiao J.K., Ball B.A., Morrison P.F., Mefford I.N. and Bungay P.M. (1990). Effects of different semipermeable membranes on *in vitro* and *in vivo* performance of microdialysis probes. *J. Neurochem.* **54**:1449-52.

Johansen J.P., Fields H.L. and Manning B.H. (2001). The affective component of pain in rodents: Direct evidence for a contribution of the anterior cingulate cortex. *Proc. Nat. Acad. Sci. USA* **98**:8077-8082.

Johansen J.P. and Fields H.L. (2004). Glutamatergic activation of anterior cingulate cortex produces an aversive teaching signal. *Nature Neurosci.* **7**:398-403.

Jones S.R., Gainetdinov R.R., Wightman R.M and Caron M.G. (1998). Mechanisms of amphetamine action revealed in mice lacking the dopamine transporter. *J. Neurosci.* **18**:1979-1986.

Jones B.F., Groenewegen H.J. and Witter M.P. (2005). Intrinsic connections of the cingulate cortex in the rat suggest the existence of multiple functionally segregated networks. *Neurosci.* **133**:193-207.

Joseph M.H. and Davies P. (1983). Electrochemical activity of *o*-phthalaldehyde-mercaptoethanol derivatives of amino acids. Application to high-performance liquid chromatographic determination of amino acids in plasma and other biological materials. *J. Chromatog.* **277**:125-36.

Kanai Y., Bhide P.G., DiFiglia M. and Hediger M.A. (1995a). Neuronal high-affinity glutamate transport in the rat central nervous system. *NeuroReport* **6**:2357–62.

Kanai Y., Nussberger S., Romero M.F., Boron W.F., Hebert S.C. and Hediger M.A. (1995b). Electrogenic properties of the epithelial and neuronal high affinity glutamate transporter. *J. Biol. Chem.* **270**:16561–8.

Kanai Y., Hediger M.A., Wang Y., Schielke J.P. and Welty D.F. (1996). Knockout of glutamate transporters reveals a major role for astroglial transport in excitotoxicity and clearance of glutamate. *Neuron* **16**:675–86.

Kanai Y. and Hediger M.A. (2003). The glutamate and neutral amino acid transporter family: physiological and pharmacological implications. *Eur. J. Pharmacol.* **479**:237-247.

Kanai Y. and Hediger M.A. (2004). The glutamate/neutral amino acid transporter family SLC1: molecular, physiological and pharmacological aspects. *Pflugers Arch.* **447**:469-79.

Kapetanovic I.M., Sweeney D.J. and Rapport S.I. (1982). Age effects on haloperidol pharmacokinetics in male, Fischer-344 rats. *J. Pharmacol. Exp. Ther.* **221**:434-8.

Kia H.K., Brisorquiel M.J., Hamon M., Calas A. and Verge D. (1996). Ultrastructural localisation of 5-hydroxytryptamine_{1A} receptors in the rat brain. *J. Neurosci. Res.* **46**:697-708.

Kimelberg H.K., Goderie S.K., Higman S., Pang S. and Waniewski R.A. (1990). Swelling-induced release of glutamate, aspartate and taurine from astrocyte cultures, *J. Neurosci.* **10**:1583-91.

Klitenick M.A., Deutch A.Y., Churchill L. and Kalivas P.W. (1992). Topography and functional role of dopaminergic projections from the ventral mesencephalic tegmentum to the ventral pallidum. *Neurosci.* **50**:371-86.

Kolb B. (1984). Functions of the frontal cortex of the rat: a comparative review. *Brain Res.* **320**:65-98.

Kondziella D., Brenner E., Eyjolfsson E.M., Markinhuhta K.R., Carlsson M.L. and Sonnewald U. (2006). Glial-neuronal interactions are impaired in the schizophrenia model of repeated MK-801 exposure. *Neuropsychopharmacol.* **31**:1880-7.

Kondziella D., Brenner E., Eyjolfsson E.M. and Sonnewald U. (2007). How do glial-neuronal interactions fit into current neurotransmitter hypotheses of schizophrenia? *Neurochem. Int.* **50**:291-301.

Kuczenski R. and Segal D.S. (1990). *In vivo* measurements of monoamines during amphetamine-induced behaviours in rats. *Prog. Neuropsychopharmacol. Biol. Psychiatry* **14**:S37-50.

Kvamme E., Roberg B. and Torgner I.A. (2000). Phosphate-activated glutaminase and mitochondrial glutamine transport in the brain. *Neurochem. Res.* **25**:1407-19.

Legendre R. and Pieron H. (1910). Des resultats histophysiologiques de l'injection intraoccipito-atlantoidienne de liquides insominiques. *C. R. Soc. Biol.* **1**:1108-9.

Lidow M.S., Goldman-Rakic P.S., Gallager D.W. and Rakic P. (1991). Distribution of dopaminergic receptors in the primate cerebral cortex: quantitative autoradiographic analysis using [3H]raclopride, [3H]spiperone and [3H]SCH23390. *Neuroscience* **40**:657-671.

Lindvall O. and Bjorklund A. (1974). The glyoxylic acid fluorescence histochemical method: a detailed account of the methodology for the visualisation of central catecholamine neurons. *Histochemistry* **39**:97-127.

Lindvall O. and Bjorklund A. (1978). Anatomy of the dopaminergic neuron systems in the rat brain. *Adv. Biochem. Psychopharmacol.* **19**:1-23.

Lindvall O., Bjorklund A. and Divac I. (1978). Organisation of catecholamine neurones projecting to the frontal cortex in the rat. *Brain Res.* **142**:1-24.

Lonroth P., Jansson P.A. and Smith U. (1987). A microdialysis method for allowing characterization of intercellular water space in humans. *Am. J. Physiol.* **253**:E228-31.

Lorrain D.S., Baccei C.S., Bristow L.J., Anderson J.J. and Varney M.A. (2003). Effects of ketamine and N-methyl-D-aspartate on glutamate and dopamine release in the rat prefrontal cortex: modulation by a group II selective metabotropic glutamate receptor agonist LY379268. *Neurosci.* **117**:697-706.

Louis M. and Clarke P.B.S. (1998). Effect of ventral tegmental 6-hydroxydopamine lesions on the locomotor stimulant action of nicotine in rats. *Neuropharm.* **37**: 1503-1513.

Maki R., Robinson M.B. and Dichter M.A. (1994). The glutamate uptake inhibitor L-*trans*-pyrrolidine-2,4-dicarboxylate depresses excitatory synaptic transmission via a presynaptic mechanism in cultured hippocampal neurons. *J. Neurosci.* **14**:6754-62.

Malin E.L., Ibrahim D.Y., Tu J.W. and McGaugh J.L. (2007). Involvement of the rostral anterior cingulate cortex in consolidation of inhibitory avoidance memory: interaction with the basolateral amygdale. *Neurobiol. Learn Mem.* **87**:295-302.

Massieu L., Morales-Villagran A. and Tapia R. (1995). Accumulation of extracellular glutamate is not sufficient for inducing neuronal damage: an *in vivo* microdialysis study. *J. Neurochem.* **64**:2262-72.

Mazei M.S., Pluto C.P., Kirkbride B. and Pehek E.A. (2002). Effects of catecholamine uptake blockers in the caudate-putamen and subregions of the medial prefrontal cortex of the rat. *Brain Res.* **936**:58-67.

McQuade R.D., Ford D., Duffy R.A., Chipkin R.E., Iorio L.C. and Barnett A. (1988). Serotonergic component of SCH23390: *in vitro* and *in vivo* binding analyses. *Life Sci.* **43**:1861-9.

Melendez R.I., Vuthiganon J. and Kalivas P.W. (2005). Regulation of extracellular glutamate in the prefrontal cortex: focus on the cystine glutamate exchanger and group I metabotropic glutamate receptors. *J. Pharmacol. Exp. Ther.* **314**: 139-47.

Miele M., Boutelle M.G. and Fillenz M. (1996). The source of physiologically stimulated glutamate efflux from striatum of conscious rats. *J. Physiol.* **497**:745-751.

Miyazaki I., Asanuma M., Diaz-Corrales F.J., Miyoshi K. and Ogawa N. (2004). Direct evidence for expression of dopamine receptors in astrocytes from basal ganglia. *Brain Res.* **1029**:120-123.

Moghaddam B. and Bunney B.S. (1989). Ionic composition of microdialysis perfusing solution alters the pharmacological responsiveness and basal outflow of striatal dopamine. *J. Neurochem.* **53**:652-4.

Moghaddam B. and Adams B.W. (1998). Reversal of phencyclidine effects by a group II metabotropic glutamate receptor agonist in rats. *Science* **281**:1349-52.

Moghaddam B. (2002). Stress activation of glutamate neurotransmission in the prefrontal cortex: implications for dopamine-associated psychiatric disorders. *Biol. Psych.* **51**:775-87.

Montana V., Malarkey E.B., Verderio C., Matteoli M. and Pappas V. (2006). Vesicular transmitter release from astrocytes. *Glia* **54**:700-715.

Moore S. and Stein W.H. (1951). Chromatography of amino acids on sulfonated polystyrene resins. *J. Biol. Chem.* **192**:663-81.

Muly E.C., Szigeti K. and Goldman-Rakic P.S. (1998). D₁ receptor in interneurons of macaque prefrontal cortex: distribution and subcellular localisation. *J. Neurosci.* **18**:10553-10565.

Mukherjee J., Christian B.T., Narayanan T.K., Shi B. and Mantil J. (2001). Evaluation of dopamine D-2 receptor occupancy by clozapine, risperidone, and haloperidol in vivo in the rodent and nonhuman primate brain using 18F-fallypride. *Neuropsychopharmacol.* **25**:476-88.

Muschamp J.W., Regina M.J., Hull E.M., Winter J.C. and Rabin R.A. (2004). Lysergic acid diethylamide and [-]-2,5-dimethoxy-4-methylamphetamine increase extracellular glutamate in rat prefrontal cortex. *Brain Res.* **1023**:134-40.

Musil S.Y. and Olson C.R. (1988). Organisation of cortical and subcortical projections to the anterior cingulate cortex in the cat. *J. Comp. Neurol.* **272**:203-18.

Nagao S., Kwak S. and Kanazawa I. (1997). EAAT4, a glutamate transporter with properties of a chloride channel, is predominantly localised in Purkinje cell dendrites, and forms parasagittal compartments in rat cerebellum. *Neurosci.* **78**:929-33.

Negyessy L. and Goldman-Rakic P.S. (2005). Subcellular localisation of the dopamine D₂ receptor and coexistence with the calcium-binding protein neuronal calcium sensor-1 in the primate prefrontal cortex. *J. Comp. Neurol.* **488**:464-475.

Ohishi H., Shigemoto R., Nakanishi S. and Mizuno N. (1993). Distribution of the mRNA for a metabotropic glutamate receptor (mGluR3) in the rat brain: an in situ hybridization study. *J. Comp. Neurol.* **335**:252-66.

Ohrmann P., Siegmund A., Suslow T., Spitzberg K., Kersting A., Arolt V., Heindel W. and Pfeleiderer B. (2005). Evidence for glutamatergic neuronal dysfunction in the prefrontal cortex in chronic but not in first-episode patients with schizophrenia: a proton magnetic resonance spectroscopy study. *Schizophr. Res.* **73**:153-157.

Osborne P.G., O'Connor W.T. and Ungerstedt U. (1991). Effect of varying the ionic concentration of a microdialysis perfusate on basal striatal dopamine levels in awake rats. *J. Neurochem.* **56**:452-6.

Pan W.H., Yang S.Y. and Lin S.K. (2004). Neurochemical interaction between dopaminergic and noradrenergic neurones in the medial prefrontal cortex. *Synapse* **53**:44-52.

Parpura V., Basarsky T.A., Liu F., Jęftinija K., Jęftinija S. and Haydon P.G. (1994). Glutamate-mediated astrocyte-neurone signaling. *Nature* **369**:744-7.

Parsons S.M. (2000). Transport mechanisms in acetylcholine and monoamine storage. *FASEB J.* **14**:2423-34.

Paxinos G. and Watson C. (2005). The rat brain in stereotaxic coordinates (5th edition), Academic Press., London.

Petralia R.S., Wang Y.X., Niedzielski A.S. and Wenthold R.J. (1996). The metabotropic glutamate receptors, mGluR2 and mGluR3, show unique postsynaptic, presynaptic and glial localizations. *Neurosci.* **71**:949-76.

Pifl C., Drobny H., Reither H., Hornykiewicz O. and Singer E.A. (1995). Mechanism of the dopamine-releasing actions of amphetamine and cocaine: plasmalemmal dopamine transporter versus vesicular monoamine transporter. *Mol. Pharmacol.* **47**:368-373

Pifl C., Agneter E., Drobny H., Sitte H.H. and Singer E.A. (1999). Amphetamine reverses or blocks the operation of the human noradrenaline transporter depending on its concentration: superfusion studies on transfected cells. *Neuropharmacol.* **38**:157-165.

Pin J.P. and Duvoisin R. (1995). The metabotropic glutamate receptors: structure and function. *Neuropharmacology* **34**:1-26.

Pines G., Danbolt N.C., Bjoras M., Zhang Y., Bendahan A., Eide L., Koepsell H., Storm-Mathisen J., Seeberg E. and Kanner B.I. (1992). Cloning and expression of a rat brain L-glutamate transporter. *Nature* **360**:464-467.

Porter J.T. and McCarthy K.D. (1997). Astrocytic neurotransmitter receptors *in situ* and *in vivo*. *Prog. Neurobiol.* **51**:439-55.

Pow D.V. (2001). Visualising the activity of the cystine-glutamate antiporter in glial cells using antibodies to amino adipic acid, a selectively transported substrate. *Glia* **34**:27-38.

Reid M.S., Hsu K. and Berger S.P. (1997). Cocaine and amphetamine preferentially stimulate glutamate release in the limbic system: studies on the involvement of dopamine. *Synapse* **27**:95-105.

Reuss B. and Unsicker K. (2001). Atypical neuroleptic drugs downregulate dopamine sensitivity in rat cortical and striatal astrocytes, *Molec. Cell Neurosci.* **18**:197-209.

Richfield E.K., Penney J.B. and Young A.B. (1989). Anatomical and affinity state comparisons between dopamine D₁ and D₂ receptors in the rat central nervous system. *Neurosci.* **30**:767-77.

Robinson M.B., Hunter-Ensor M. and Sinor J. (1991). Pharmacologically distinct sodium-dependent L-[3H]-glutamate transport processes in rat brain. *Brain Res.* **544**:196-202.

Rossi D.J., Oshima T. and Atwell D. (2000). Glutamate release in severe brain ischaemia is mainly by reversed uptake. *Nature* **403**:316-21.

Rothman R.B., Blough B.E. and Baumann M.H. (2002). Appetite suppressants as agonist substitution therapies for stimulant dependence. *Ann. NY. Acad. Sci.* **965**:109-126.

Rothstein J.D., Dykes-Hoberg M., Pardo C.A., Bristol L.A., Jin L., Kuncl R.W., Kanai Y., Hediger M.A., Wang Y., Schielke J.P. and Welty D.F. (1996). Knockout of glutamate transporters reveals a major role for astroglial transport in excitotoxicity and clearance of glutamate. *Neuron* **16**:675-686.

Rothstein J.D., Dykes-Hoberg M., Pardo C.A., Bristol L.A., Jin L., Kuncl R.W., Arriza J.L., Eliasof S., Kavanaugh M.P. and Amara S.G. (1997). Excitatory amino acid transporter 5, a retinal glutamate transporter coupled to a chloride conductance. *Proc. Natl. Acad. Sci. U. S. A.* **94**:4155-60.

Rowley H.L., Martin K.F. and Marsden C.A. (1995). Determination of *in vivo* amino acid neurotransmitters by high-performance liquid chromatography with o-phthalaldehyde-sulphite derivatisation. *J. Neurosci. Meth.* **57**:93-9.

Rowley H.L., Butler S.A., Prow M.R., Dykes S.G., Aspley S., Kilpatrick I.C. and Heal D.J. (2000). Comparison of the effects of sibutramine and other weight-modifying drugs on extracellular dopamine in the nucleus accumbens of freely-moving rats. *Synapse* **38**:167-76.

Sabol K.E. and Seiden L.S. (1998). Reserpine attenuates *d*-amphetamine and MDMA-induced transmitter release *in vivo*: a consideration of dose, core temperature and dopamine synthesis. *Brain Res.* **806** :69-78.

Santana N., Bortolozzi A., Serrats J., Mengod G. and Artigas F. (2004). Expression of serotonin_{1A} and serotonin_{2A} receptors in pyramidal and GABAergic neurones of the rat prefrontal cortex. *Cereb. Cortex* **14**:1100-9.

Santiago M, Cano J. and Westerink B.M. (1993). Are bilateral nigrostriatal pathways functionally linked in the rat brain? A microdialysis study in conscious rats. *Brain Res.* **628**:187-92.

Sattler R., Xiong Z., Lu W.Y., MacDonald J.F. and Tymianski M. (2000). Distinct roles of synaptic and extrasynaptic NMDA receptors in excitotoxicity. *J. Neurosci.* **20**:22-33.

Segovia G., Del Arco A. and Mora F. (1997). Endogenous glutamate increases the extracellular concentrations of dopamine, GABA and taurine through NMDA and AMPA/kainate receptors in striatum of the freely-moving rat: a microdialysis study. *J. Neurochem.* **69**:1476-83.

Segovia G., Del Arco A. and Mora F. (1999). Effects of aging on the interaction between glutamate, dopamine and GABA in striatum and nucleus accumbens of the awake rat. *J. Neurochem.* **73**:2063-72.

Seki Y., Feustel P.J., Keller R.W. Jr., Tranmer B.I. and Kimelberg H.K. (1999). Inhibition of ischaemia-induced glutamate release in rat striatum by dihydrokainate and an anion channel blocker. *Stroke* **30**:433-40.

Semba J. and Wakuta M.S. (1998). Regional differences in the effects of glutamate uptake inhibitor *L-trans*-pyrrolidine-2,4-dicarboxylic acid on extracellular amino acids and dopamine in rat brain: an *in vivo* microdialysis study. *Gen. Pharmacol.* **31**:399-404.

Semyanov A. and Kullmann D.M. (2000). Modulation of GABAergic signaling among interneurons by metabotropic glutamate receptors. *Neuron* **25**:663-72.

Sesack S.R. and Pickel V.M. (1992). Dual ultrastructural localization of enkephalin and tyrosine hydroxylase immunoreactivity in the rat ventral tegmental area: multiple substrates for opiate-dopamine interactions. *J. Neurosci.* **12**:1335-50.

Sesack S.R., Hawrylak V.A., Matus C., Guido M.A. and Levey A.I. (1998). Dopamine axon varicosities in the prelimbic division of the rat prefrontal cortex exhibit sparse immunoreactivity for the dopamine transporter. *J. Neurosci.* **18**:1697-708.

Shank R.P., Bennett G.S., Freytag S.O. and Campbell G.L. (1985). Pyruvate carboxylase: an astrocyte-specific enzyme implicated in the replenishment of amino acid neurotransmitter pools. *Brain Res.* **329**:364-7.

Shoblock J.R., Sullivan E.B., Maisonneuve I.M. and Glick S.D. (2003). Neurochemical and behavioural differences between *d*-methamphetamine and *d*-amphetamine in rats. *Psychopharmacol.* **165**:359-369.

Silva E., Hernandez L., Contreras Q., Guerrero F. and Alba G. (2000). Noxious stimulation increases glutamate and arginine in the periaqueductal grey matter in rats: a microdialysis study. *Pain* **87**:131-5.

Sidiropoulou K., Chao S., Lu W. and Wolf M.E. (2001). Amphetamine administration does not alter protein levels of the GLT-1 and EAAC1 glutamate transporter subtypes in rat midbrain, nucleus accumbens, striatum, or prefrontal cortex. *Mol. Brain Res.* **90**:187-92.

Smiley J.F., Levey A.I., Ciliax B.J. and Goldman-Rakic P.S. (1994). D₁ dopamine receptor immunoreactivity in human and monkey cerebral cortex: predominant and extrasynaptic localisation in dendritic spines. *Proc. Natl. Acad. Sci. USA* **91**:5720-5724.

Smith J.C.E. and Whitton P.S. (2001). The regulation of NMDA-evoked dopamine release by nitric oxide in the frontal cortex and raphe nuclei of the freely-moving rat. *Brain Res.* **889**:57-62.

Smith J.A., Mo Q., Guo H., Kunko P.M. and Robinson S.E. (1995). Cocaine increases extraneuronal levels of aspartate and glutamate in the nucleus accumbens. *Brain Res.* **683**:264-269.

Sonnewald U., Qu H. and Aschner M. (2002). Pharmacology and toxicology of astrocyte-neuron glutamate transport and cycling. *J. Pharmacol. Exp. Ther.* **301**:1-6.

Spackman D.H., Stein W.H. and Moore S. (1958). Automatic recording apparatus for use in the chromatography of amino acids. *Anal. Chem.* **30**:1190-206.

Stanley J.A. (2002). *In vivo* magnetic resonance spectroscopy and its application to neuropsychiatric disorders. *Can. J. Psychiatry* **47**:315-26.

Stamford J.A. (1989). *In vivo* voltammetry – prospects for the next decade. *TINS* **12**:407-12.

Stenken J.A. (1999). Methods and issues in microdialysis calibration. *Analytica Chim. Act.* **379**:337-58.

Storck T., Schulte S., Hofmann K. and Stoffel W. (1992). Structure, expression, and functional analysis of a Na⁺-dependent glutamate/aspartate transporter from rat brain. *PNAS* **89**:10955-10959.

Sulzer D., Sonders M.S., Paulsen N.W. and Galli A. (2005). Mechanisms of neurotransmitter release by amphetamines: A review. *Progress Neurobiol.* **75**:406-33.

Swatkowski M., Barbour B. and Attwell D. (1990). Non-vesicular release of glutamate from glial cells by reversed electrogenic glutamate uptake. *Nature* **348**:443-446.

Takahata R. and Moghaddam B. (1998). Glutamatergic regulation of basal and stimulus-activated dopamine release in the prefrontal cortex. *J. Neurochem.* **71**:1443-1449.

Tanaka K., Watase K., Manabe T., Yamada K., Watanabe M., Takahashi K., Iwama H., Nishikawa T., Ichihara N., Kikuchi T., Okuyama S., Kawashima N., Hori S., Takimoto M. and Wada K. (1997). Epilepsy and exacerbation of brain injury in mice lacking the glutamate transporter GLT-1. *Science* **276**:1699-702.

Thierry A.M., Deniau J.M. and Feger J. (1979). Effects of stimulation of the frontal cortex on identified output VMT cells in the rat. *Neurosci. Lett.* **15**:102-7.

Timmerman W. and Westerink B.H. (1997). Brain microdialysis of GABA and glutamate: what does it signify? *Synapse* **27**:242-261.

Tissari A.H. (1982). Increase of dopamine synthesis in synaptosomes from rats treated with neuroleptics or reserpine. *Med. Biol.* **60**:38-41.

Tsai G., Passani L.A., Slusher B.S., Carter R., Buer L., Kleinman J.E. and Coyle J.T. (1995). Abnormal excitatory neurotransmitter metabolism in schizophrenic brain. *Arch. Gen. Psychiatry* **52**:829-36.

Van Eden C.G., Hoorneman E.M.D., Buus R.M., Mathussen M.A.H., Geffard M. and Uylings H.B.M. (1987). Immunocytochemical localization of dopamine in the prefrontal cortex of the rat at the light and electron microscopical level. *Neurosci.* **22**:849-62.

Vincent S.L., Khan Y. and Benes F.M. (1993). Cellular distribution of D₁ and D₂ receptors in rat medial prefrontal cortex. *J. Neurosci.* **13** :2551-2564.

Vogt B.A., Derbyshire S. and Jones A.K. (1996). Pain processing in four regions of human cingulate cortex localized with co-registered PET and MR imaging. *Eur. J. Neurosci.* **8**:1461-73.

Volterra A. and Steinhauser C. (2004). Glial modulation of synaptic transmission in the hippocampus. *Glia* **47**:249-57.

Wall S.C., Gu H. and Rudnick G. (1995). Biogenic amine flux mediated by cloned transporters stably expressed in cultured cell lines: amphetamine specificity for inhibition and efflux. *Mol. Pharmacol.* **47**:544-50.

Warr O., Takahashi M. and Attwell D. (1999). Modulation of extracellular glutamate concentration in rat brain slices by cystine-glutamate exchange. *J. Physiol.* **514**:783-93.

Wayment H.K., Schenk J.O. and Sorg B.A. (2001). Characterisation of extracellular dopamine clearance in the medial prefrontal cortex: role of monoamine uptake and monoamine oxidase inhibition. *J. Neurosci.* **21**:35-44.

Westerink B.H. and De Vries J.B. (1988). Characterisation of *in vivo* dopamine release as determined by brain microdialysis after acute and subchronic implantations: methodological aspects. *J. Neurochem.* **51**:683-7.

Westerink B.H. (1995). Brain microdialysis and its application for the study of animal behaviour. *Behav. Brain Res.* **70**:103-24.

Wilhelm A., Volkandt W., Langer D., Nolte C., Kettenmann H. and Zimmerman H. (2004). Localisation of SNARE proteins and secretory organelle proteins in astrocytes *in vitro* and *in situ*. *Neurosci. Res.* **48**:249-57.

Wolf M.E. and Xue C.J. (1999). Amphetamine-induced glutamate efflux in the rat ventral tegmental area is prevented by MK-801, SCH 23390, and ibotenic acid lesions of the prefrontal cortex. *J. Neurochem.* **73**:1529-38.

Wolf M.E., Xue C.J., Li Y. and Wavak D. (2000). Amphetamine increases glutamate efflux in the rat ventral tegmental area by a mechanism involving glutamate transporters and reactive oxygen species. *J. Neurochem.* **75**:1634-1644.

Wortley K.E., Hughes Z.A., Heal D.J. and Stanford S.C. (1999). Comparison of changes in the extracellular concentration of noradrenaline in the rat frontal cortex induced by sibutramine or *d*-amphetamine: modulation by α_2 -adrenoceptors. *Br. J. Pharmacol.* **127**:1860-6.

Xi Z.X., Shen H., Baker D.A. and Kalivas P.W. (2003). Inhibition of non-vesicular glutamate release by group III metabotropic glutamate receptors in the nucleus accumbens. *J. Neurochem.* **87**:1204-1212.

Ye Z.C., Wyeth S.W., Baltan-Tekkoh S. and Ransom B.R. (2003). Functional hemichannels in astrocytes: A novel mechanism of glutamate release. *J. Neurosci.* **23**:3588-96.

Yücel M., Wood S.J., Fornito A., Riffkin J., Velakoulis D. and Pantelis C. (2003). Anterior cingulate dysfunction: Implications for psychiatric disorders? *Rev. Psychiatr. Neurosci.* **28**:350-354.

Zetterstrom T., Vernet L., Ungerstadt U., Tossman U., Jonzon B. and Fredholm B.B. (1982). Purine levels in the intact rat brain. Studies with an implanted perfused hollow fibre. *Neurosci. Lett.* **29**:111-5.

Zoli M. and Agnati L.F. (1996). Wiring and volume transmission in the nervous system: the concept of closed and open synapses. *Prog. Neurobiol.* **80**.

Zuo D-Y., Zhang Y-H., Cao Y., Wu C-F., Tanaka M. And Wu Y-L. (2006). Acute and chronic MK-801 administration on extracellular glutamate and acid release in the prefrontal cortex of freely moving mice on line with behaviour. *Life Sci.* **78**:2172-8.